SPACE, TELECOMMUNICATIONS AND RADIOSCIENCE LABORATORY

STARLAB
DEPARTMENT OF ELECTRICAL ENGINEERING
STANFORD UNIVERSITY • STANFORD, CA 94305

Seasonal Variations of Globally Measured ELF/VLF Radio Noise

by

D. A. Chrissan
A. C. Fraser-Smith

Technical Report D177-1

December 1996

Sponsored by
The Office of Naval Research
through
Grants No. N00014-92-J-1576 and No. N00014-93-1-1073

UNCLASSIFIED

SECURITY CLASSIFICATION OF THIS PAGE *(When Data Entered)*

REPORT DOCUMENTATION PAGE		READ INSTRUCTIONS BEFORE COMPLETING FORM
1. REPORT NUMBER D 177-1	2. GOVT ACCESSION NO.	3. RECIPIENT'S CATALOG NUMBER
4. TITLE *(and Subtitle)* SEASONAL VARIATIONS OF GLOBALLY MEASURED ELF/VLF RADIO NOISE		5. TYPE OF REPORT & PERIOD COVERED TECHNICAL 6. PERFORMING ORG. REPORT NUMBER
7. AUTHOR(s) D.A. Chrissan and A.C. Fraser-Smith		8. CONTRACT OR GRANT NUMBER(s) GRANT No. N00014-92-J-1576 GRANT No. N00014-93-1-1073
9. PERFORMING ORGANIZATION NAME AND ADDRESS SPACE, TELECOMMUNICATIONS AND RADIOSCIENCE LAB. DURAND BUILDING, STANFORD UNIVERSITY, 94305-9515		10. PROGRAM ELEMENT, PROJECT, TASK AREA & WORK UNIT NUMBERS
11. CONTROLLING OFFICE NAME AND ADDRESS OFFICE OF NAVAL RESEARCH, CODE 321SR 800 QUINCY STREET ARLINGTON, VA 22217		12. REPORT DATE DECEMBER 1996 13. NUMBER OF PAGES
14. MONITORING AGENCY NAME & ADDRESS*(if different from Controlling Office)*		15. SECURITY CLASS. *(of this report)* UNCLASSIFIED 15a. DECLASSIFICATION/DOWNGRADING SCHEDULE

16. DISTRIBUTION STATEMENT *(of this Report)*

DISTRIBUTION UNLIMITED, APPROVED FOR PUBLIC RELEASE AND SALE.

17. DISTRIBUTION STATEMENT *(of the abstract entered in Block 20, if different from Report)*

18. SUPPLEMENTARY NOTES

19. KEY WORDS *(Continue on reverse side if necessary and identify by block number)*

ELF NOISE VLF NOISE SFERICS CHORUS
HISS GLOBAL NOISE MEASUREMENTS RADIO NOISE STATISTICS
LONG-TERM NOISE MEASUREMENTS
SEASONAL VARIATIONS

20. ABSTRACT *(Continue on reverse side if necessary and identify by block number)*

THE SPACE, TELECOMMUNICATIONS AND RADIOSCIENCE (STAR) LABORATORY AT STANFORD HAS BEEN CONDUCTING A GLOBAL SURVEY OF EXTREMELY-LOW FREQUENCY (ELF) AND VERY-LOW FREQUENCY (VLF) RADIO NOISE SINCE FEBRUARY 1985. EIGHT MEASUREMENT STATIONS AROUND THE WORLD RECORD THE INSTANTANEOUS NOISE AMPLITUDE IN EACH OF SIXTEEN NARROW FREQUENCY BANDS IN THE 10 Hz - 32 kHz FREQUENCY RANGE, AND THIS REPORT PRESENTS CALCULATIONS OF THE MONTHLY AVERAGES FOR THE FOUR STATIONS WITH THE LONGEST TIMES OF OPERATION. (over)

BLOCK 20 CONT.

THE DATA PRESENTED HERE SUPPLEMENT THOSE IN A PAPER IN RADIO SCIENCE BY THE SAME AUTHORS; HOWEVER, THIS REPORT INCLUDES A MUCH MORE DETAILED AND EXTENSIVE PRESENTATION OF THE SEASONAL VARIATION DATA THAN DOES THE PUBLISHED PAPER. SPECIFICALLY, THIS REPORT CONTAINS: (1) SEASONAL VARIATION DATA FOR SPECIFIC DIURNAL TIME PERIODS, AND (2) THE SEASONAL VARIATIONS FOR INDIVIDUAL YEARS.

Seasonal Variations of Globally Measured ELF/VLF Radio Noise

by

D. A. Chrissan and A. C. Fraser-Smith

Technical Report D177-1

December 1996

Sponsored by

The Office of Naval Research

Grants No. N00014-92-J-1576 and No. N00014-93-1-1073

Abstract

The Space, Telecommunications and Radioscience (STAR) Laboratory at Stanford has been conducting a global survey of extremely-low frequency (ELF) and very-low frequency (VLF) radio noise since February 1985. Eight measurement stations around the world record the instantaneous noise amplitude in each of sixteen narrow frequency bands in the 10 Hz – 32 kHz frequency range, and this report presents calculations of the monthly averages of these amplitudes for the four stations with the longest times of operation.

The data presented here supplement those in a paper in *Radio Science* by the same authors [*Chrissan and Fraser-Smith,* 1996]; however, this report includes a much more detailed and extensive presentation of the seasonal variation data than does the published paper. Specifically, this report contains: (1) seasonal variation data for specific diurnal time periods, and (2) the seasonal variations for individual years.

Contents

1 Introduction

During the years 1985-1986, eight ELF/VLF (10 Hz – 32 kHz) radio noise measurement systems, or radiometers, were installed at a variety of high-latitude and mid-latitude sites in an effort to fill large gaps in the information available on radio noise in this frequency range. Most of the stations operated much longer than original program expectations, and this longevity allows us to examine seasonal trends over the course of many years. A number of other ELF/VLF measurement systems have been implemented in the past, but this is the only system of its kind in terms of its geographic coverage and continuity of simultaneous data collection. It would be impossible to derive statistically significant seasonal variations without multiple years of data, since the individual seasonal variations sometimes differ significantly from year to year.

The radiometers were primarily developed to obtain new information in support of defense communications and radio navigation systems, and to this end the data have been used to develop long range ELF/VLF noise prediction models [*Warber and Field,* 1995]. However, the data have also found use in geophysical and environmental analyses, such as to study polar region events (auroral hiss and polar chorus) and the effects of solar particle events [*Fraser-Smith and Turtle,* 1993], to define the natural background noise levels at power line frequencies for comparison with those levels created by man-made power generation and distribution systems around the world [*Fraser-Smith and Bowen,* 1992], and to relate long term variations in ELF/VLF noise to seasonal weather patterns and global climate change [*Füllekrug and Fraser-Smith,* 1997].

It is this last context in which we present the data in this paper. Radio noise at ELF/VLF frequencies is caused primarily by lightning occurring throughout the world, so the noise levels can be used to study global climate change and the propagation characteristics of the electromagnetic impulses, or sferics, radiated by the various lightning sources. Four of the radiometers — Arrival Heights, Antarctica (AH; $77.8°S$, $193.3°W$); Dunedin, New Zealand (DU; $45.8°S$, $189.5°W$); Søndrestromfjørd, Greenland (SS; $67.0°N$, $50.1°W$); and Stanford, California (SU; $37.4°N$, $122.2°W$) — have provided enough good, long term data to justify a seasonal variation analysis. Fortunately these four stations cover mid- and high-latitude locations in both the northern and southern hemispheres. The other four stations (Grafton, New Hampshire; Thule, Greenland; Kochi, Japan; and L'Aquila, Italy) were

either in operation for too short a time, had too many data gaps, or were too contaminated by man-made interference to provide long term averages of naturally occuring noise. The systems at Stanford and Arrival Heights are continuing to collect data; the former has been in operation for ten years and the latter eleven and a half. They should be able to collect data beyond one solar cycle.

We present the ELF/VLF radio noise from these four stations using variations in monthly averages. For each month at each station, a single number is computed representing the average noise level for that month, then the variation by month throughout each year is determined. All the years are then averaged together to create a single plot of annual variation by month. In this report individual years are plotted as well, and we also calculate seasonal variations using only four-hour time periods in each day.

2 Radiometer System Description

A complete technical description of the radiometers used for the radio noise survey has been provided elsewhere [*Fraser-Smith et al.,* 1988], so we give only an overview as it pertains to the data being presented. Each radiometer contains two receivers, one for the 10–400 Hz frequency range (which we designate ELF in this communication) and the other for the 400 Hz – 32 kHz frequency range (designated VLF). Each receiver has its own pair of crossed loop antennas, one oriented in the N-S geomagnetic direction and the other in the E-W geomagnetic direction. The ELF antennas are 1164 turn coils which are either buried or enclosed in order to prevent noise due to wind induced motion of the coils in the earth's magnetic field. The VLF antennas are single-turn triangular above-ground loops 18m wide and 9m high.

Time series recordings are made of both the ELF and VLF receiver outputs, but only for one minute every hour. In addition to these time series recordings, continuous data collection is obtained by monitoring the outputs of a bank of sixteen narrowband channel filters with center frequencies distributed roughly logarithmically across the 10 Hz – 32 kHz band. Each of the 32 filters (the N-S and E-W loops must be filtered separately) is a six pole Chebychev bandpass filter with a two sided bandwidth equal to five percent of the center frequency. The sixteen center frequencies and bandwidths are contained in Table 1 – the first six are within the ELF receiver's frequency range and the last ten are within the VLF receiver's.

Channel	Frequency	Bandwidth
1	10 Hz	0.5 Hz
2	30	1.5
3	80	4
4	135	6.75
5	275	13.75
6	380	19
7	500	25
8	750 Hz	37.5
9	1 kHz	50
10	1.5	75
11	2	100
12	3	150
13	4	200
14	8	400
15	10.2	510
16	32 kHz	1600 Hz

Table 1: Center frequencies and bandwidths for the 16 narrowband channels of the ELF/VLF radiometer.

Each filter output is passed through an analog RMS detector which squares the input, performs a time average, and outputs the square root of the average. The RMS detector output is then sampled at a rate of ten times per second by an analog to digital converter and sent to a digital computer, which computes the root-sum-square of the N-S and E-W detector outputs to determine the RMS amplitude of the horizontal component of magnetic field for each channel. The analog to digital convertors have a useful dynamic range of 70 dB, but switchable gain amplifiers in the analog receiver circuitry increase the total system dynamic range to 100 dB.

In order to save digital tape space, the computer writes out only every tenth sample. However, it also stores the average and RMS values for each minute (600 samples), along with the minimum and maximum of the 600 values for that minute. The measurements reported here are derived from these one-minute average amplitudes.

3 ELF/VLF Noise Measurements

To provide a basic context for our ELF/VLF noise amplitude measurements, Figure 1 shows the one hour average noise amplitudes over the course of one month for one channel, the 10 Hz band measured at Arrival Heights during the month of June 1994. Each of the 720 points on this graph is an average of roughly 32,000 noise filter output samples (not 36,000 because of calibration periods). The data consist of both random and diurnal variations; they sometimes show occasional short duration impulses due to both man made and natural interference as well. The entire database contains thousands of these plots, one for each station, month and channel.

The unit $\mathrm{fT}/\sqrt{\mathrm{Hz}}$ is essentially the square root of power spectral density, obtained in this case by dividing the RMS filter amplitude output (in fT) by 0.707, the square root of the 0.5 Hz bandwidth for the 10 Hz channel filter. We present the data in fT because our system detects magnetic field. The vertical electric field component and/or the power of the incoming signal may be obtained using 377 Ω as the impedance of free space, but this is an approximation (albeit usually a good one) that assumes the impinging electromagnetic waves are planar. To convert to electric field under this assumption, the relation $B = \sqrt{\mu_0 \epsilon_0} E = \frac{E}{c}$ may be used to determine that 1fT is equivalent to $0.300 \frac{\mu \mathrm{V}}{\mathrm{m}}$. If it is desired to relate magnetic field (or magnetic flux density) B to magnetic intensity H, the relation $B = \mu_0 H$ can

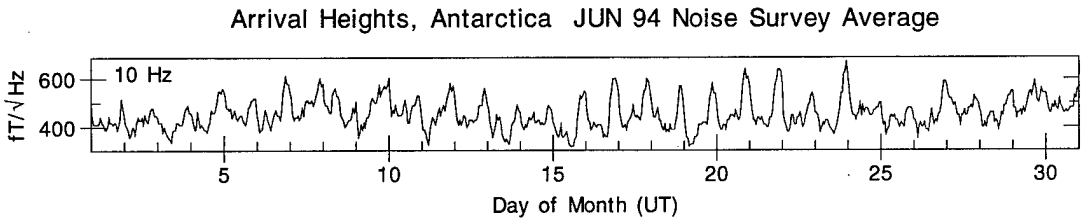

Figure 1: Noise averages in the 10 Hz frequency band recorded June, 1994, at Arrival Heights, Antarctica. Each of the 720 points on this plot is an average of one hour of data.

be used to find that 1fT is equivalent to $7.958 \times 10^{-4} \frac{\mu A}{m}$.

Determining the seasonal variations of natural radio noise over the course of many years requires two steps: (1) monthly averages are computed for each station, month, year, and frequency band (*i.e.*, all the data in Figure 1 are averaged to come up with one number for June 1994 at Arrival Heights in the 10 Hz frequency band), and (2) all the years are then averaged together, resulting in an overall variation by month at each station and in each band. All 24 hours of each day are included, but we also repeat the computation six more times including only four-hour time blocks from each day. This allows for examination of seasonal variations for certain times of day only. We also present data from individual years, with all years overlayed in order to present the data in a reasonable amount of space.

We wish to include only natural radio noise, so it is necessary to eliminate data corrupted by instrumentation problems, physical movement of the coils, or man-made interference. Down time and instrumentation problems are either reported by the system itself or detected by examining the data in the form of Figure 1. Sometimes individual channels are eliminated if hardware failures in those channels are detected; at other times all the ELF or VLF channels must be removed. Another problem occurs occasionally: huge increases in levels of the ELF channels due to movement of the coils from

local construction or agriculture, in which case the ELF channels only are neglected. The end result of these eliminations is that some months have a reduced number of samples in their final average values and other months are missing altogether; however, there are no cases where this has a significant effect on the data presented. It is of note that the 10.2 kHz band at each station is contaminated to some degree by Omega navigation signals.

4 Data Analysis

Figures 2 to 9 show the monthly variations of the noise level for all channels at the four different stations, and the error bars show the standard deviations from year to year, *i.e.*, a small error bar indicates little variation from one year to the next for that month. Note that the error bars are largely unrelated to the standard deviation of individual noise samples, which can be quite large; they are also unrelated to the standard deviation of the total average, which is minute since each point on these plots is an average of millions of sample values. Note that each individual graph has its own scale.

Every year for which a station collected valid data is included in the seasonal variation computation. For Arrival Heights, the years 1985 to 1994 are included; Dunedin includes 1986 to 1990; Søndrestrøm includes 1986 to 1991 and 1993; Stanford includes 1986 to 1993.

Figures 10 to 57 are similar to Figures 2 to 9 except that instead of including all 24 hours from each day, only four hours from each day are used. Thus each plot includes roughly one sixth as much data, and there are six times as many plots. This allows for the examination of seasonal variations based on time of day. Note that the time blocks are labeled differently in the figures' headers than in their captions (an artifact of the data processing software), but each time block does contain a full four hours of data. For example, the header "00-03 UT" refers to data in the range 00:00 UT to 03:59 UT.

Figures 58 to 65 show the individual years of data used to create Figures 2 to 9. Likewise, Figures 66 to 113 show the individual years of data used to create Figures 10 to 57. The symbols used and the years they correspond to for each station are shown in Table 2. Initial examination of the data reveals no common trend from year to year; *i.e.*, data for each year appear to be independent of those for other years.

Symbol	AH	DU	SS	SU
□	1985	1986	1986	1986
○	1986	1987	1987	1987
△	1987	1988	1988	1988
+	1988	1989	1989	1989
x	1989	1990	1990	1990
◇	1990		1991	1991
+ in ◇	1991		1993	1992
x in □	1992			1993
+ in ○	1993			
*	1994			

Table 2: Symbols used for plotting data for individual years.

5 Conclusion

We have presented the monthly variations of ELF/VLF radio noise amplitudes as calculated from several years of data taken from four sites around the world. The data exhibit strong seasonal trends which can be attributed to natural variation in global storm patterns, and which do not appear to be influenced by man-made interference. A lack of complete supporting information on the distribution of global lightning with respect to diurnal variation, month and location precludes us from determining a physical justification for every characteristic of the data; however, the data correlate well in general with known lightning distribution results [*Price and Rind,* 1992, *Goodman and Christian,* 1993]. These data thus may, in their own right, provide information on global lightning distributions.

6 Acknowledgement

This research was sponsored by the Office of Naval Research through Grants No. N00014-92-J-1576 and No. N00014-93-1-1073. Logistic support for the measurements at Søndrestromfjørd, Greenland, and Arrival Heights, Antarctica, was provided by the National Science Foundation through NSF cooperative agreement ATM 88-22560, and NSF grants DPP-8720167 and OPP-9119552, respectively. We thank Paul R. McGill for his assistance in the project, Dr. J.D. Kelly of SRI international for facilitating the measurements

at Søndrestromfjørd, and Dr. N.R. Thomson of the University of Otago for his help with the Dunedin measurements.

7 References

[*Chrissan and Fraser-Smith,* 1996] Chrissan, D., and A.C. Fraser-Smith, Seasonal variations of globally measured ELF/VLF radio noise, *Radio Sci., 31*(5), 1141-1152, 1996.

[*Fraser-Smith and Bowen,* 1992] Fraser-Smith, A.C., and M.M. Bowen, The natural background levels of 50/60 Hz radio noise, *IEEE Trans. Elecromagn. Compat., 34,* pp. 330–337, 1992.

[*Fraser-Smith and Turtle,* 1993] Fraser-Smith, A.C., and J.P. Turtle, ELF/VLF radio noise measurements at high latitudes during solar particle events, *AGARD Conf. Proc. No. 529,* pp. 16-1–16-8, May 1993.

[*Fraser-Smith et al.,* 1988] Fraser-Smith, A.C., R.A. Helliwell, B.R. Fortnam, P.R. McGill and C.C. Teague, A new global survey of ELF/VLF radio noise, Conf. on Effects of Electromagnetic Noise and Interference on Performance of Military Radio Communication Systems, Lisbon, Portugal, 26-30 October, 1987. Published in *AGARD Conf. Proc. No. 420,* pp. 4A-1–4A-7, 1988.

[*Füllekrug and Fraser-Smith,* 1997] Füllekrug,M., and A.C. Fraser-Smith, Global lightning and climate variability inferred from ELF magnetic field variations, to appear in *Geophys. Res. Letters,* 1997.

[*Goodman and Christian,* 1993] Goodman, S.J., and H.J. Christian, Global observations of lightning, in *Atlas of Satellite Observations Related to Global Change,* (R.J. Gurney, ed.),

Cambridge University Press, New York, N.Y., 1993.

[*Price and Rind,* 1992] Price, C., and D. Rind, Simulating global lightning distributions from satellite cloud data, in *Proceedings of the 9th Int. Conf. on Atmospheric Electricity,* St. Petersburg, Russia, pp. 327–330, 1992.

[*Warber and Field,* 1995] Warber, C.R., and E.C. Field, Jr., A long wave transverse electric-transverse magnetic noise prediction model, *Radio Sci., 30*(3), 783–797, 1995.

8 Seasonal Variation Figures

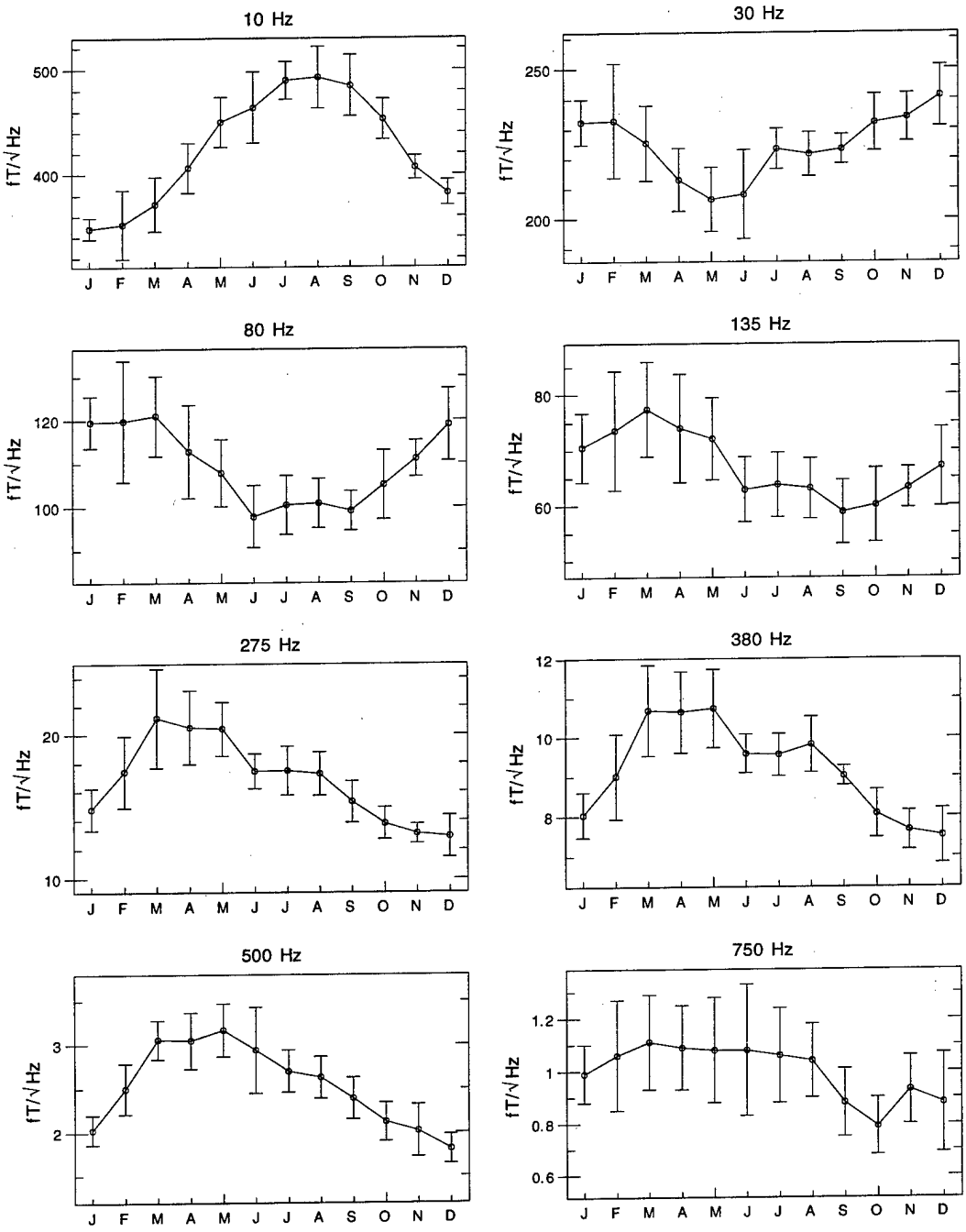

Figure 2: Monthly variation of ELF/VLF radio noise at Arrival Heights, Antarctica, for the eight lowest-frequency channels. The years 1985 to 1994 are included.

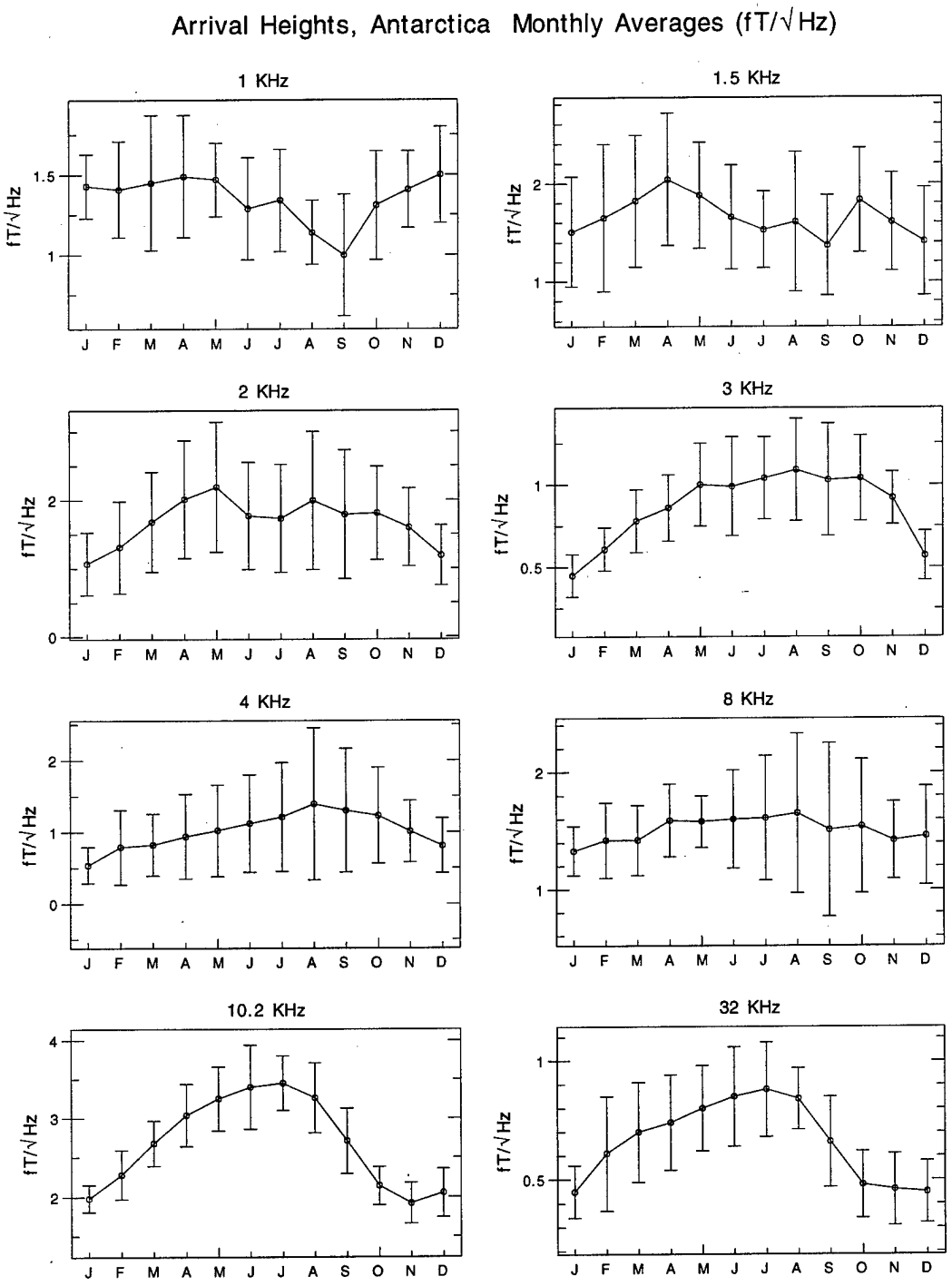

Figure 3: Monthly variation of ELF/VLF radio noise at Arrival Heights, Antarctica, for the eight highest-frequency channels. The years 1985 to 1994 are included.

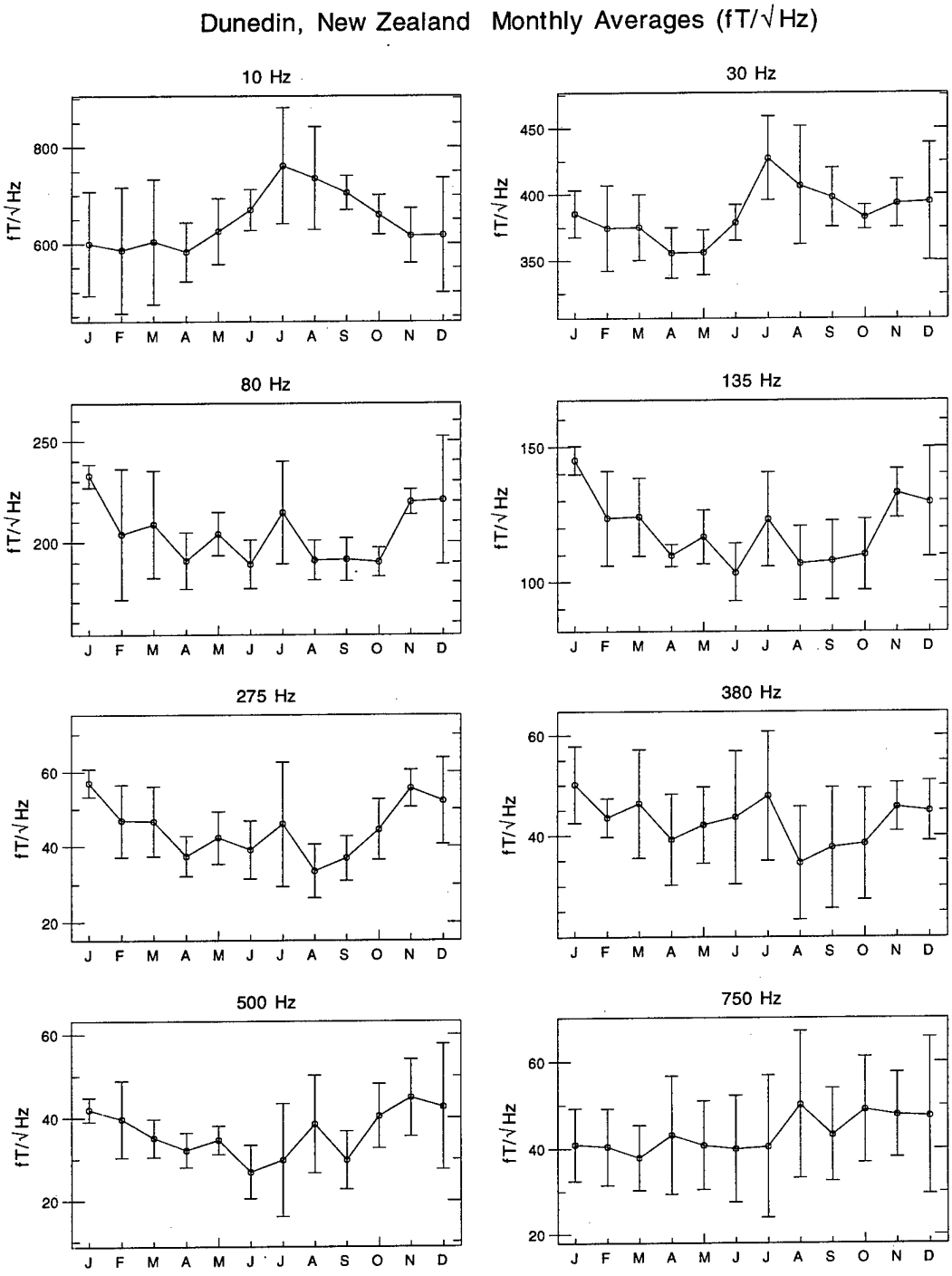

Figure 4: Monthly variation of ELF/VLF radio noise at Dunedin, New Zealand, for the eight lowest-frequency channels. The years 1986 to 1990 are included.

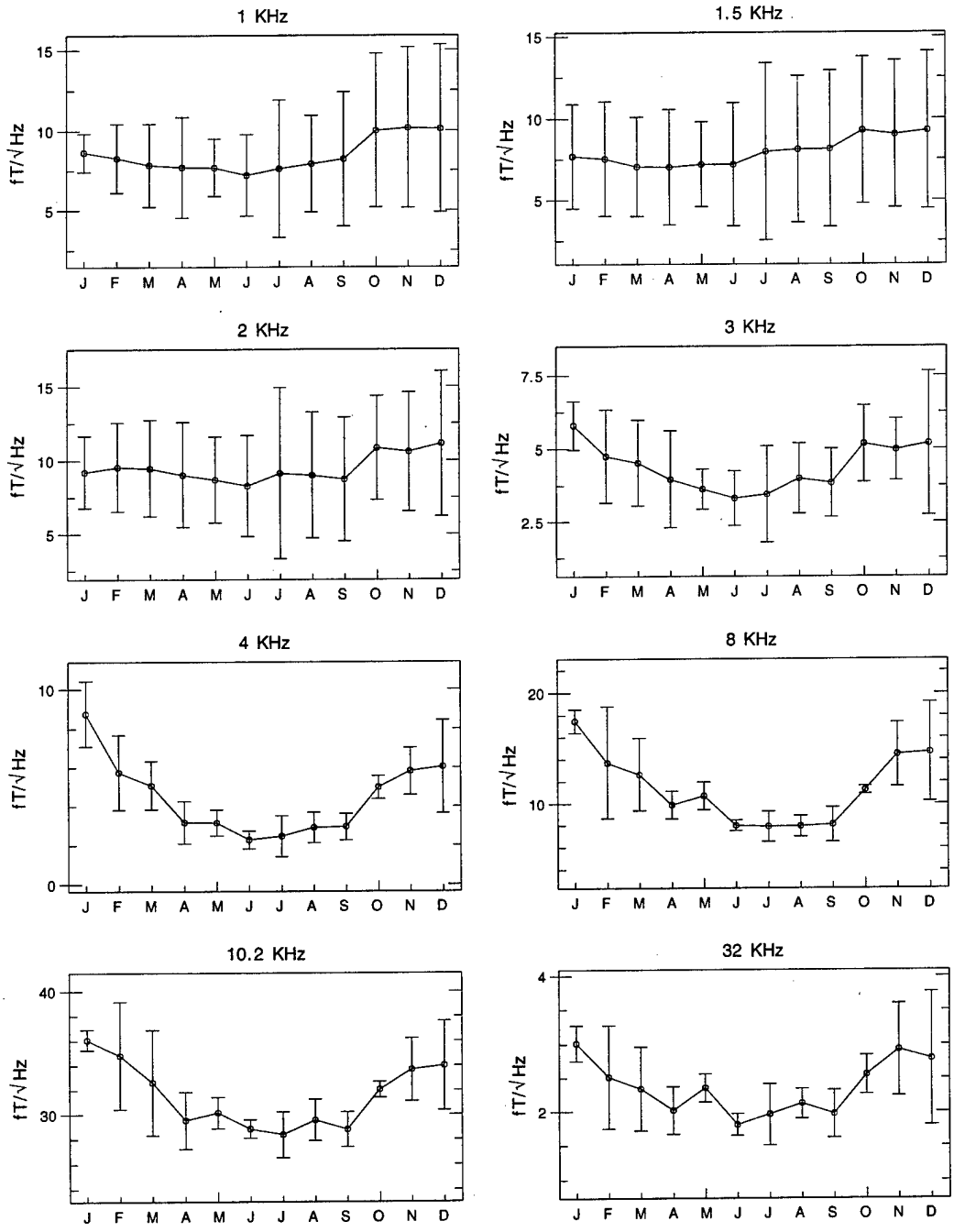

Figure 5: Monthly variation of ELF/VLF radio noise at Dunedin, New Zealand, for the eight highest-frequency channels. The years 1986 to 1990 are included.

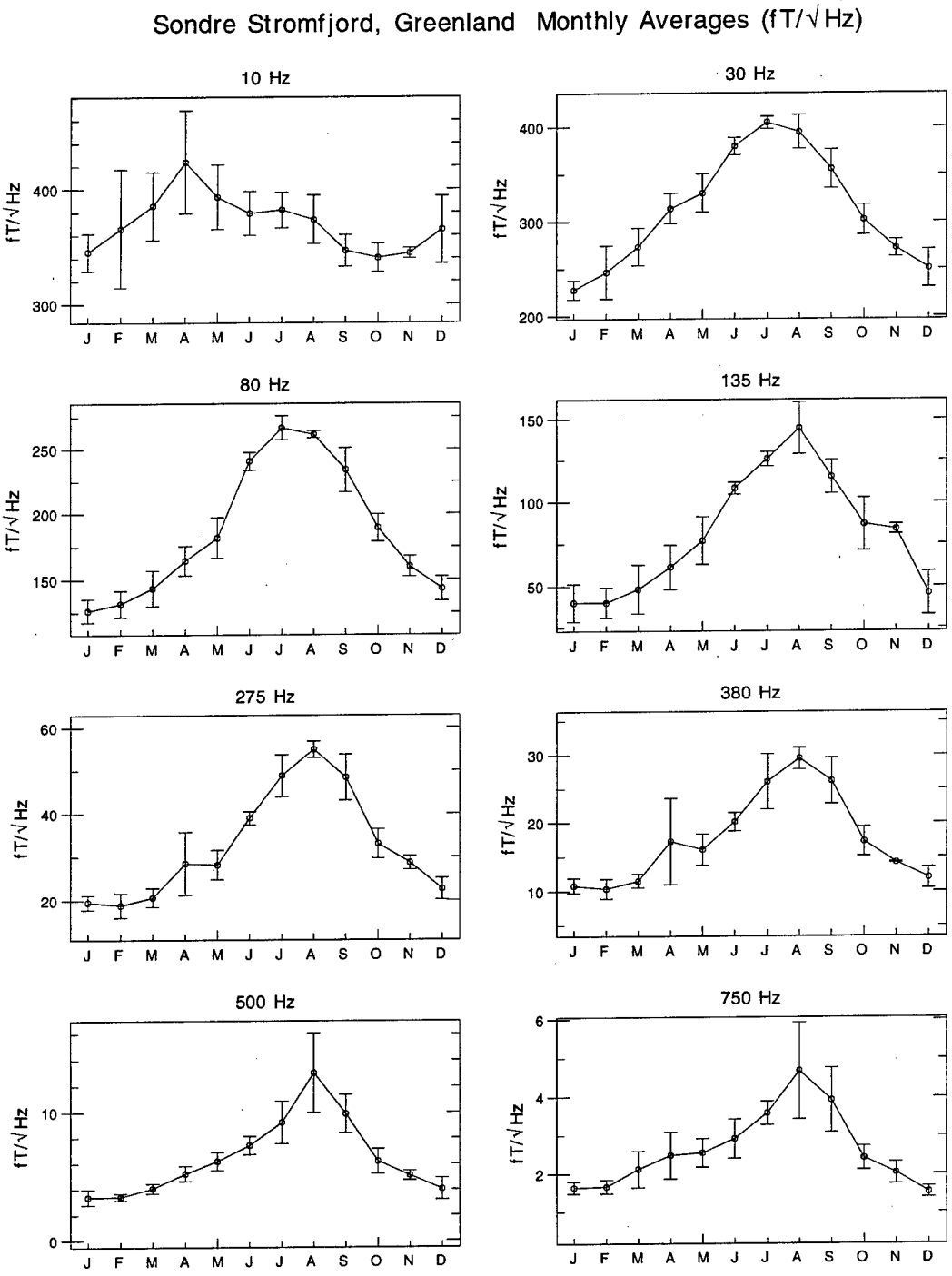

Figure 6: Monthly variation of ELF/VLF radio noise at Søndrestrøm, Greenland, for the eight lowest-frequency channels. The years 1986 to 1991 and 1993 are included.

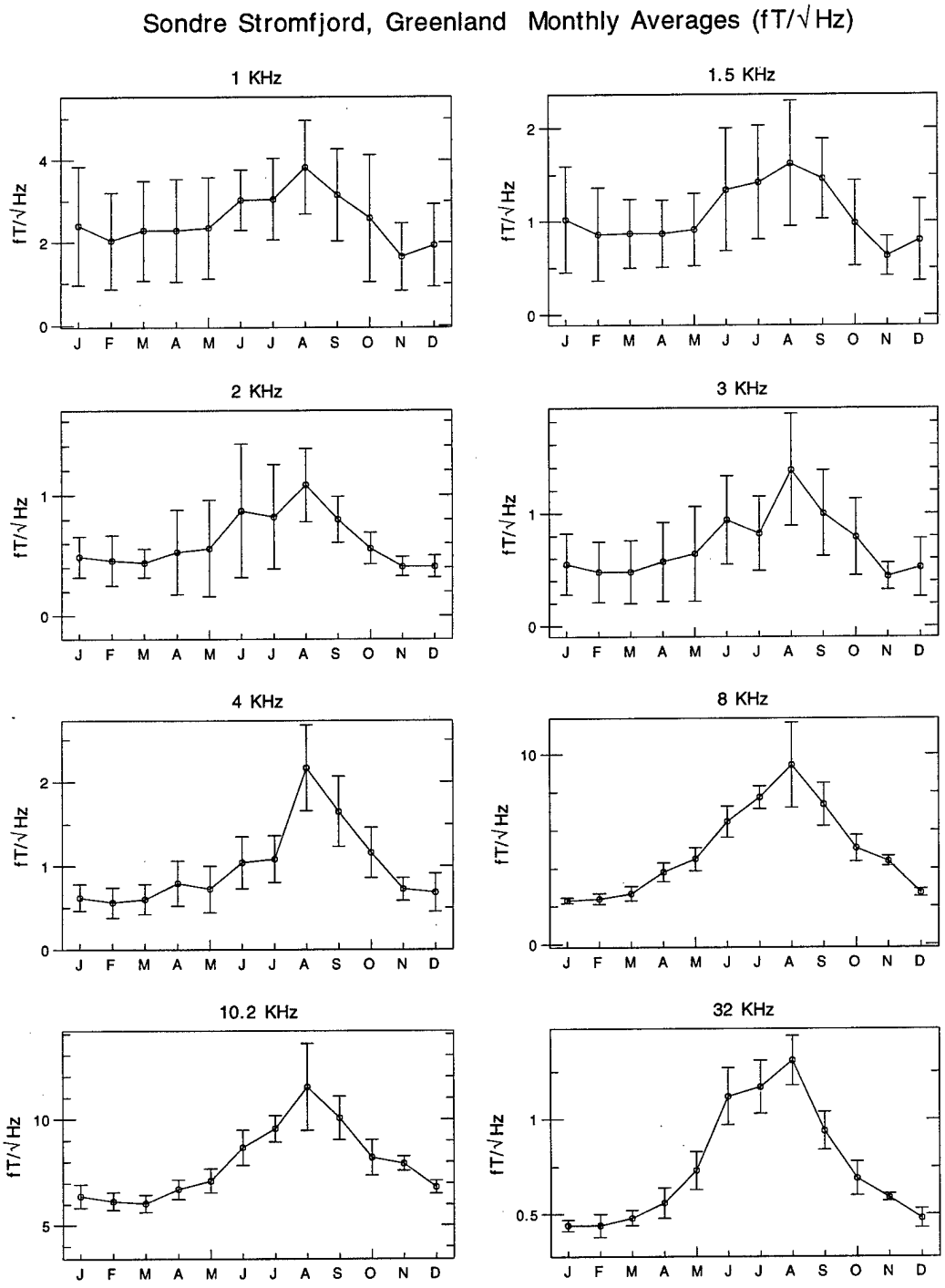

Figure 7: Monthly variation of ELF/VLF radio noise at Søndrestrøm, Greenland, for the eight highest-frequency channels. The years 1986 to 1991 and 1993 are included.

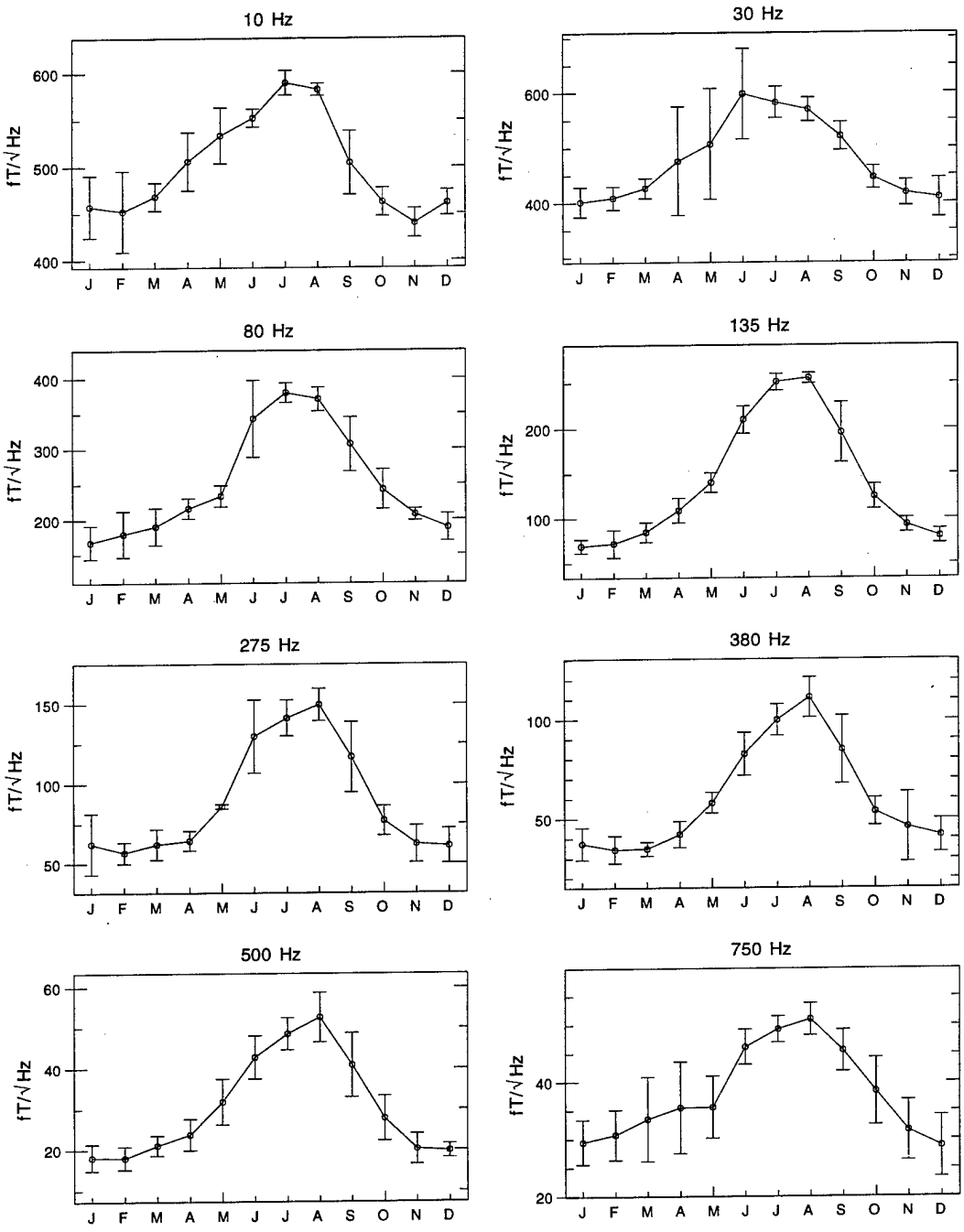

Figure 8: Monthly variation of ELF/VLF radio noise at Stanford, California, for the eight lowest-frequency channels. The years 1986 to 1993 are included.

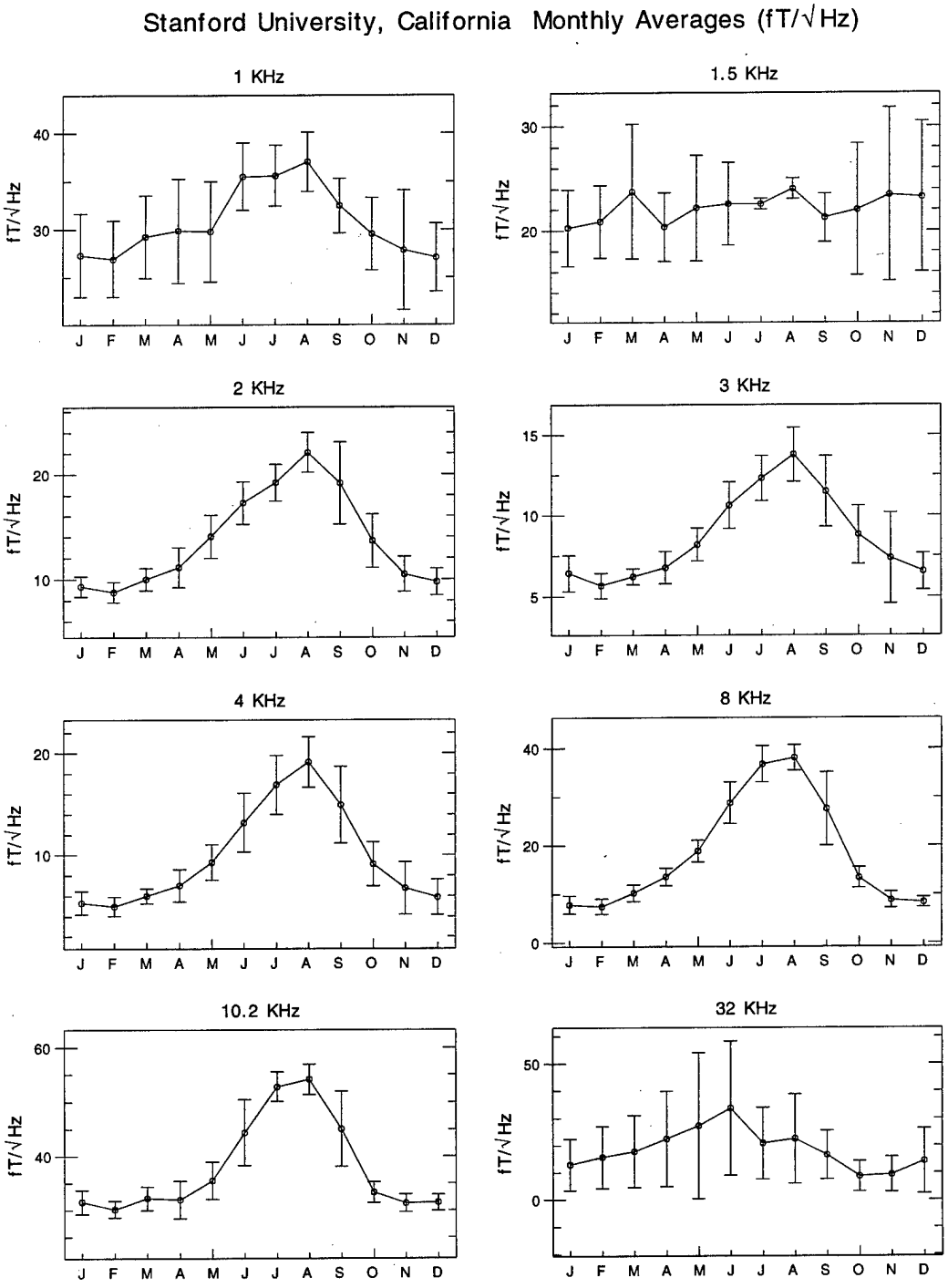

Figure 9: Monthly variation of ELF/VLF radio noise at Stanford, California, for the eight highest-frequency channels. The years 1986 to 1993 are included.

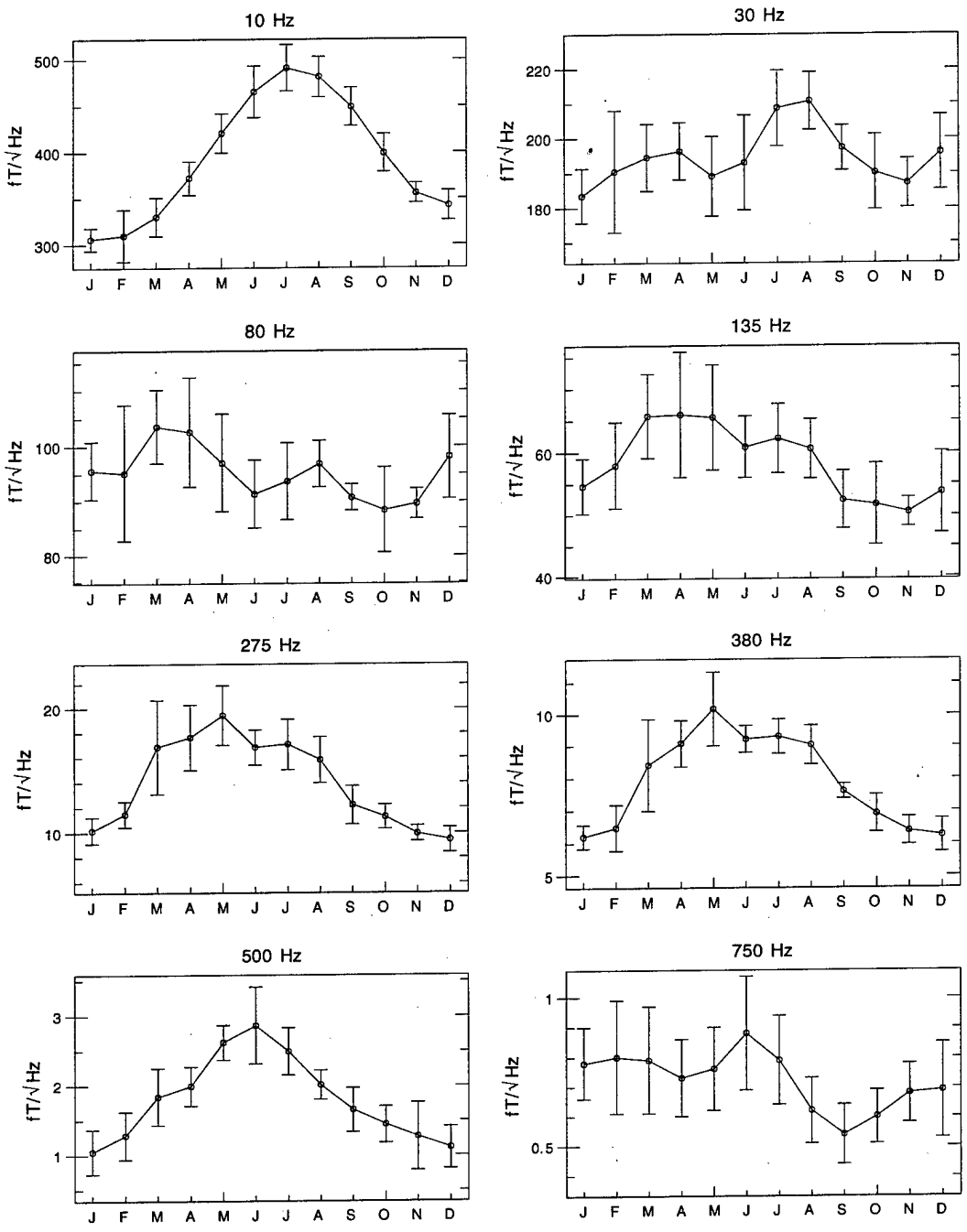

Figure 10: Monthly variation of ELF/VLF radio noise at Arrival Heights, Antarctica, for the eight lowest-frequency channels and the 00-04 UT time block. The years 1985 to 1994 are included.

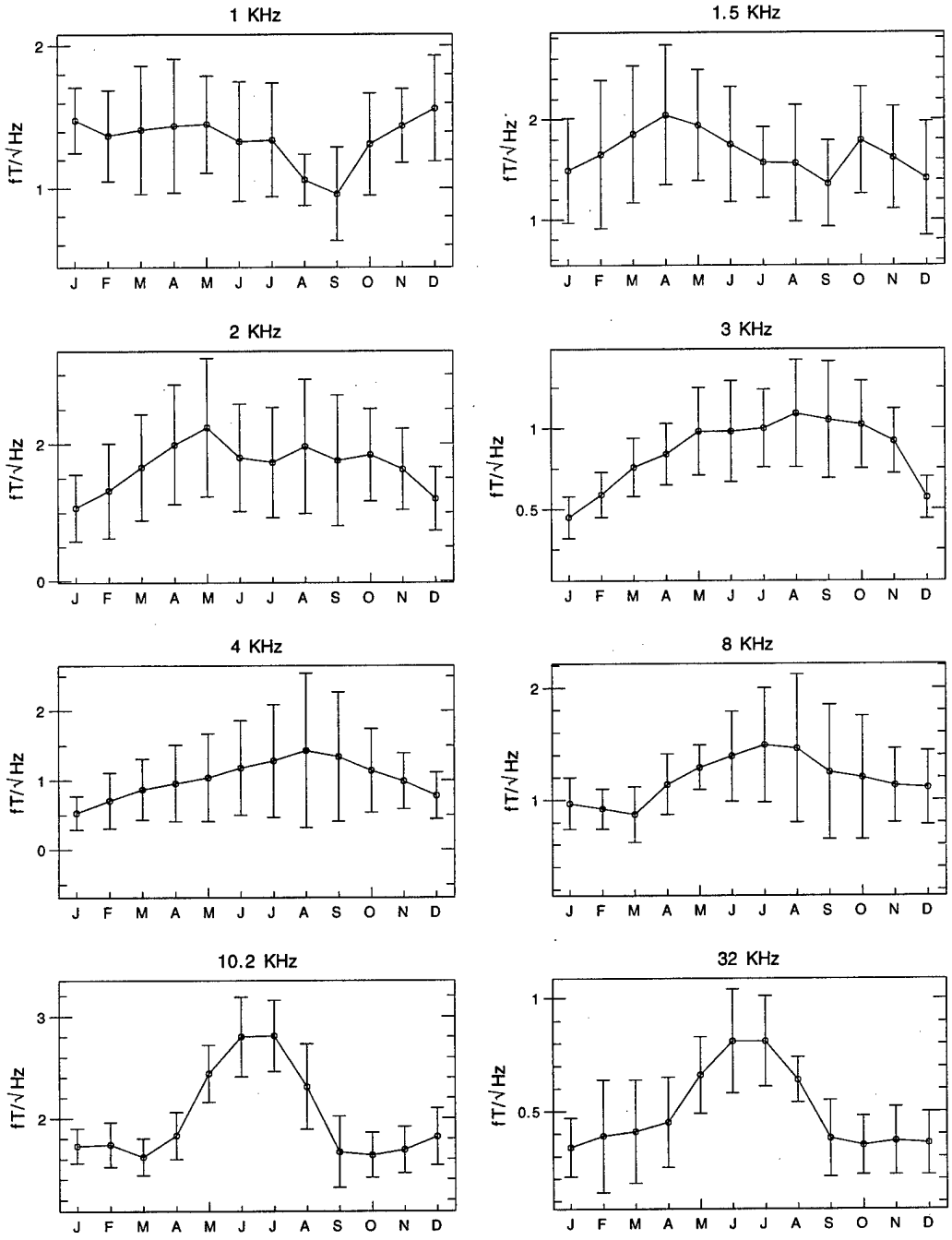

Figure 11: Monthly variation of ELF/VLF radio noise at Arrival Heights, Antarctica, for the eight highest-frequency channels and the 00-04 UT time block. The years 1985 to 1994 are included.

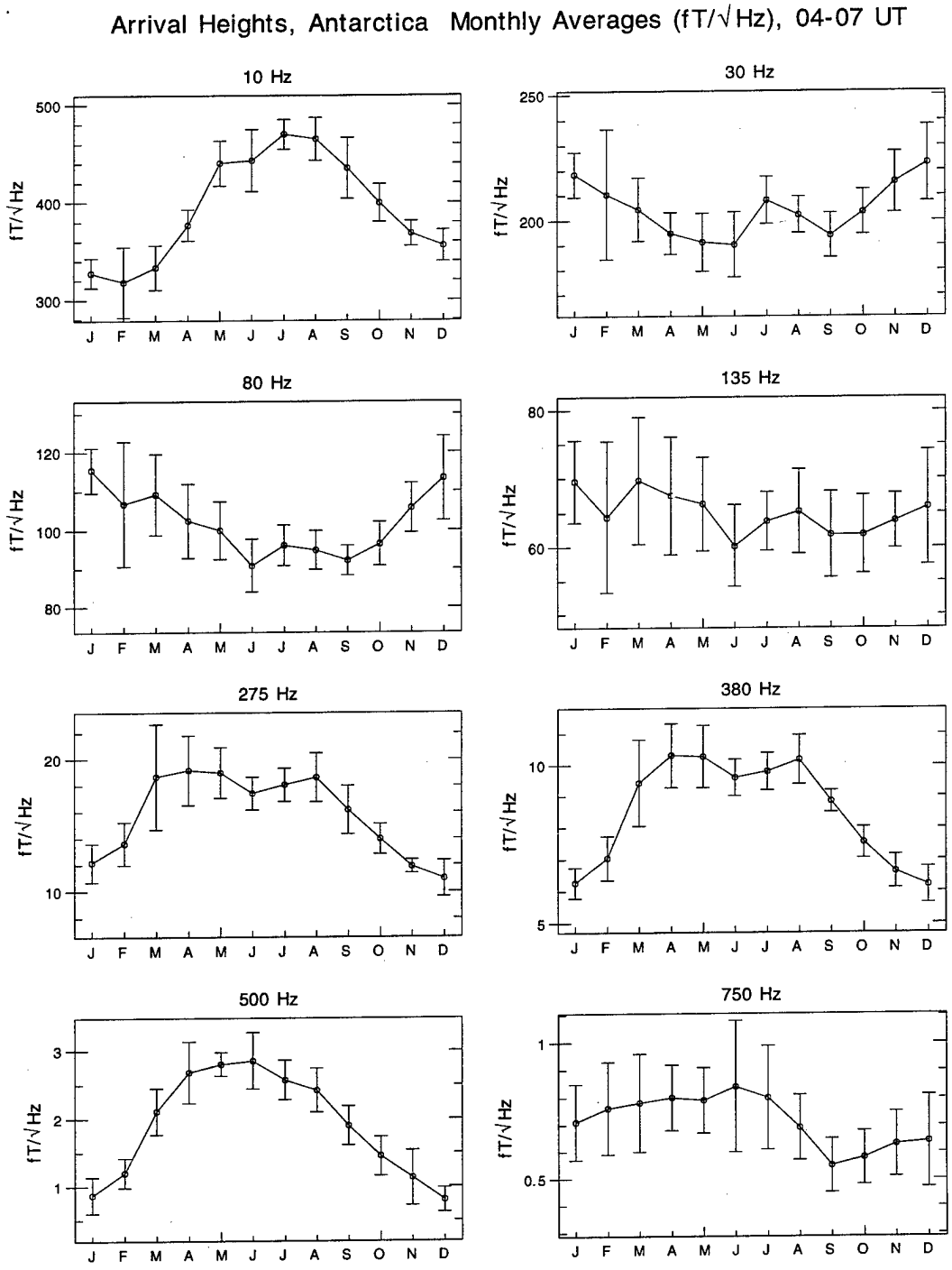

Figure 12: Monthly variation of ELF/VLF radio noise at Arrival Heights, Antarctica, for the eight lowest-frequency channels and the 04-08 UT time block. The years 1985 to 1994 are included.

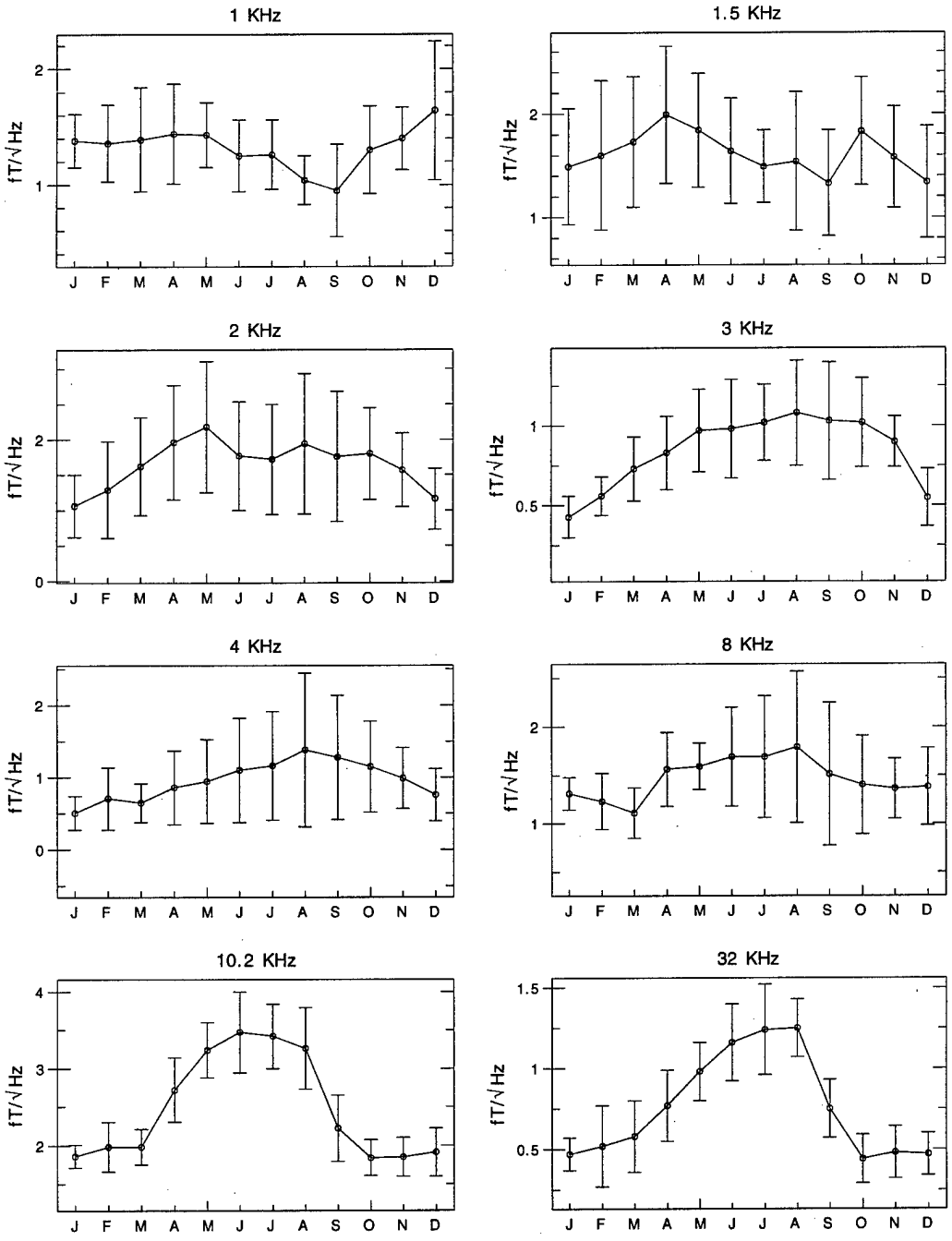

Figure 13: Monthly variation of ELF/VLF radio noise at Arrival Heights, Antarctica, for the eight highest-frequency channels and the 04-08 UT time block. The years 1985 to 1994 are included.

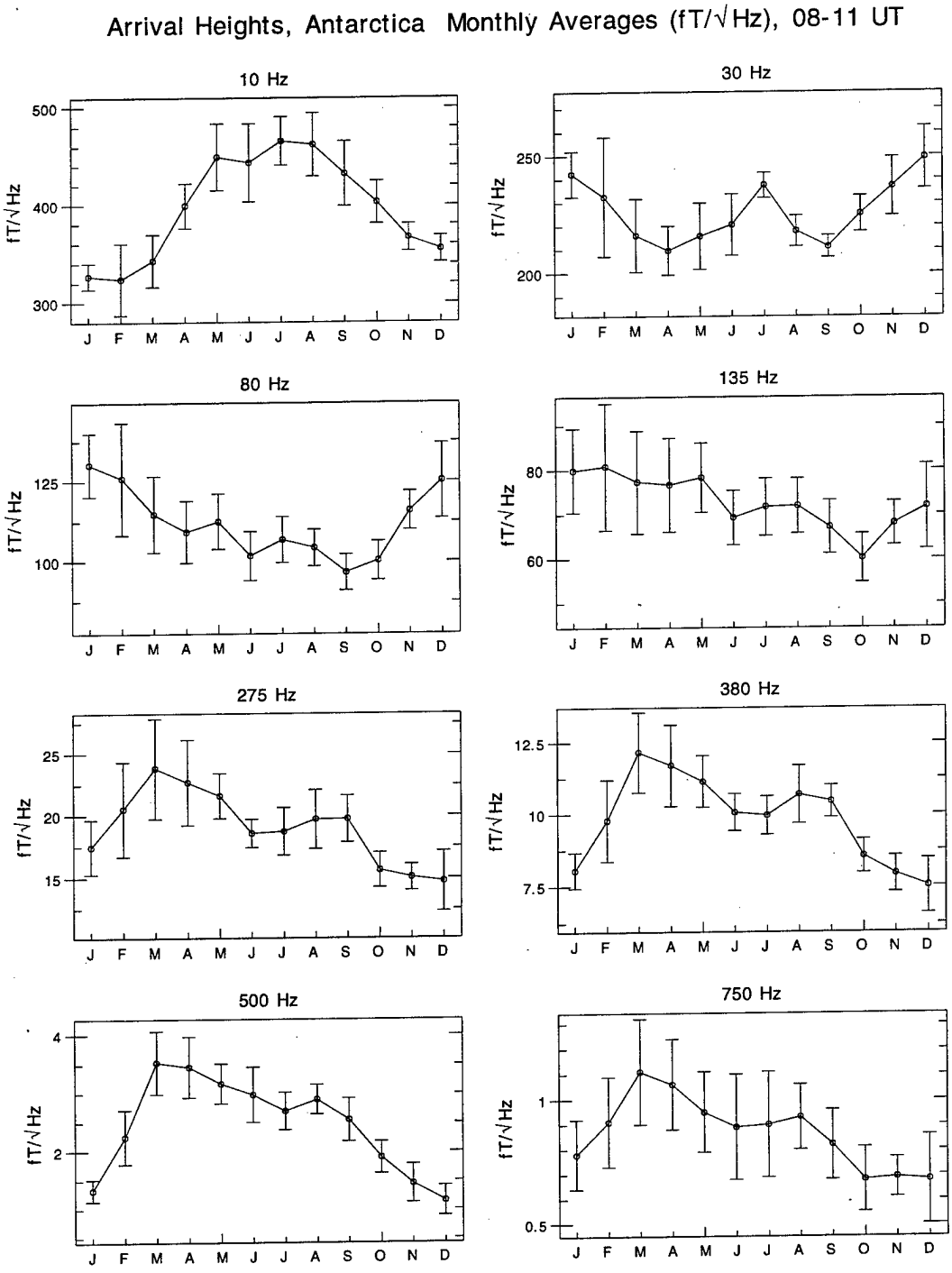

Figure 14: Monthly variation of ELF/VLF radio noise at Arrival Heights, Antarctica, for the eight lowest-frequency channels and the 08-12 UT time block. The years 1985 to 1994 are included.

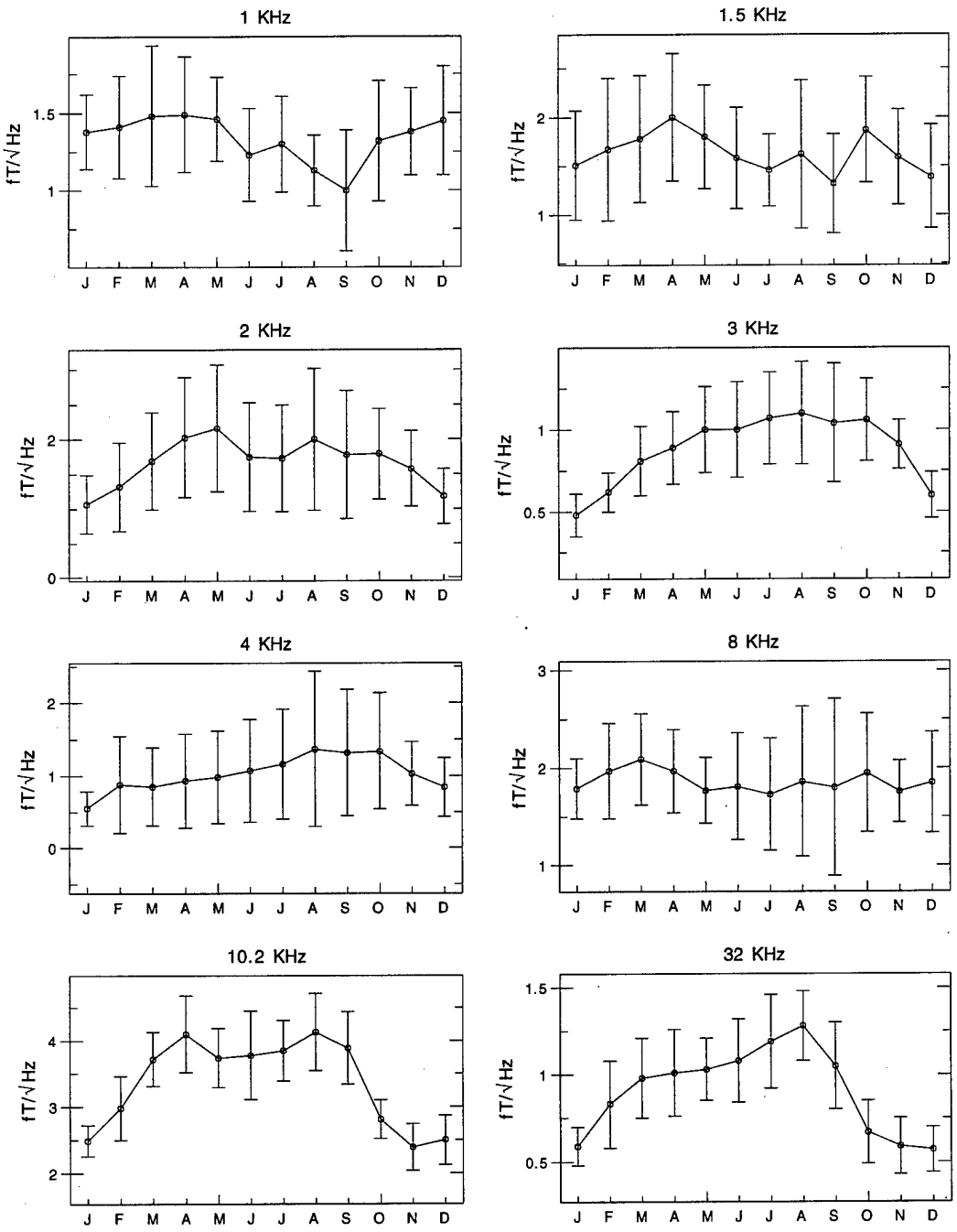

Figure 15: Monthly variation of ELF/VLF radio noise at Arrival Heights, Antarctica, for the eight highest-frequency channels and the 08-12 UT time block. The years 1985 to 1994 are included.

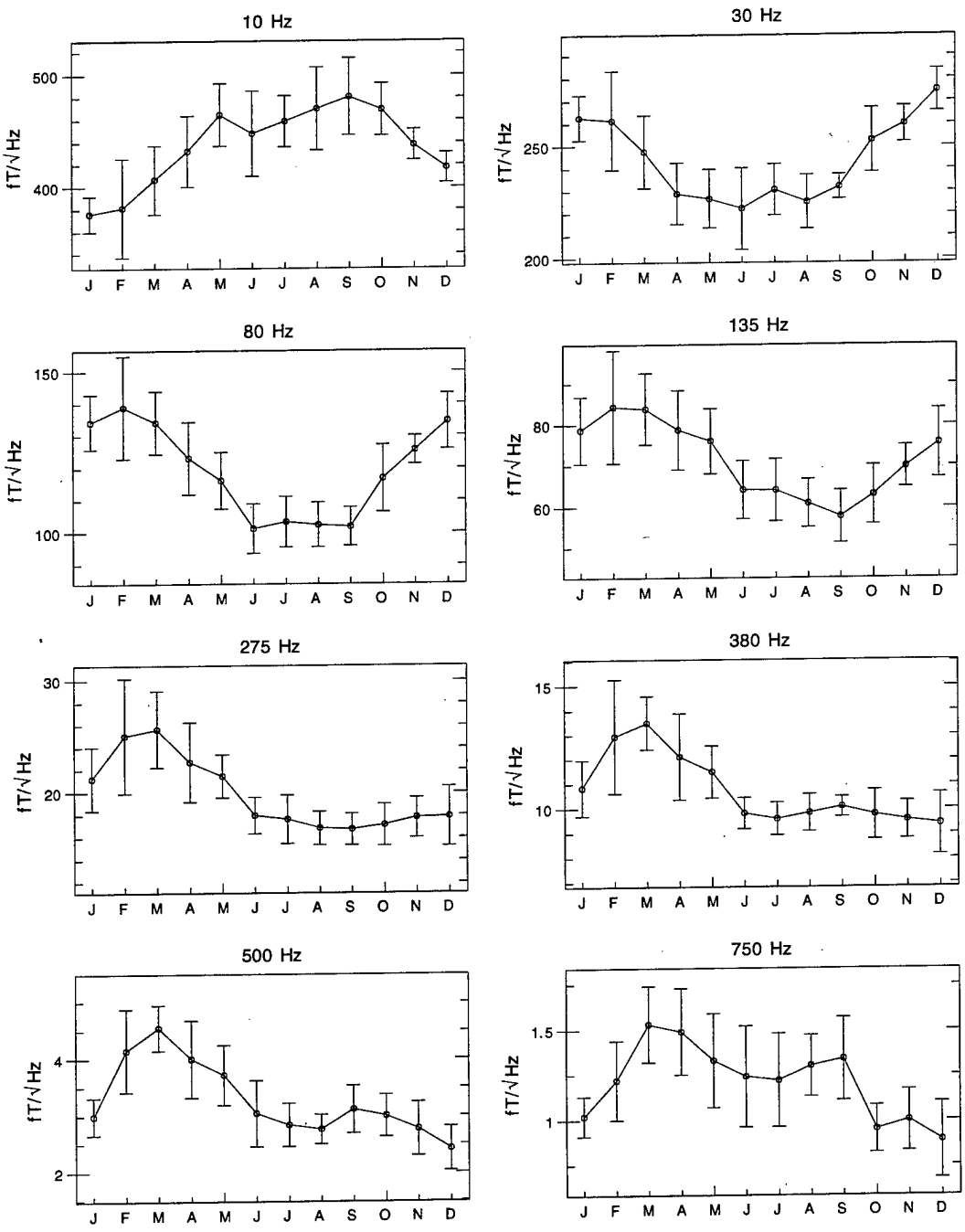

Figure 16: Monthly variation of ELF/VLF radio noise at Arrival Heights, Antarctica, for the eight lowest-frequency channels and the 12-16 UT time block. The years 1985 to 1994 are included.

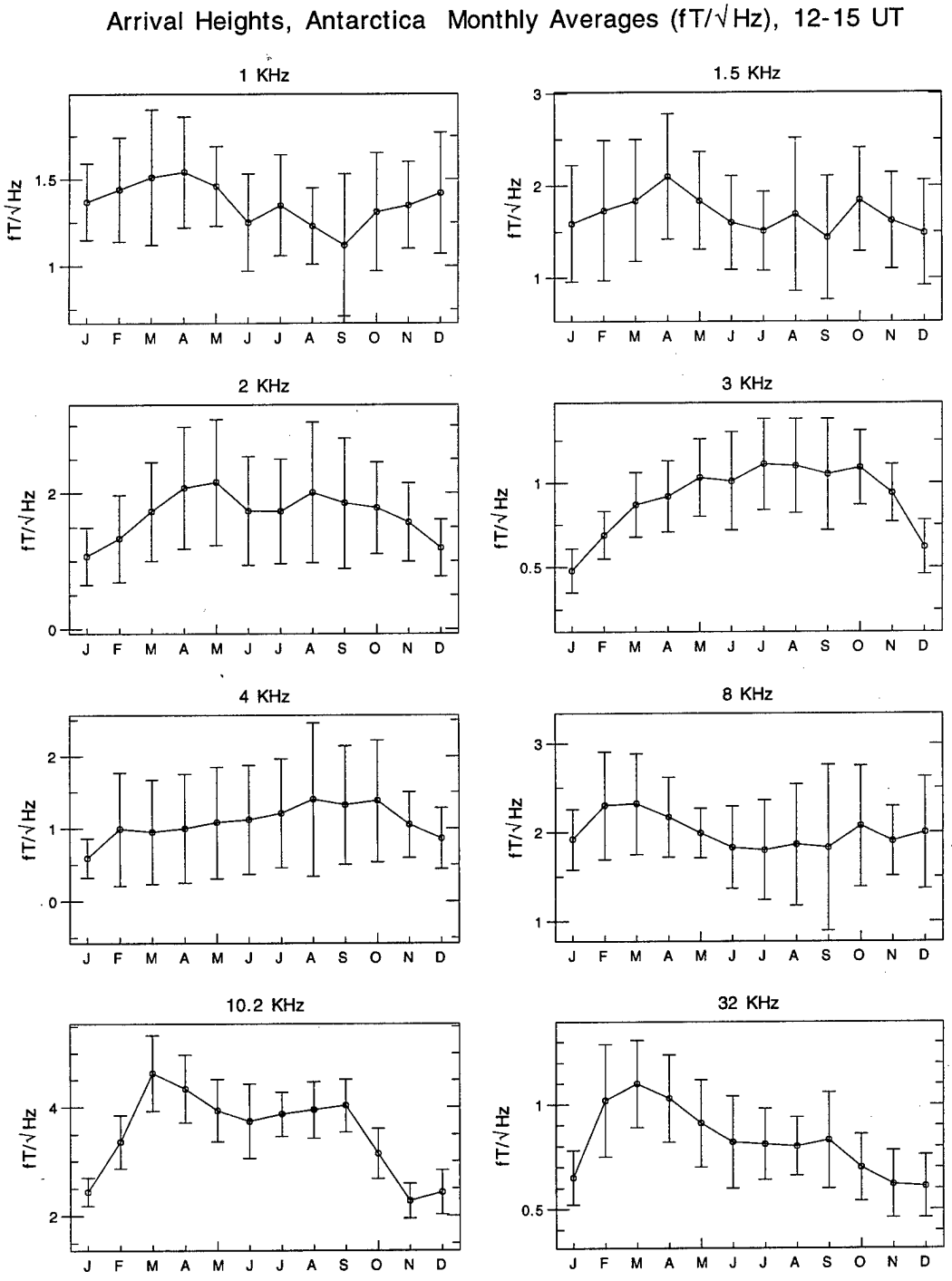

Figure 17: Monthly variation of ELF/VLF radio noise at Arrival Heights, Antarctica, for the eight highest-frequency channels and the 12-16 UT time block. The years 1985 to 1994 are included.

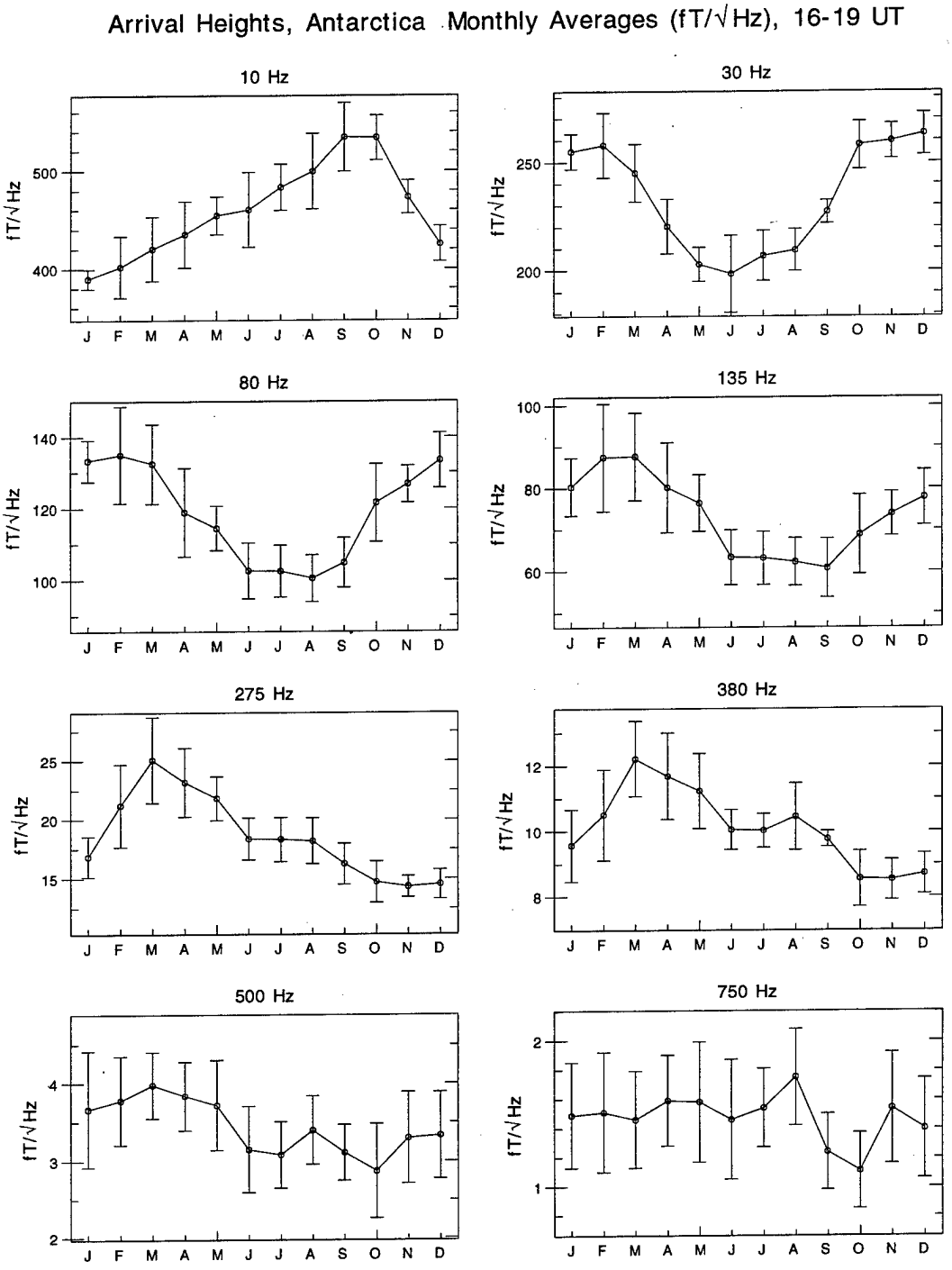

Figure 18: Monthly variation of ELF/VLF radio noise at Arrival Heights, Antarctica, for the eight lowest-frequency channels and the 16-20 UT time block. The years 1985 to 1994 are included.

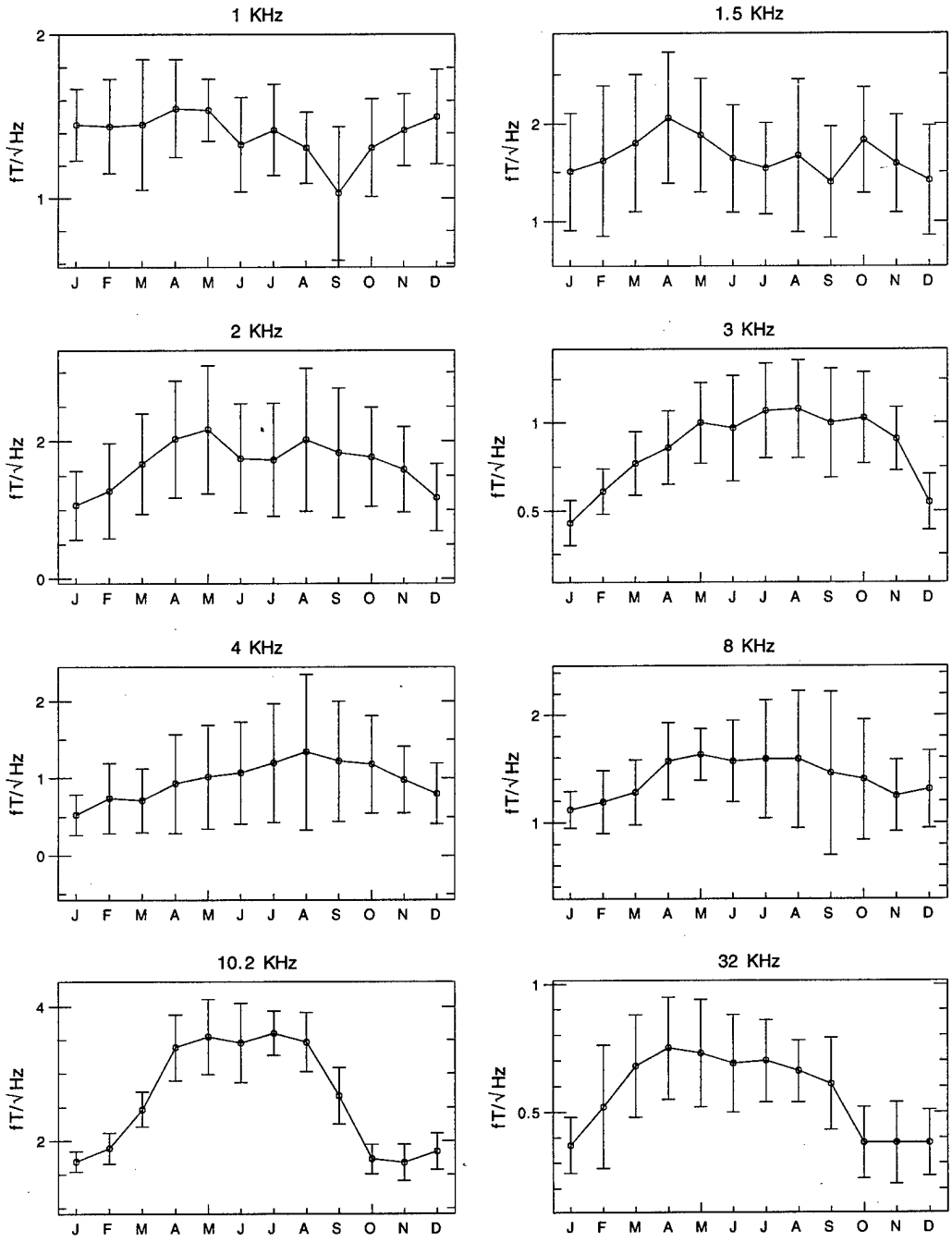

Figure 19: Monthly variation of ELF/VLF radio noise at Arrival Heights, Antarctica, for the eight highest-frequency channels and the 16-20 UT time block. The years 1985 to 1994 are included.

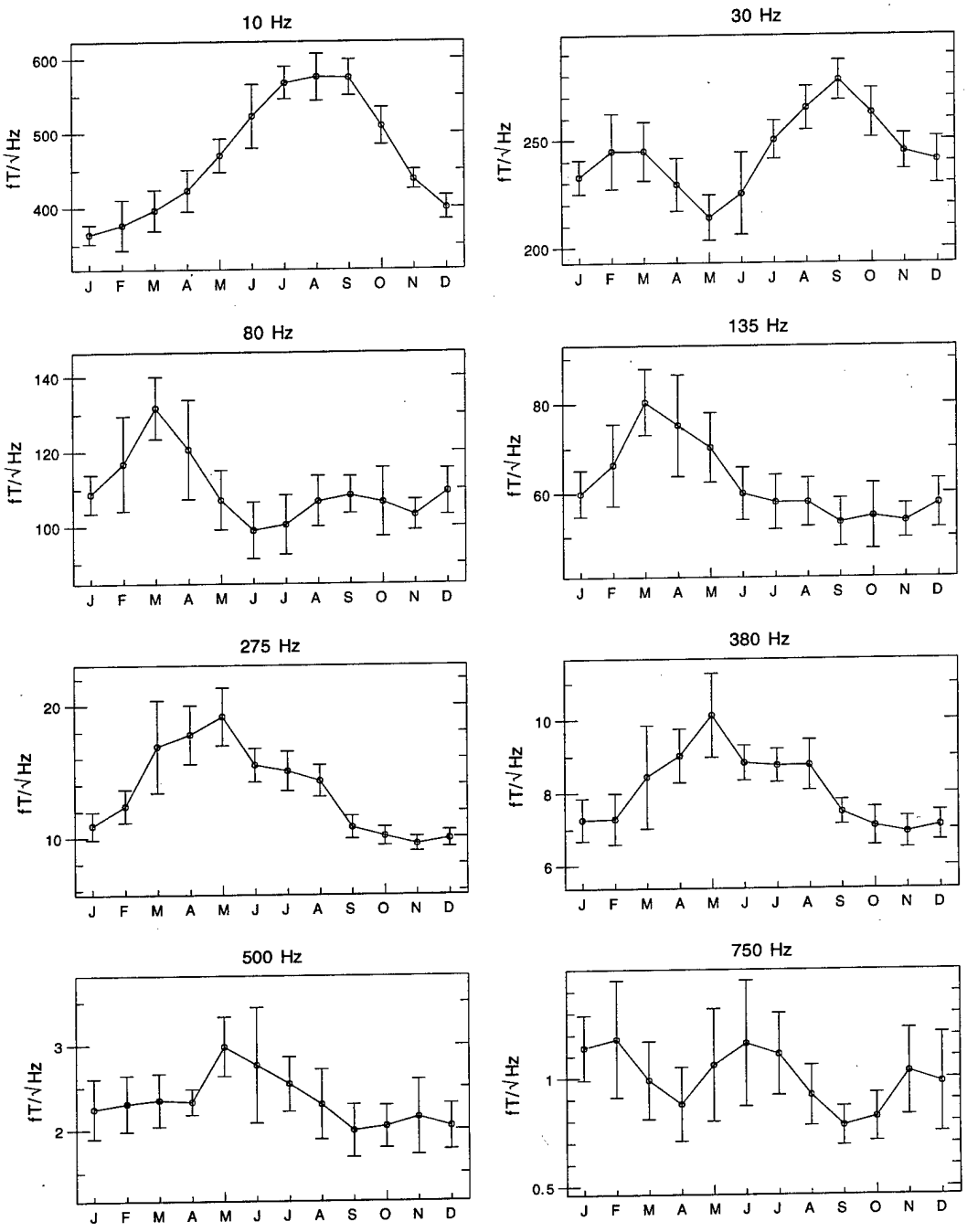

Figure 20: Monthly variation of ELF/VLF radio noise at Arrival Heights, Antarctica, for the eight lowest-frequency channels and the 20-24 UT time block. The years 1985 to 1994 are included.

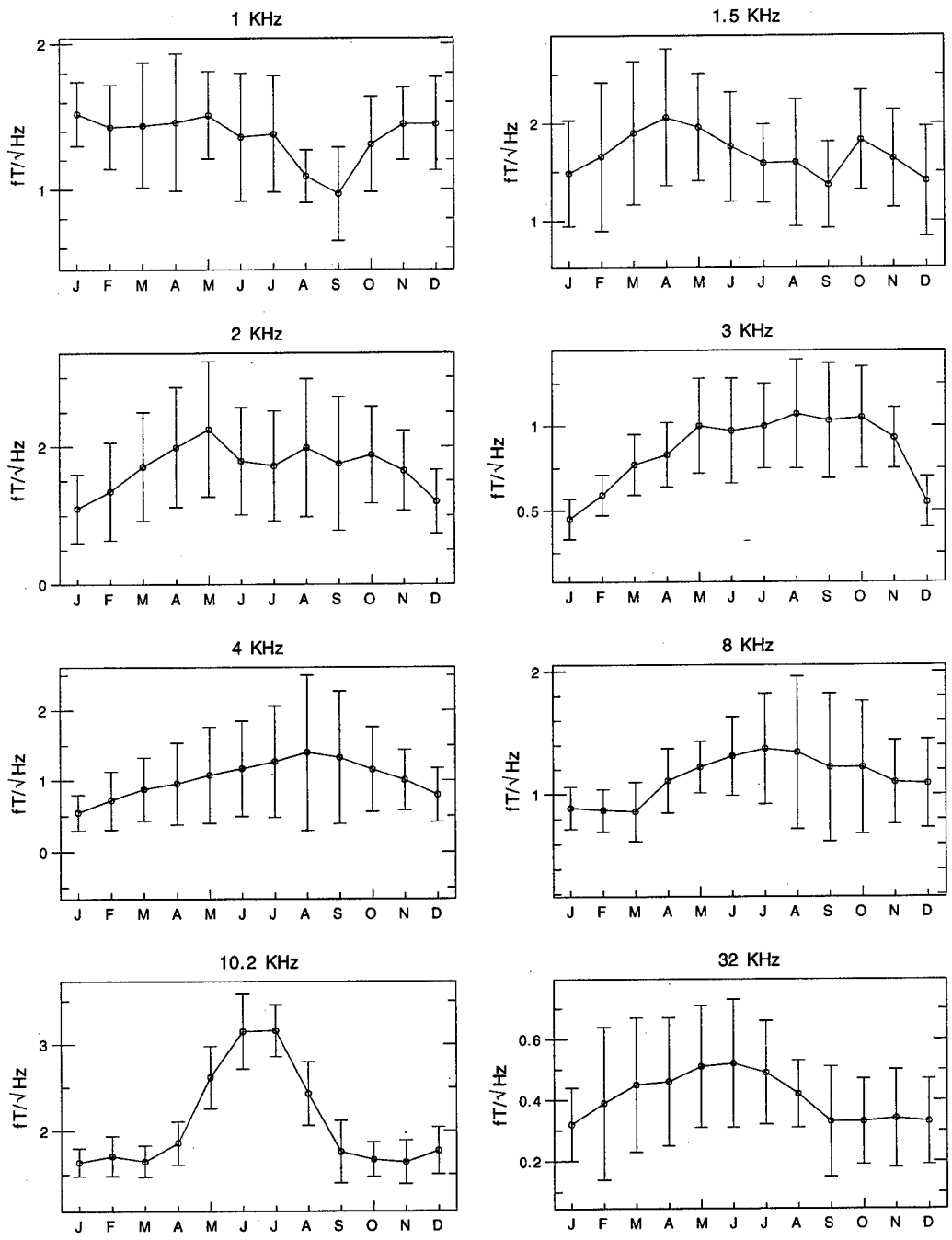

Figure 21: Monthly variation of ELF/VLF radio noise at Arrival Heights, Antarctica, for the eight highest-frequency channels and the 20-24 UT time block. The years 1985 to 1994 are included.

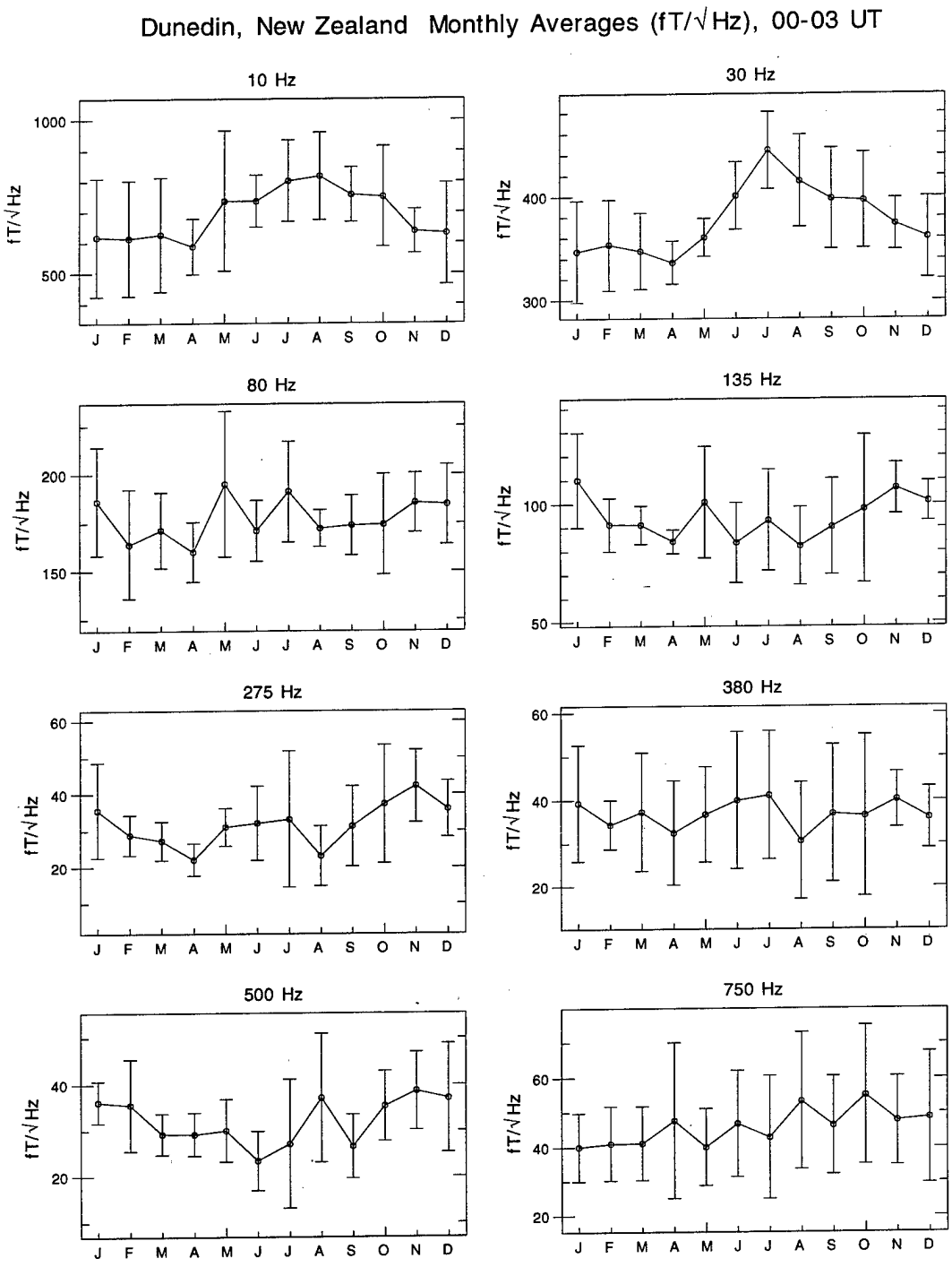

Figure 22: Monthly variation of ELF/VLF radio noise at Dunedin, New Zealand, for the eight lowest-frequency channels and the 00-04 UT time block. The years 1986 to 1990 are included.

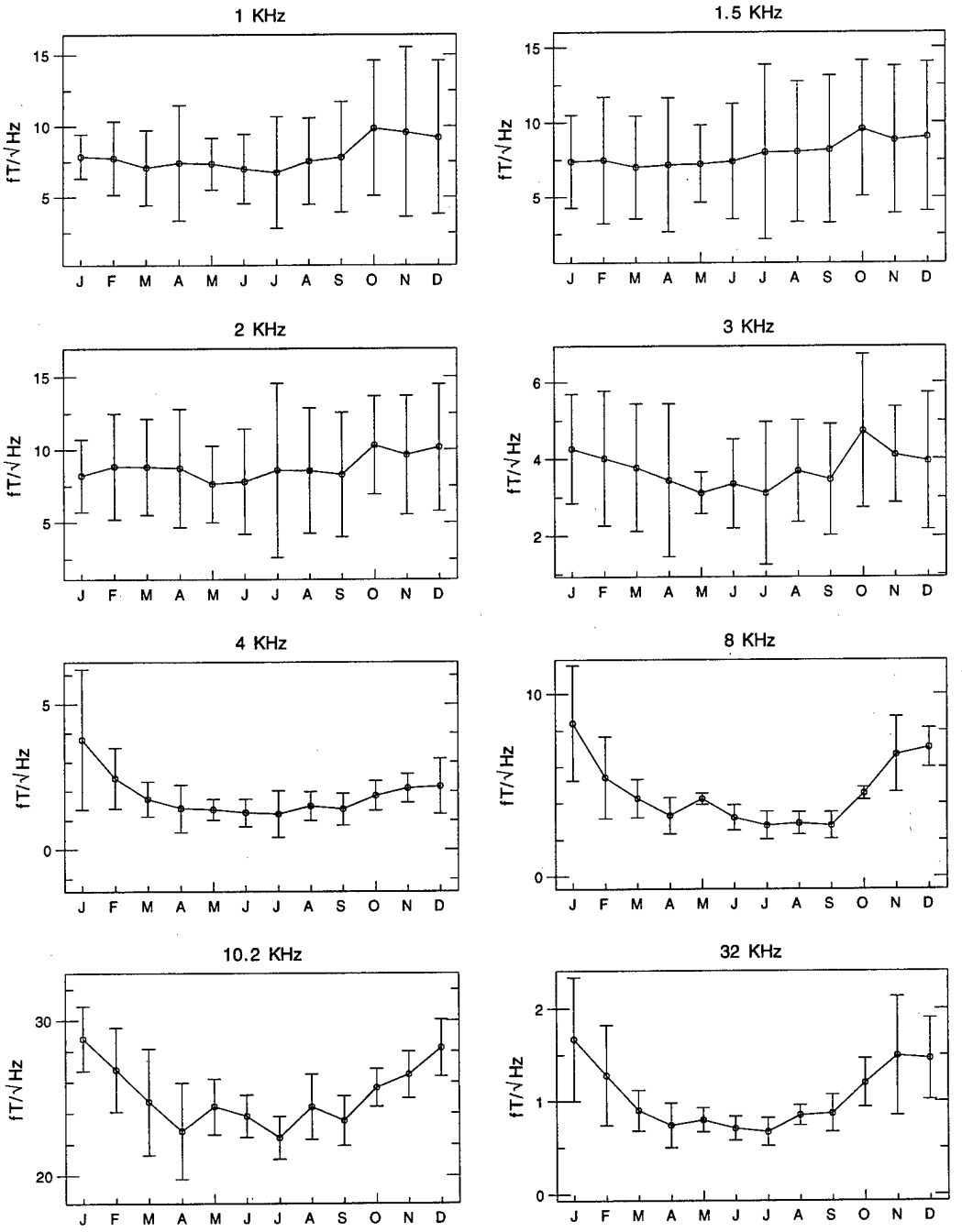

Figure 23: Monthly variation of ELF/VLF radio noise at Dunedin, New Zealand, for the eight highest-frequency channels and the 00-04 UT time block. The years 1986 to 1990 are included.

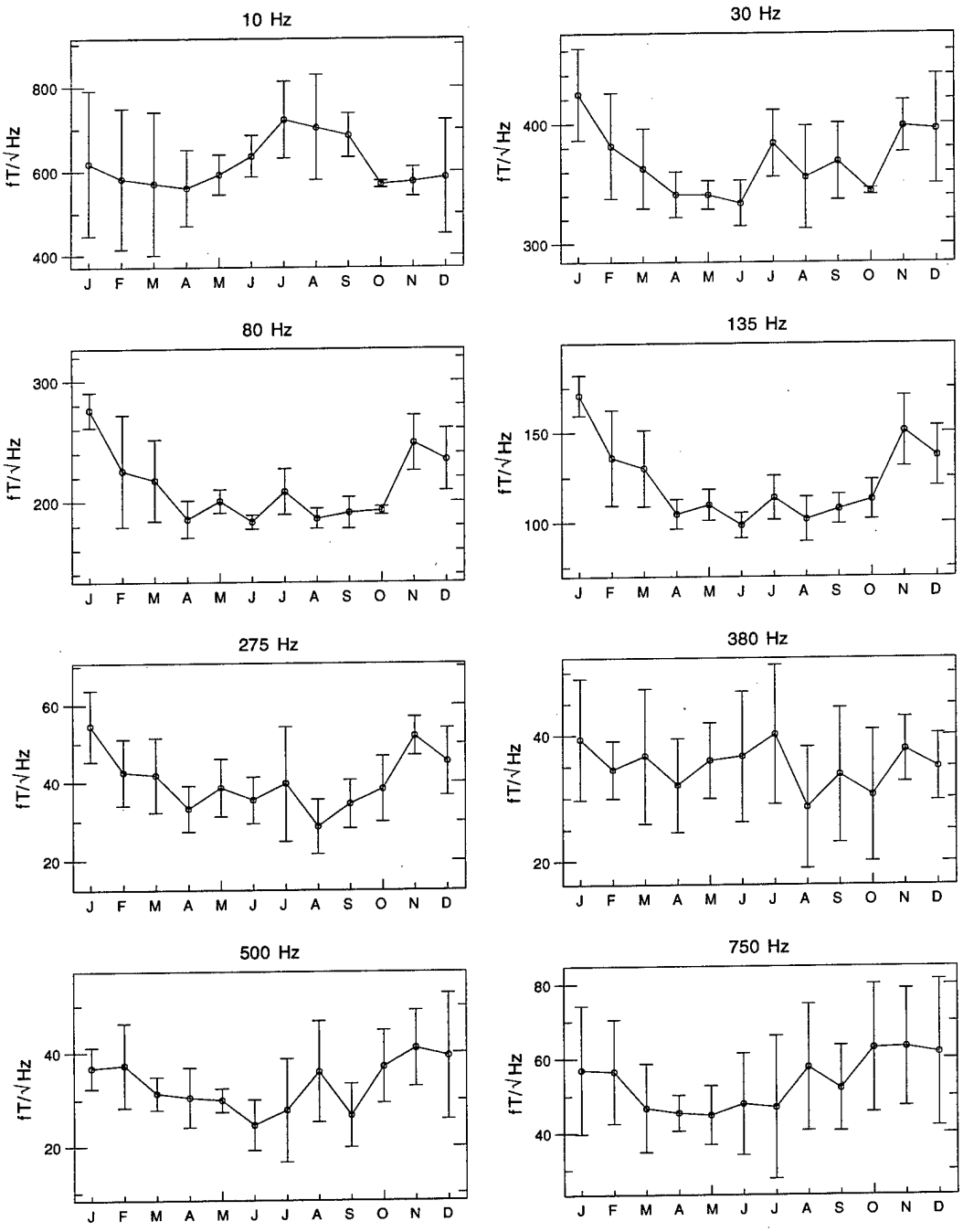

Figure 24: Monthly variation of ELF/VLF radio noise at Dunedin, New Zealand, for the eight lowest-frequency channels and the 04-08 UT time block. The years 1986 to 1990 are included.

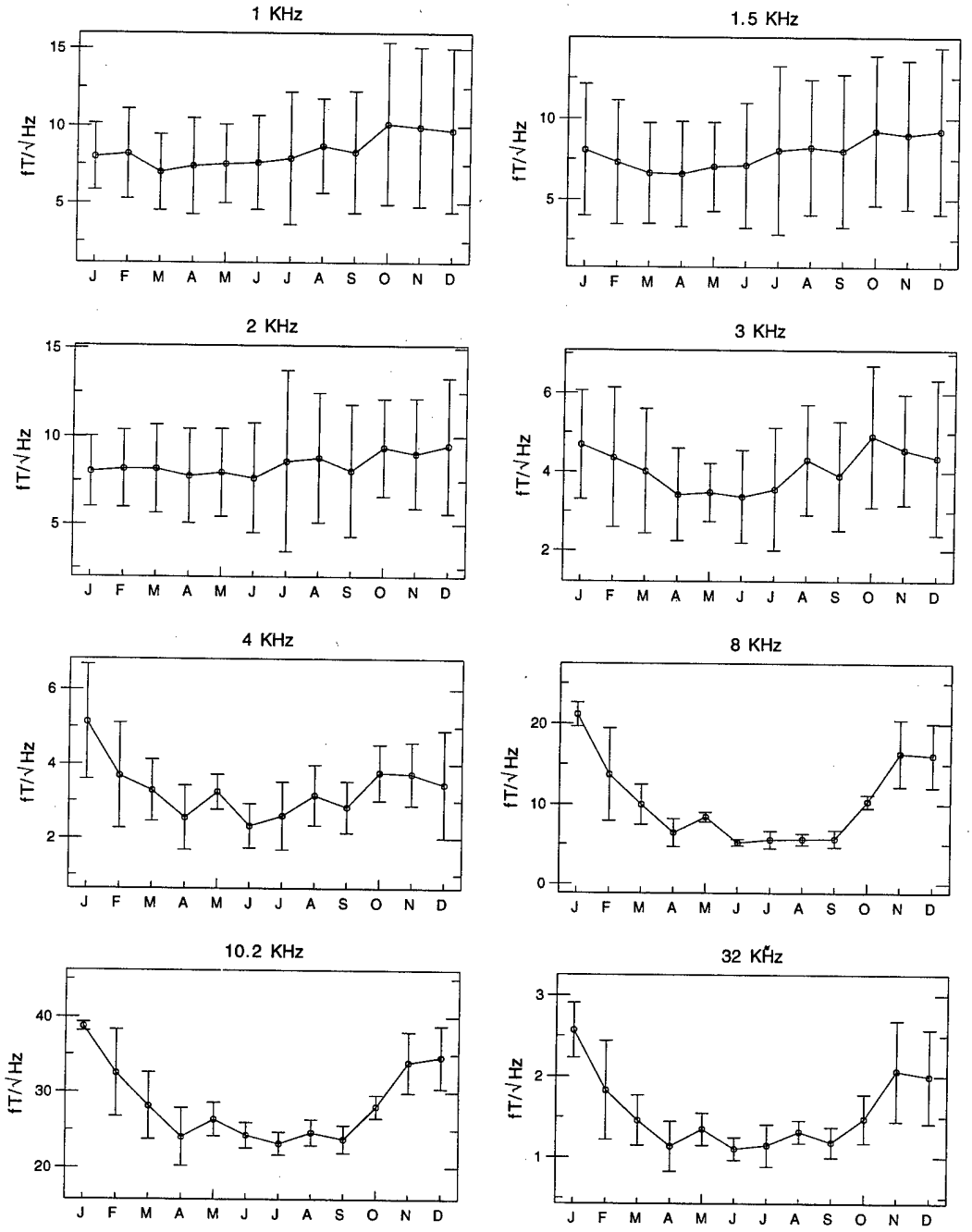

Figure 25: Monthly variation of ELF/VLF radio noise at Dunedin, New Zealand, for the eight highest-frequency channels and the 04-08 UT time block. The years 1986 to 1990 are included.

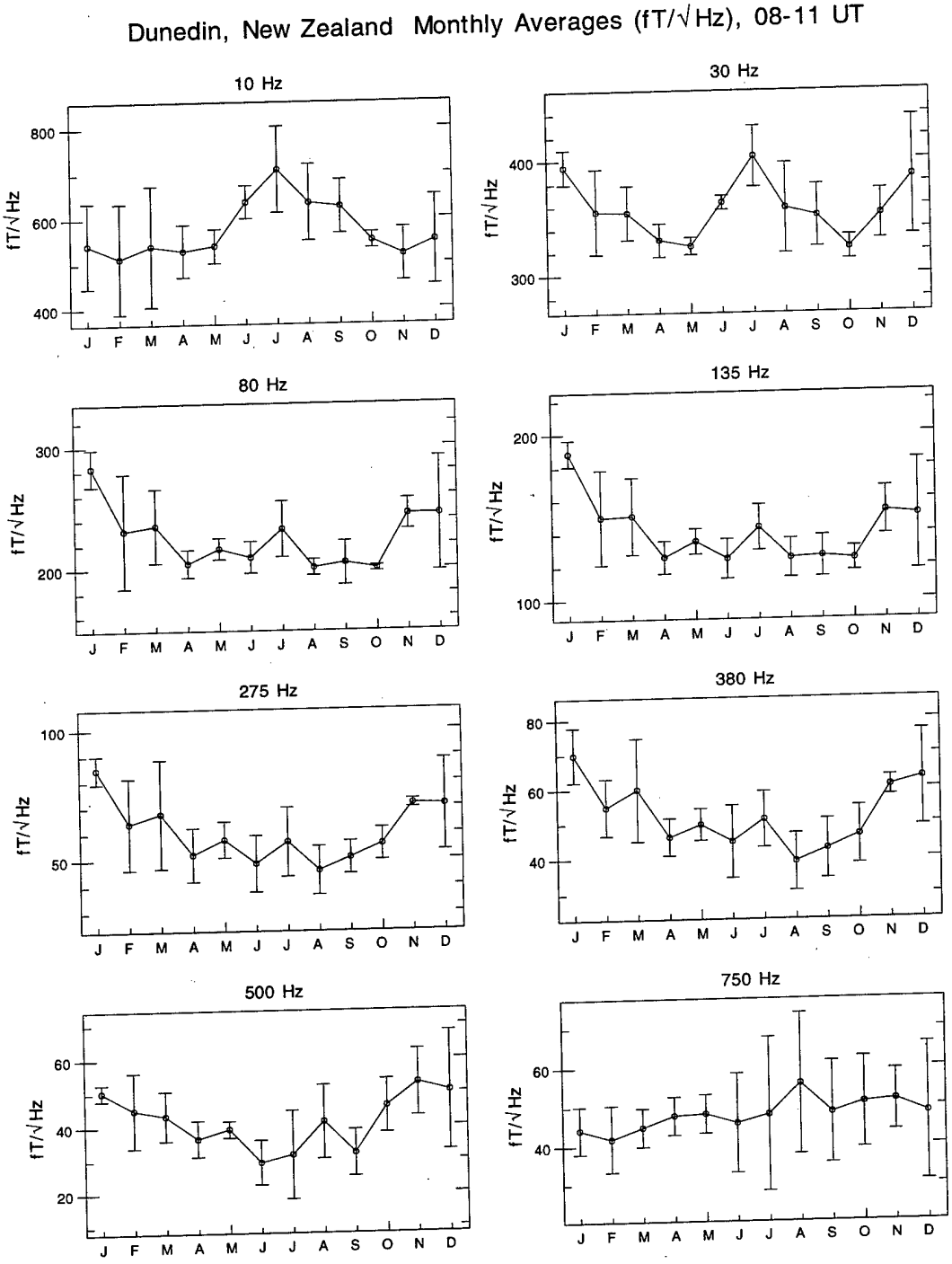

Figure 26: Monthly variation of ELF/VLF radio noise at Dunedin, New Zealand, for the eight lowest-frequency channels and the 08-12 UT time block. The years 1986 to 1990 are included.

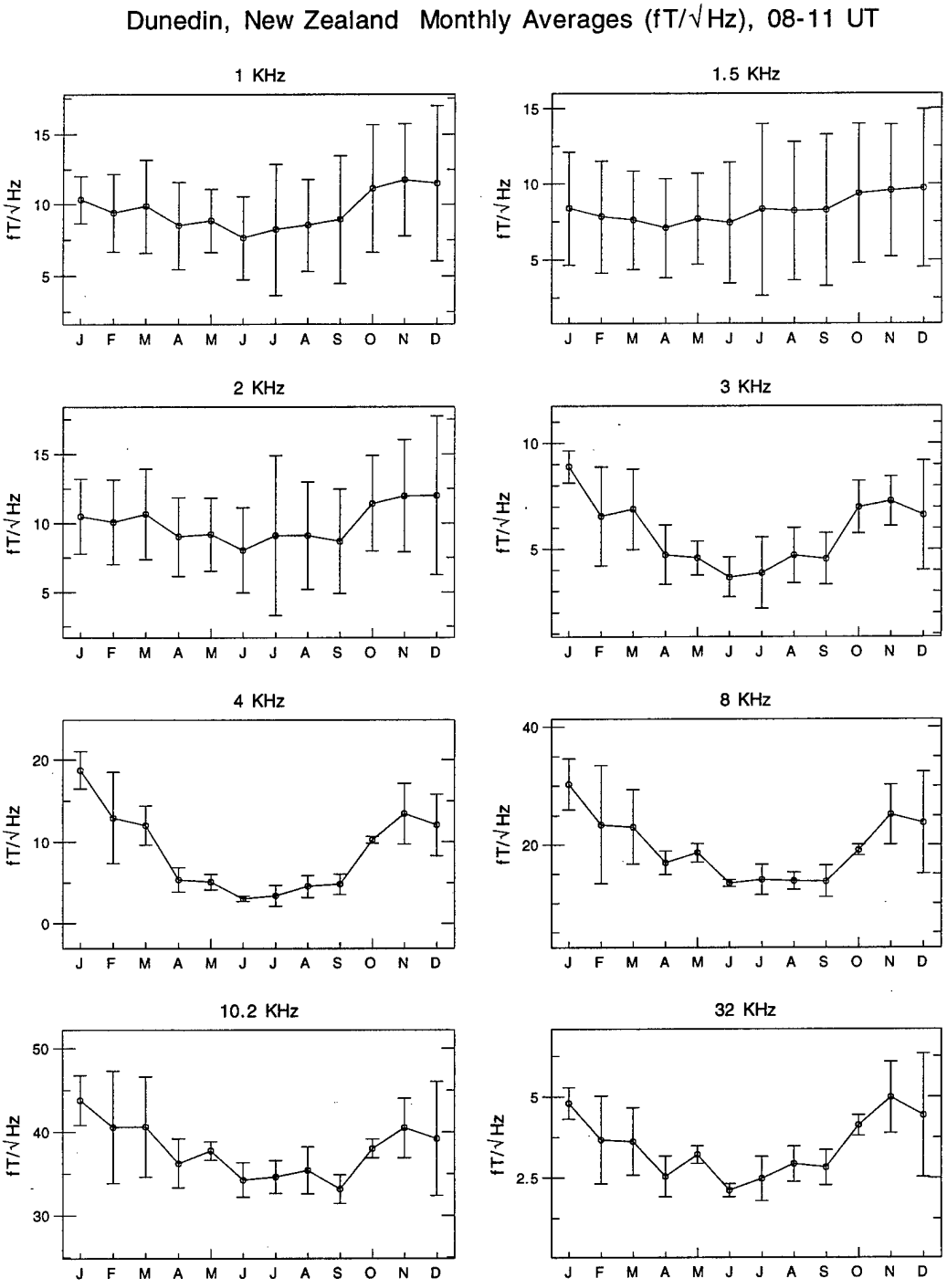

Figure 27: Monthly variation of ELF/VLF radio noise at Dunedin, New Zealand, for the eight highest-frequency channels and the 08-12 UT time block. The years 1986 to 1990 are included.

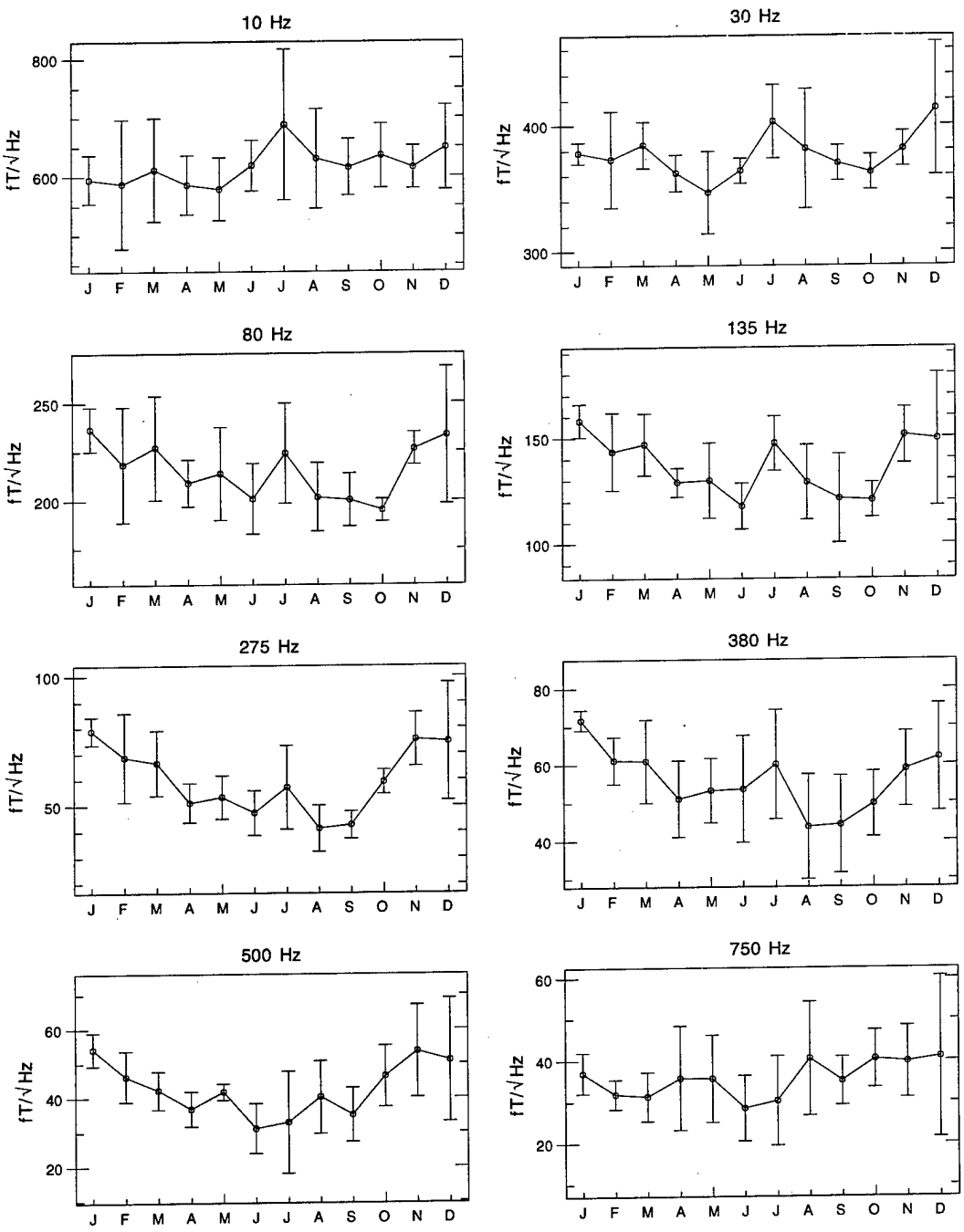

Figure 28: Monthly variation of ELF/VLF radio noise at Dunedin, New Zealand, for the eight lowest-frequency channels and the 12-16 UT time block. The years 1986 to 1990 are included.

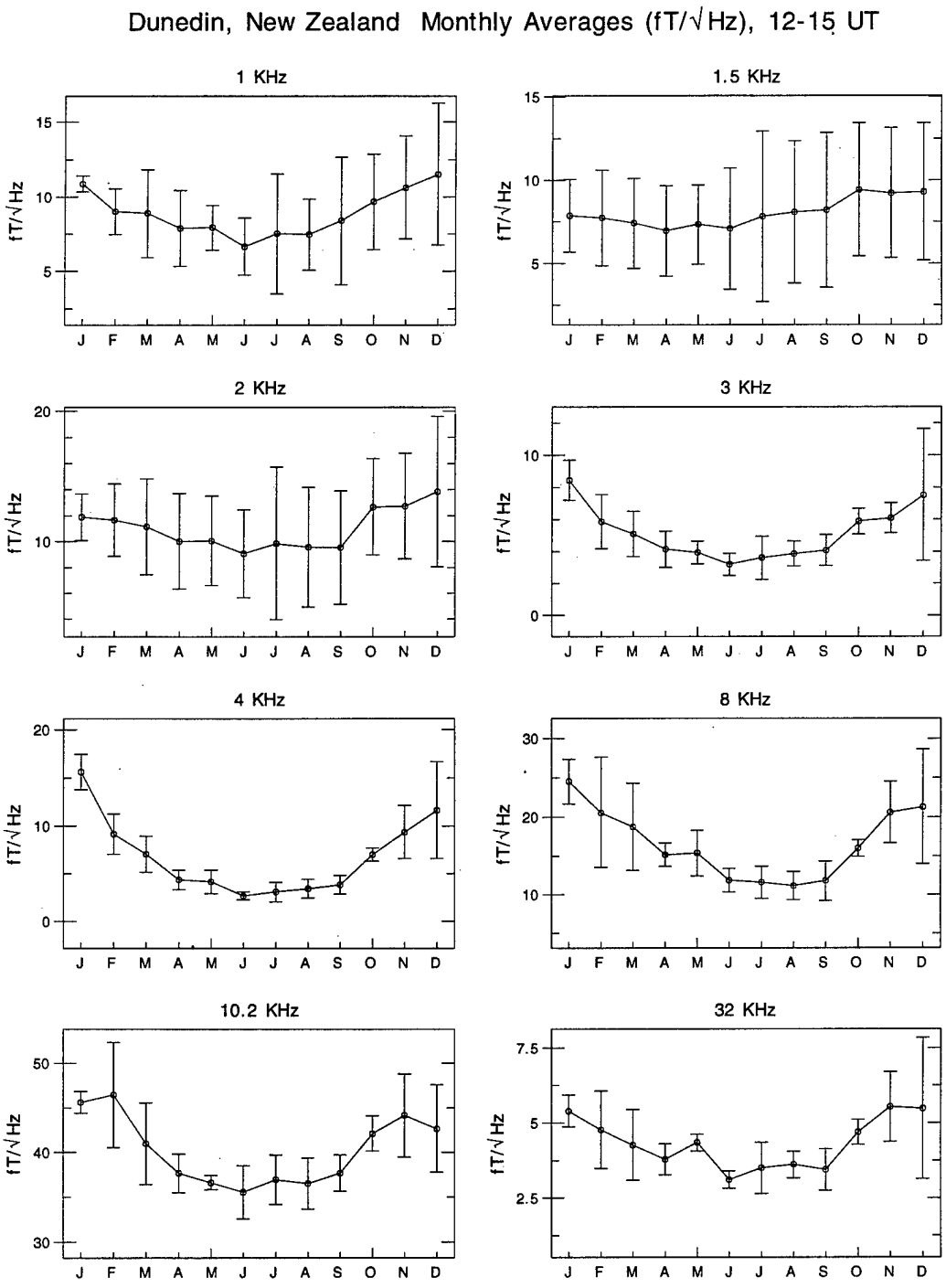

Figure 29: Monthly variation of ELF/VLF radio noise at Dunedin, New Zealand, for the eight highest-frequency channels and the 12-16 UT time block. The years 1986 to 1990 are included.

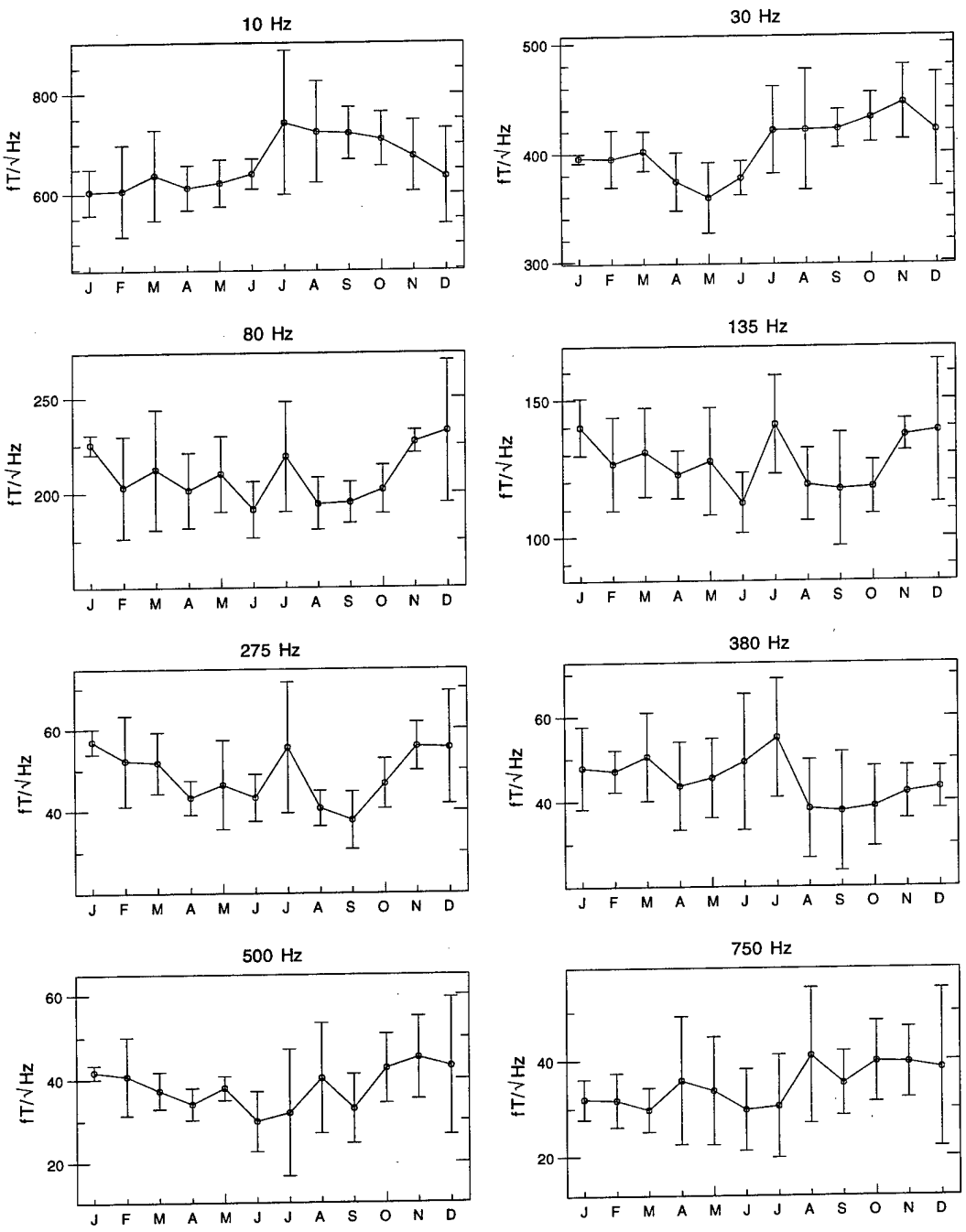

Figure 30: Monthly variation of ELF/VLF radio noise at Dunedin, New Zealand, for the eight lowest-frequency channels and the 16-20 UT time block. The years 1986 to 1990 are included.

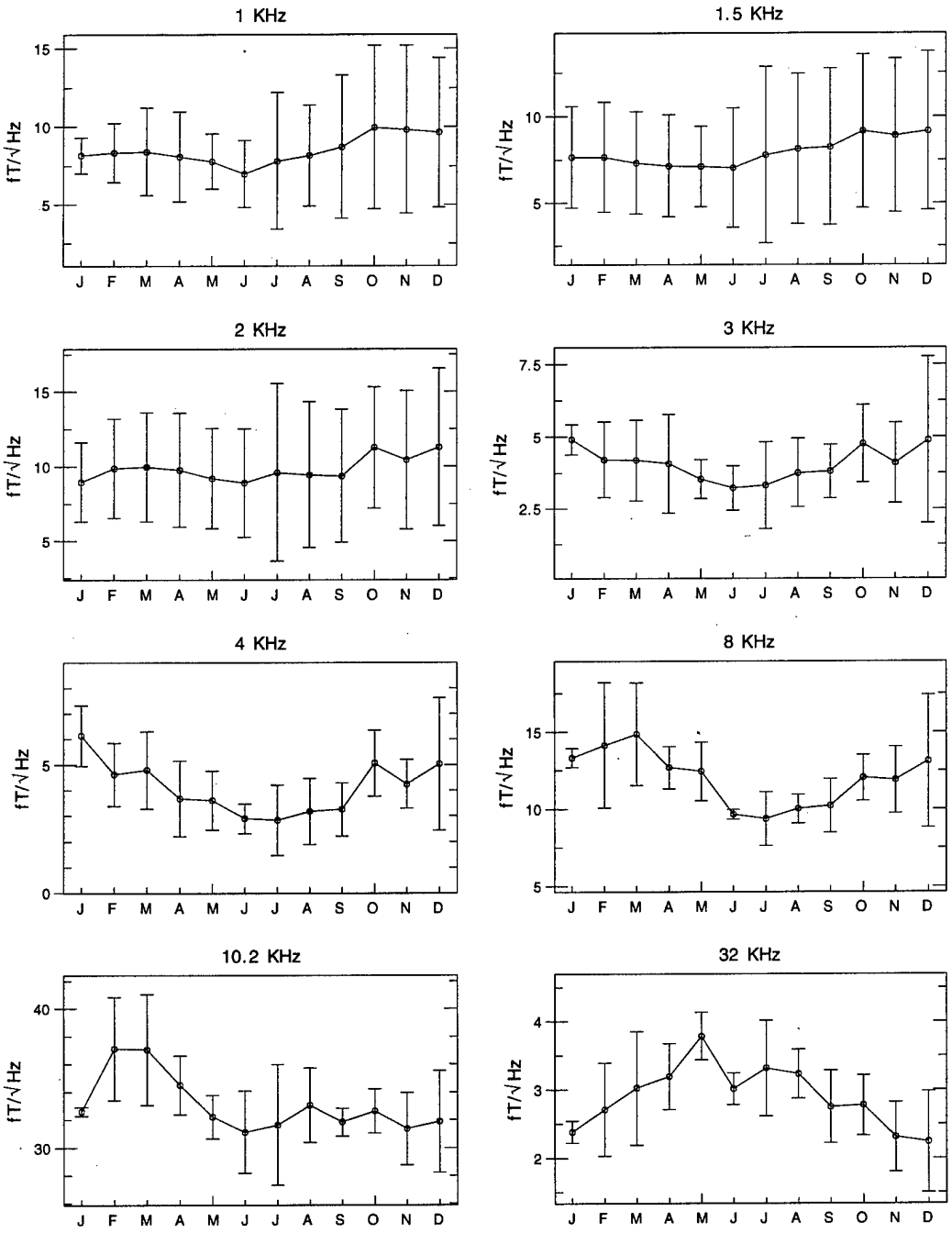

Figure 31: Monthly variation of ELF/VLF radio noise at Dunedin, New Zealand, for the eight highest-frequency channels and the 16-20 UT time block. The years 1986 to 1990 are included.

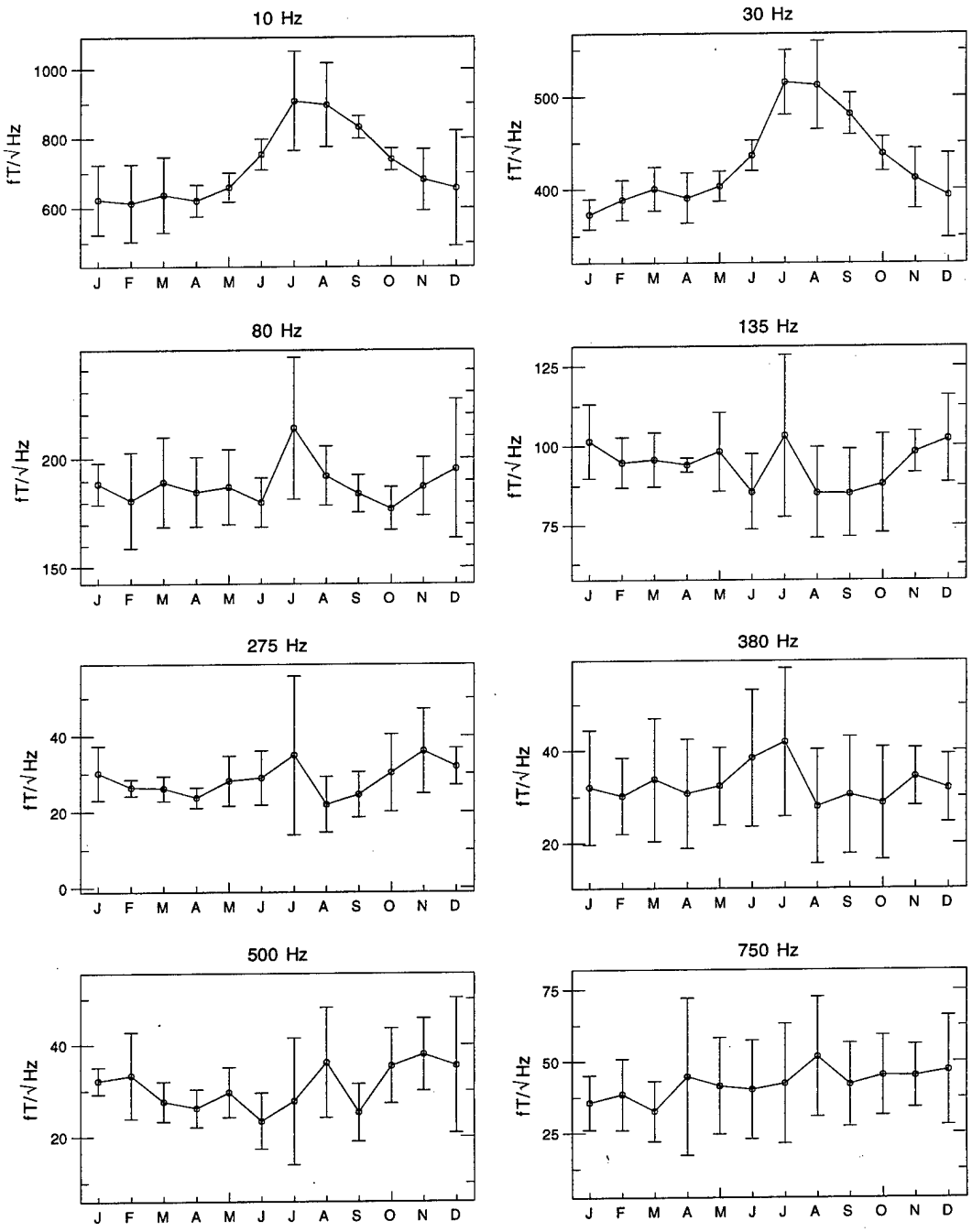

Figure 32: Monthly variation of ELF/VLF radio noise at Dunedin, New Zealand, for the eight lowest-frequency channels and the 20-24 UT time block. The years 1986 to 1990 are included.

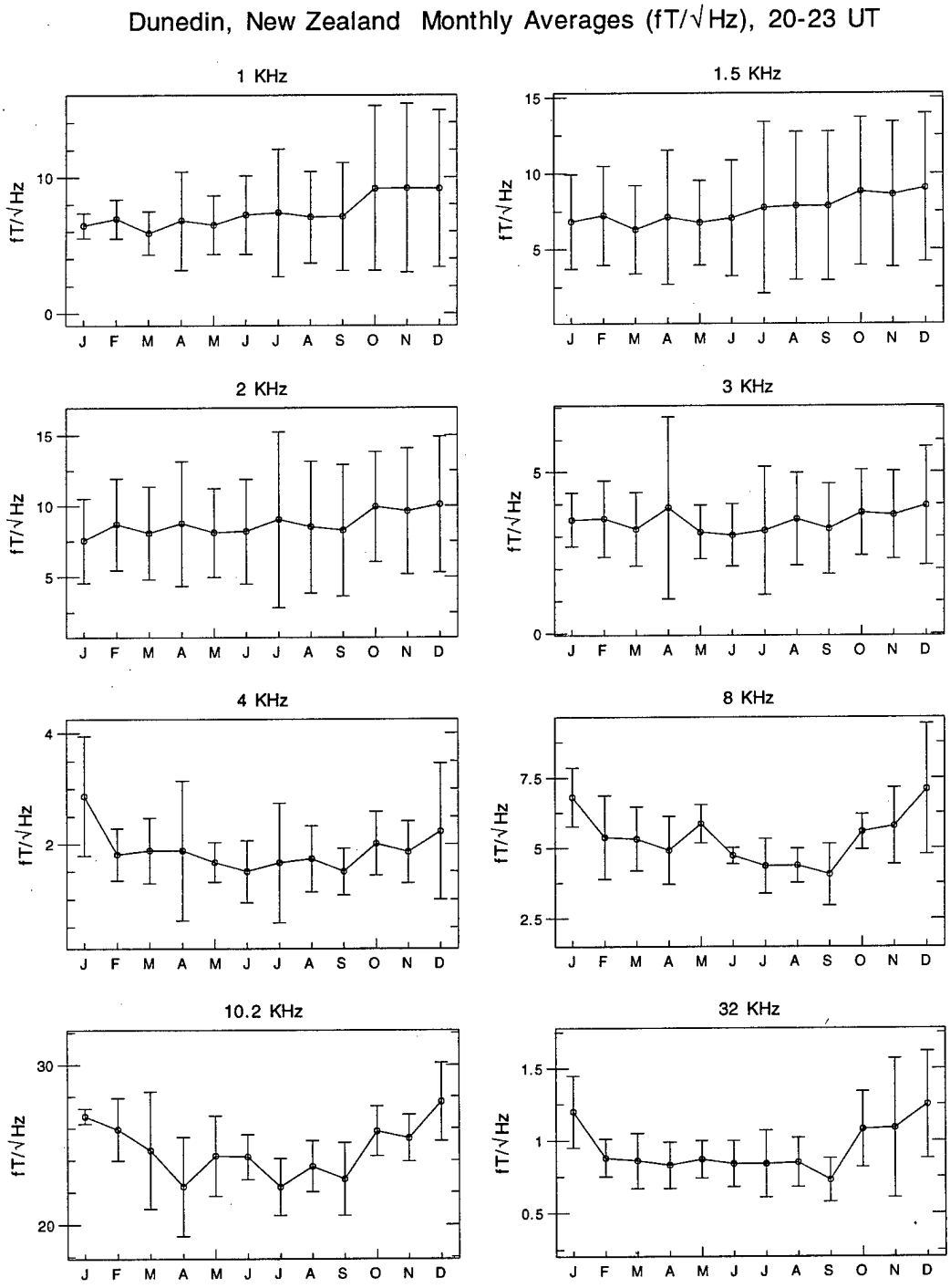

Figure 33: Monthly variation of ELF/VLF radio noise at Dunedin, New Zealand, for the eight highest-frequency channels and the 20-24 UT time block. The years 1986 to 1990 are included.

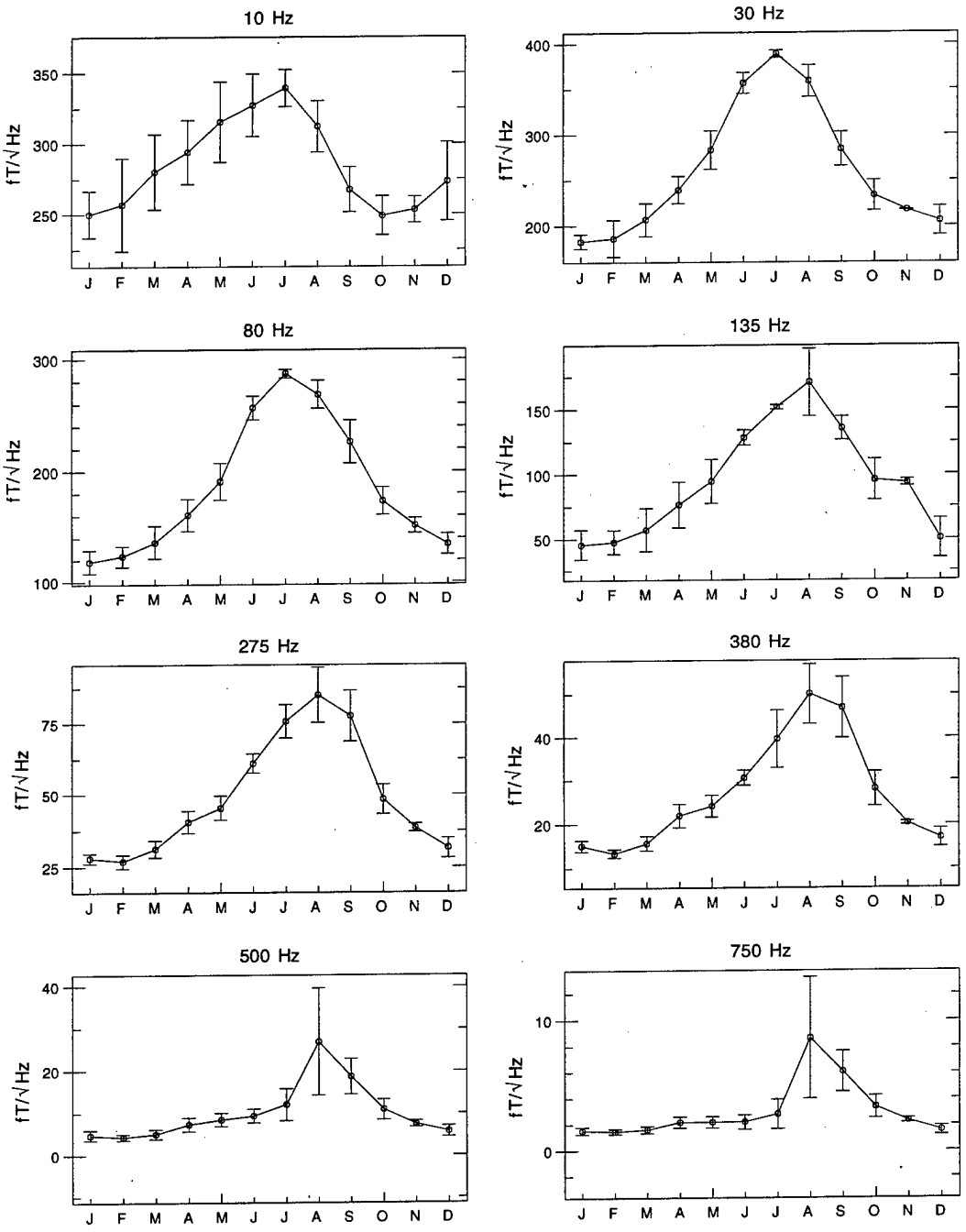

Figure 34: Monthly variation of ELF/VLF radio noise at Søndrestrøm, Greenland, for the eight lowest-frequency channels and the 00-04 UT time block. The years 1986 to 1991 and the year 1993 are included.

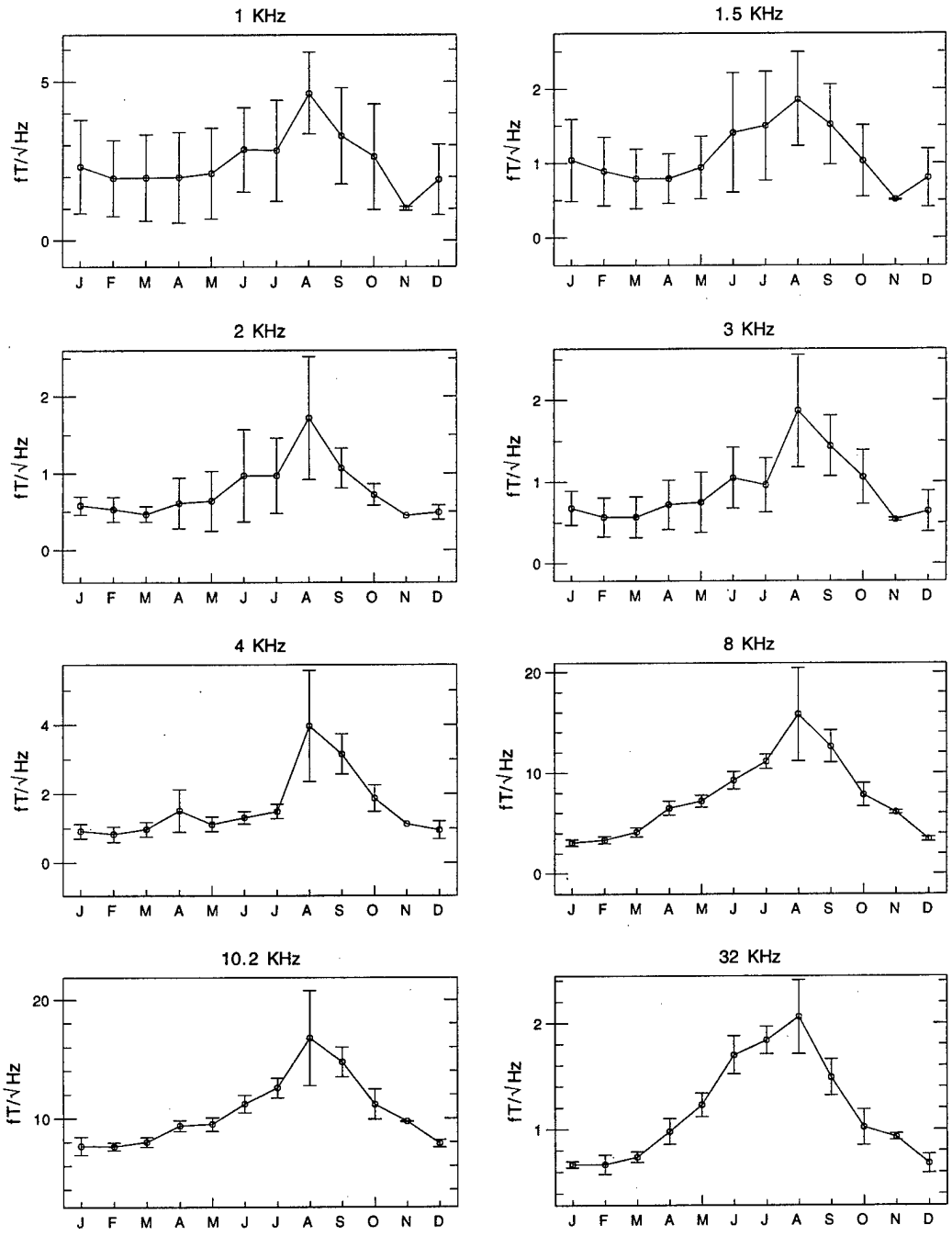

Figure 35: Monthly variation of ELF/VLF radio noise at Søndrestrøm, Greenland, for the eight highest-frequency channels and the 00-04 UT time block. The years 1986 to 1991 and the year 1993 are included.

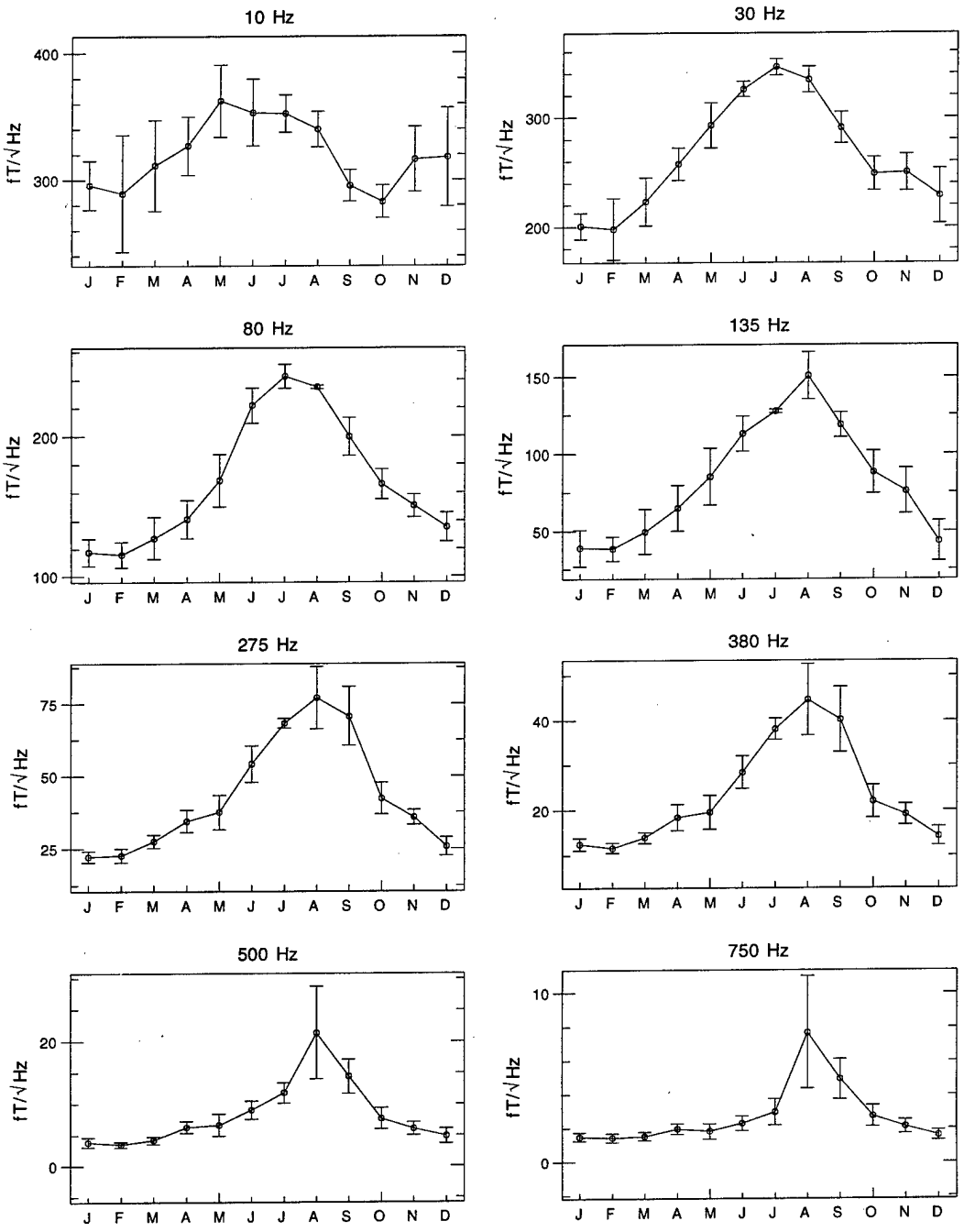

Figure 36: Monthly variation of ELF/VLF radio noise at Søndrestrøm, Greenland, for the eight lowest-frequency channels and the 04-08 UT time block. The years 1986 to 1991 and the year 1993 are included.

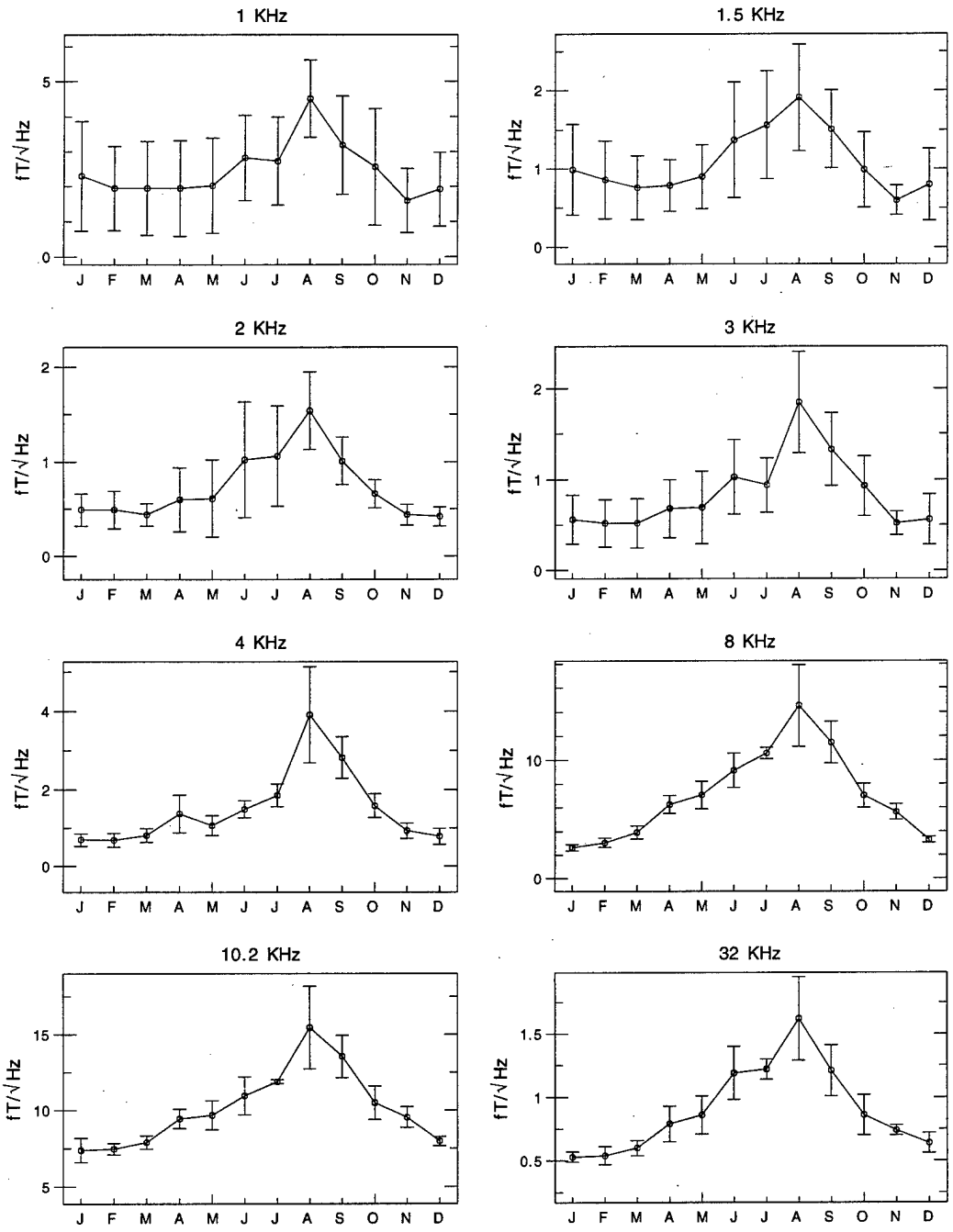

Figure 37: Monthly variation of ELF/VLF radio noise at Søndrestrøm, Greenland, for the eight highest-frequency channels and the 04-08 UT time block. The years 1986 to 1991 and the year 1993 are included.

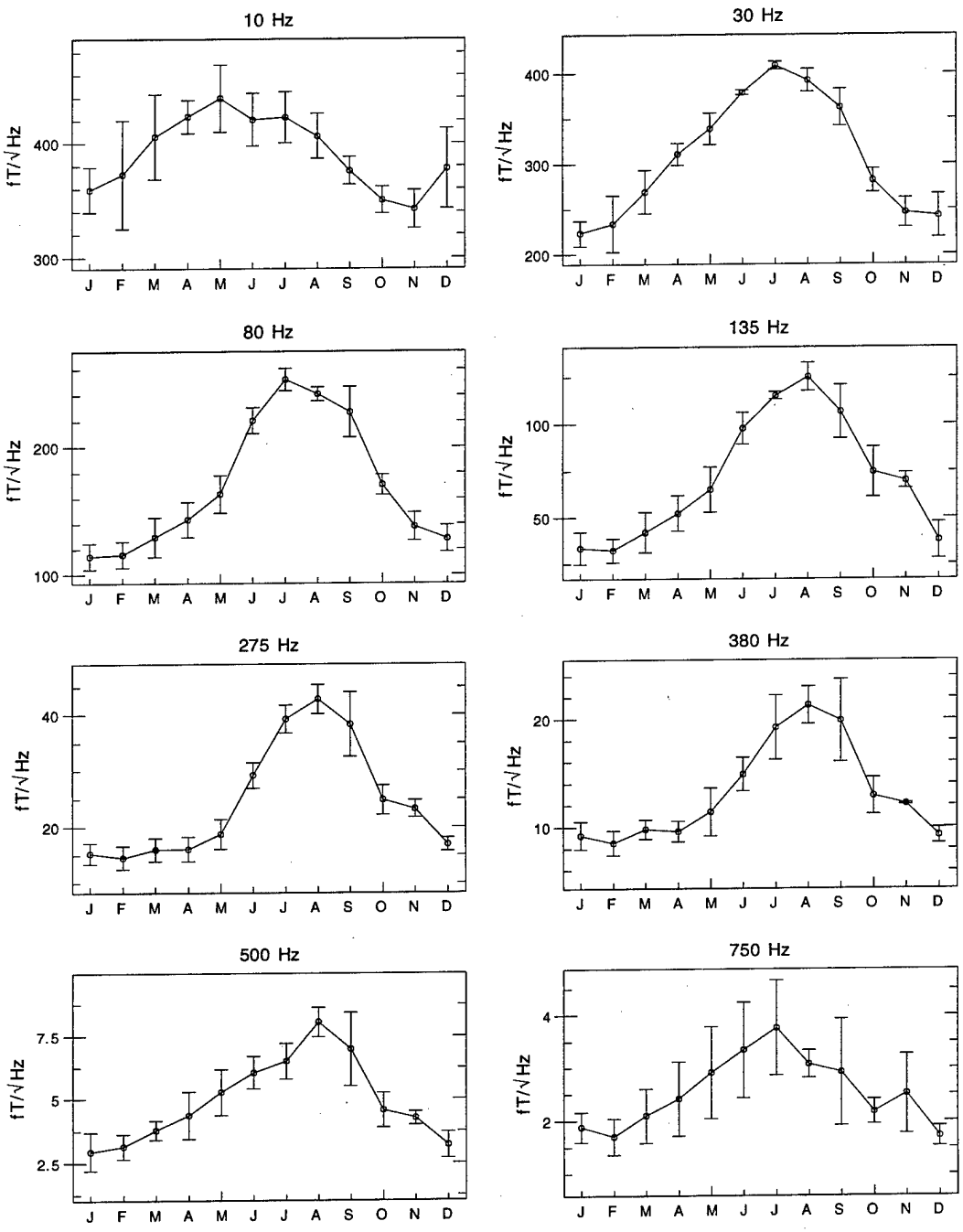

Figure 38: Monthly variation of ELF/VLF radio noise at Søndrestrøm, Greenland, for the eight lowest-frequency channels and the 08-12 UT time block. The years 1986 to 1991 and the year 1993 are included.

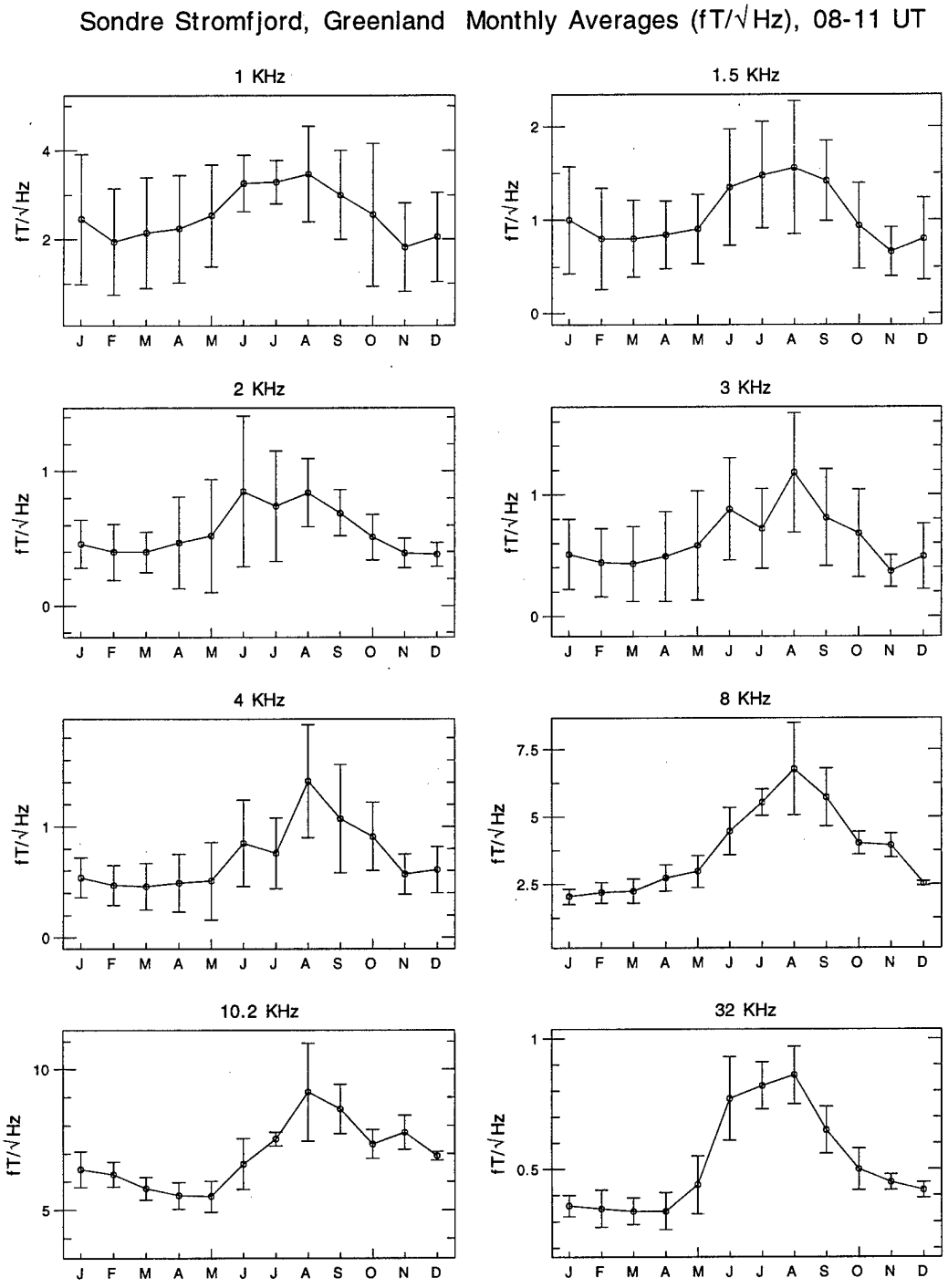

Figure 39: Monthly variation of ELF/VLF radio noise at Søndrestrøm, Greenland, for the eight highest-frequency channels and the 08-12 UT time block. The years 1986 to 1991 and the year 1993 are included.

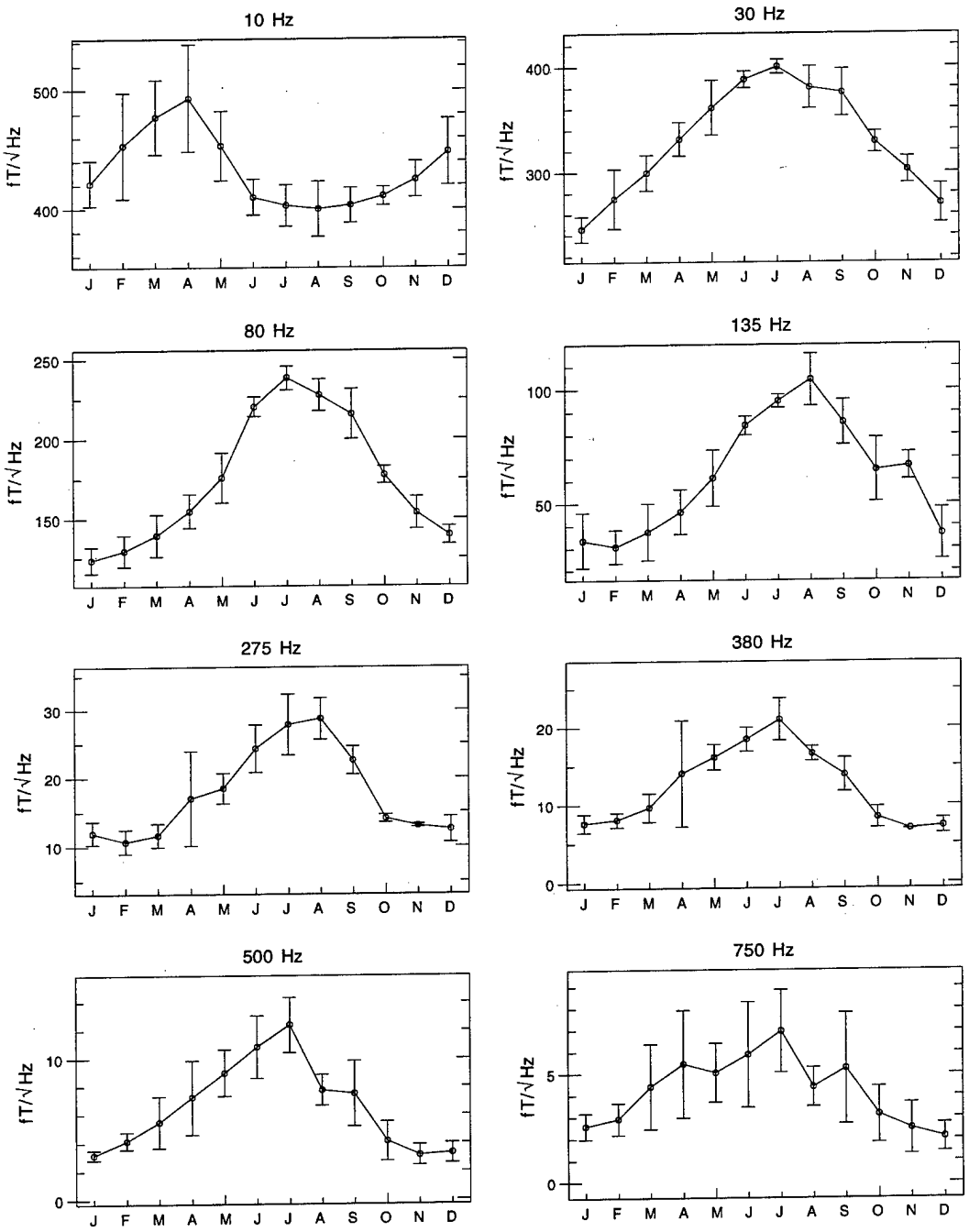

Figure 40: Monthly variation of ELF/VLF radio noise at Søndrestrøm, Greenland, for the eight lowest-frequency channels and the 12-16 UT time block. The years 1986 to 1991 and the year 1993 are included.

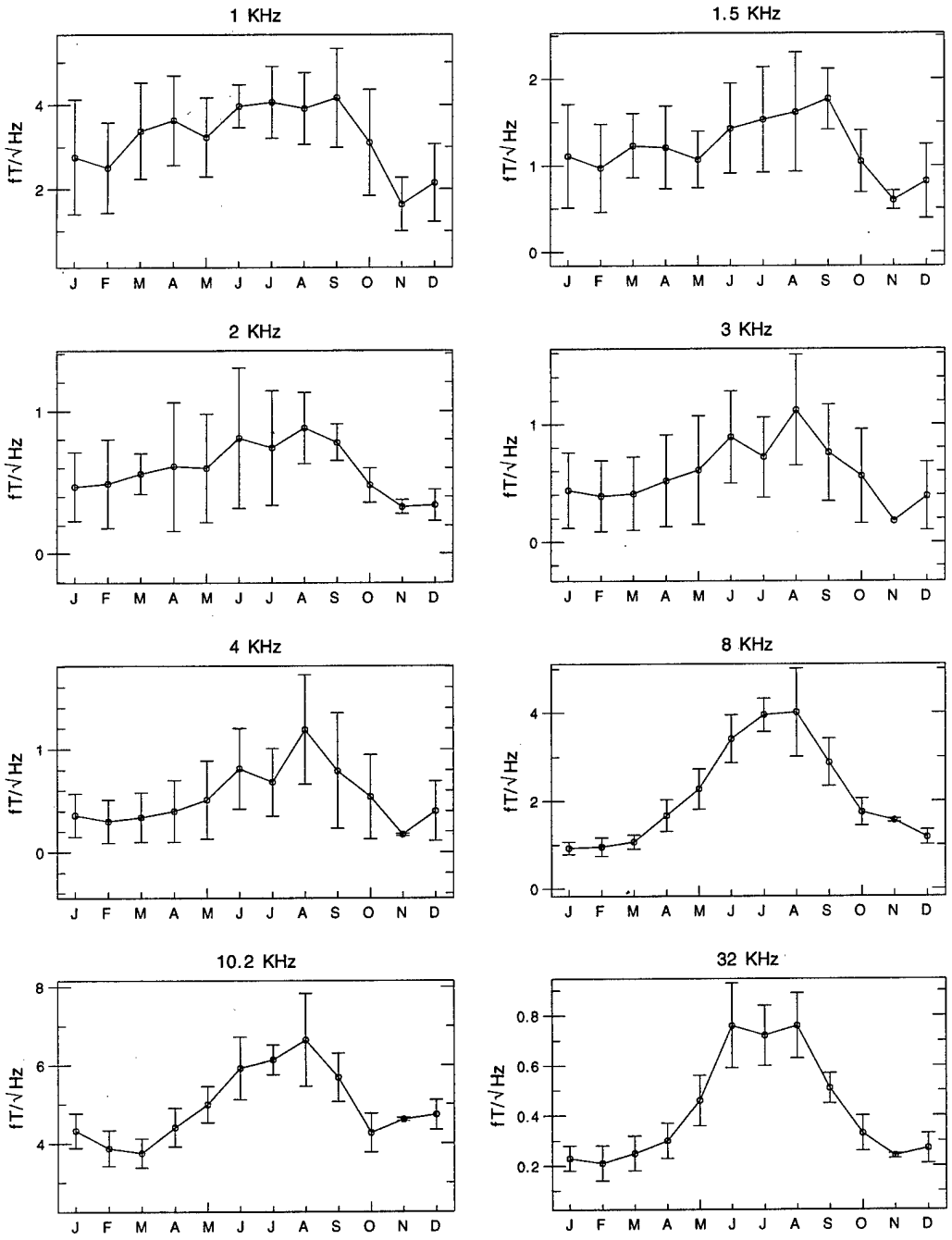

Figure 41: Monthly variation of ELF/VLF radio noise at Søndrestrøm, Greenland, for the eight highest-frequency channels and the 12-16 UT time block. The years 1986 to 1991 and the year 1993 are included.

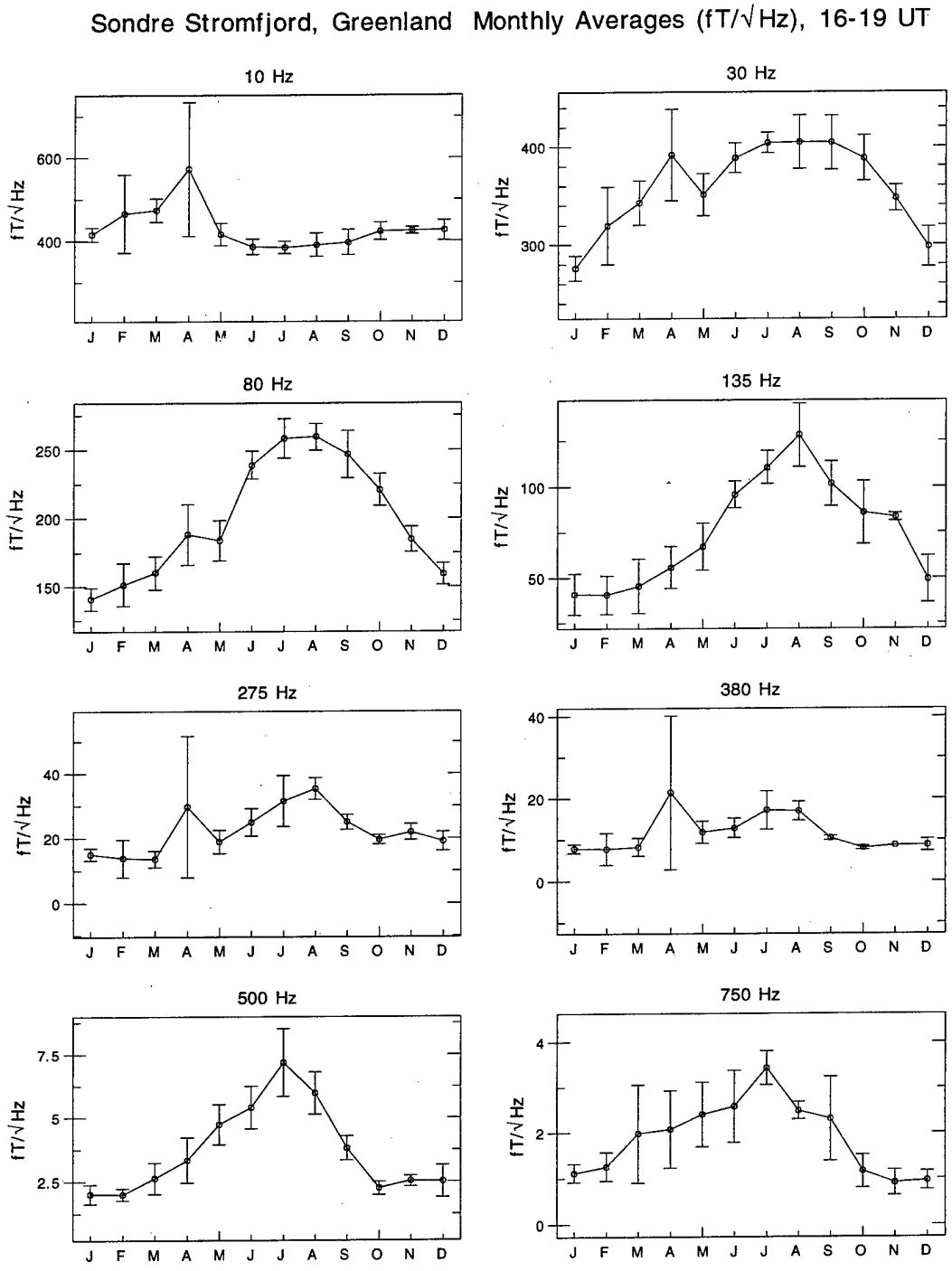

Figure 42: Monthly variation of ELF/VLF radio noise at Søndrestrøm, Greenland, for the eight lowest-frequency channels and the 16-20 UT time block. The years 1986 to 1991 and the year 1993 are included.

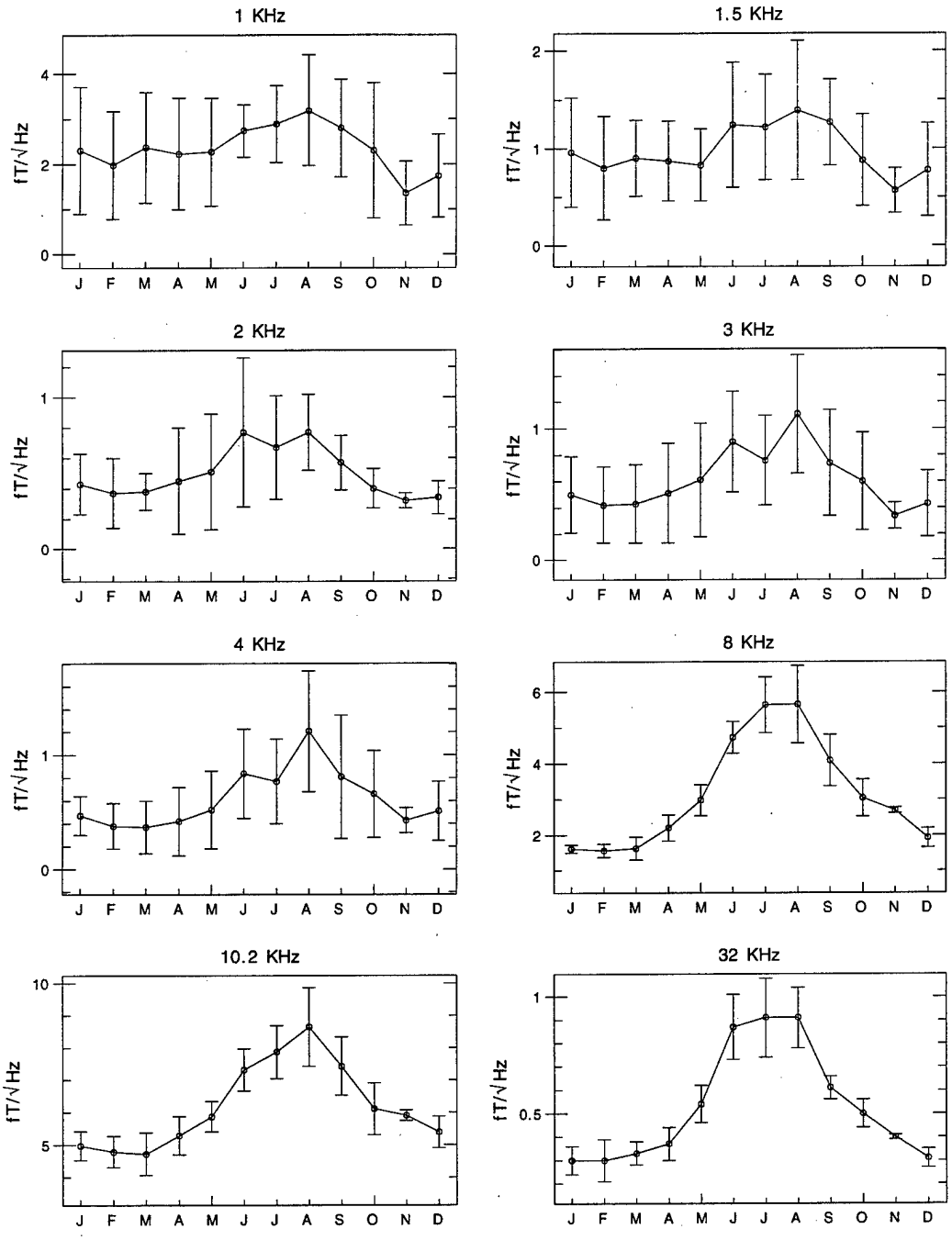

Figure 43: Monthly variation of ELF/VLF radio noise at Søndrestrøm, Greenland, for the eight highest-frequency channels and the 16-20 UT time block. The years 1986 to 1991 and the year 1993 are included.

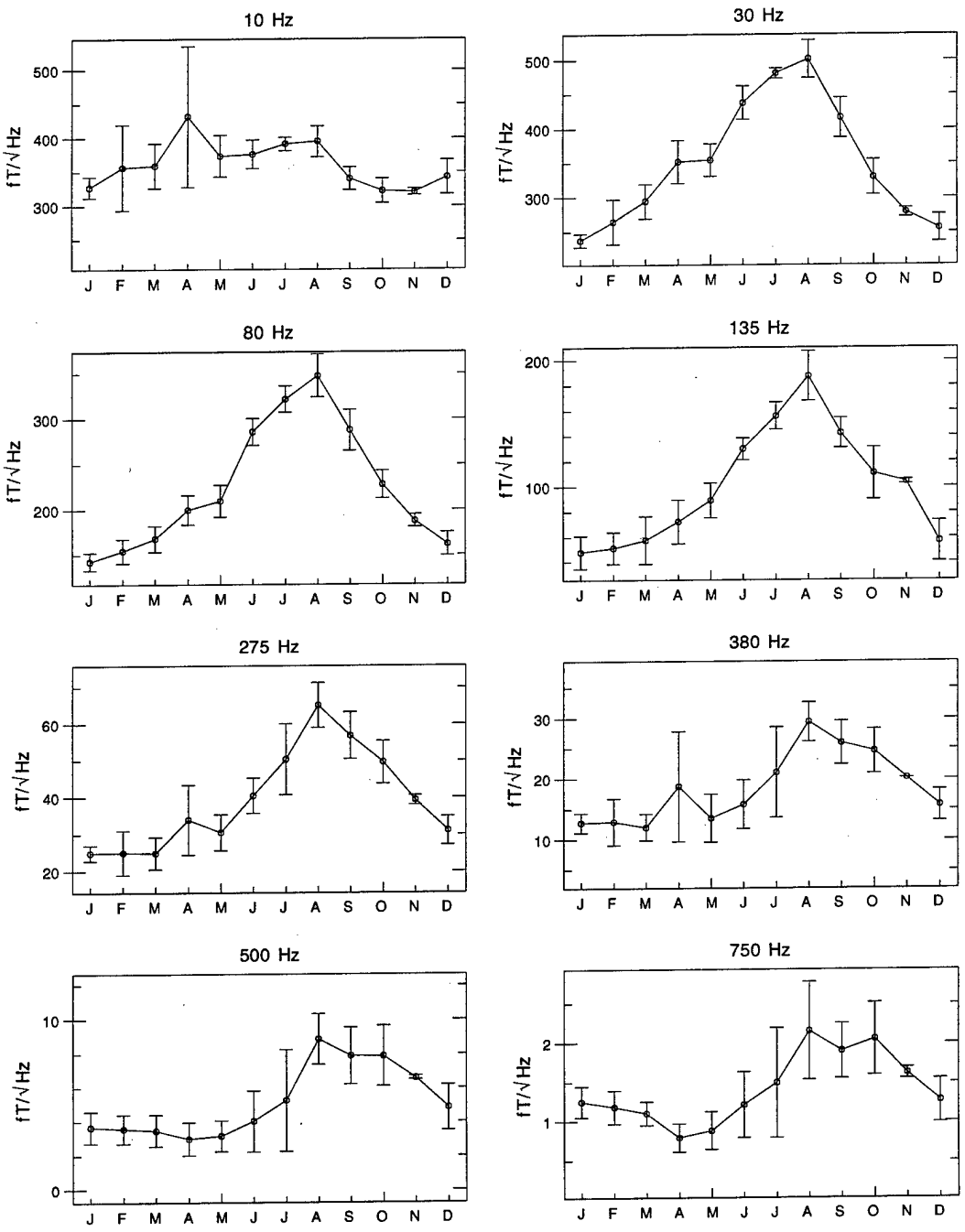

Figure 44: Monthly variation of ELF/VLF radio noise at Søndrestrøm, Greenland, for the eight lowest-frequency channels and the 20-24 UT time block. The years 1986 to 1991 and the year 1993 are included.

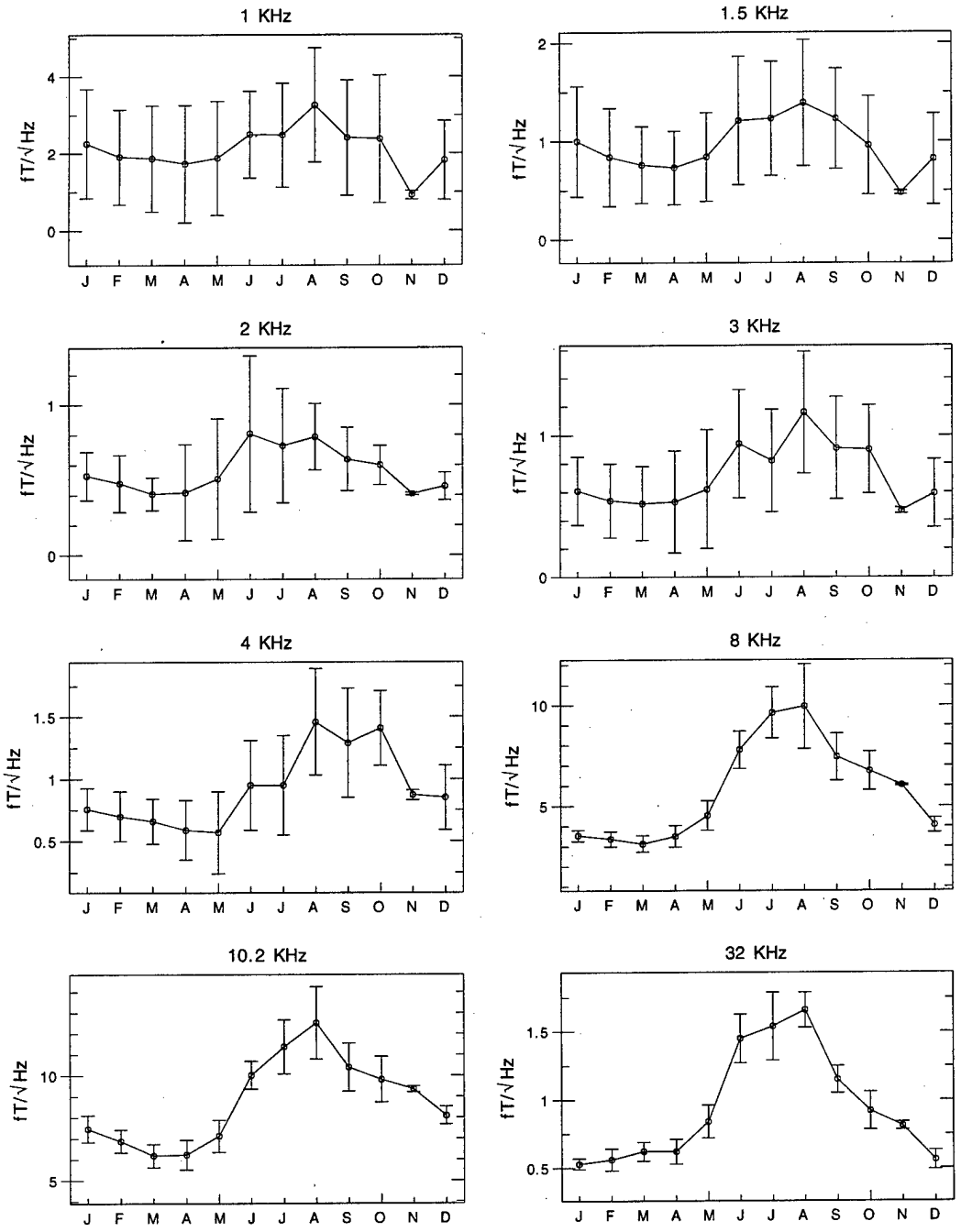

Figure 45: Monthly variation of ELF/VLF radio noise at Søndrestrøm, Greenland, for the eight highest-frequency channels and the 20-24 UT time block. The years 1986 to 1991 and the year 1993 are included.

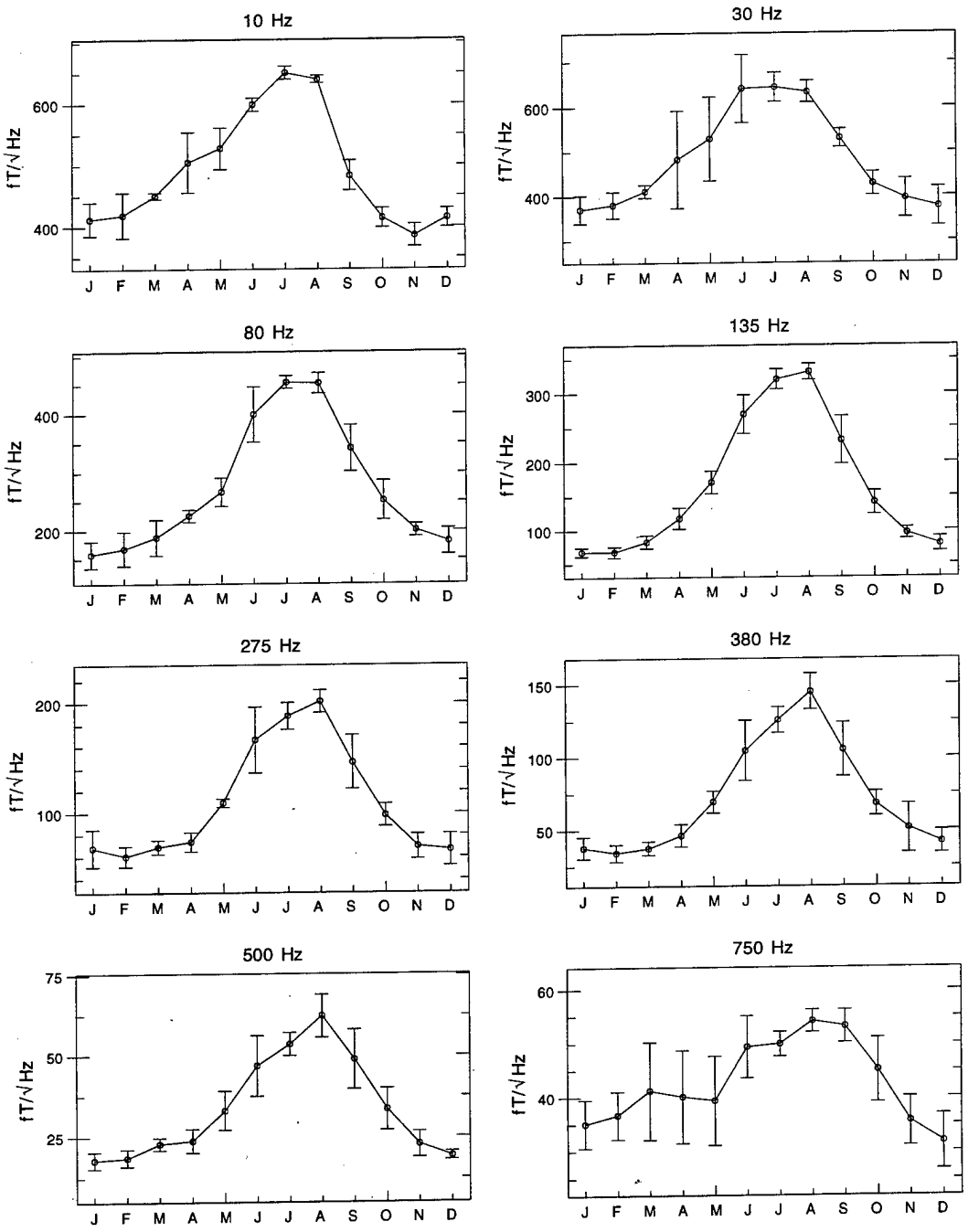

Figure 46: Monthly variation of ELF/VLF radio noise at Stanford, California, for the eight lowest-frequency channels and the 00-04 UT time block. The years 1986 to 1993 are included.

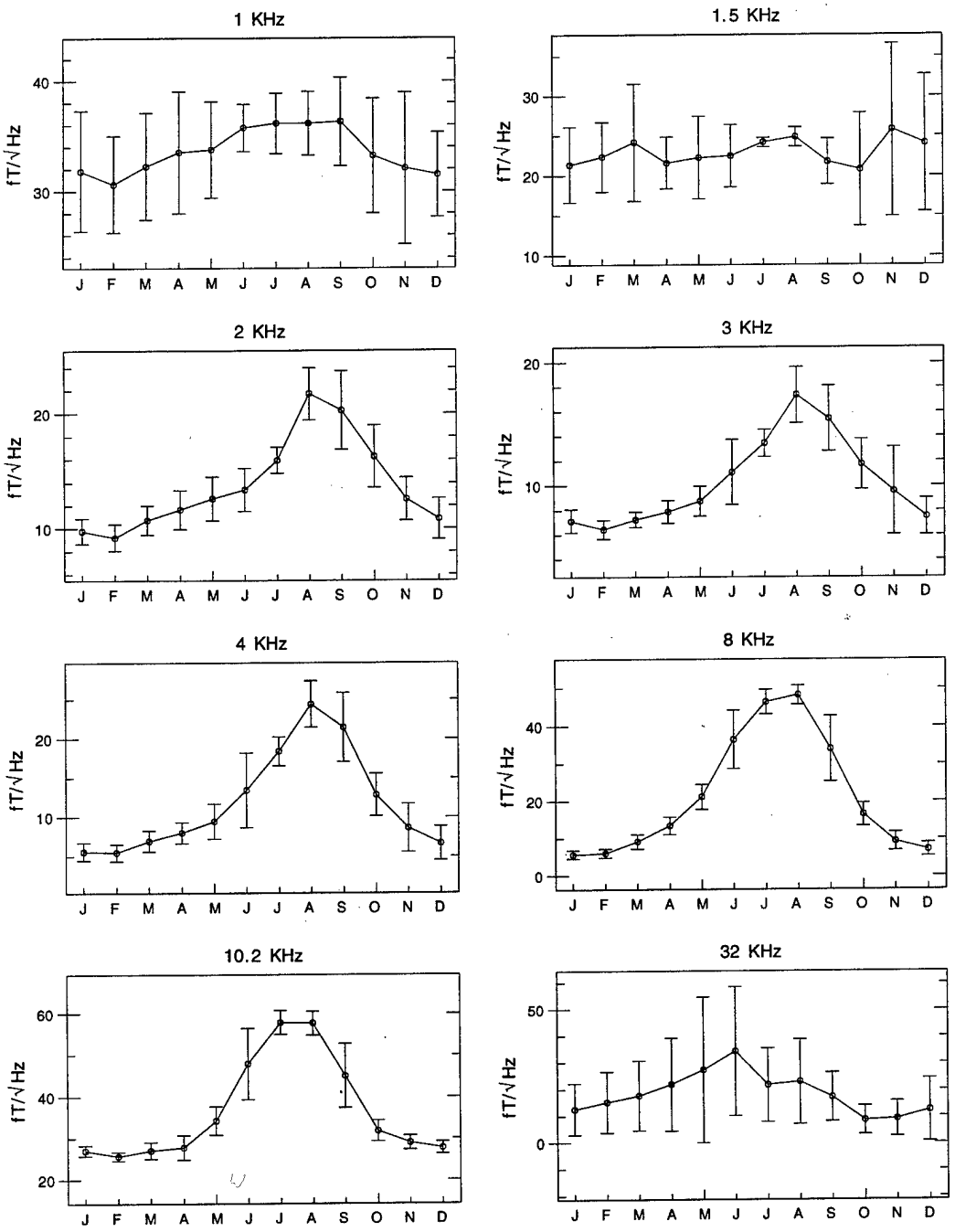

Figure 47: Monthly variation of ELF/VLF radio noise at Stanford, California, for the eight highest-frequency channels and the 00-04 UT time block. The years 1986 to 1993 are included.

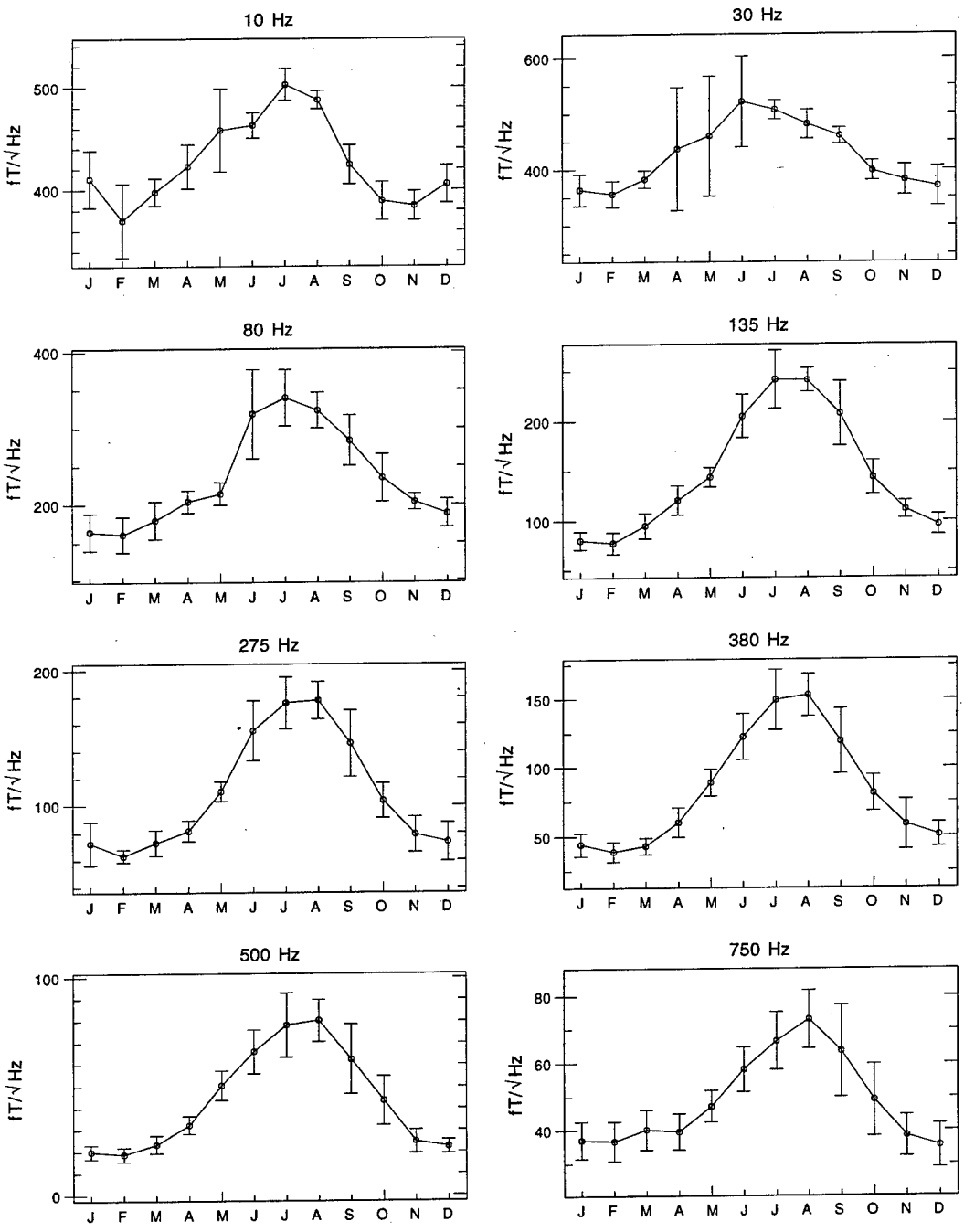

Figure 48: Monthly variation of ELF/VLF radio noise at Stanford, California, for the eight lowest-frequency channels and the 04-08 UT time block. The years 1986 to 1993 are included.

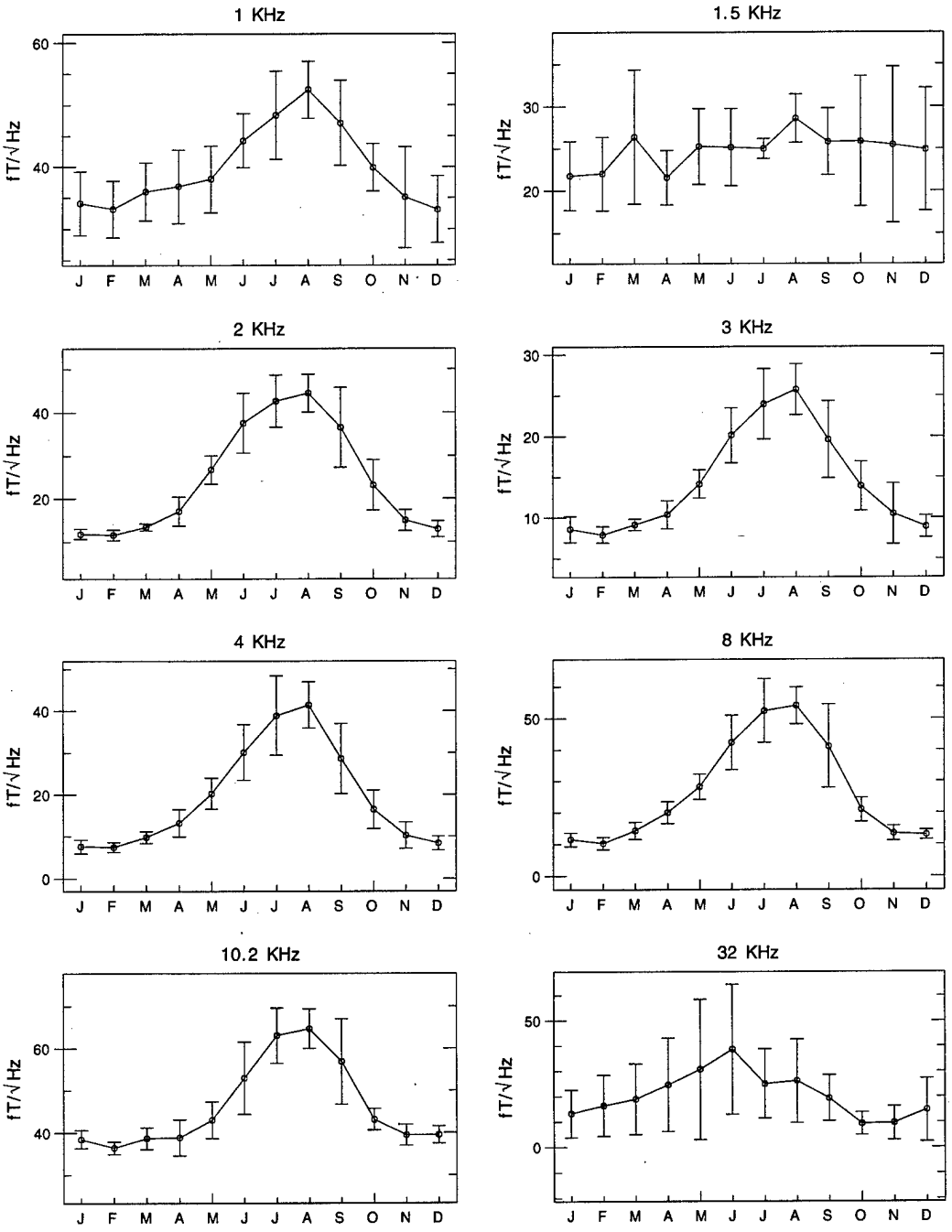

Figure 49: Monthly variation of ELF/VLF radio noise at Stanford, California, for the eight highest-frequency channels and the 04-08 UT time block. The years 1986 to 1993 are included.

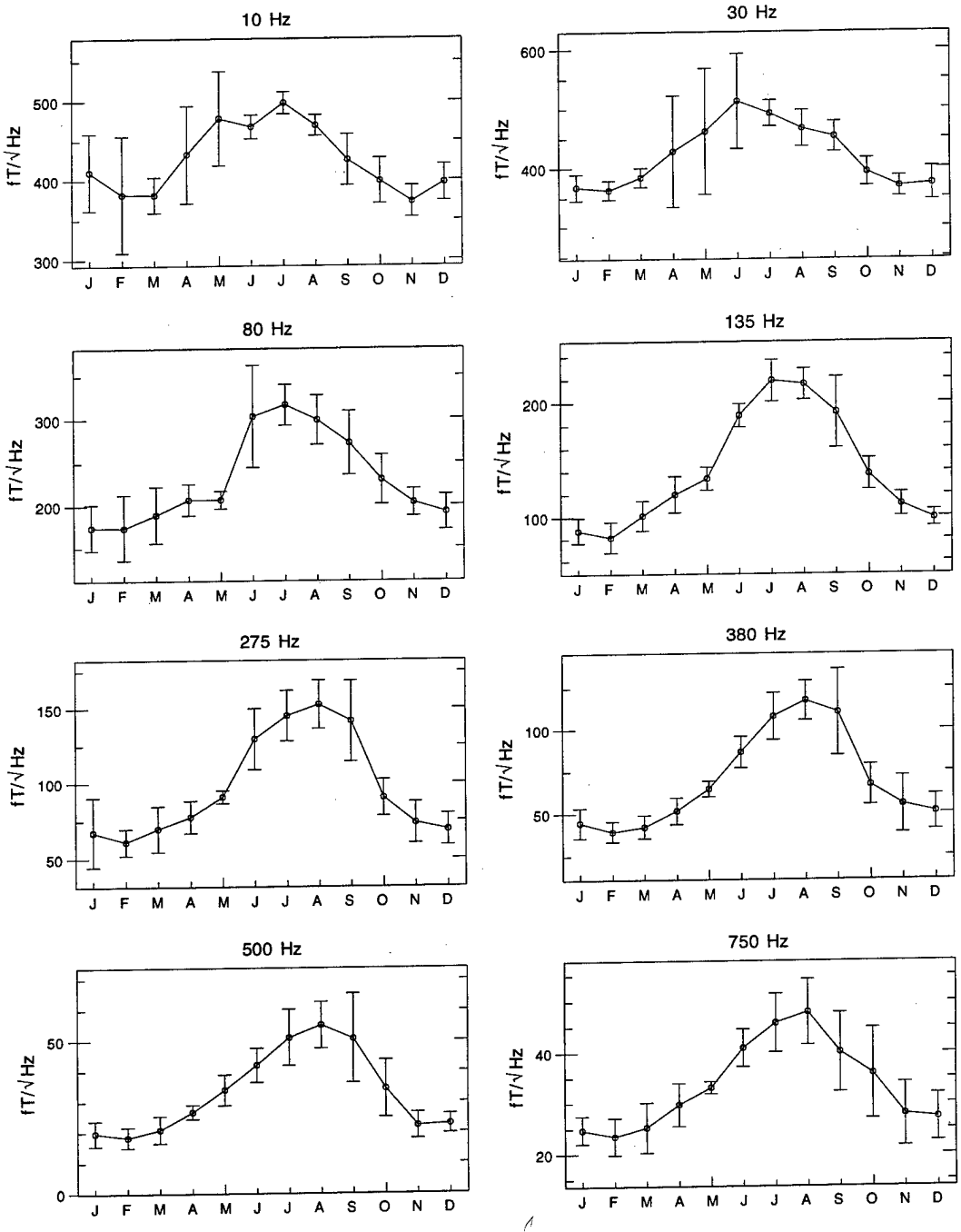

Figure 50: Monthly variation of ELF/VLF radio noise at Stanford, California, for the eight lowest-frequency channels and the 08-12 UT time block. The years 1986 to 1993 are included.

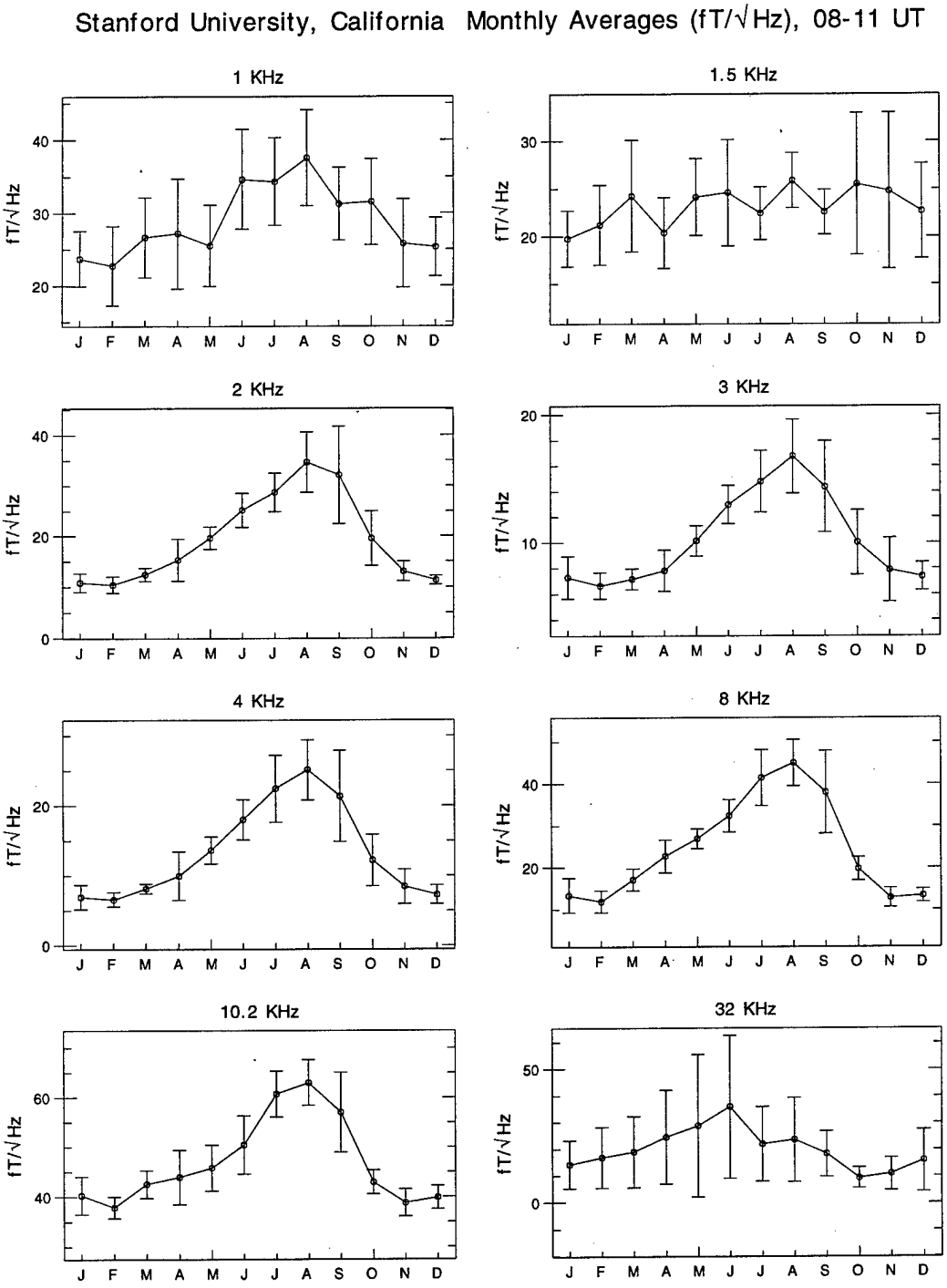

Figure 51: Monthly variation of ELF/VLF radio noise at Stanford, California, for the eight highest-frequency channels and the 08-12 UT time block. The years 1986 to 1993 are included.

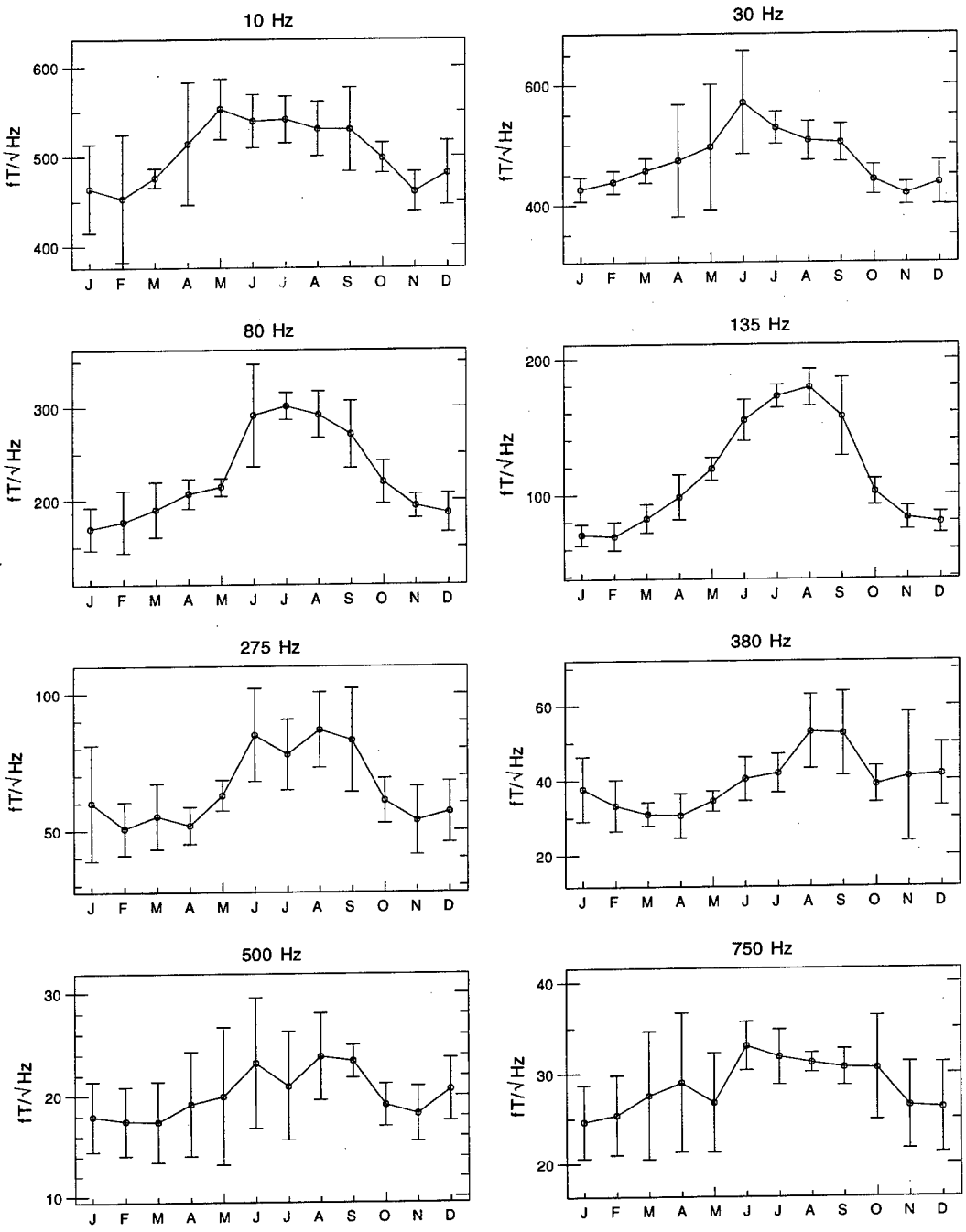

Figure 52: Monthly variation of ELF/VLF radio noise at Stanford, California, for the eight lowest-frequency channels and the 12-16 UT time block. The years 1986 to 1993 are included.

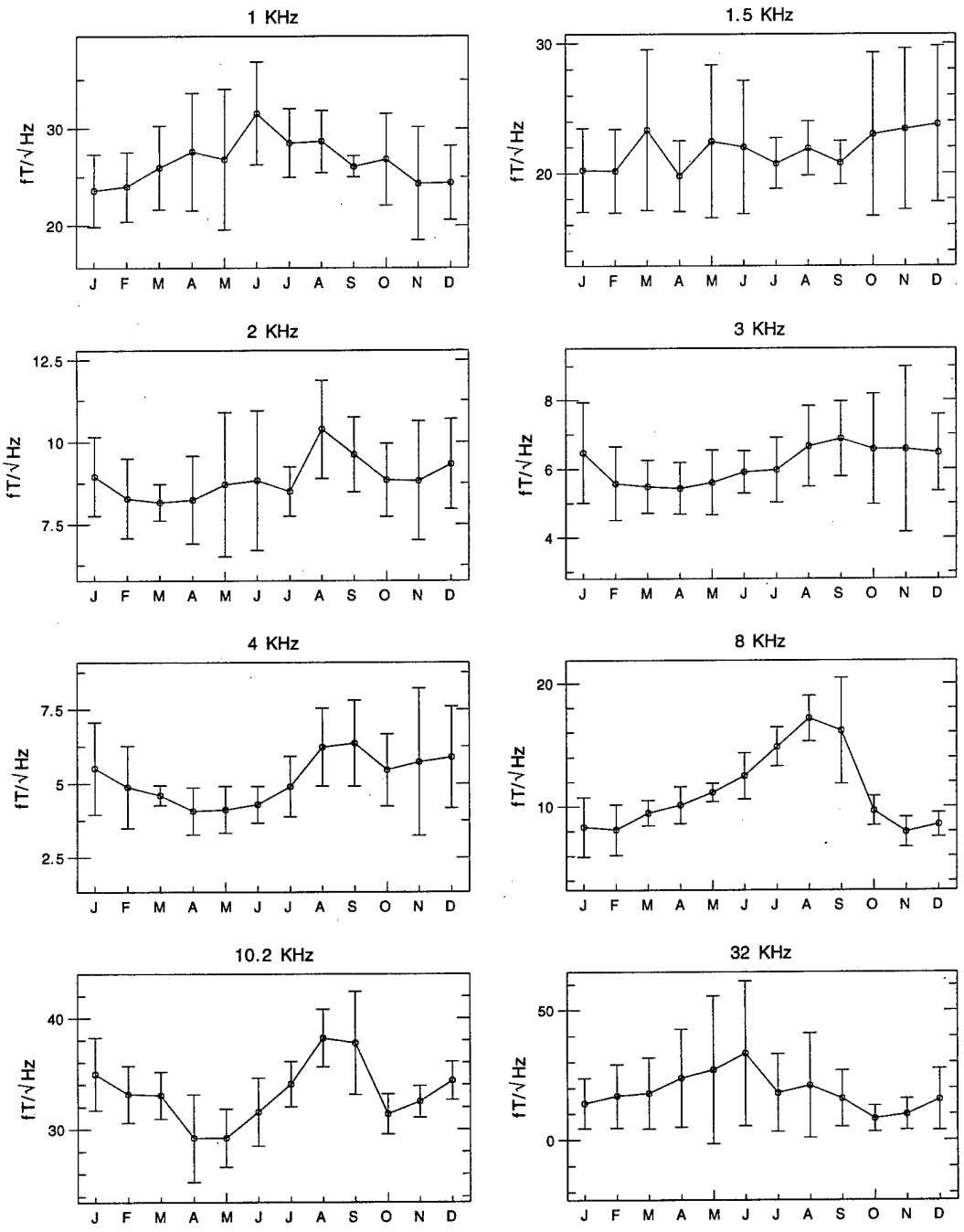

Figure 53: Monthly variation of ELF/VLF radio noise at Stanford, California, for the eight highest-frequency channels and the 12-16 UT time block. The years 1986 to 1993 are included.

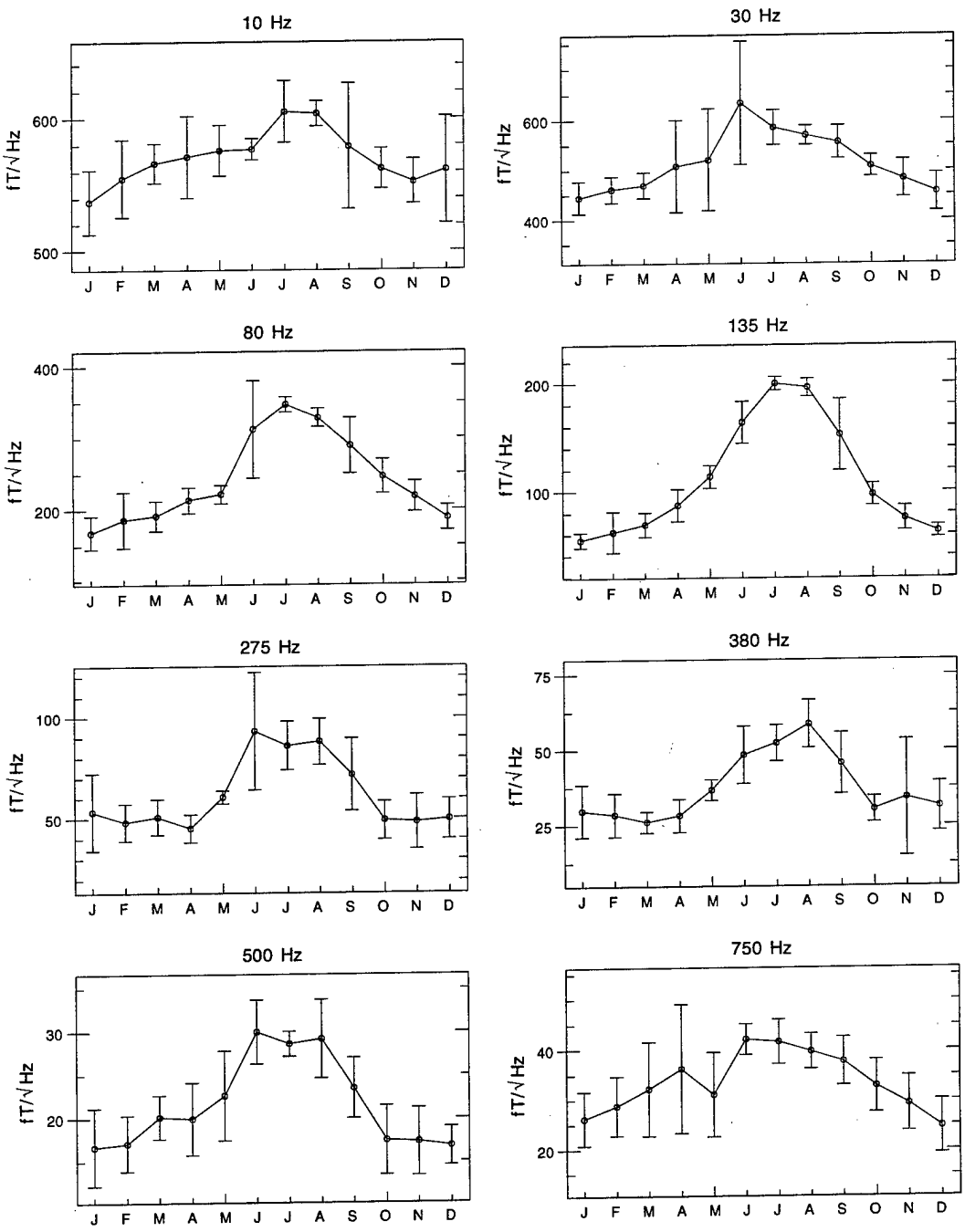

Figure 54: Monthly variation of ELF/VLF radio noise at Stanford, California, for the eight lowest-frequency channels and the 16-20 UT time block. The years 1986 to 1993 are included.

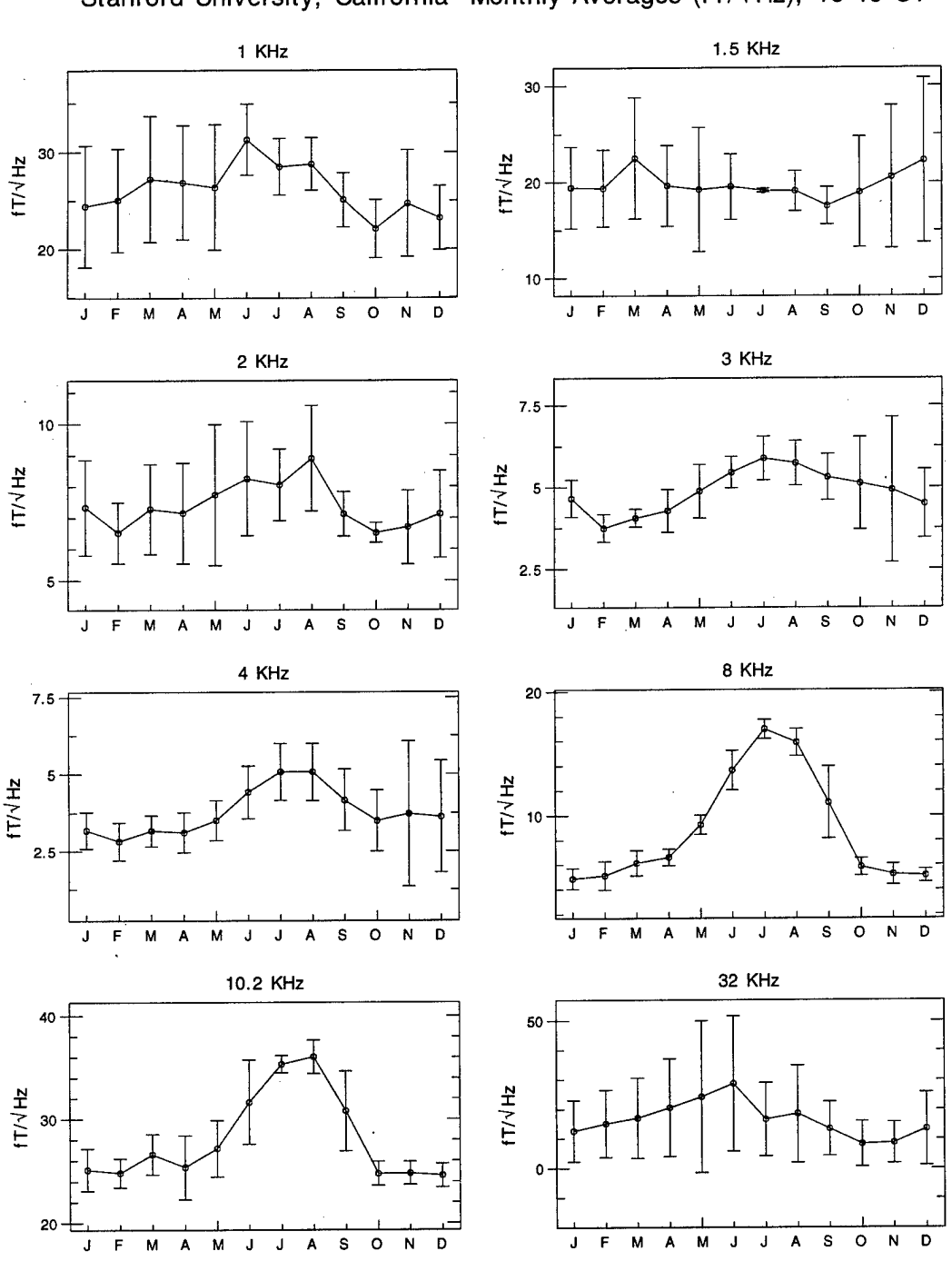

Figure 55: Monthly variation of ELF/VLF radio noise at Stanford, California, for the eight highest-frequency channels and the 16-20 UT time block. The years 1986 to 1993 are included.

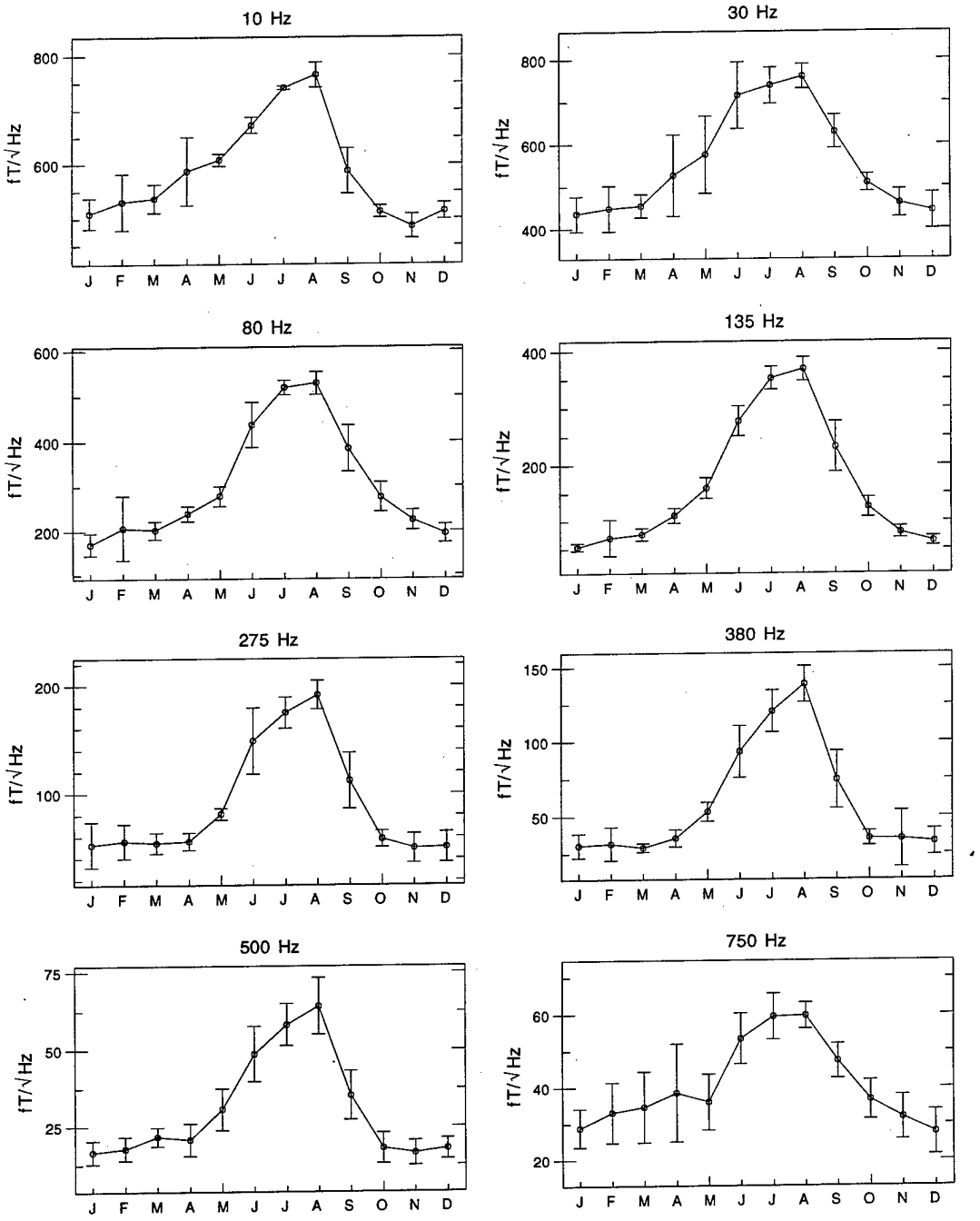

Figure 56: Monthly variation of ELF/VLF radio noise at Stanford, California, for the eight lowest-frequency channels and the 20-24 UT time block. The years 1986 to 1993 are included.

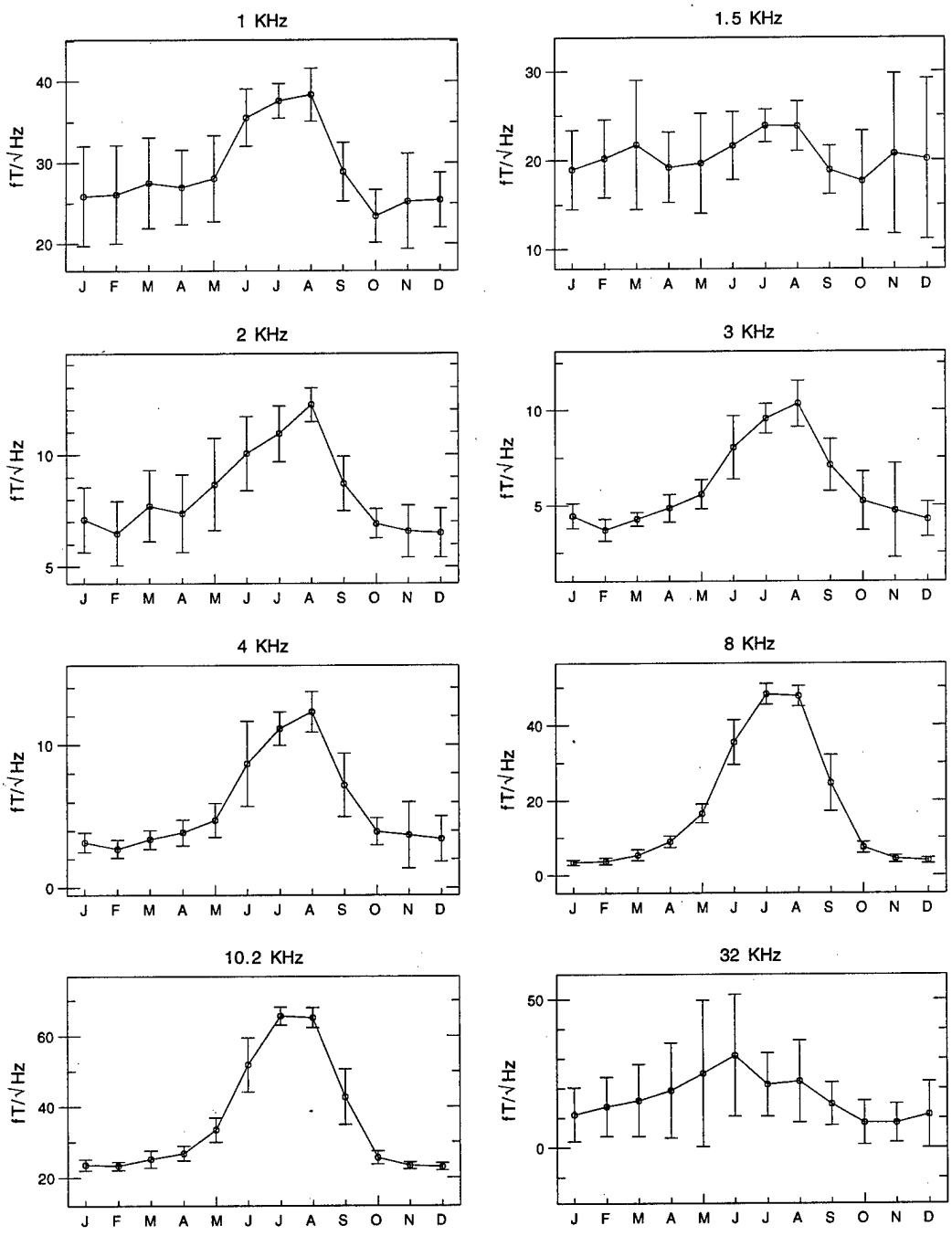

Figure 57: Monthly variation of ELF/VLF radio noise at Stanford, California, for the eight highest-frequency channels and the 20-24 UT time block. The years 1986 to 1993 are included.

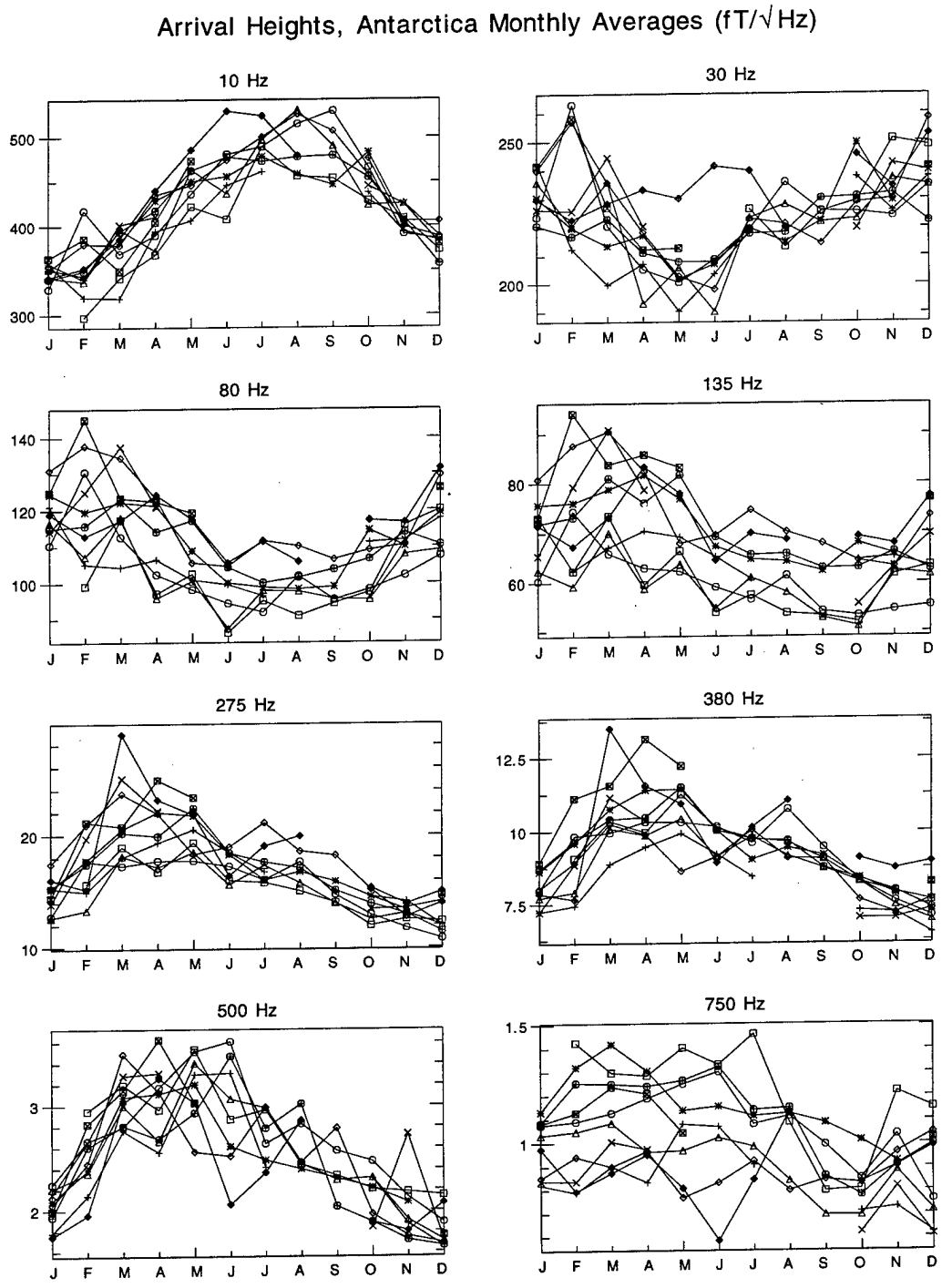

Figure 58: Monthly variation of ELF/VLF radio noise at Arrival Heights, Antarctica, for the eight lowest-frequency channels, each year shown individually. The years 1985 to 1994 are included.

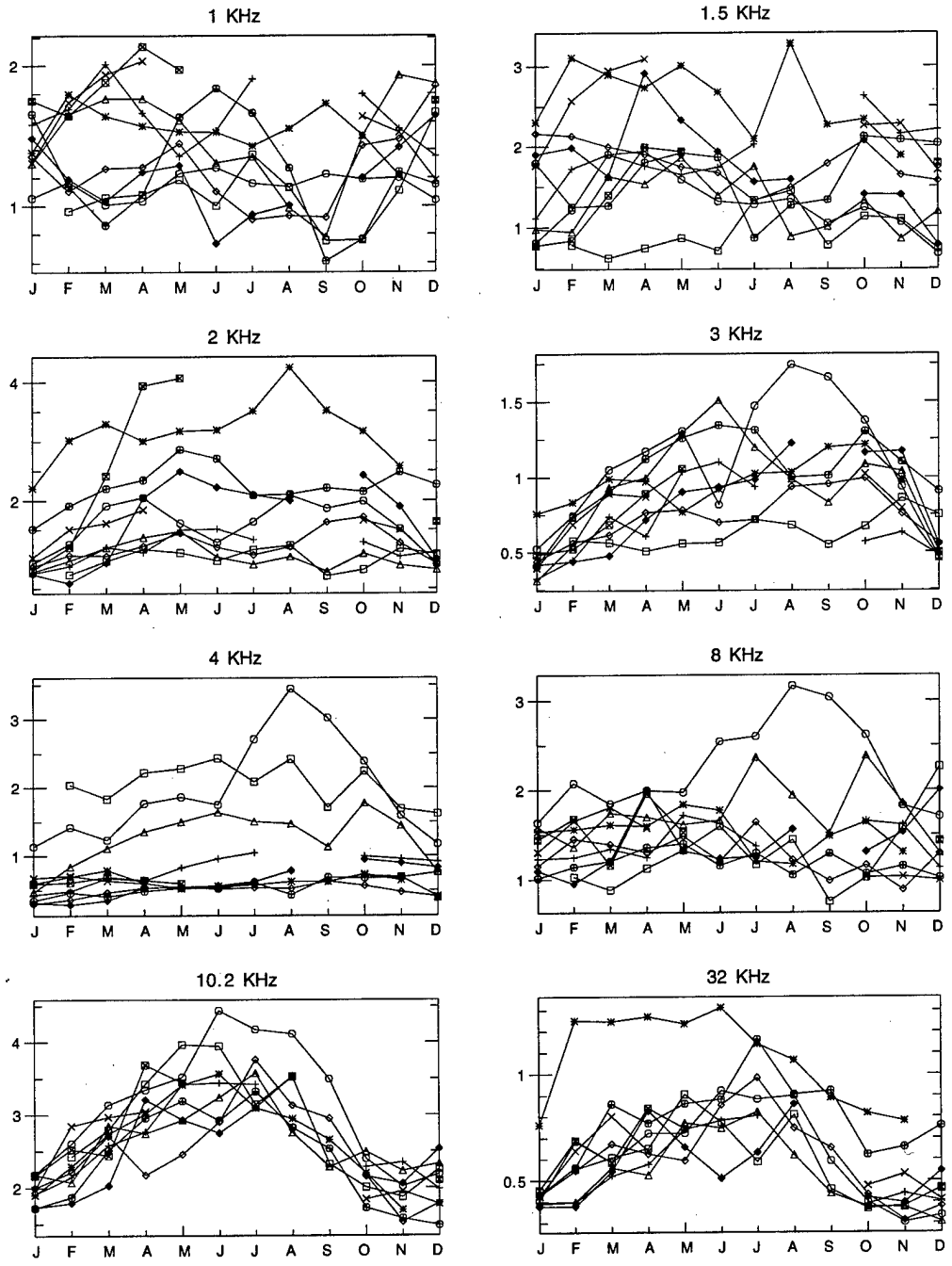

Figure 59: Monthly variation of ELF/VLF radio noise at Arrival Heights, Antarctica, for the eight highest-frequency channels, each year shown individually. The years 1985 to 1994 are included.

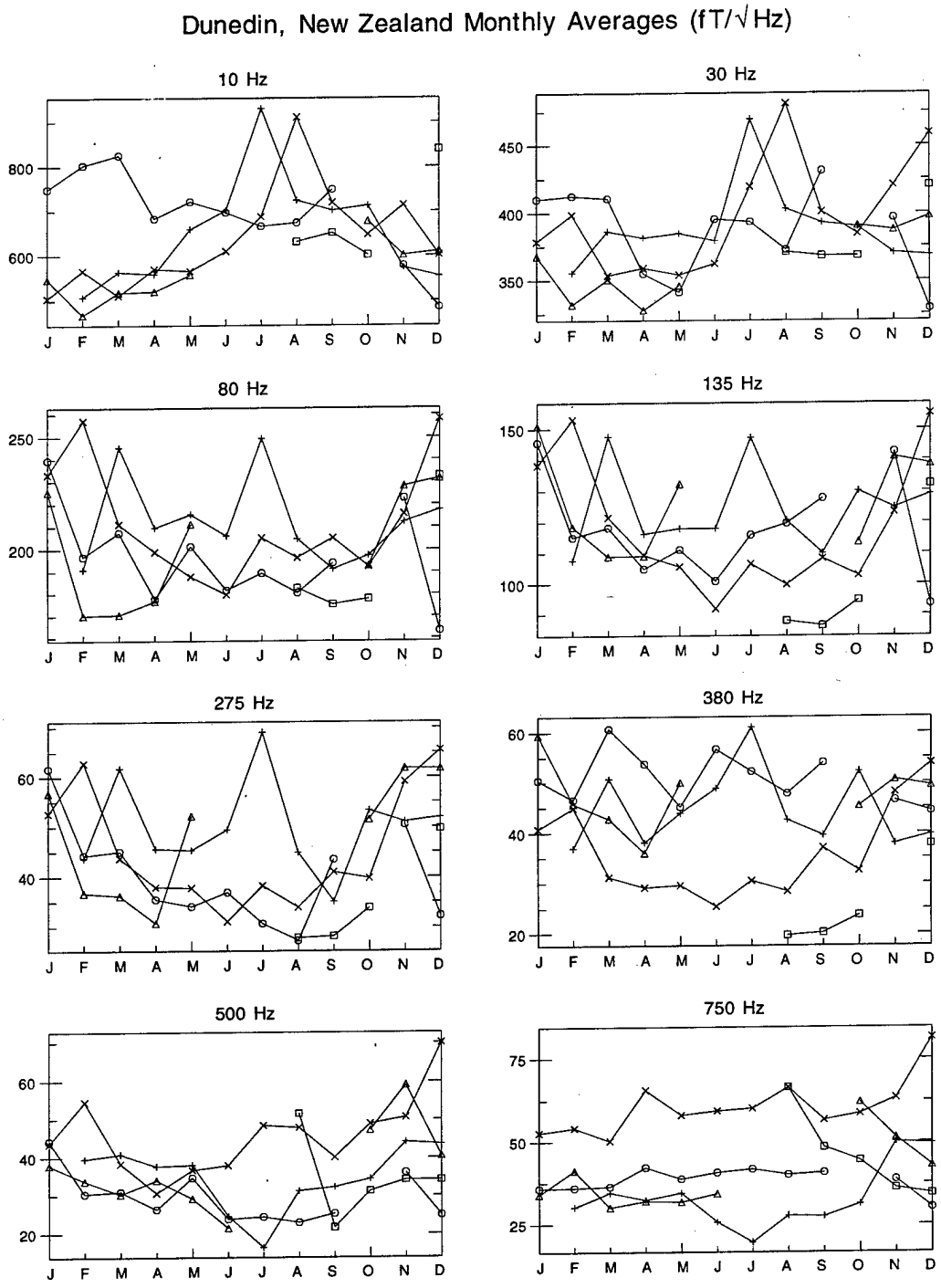

Figure 60: Monthly variation of ELF/VLF radio noise at Dunedin, New Zealand, for the eight lowest-frequency channels, each year shown individually. The years 1986 to 1990 are included.

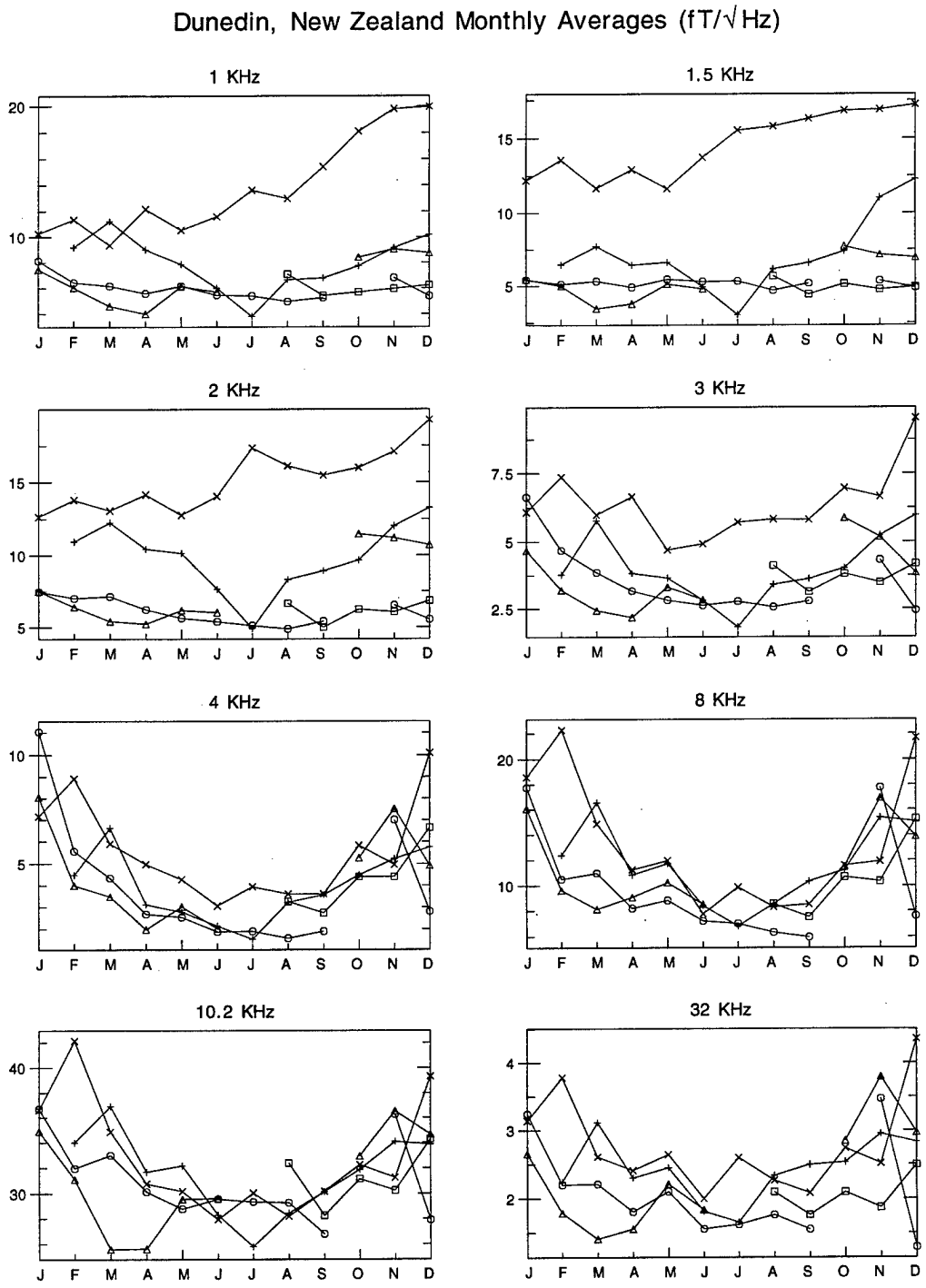

Figure 61: Monthly variation of ELF/VLF radio noise at Dunedin, New Zealand, for the eight highest-frequency channels, each year shown individually. The years 1986 to 1990 are included.

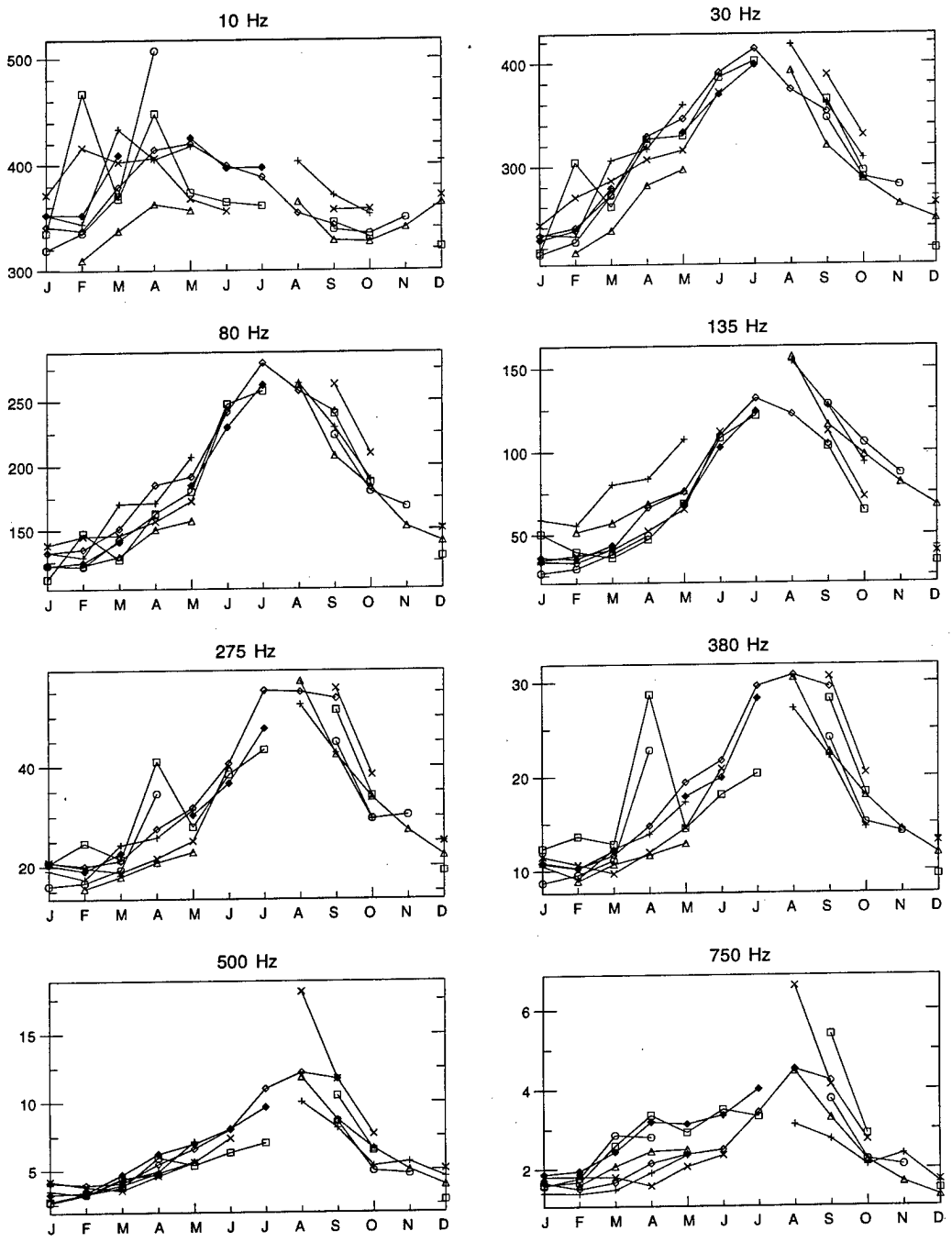

Figure 62: Monthly variation of ELF/VLF radio noise at Søndrestrøm, Greenland, for the eight lowest-frequency channels, each year shown individually. The years 1986 to 1991 and the year 1993 are included.

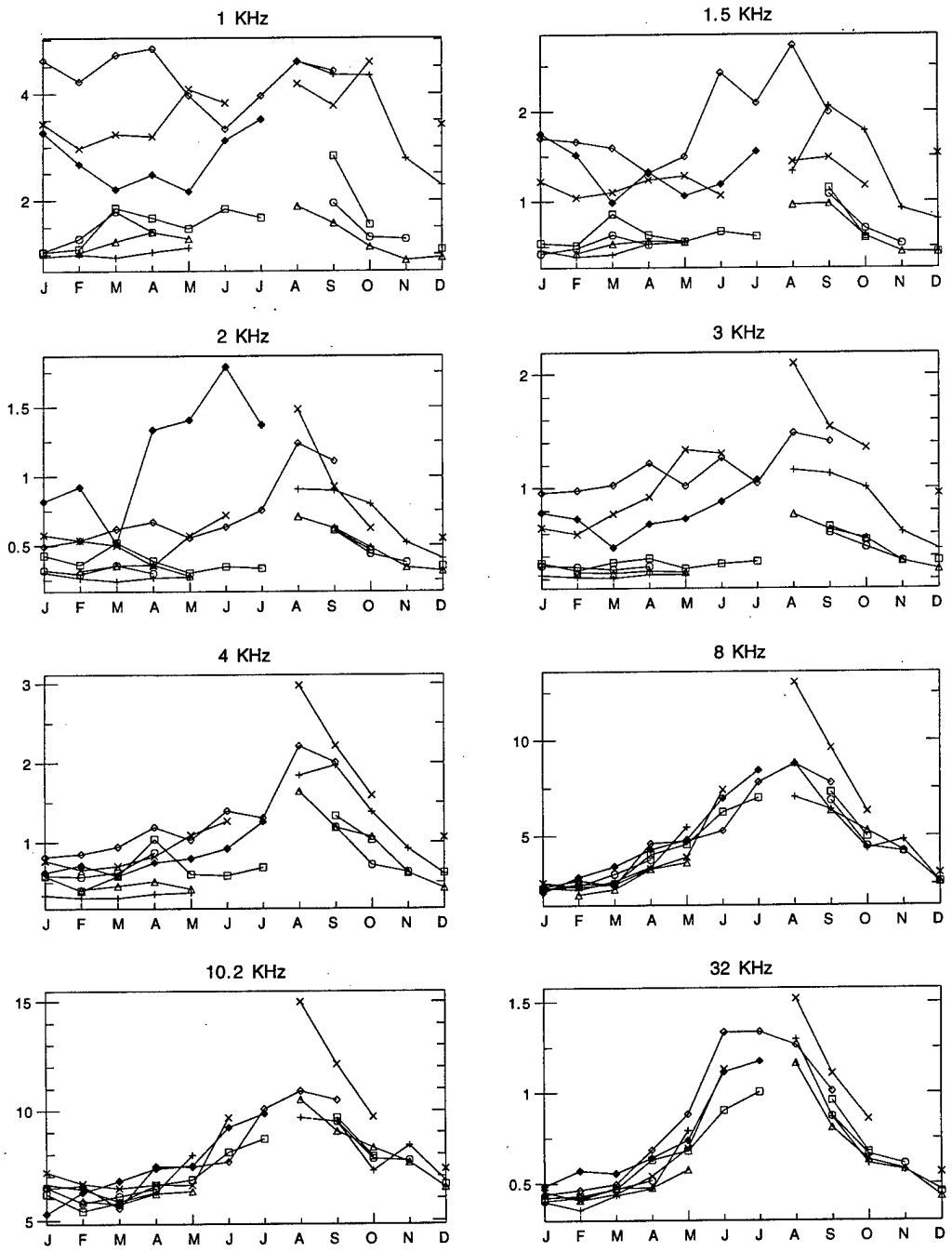

Figure 63: Monthly variation of ELF/VLF radio noise at Søndrestrøm, Greenland, for the eight highest-frequency channels, each year shown individually. The years 1986 to 1991 and the year 1993 are included.

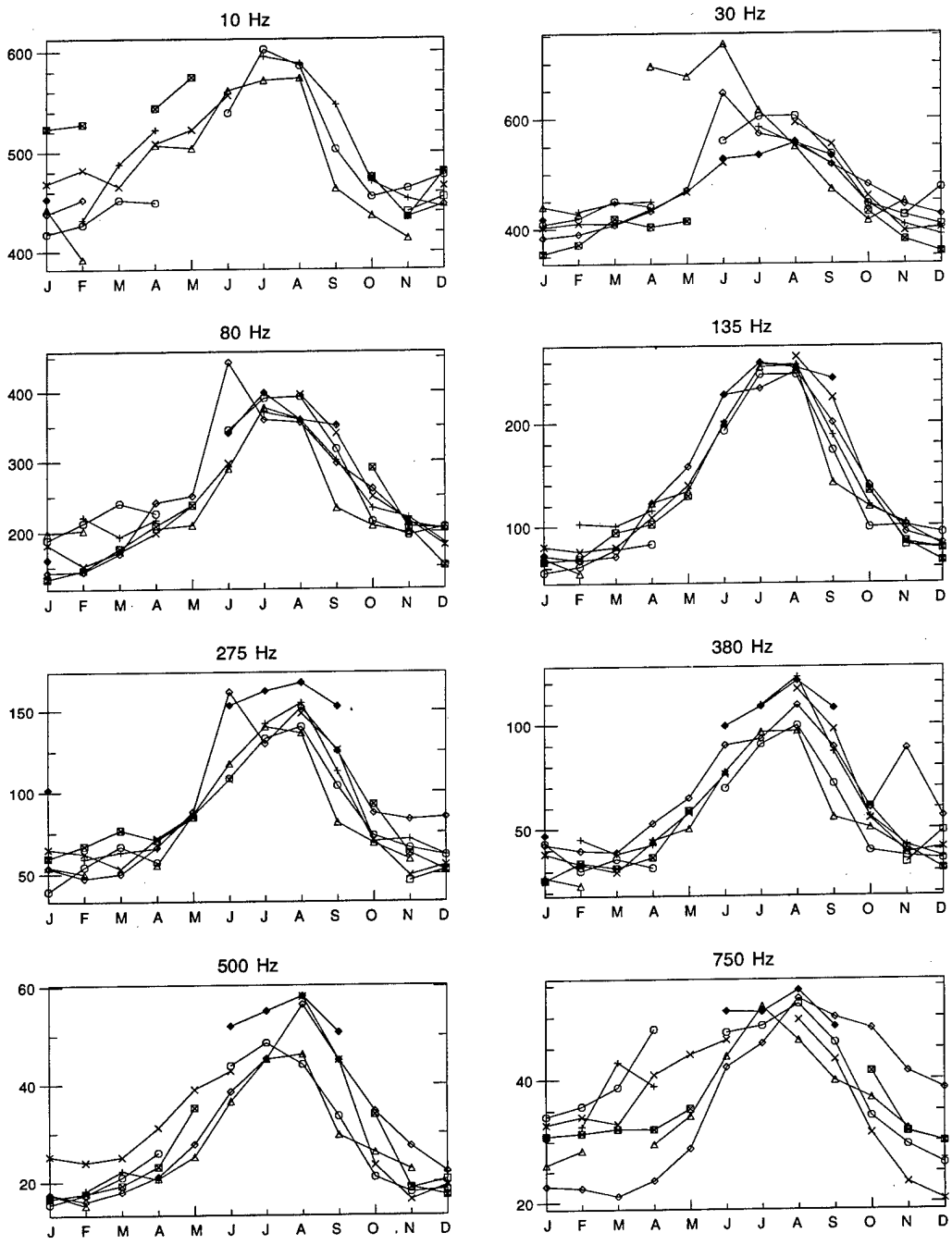

Figure 64: Monthly variation of ELF/VLF radio noise at Stanford, California, for the eight lowest-frequency channels, each year shown individually. The years 1986 to 1993 are included.

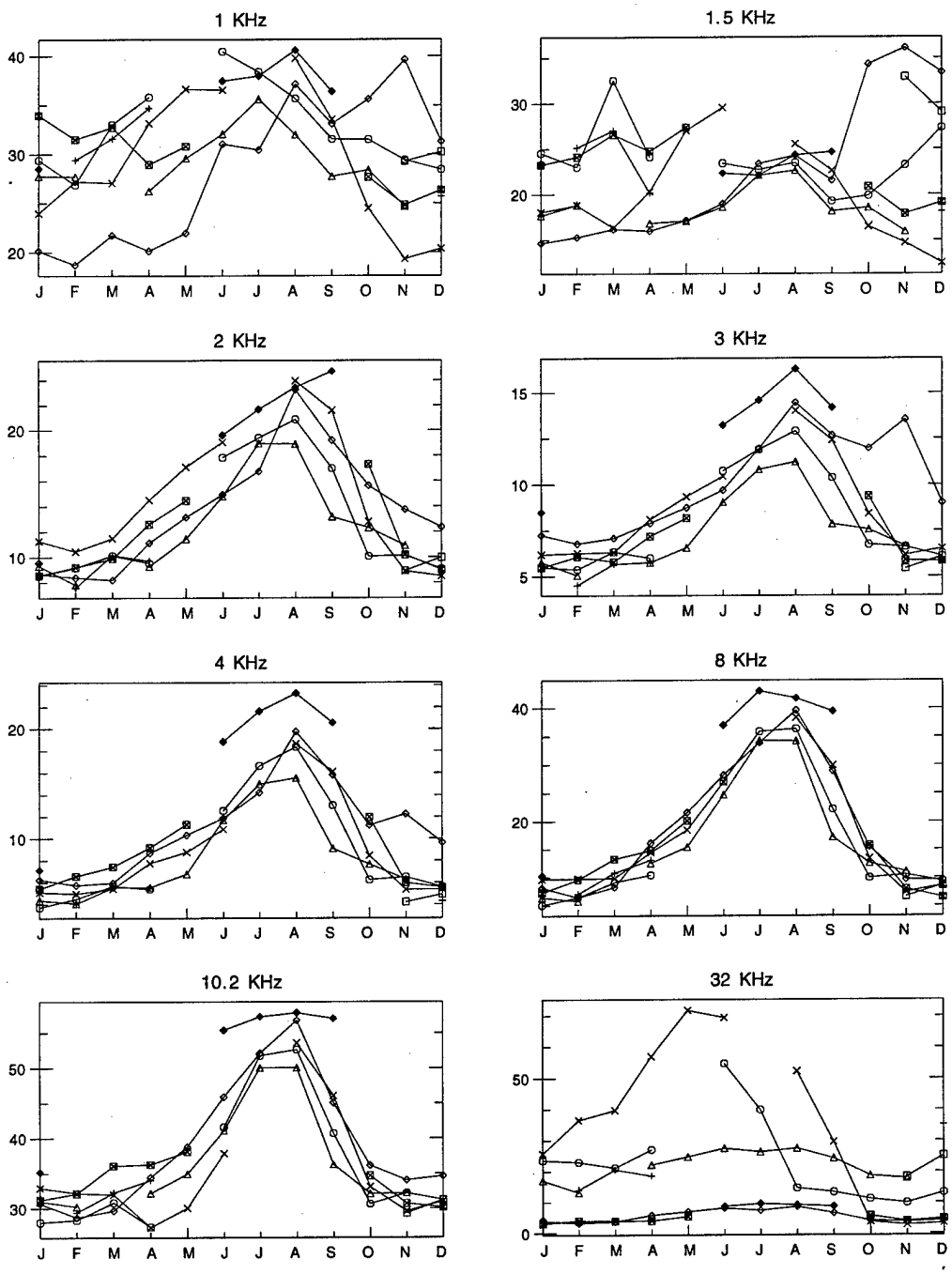

Figure 65: Monthly variation of ELF/VLF radio noise at Stanford, California, for the eight highest-frequency channels, each year shown individually. The years 1986 to 1993 are included.

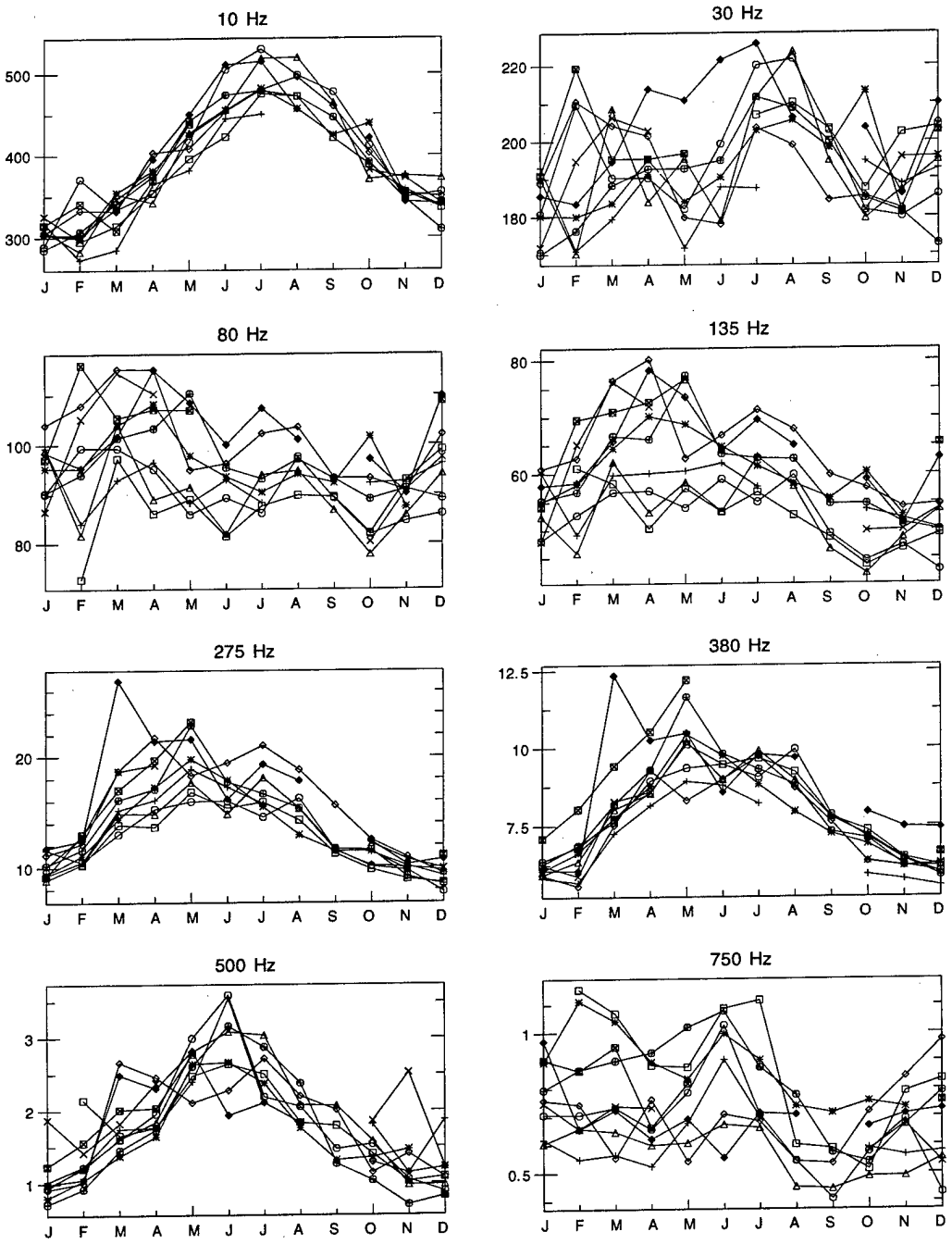

Figure 66: Monthly variation of ELF/VLF radio noise at Arrival Heights, Antarctica, for the eight lowest-frequency channels and the 00-04 UT time block, each year shown individually. The years 1985 to 1994 are included.

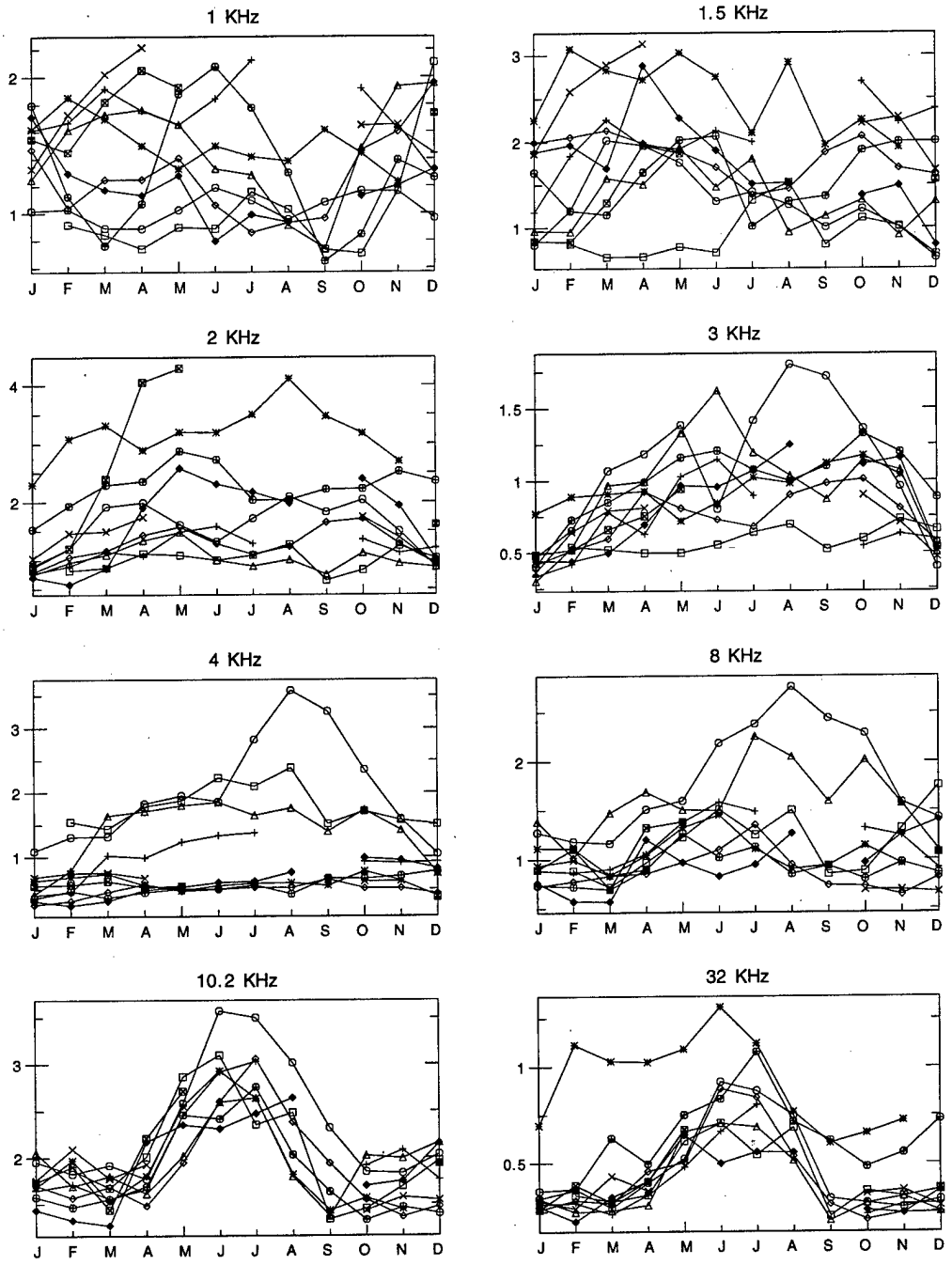

Figure 67: Monthly variation of ELF/VLF radio noise at Arrival Heights, Antarctica, for the eight highest-frequency channels and the 00-04 UT time block, each year shown individually. The years 1985 to 1994 are included.

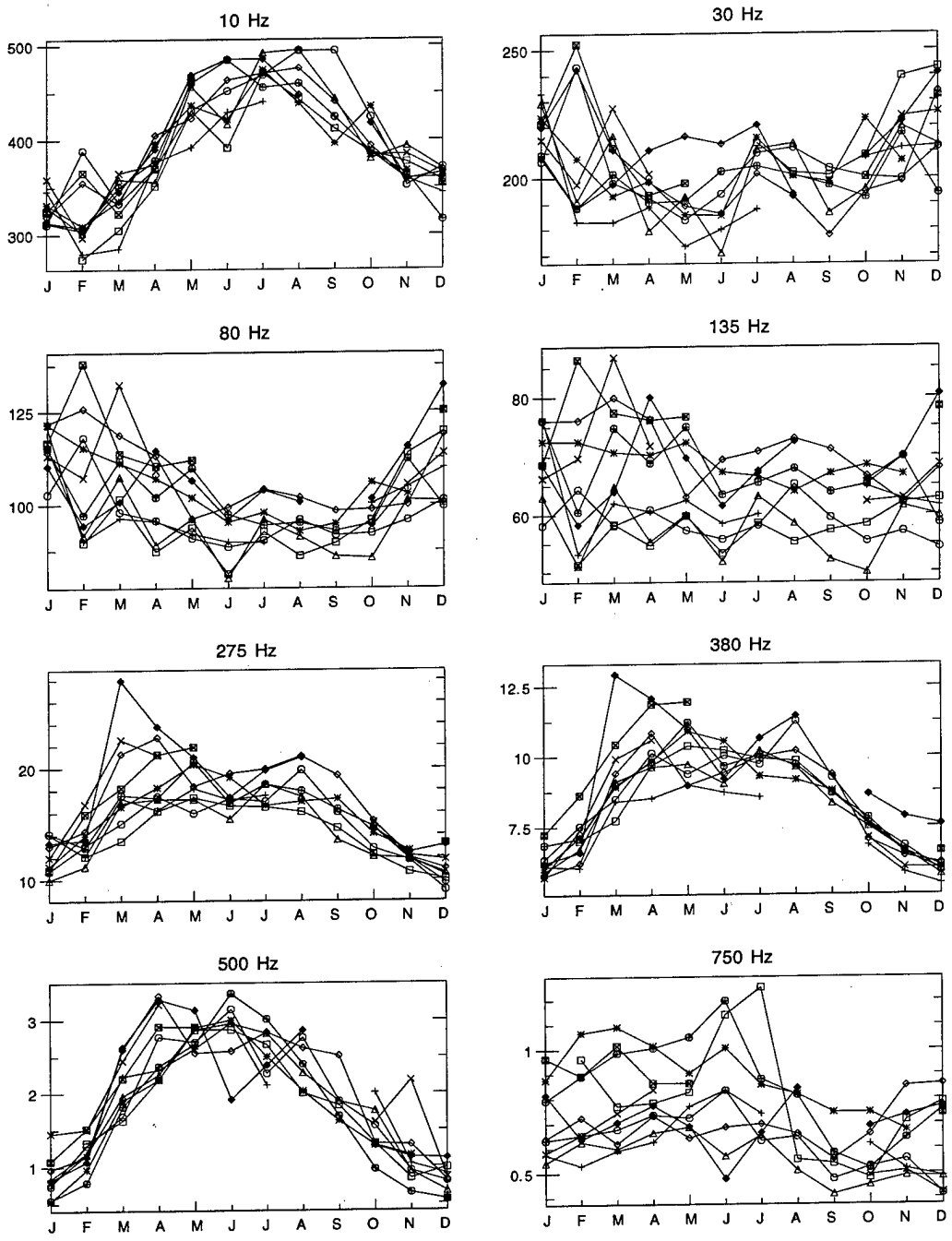

Figure 68: Monthly variation of ELF/VLF radio noise at Arrival Heights, Antarctica, for the eight lowest-frequency channels and the 04-08 UT time block, each year shown individually. The years 1985 to 1994 are included.

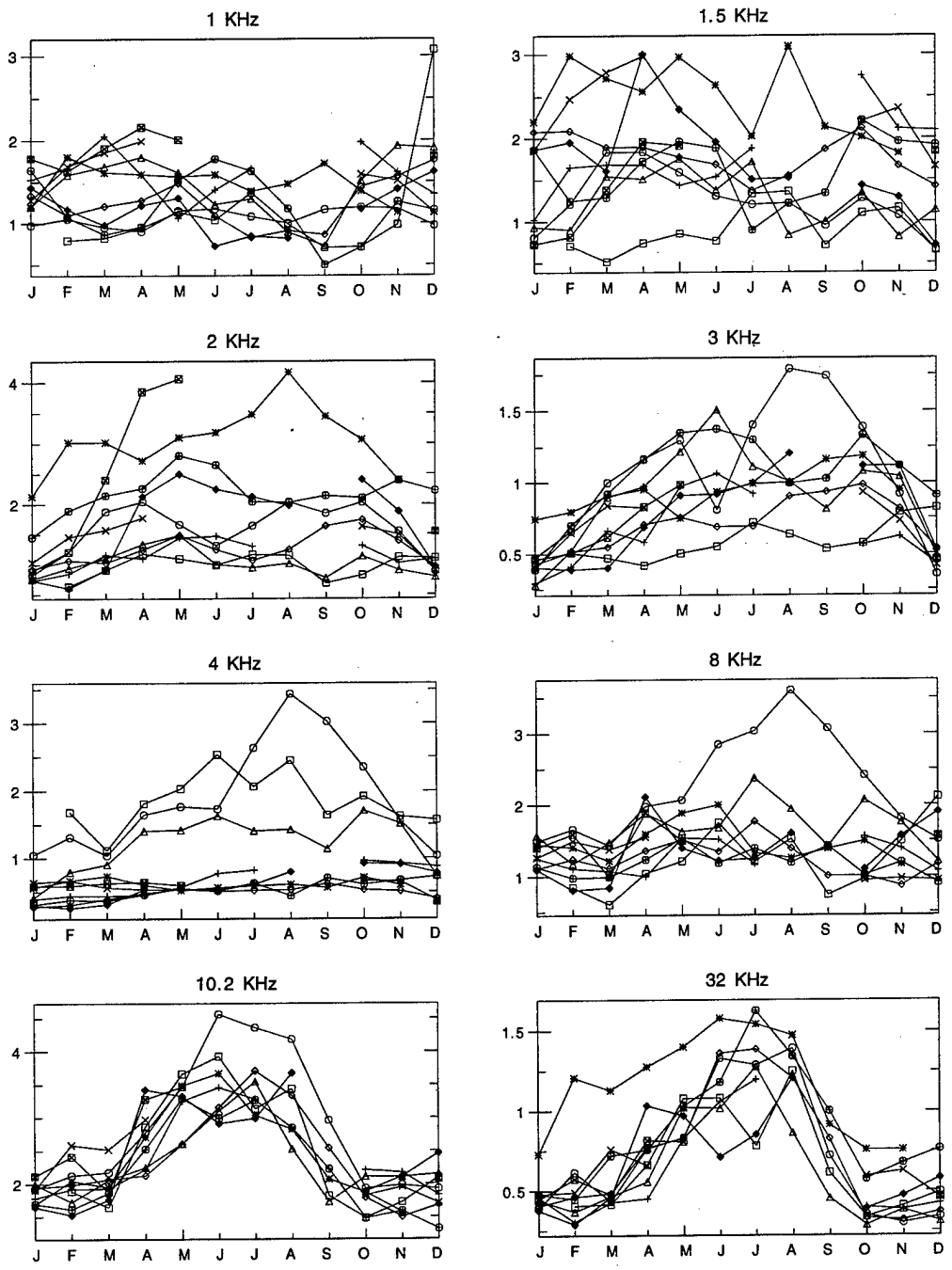

Figure 69: Monthly variation of ELF/VLF radio noise at Arrival Heights, Antarctica, for the eight highest-frequency channels and the 04-08 UT time block, each year shown individually. The years 1985 to 1994 are included.

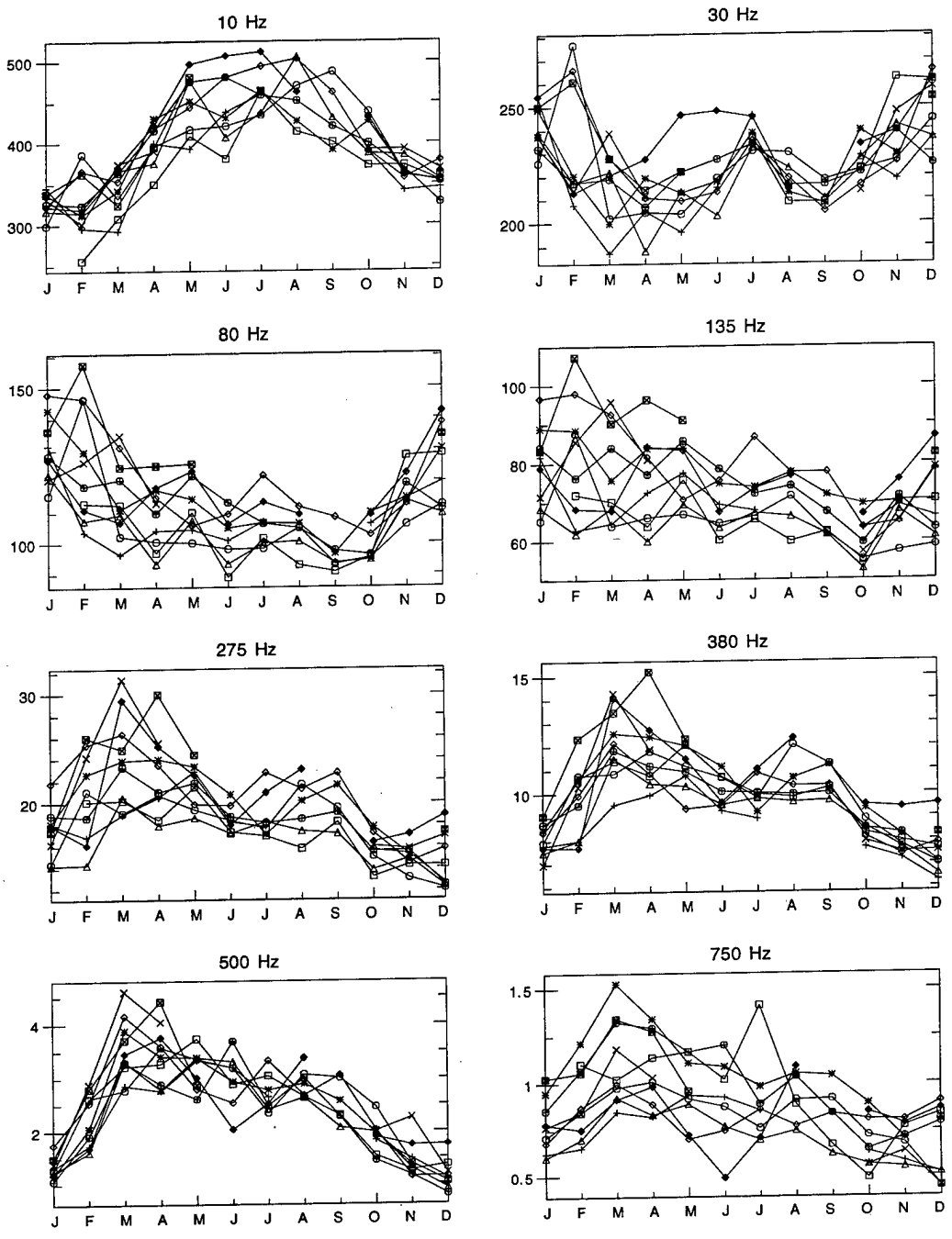

Figure 70: Monthly variation of ELF/VLF radio noise at Arrival Heights, Antarctica, for the eight lowest-frequency channels and the 08-12 UT time block, each year shown individually. The years 1985 to 1994 are included.

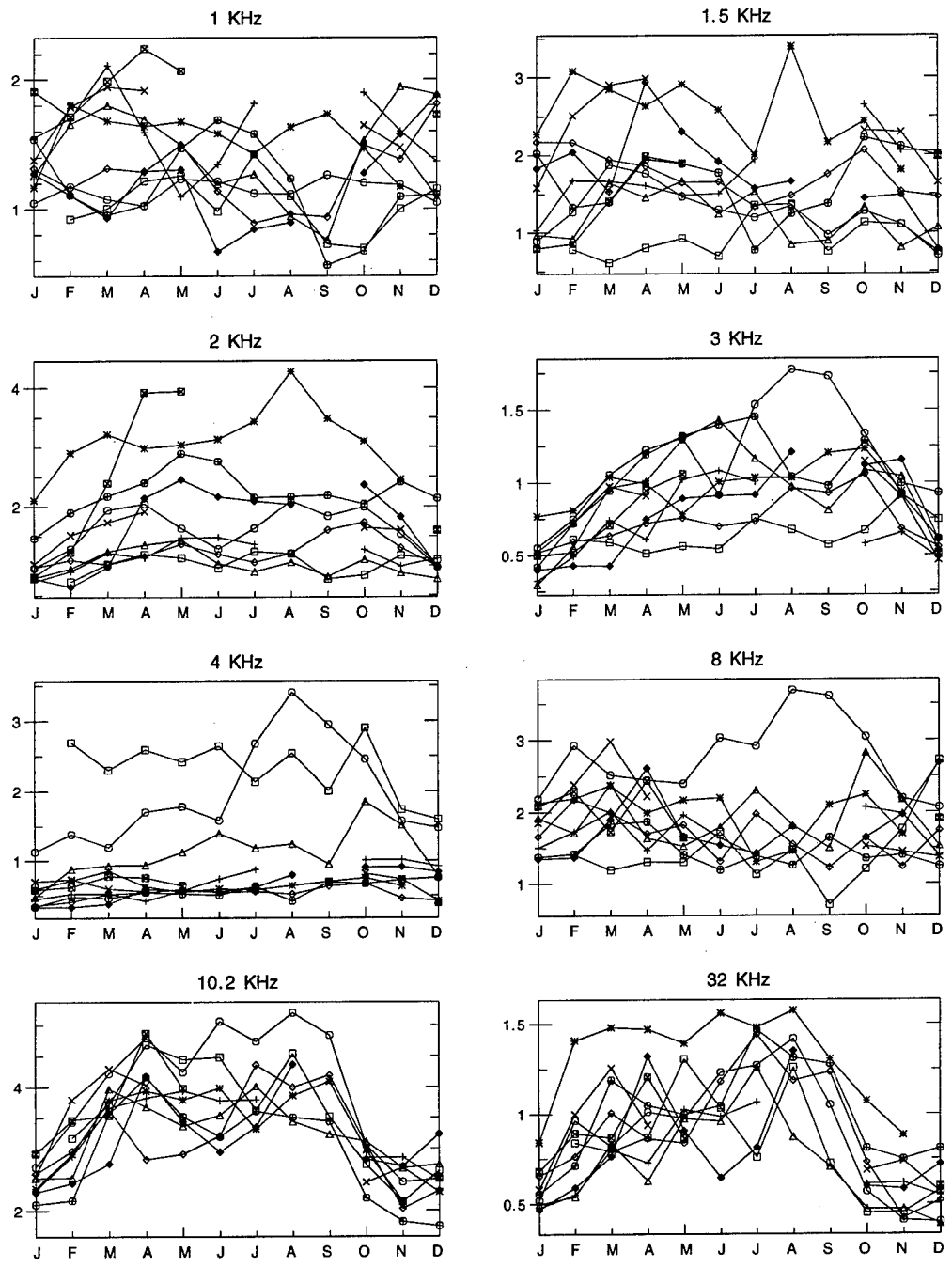

Figure 71: Monthly variation of ELF/VLF radio noise at Arrival Heights, Antarctica, for the eight highest-frequency channels and the 08-12 UT time block, each year shown individually. The years 1985 to 1994 are included.

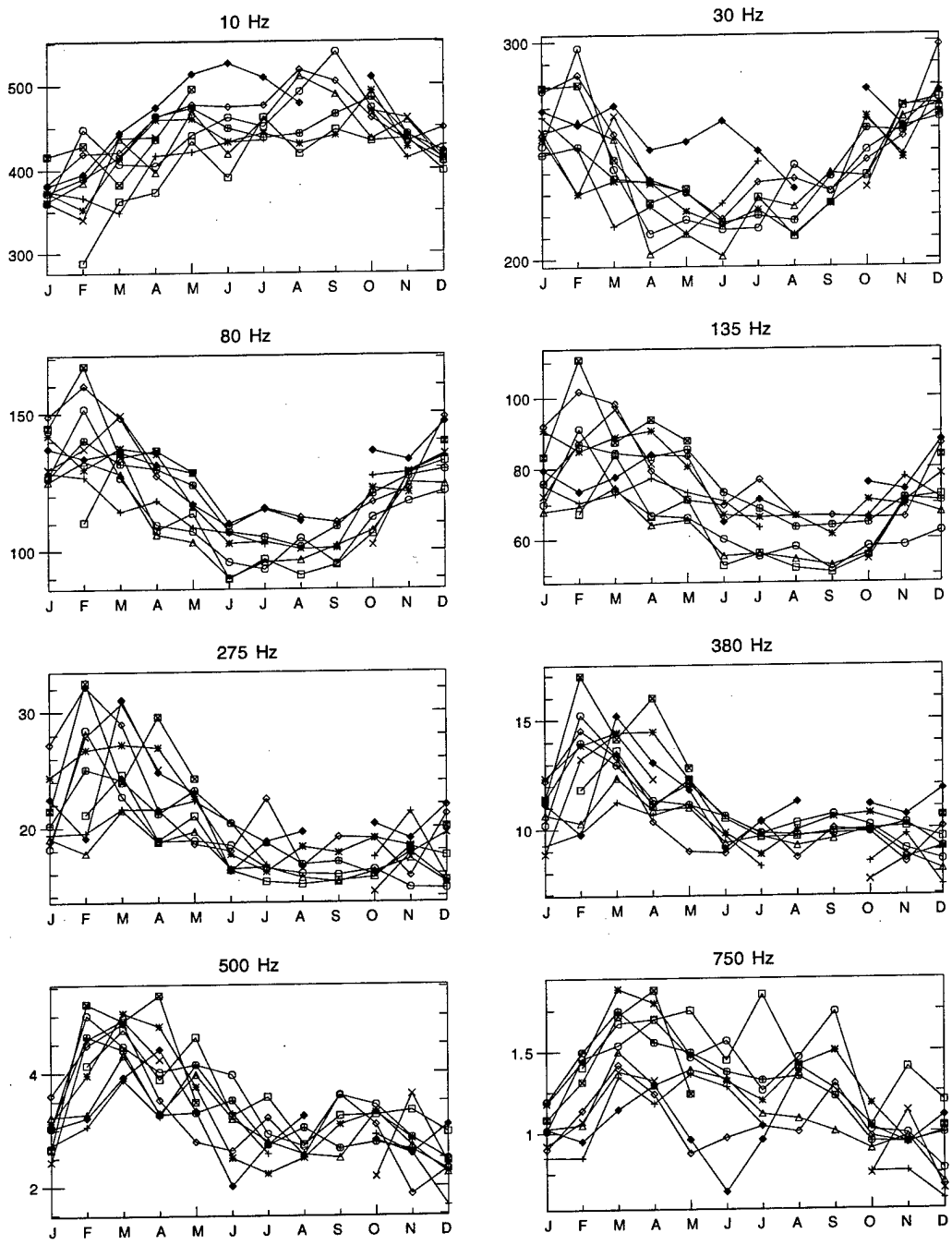

Figure 72: Monthly variation of ELF/VLF radio noise at Arrival Heights, Antarctica, for the eight lowest-frequency channels and the 12-16 UT time block, each year shown individually. The years 1985 to 1994 are included.

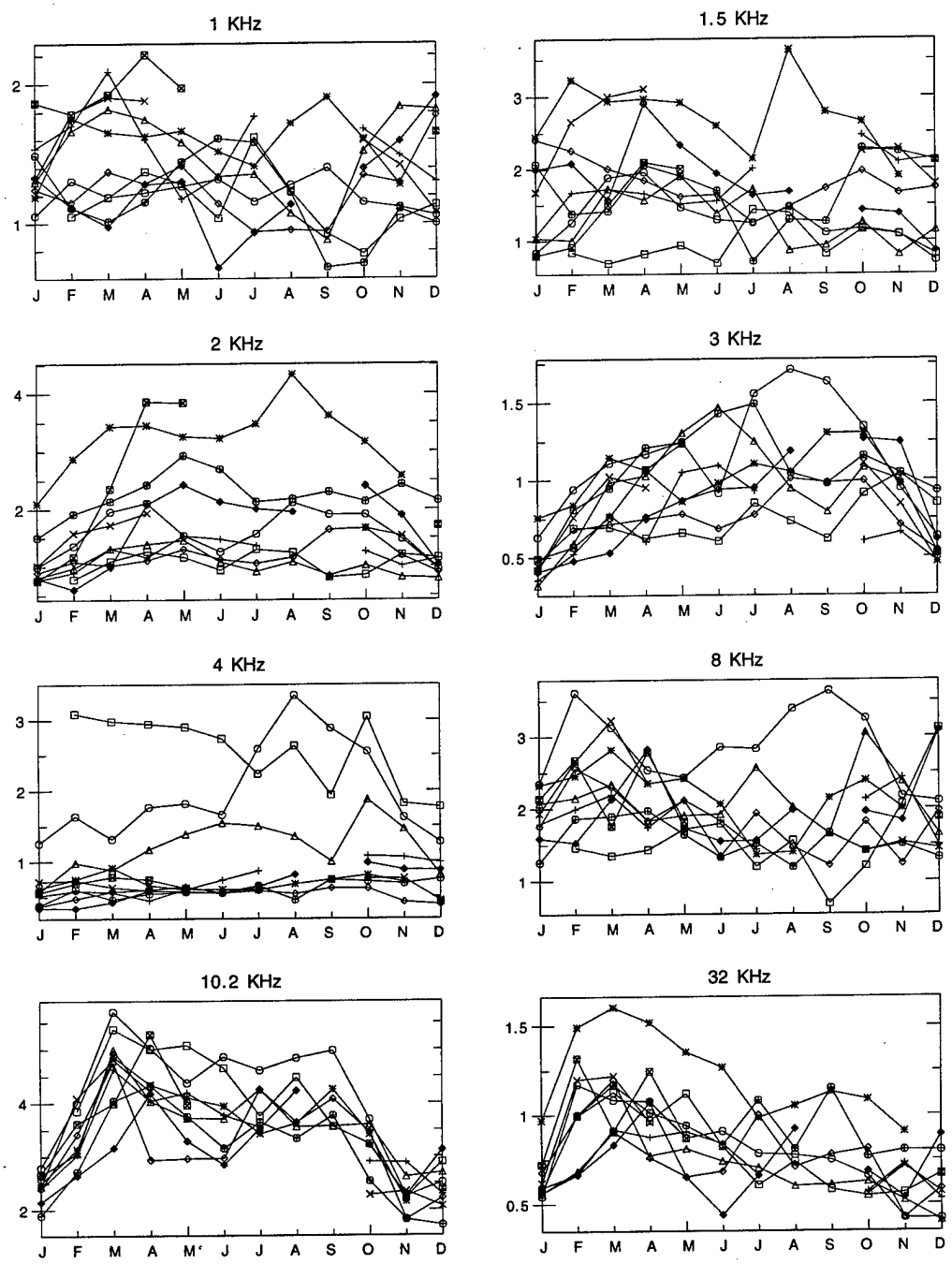

Figure 73: Monthly variation of ELF/VLF radio noise at Arrival Heights, Antarctica, for the eight highest-frequency channels and the 12-16 UT time block, each year shown individually. The years 1985 to 1994 are included.

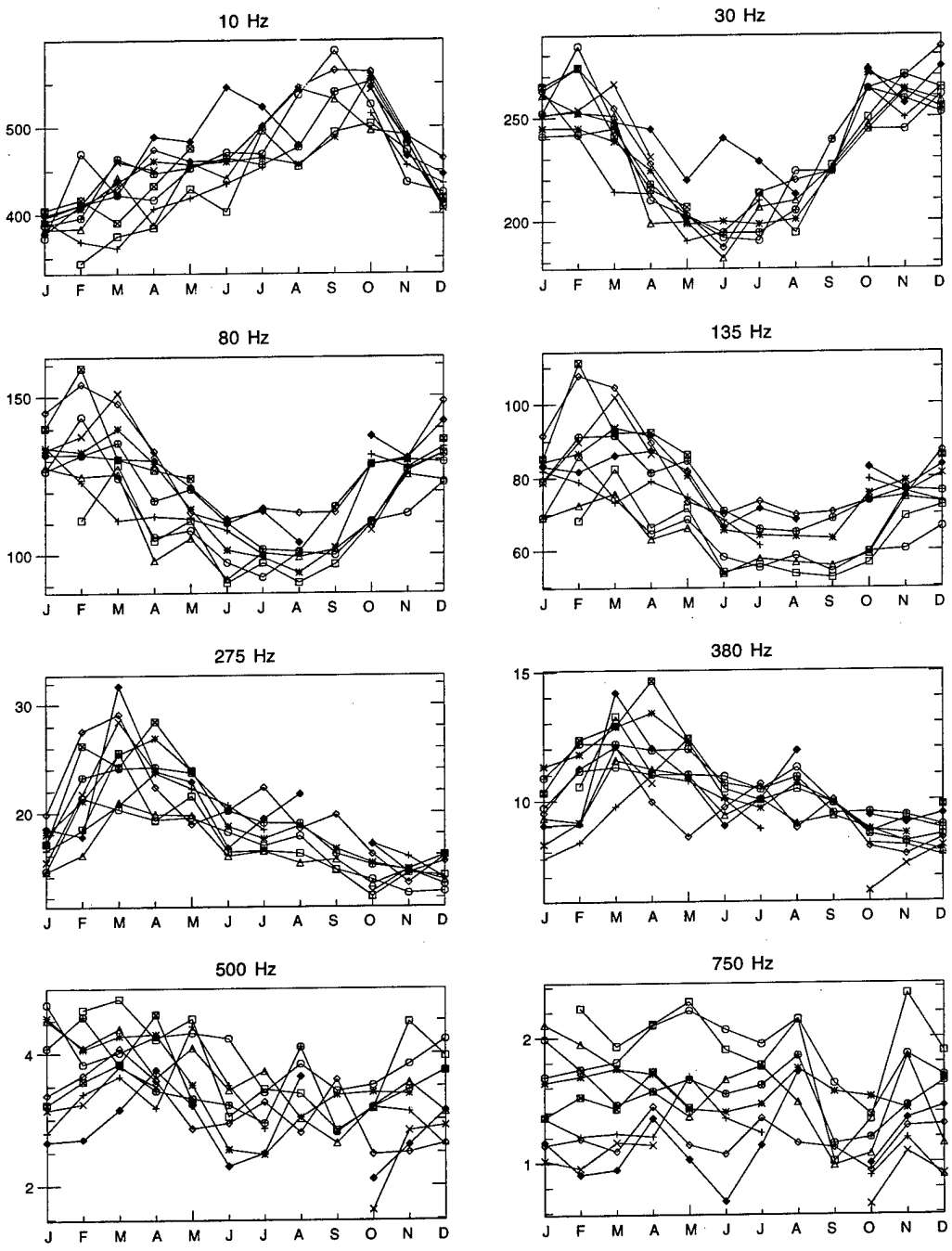

Figure 74: Monthly variation of ELF/VLF radio noise at Arrival Heights, Antarctica, for the eight lowest-frequency channels and the 16-20 UT time block, each year shown individually. The years 1985 to 1994 are included.

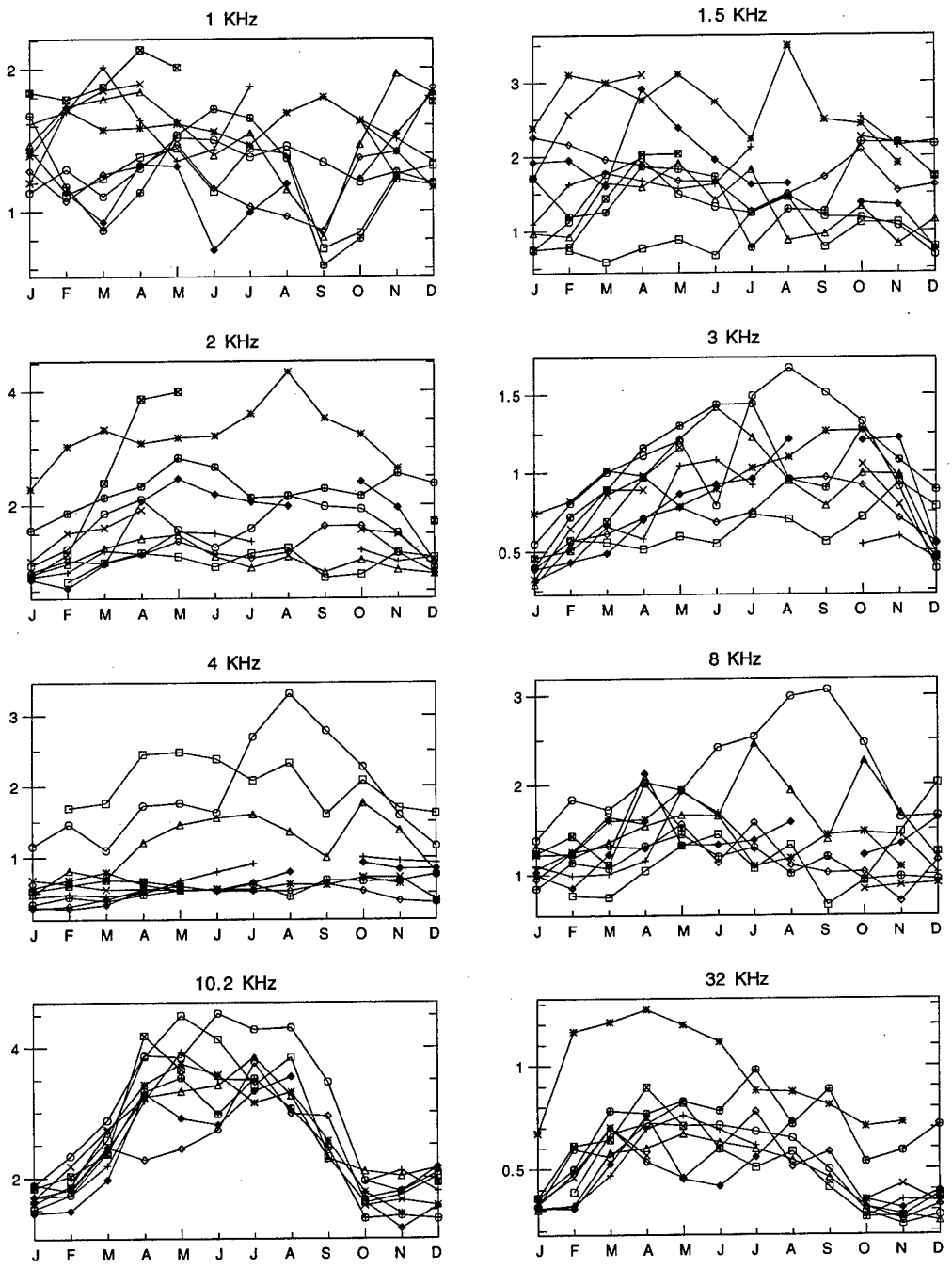

Figure 75: Monthly variation of ELF/VLF radio noise at Arrival Heights, Antarctica, for the eight highest-frequency channels and the 16-20 UT time block, each year shown individually. The years 1985 to 1994 are included.

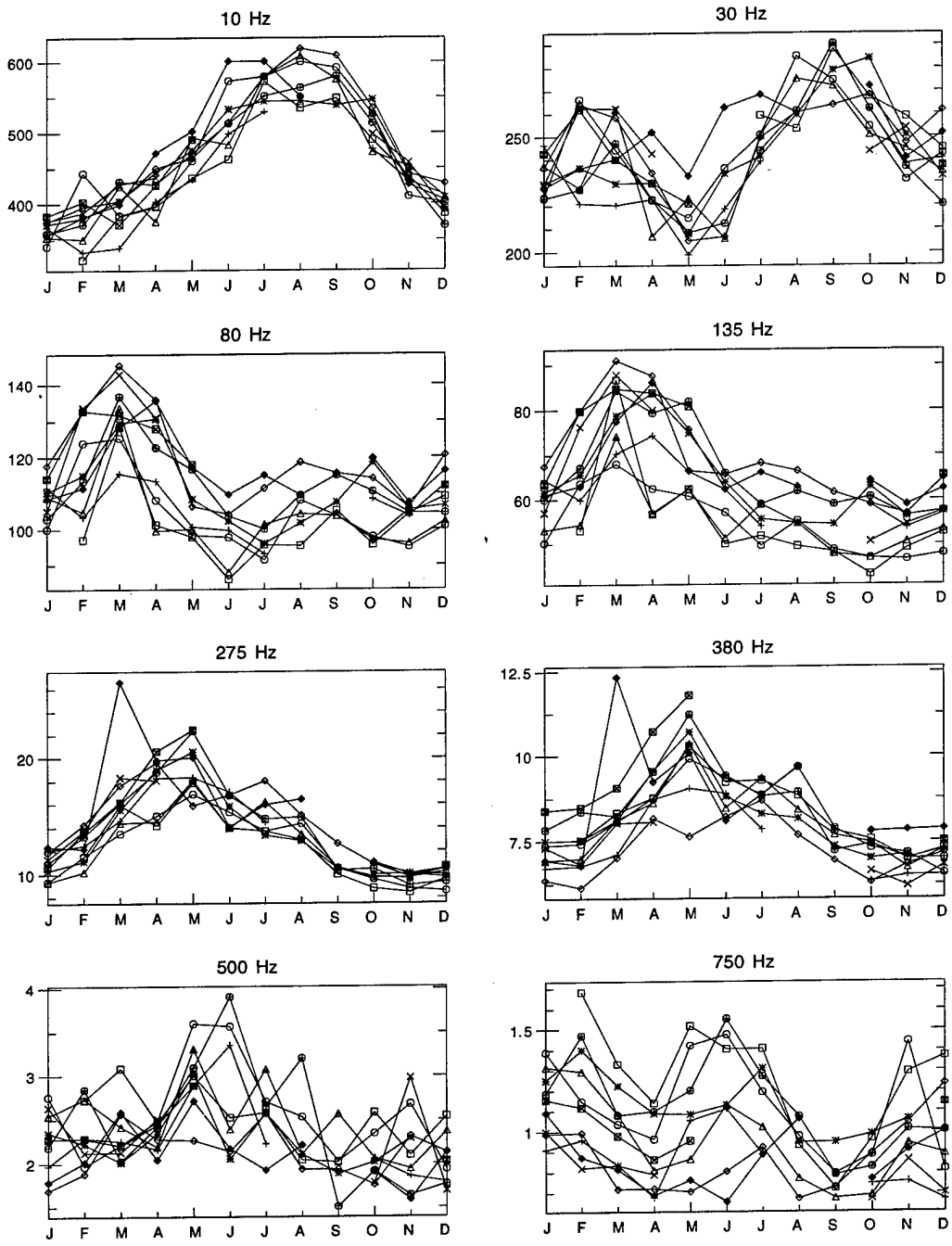

Figure 76: Monthly variation of ELF/VLF radio noise at Arrival Heights, Antarctica, for the eight lowest-frequency channels and the 20-24 UT time block, each year shown individually. The years 1985 to 1994 are included.

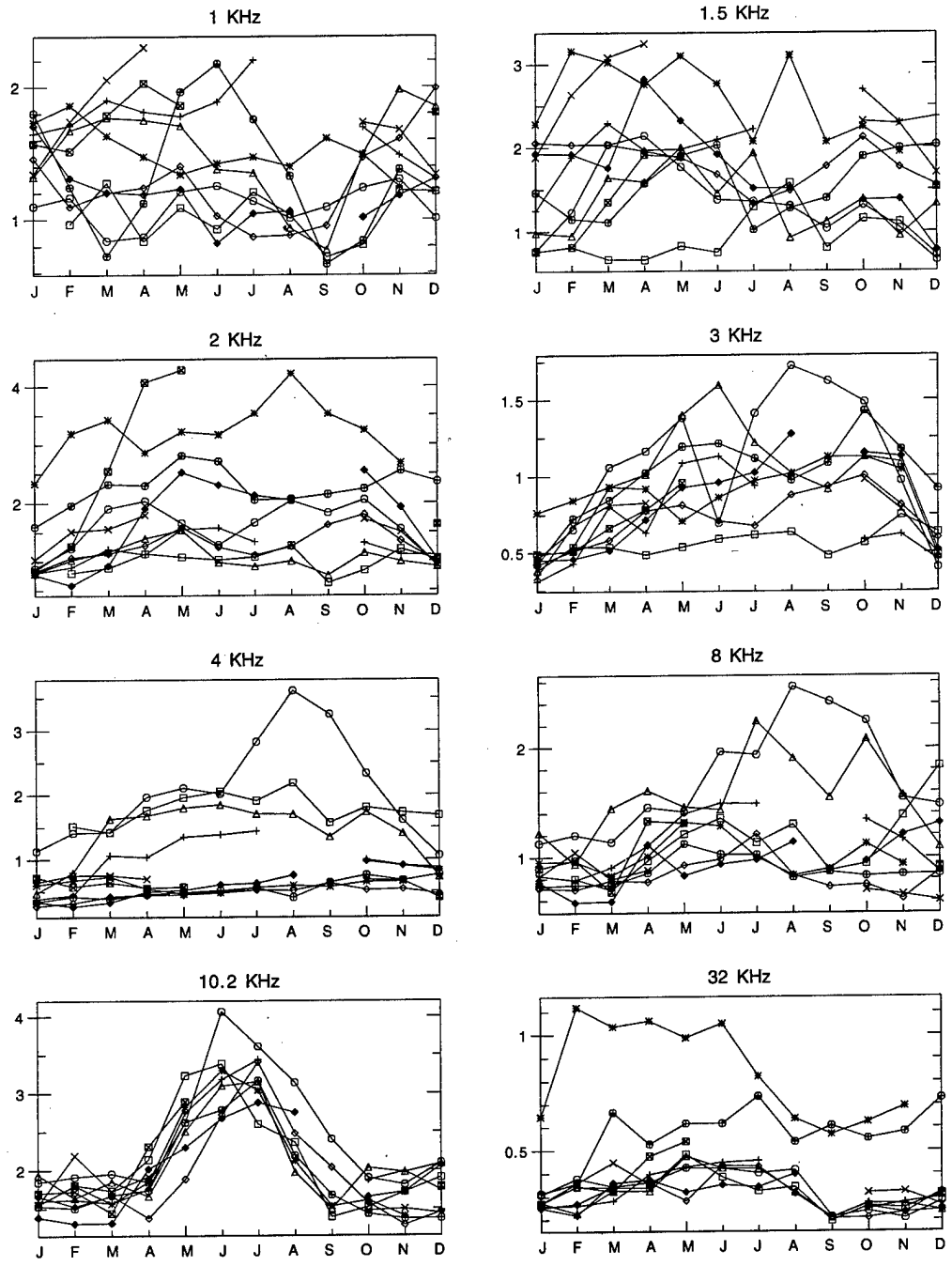

Figure 77: Monthly variation of ELF/VLF radio noise at Arrival Heights, Antarctica, for the eight highest-frequency channels and the 20-24 UT time block, each year shown individually. The years 1985 to 1994 are included.

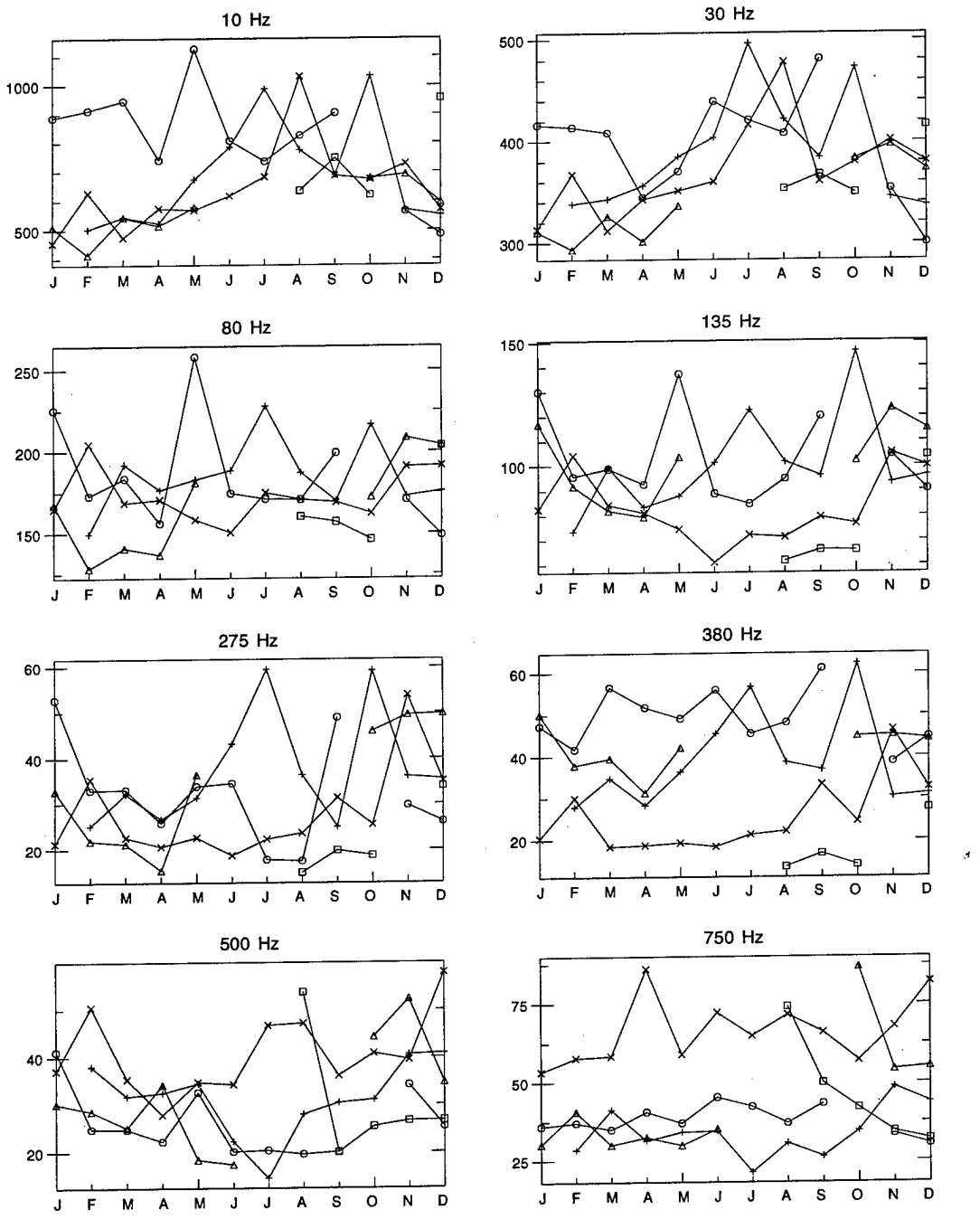

Figure 78: Monthly variation of ELF/VLF radio noise at Dunedin, New Zealand, for the eight lowest-frequency channels and the 00-04 UT time block, each year shown individually. The years 1986 to 1990 are included.

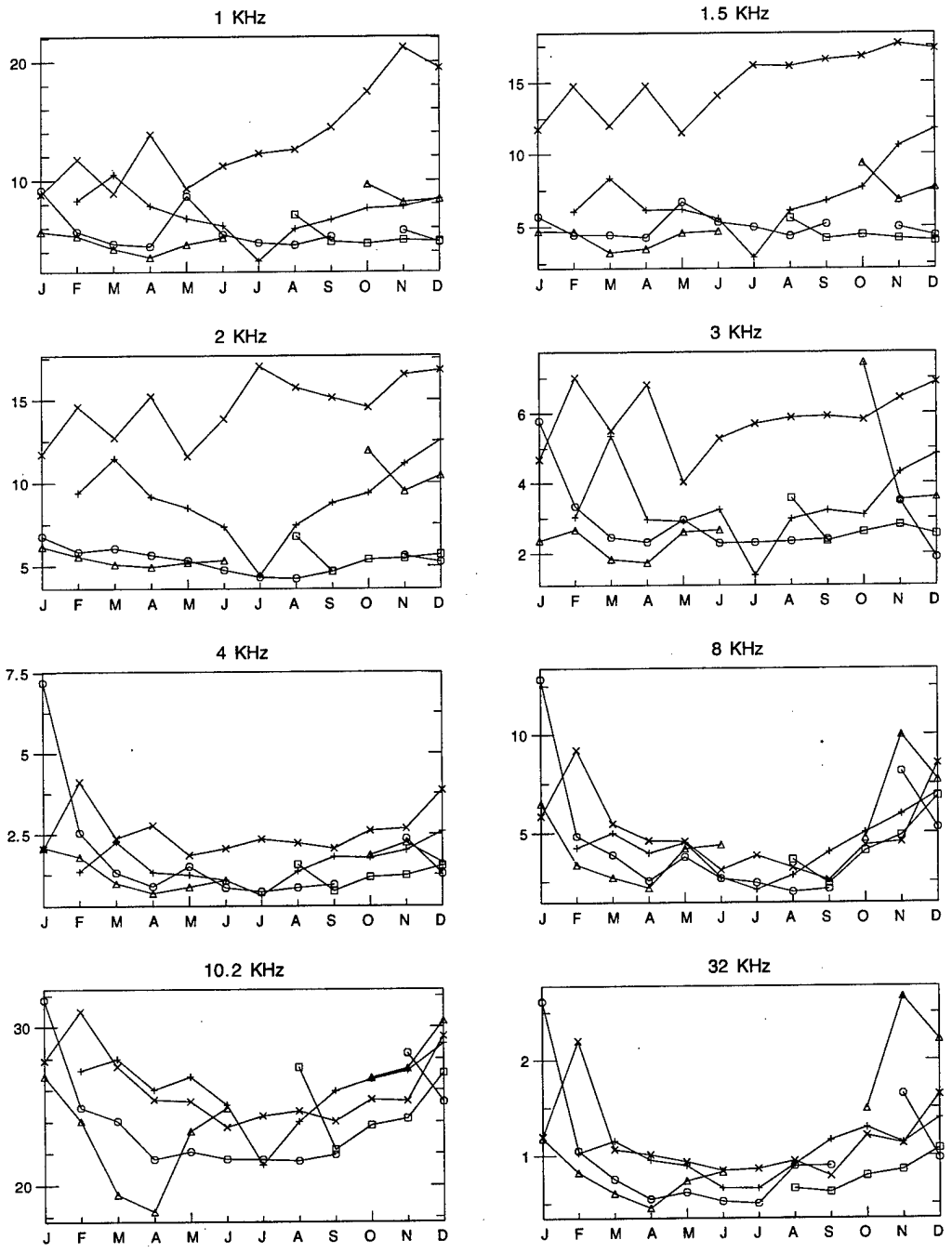

Figure 79: Monthly variation of ELF/VLF radio noise at Dunedin, New Zealand, for the eight highest-frequency channels and the 00-04 UT time block, each year shown individually. The years 1986 to 1990 are included.

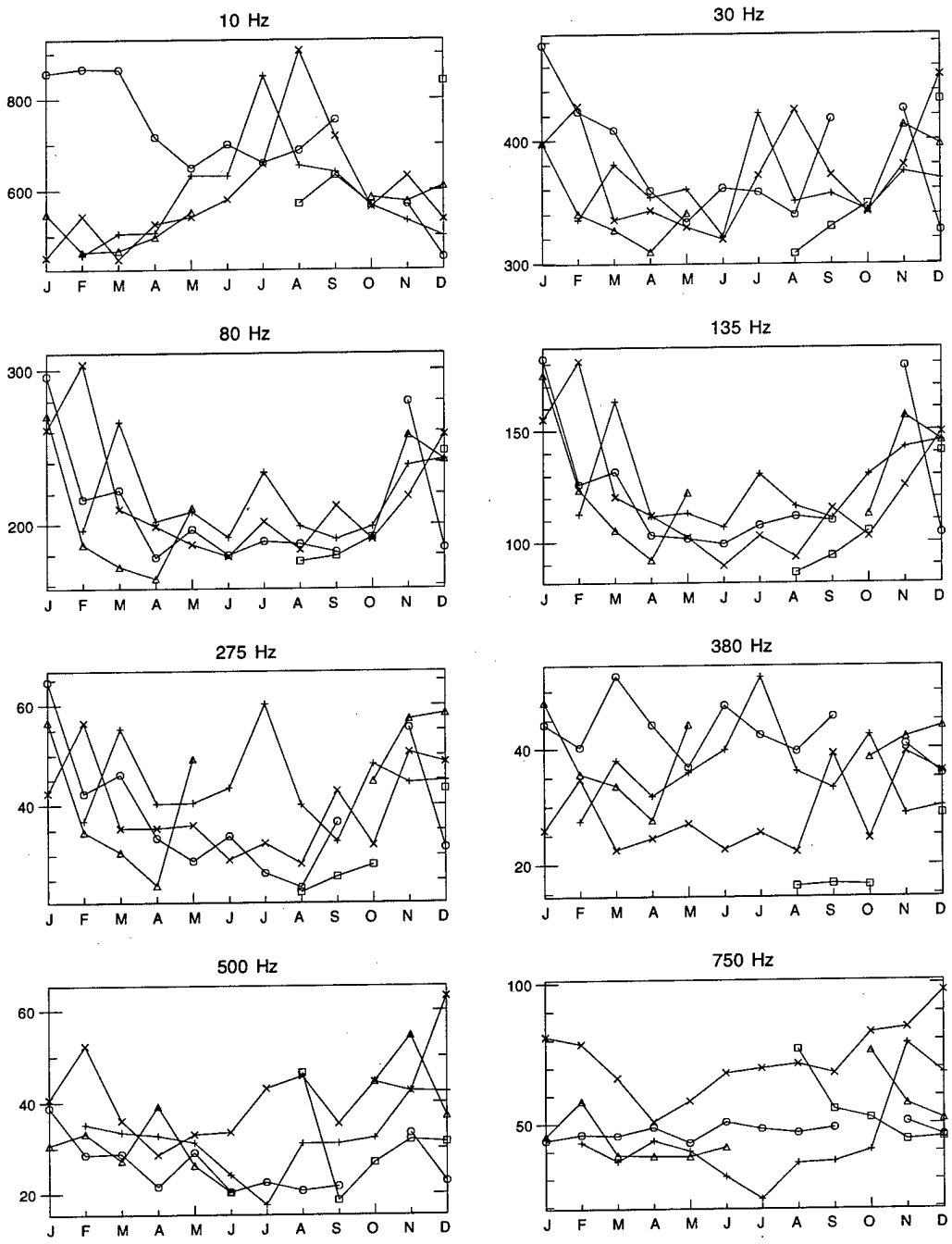

Figure 80: Monthly variation of ELF/VLF radio noise at Dunedin, New Zealand, for the eight lowest-frequency channels and the 04-08 UT time block, each year shown individually. The years 1986 to 1990 are included.

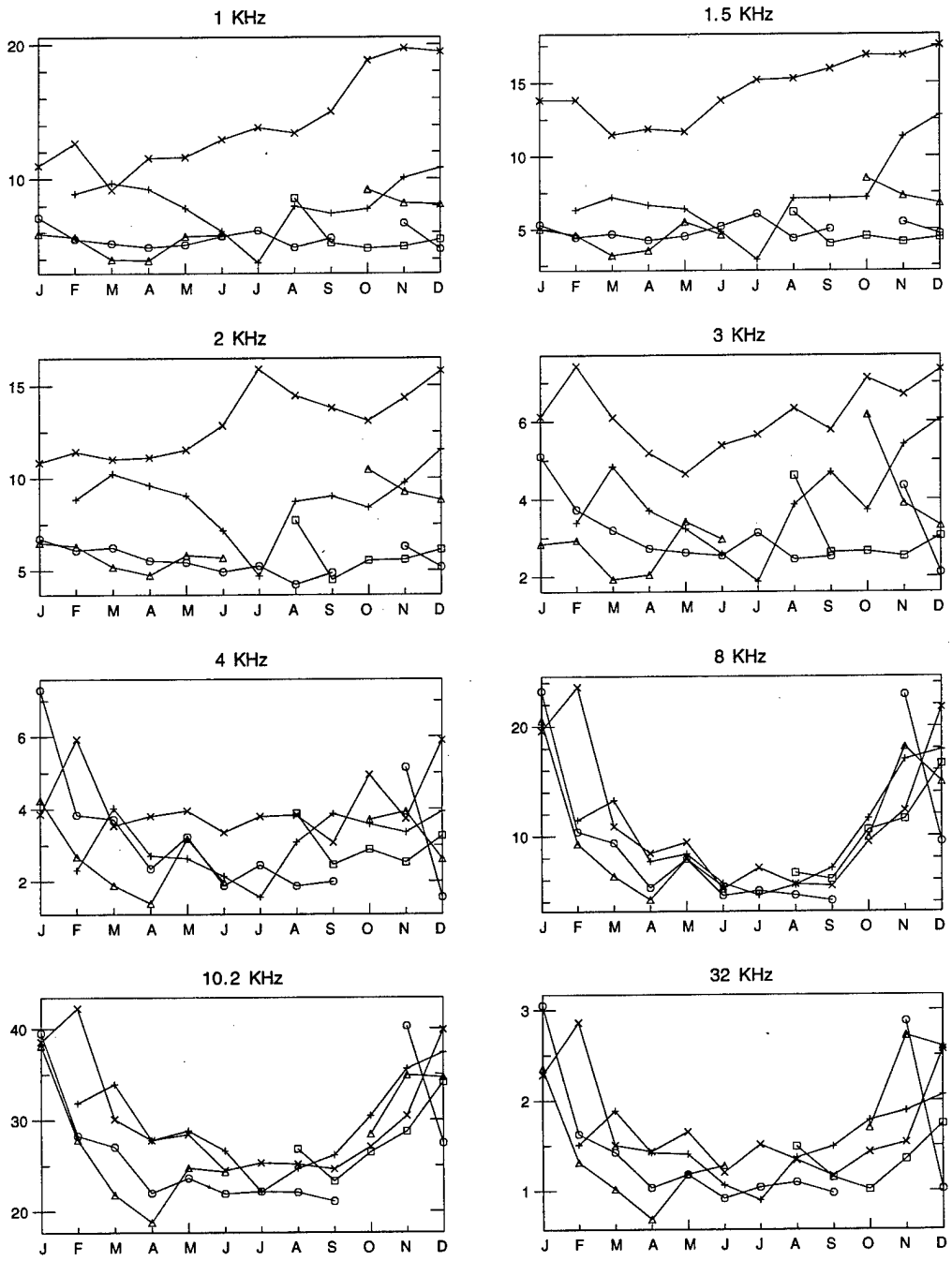

Figure 81: Monthly variation of ELF/VLF radio noise at Dunedin, New Zealand, for the eight highest-frequency channels and the 04-08 UT time block, each year shown individually. The years 1986 to 1990 are included.

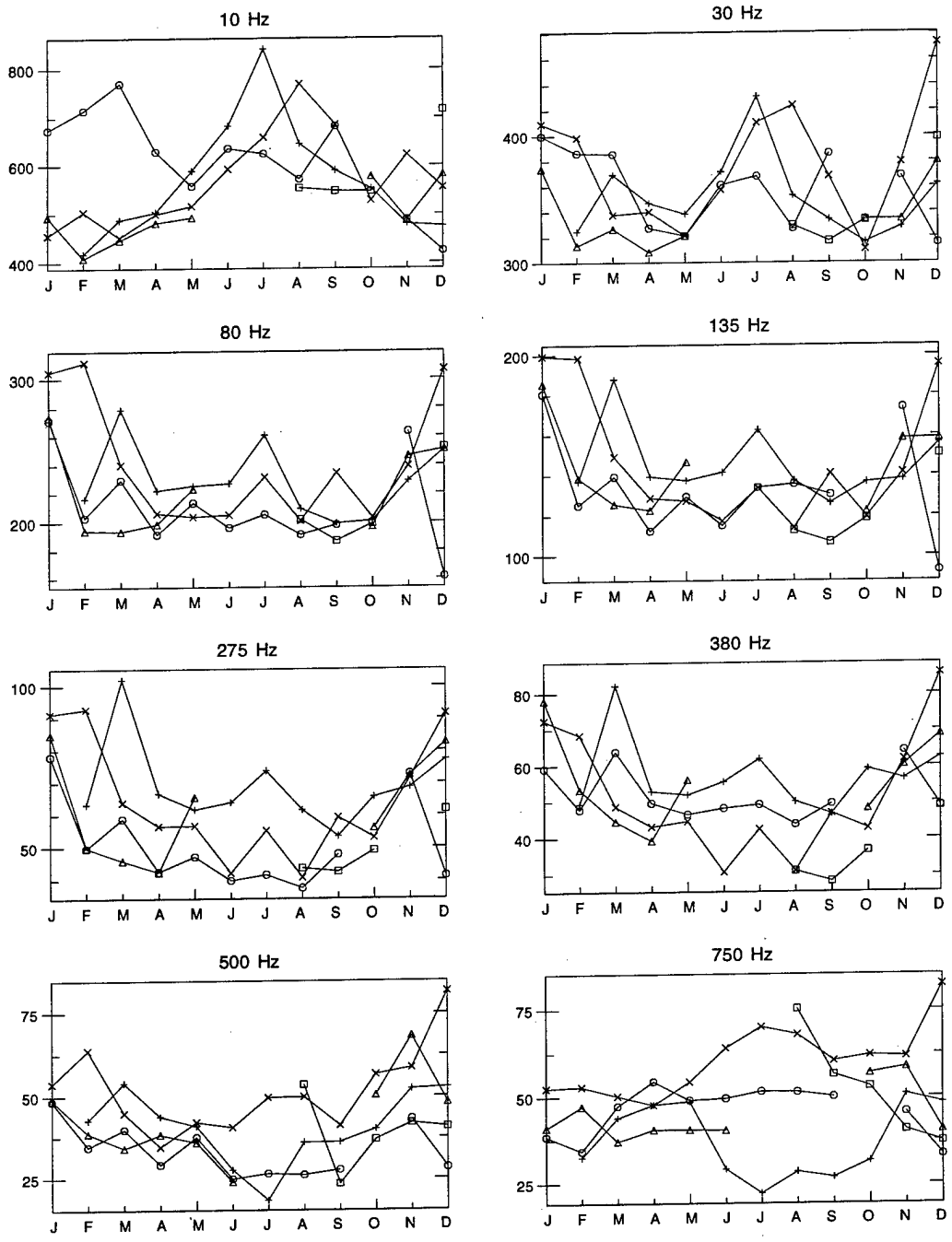

Figure 82: Monthly variation of ELF/VLF radio noise at Dunedin, New Zealand, for the eight lowest-frequency channels and the 08-12 UT time block, each year shown individually. The years 1986 to 1990 are included.

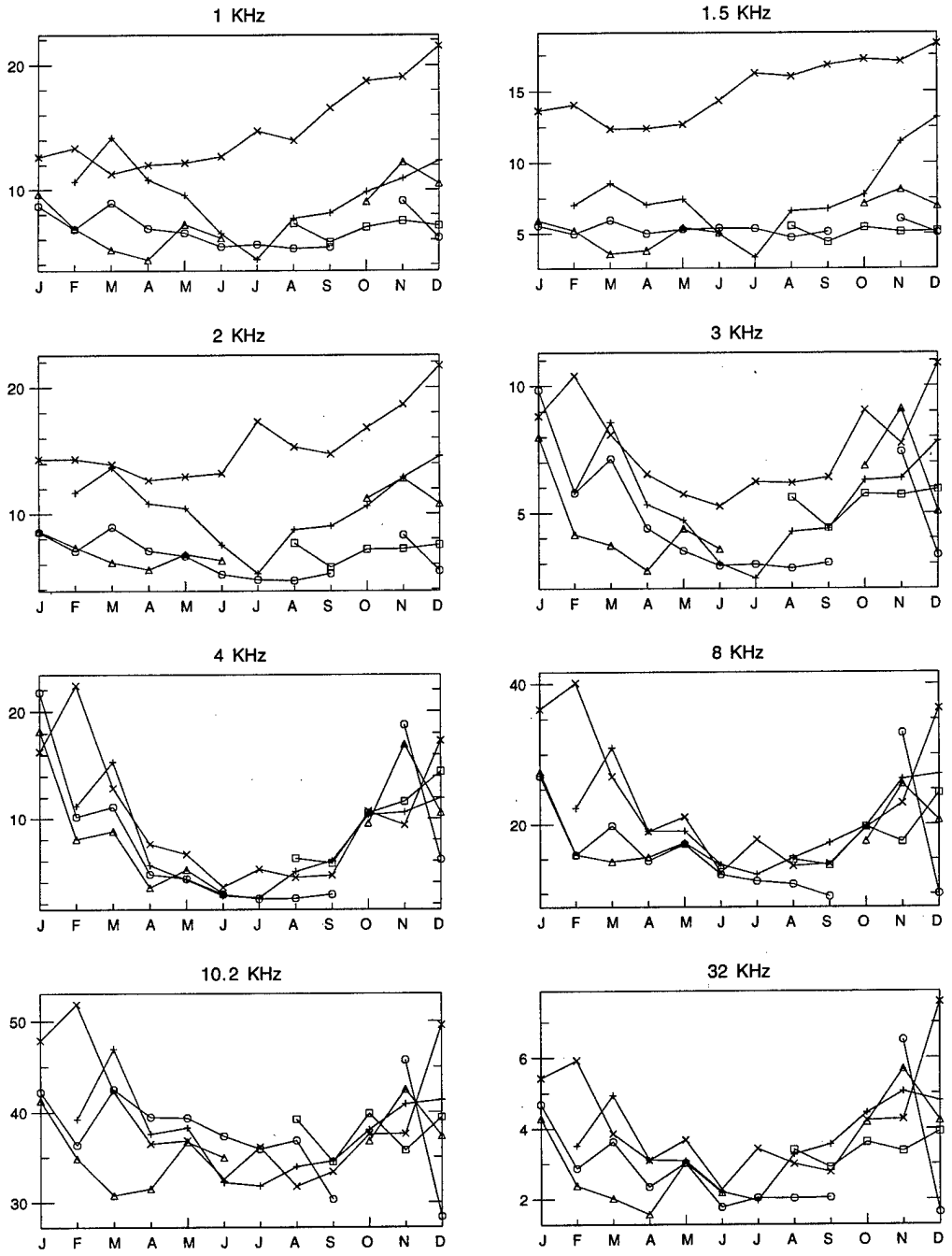

Figure 83: Monthly variation of ELF/VLF radio noise at Dunedin, New Zealand, for the eight highest-frequency channels and the 08-12 UT time block, each year shown individually. The years 1986 to 1990 are included.

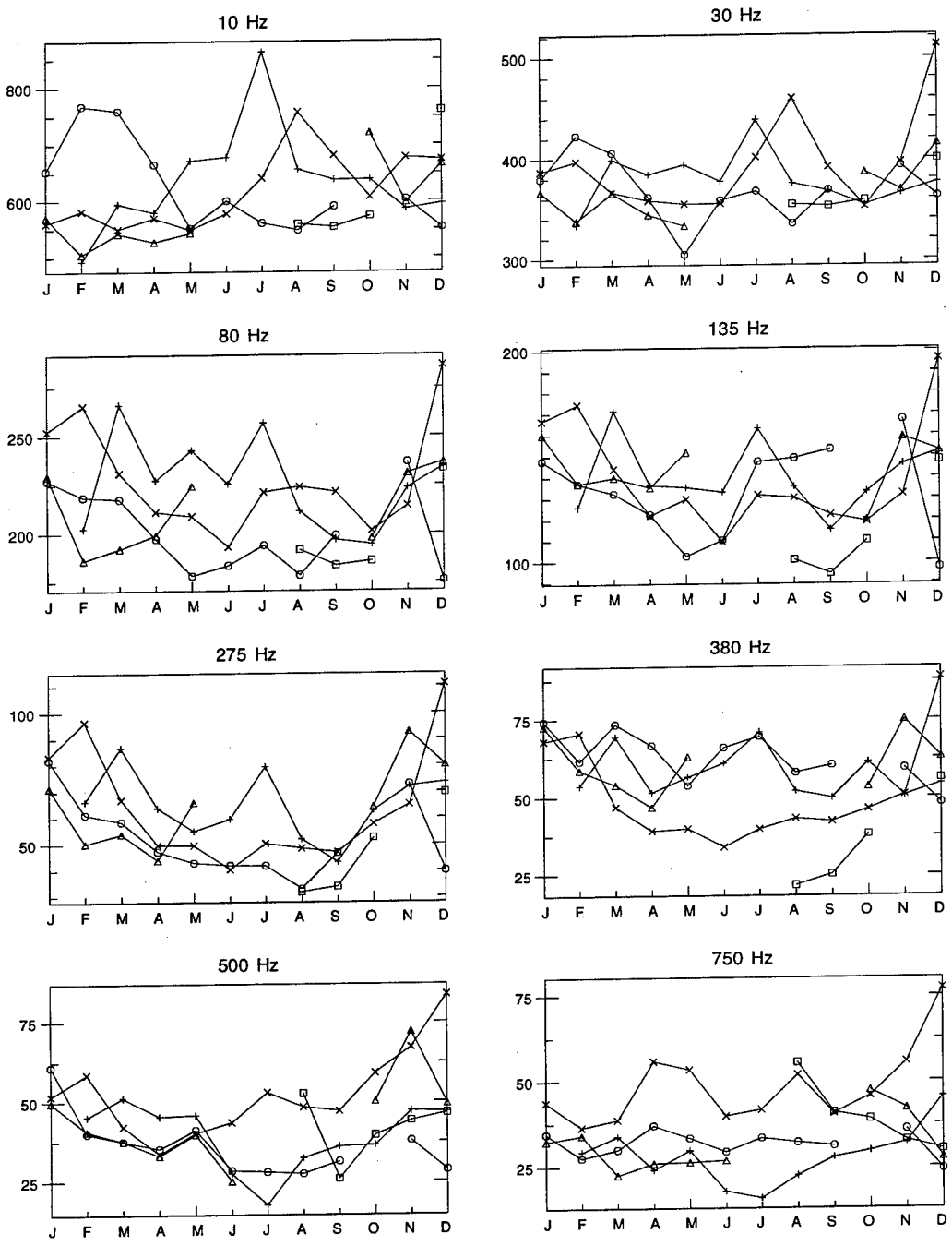

Figure 84: Monthly variation of ELF/VLF radio noise at Dunedin, New Zealand, for the eight lowest-frequency channels and the 12-16 UT time block, each year shown individually. The years 1986 to 1990 are included.

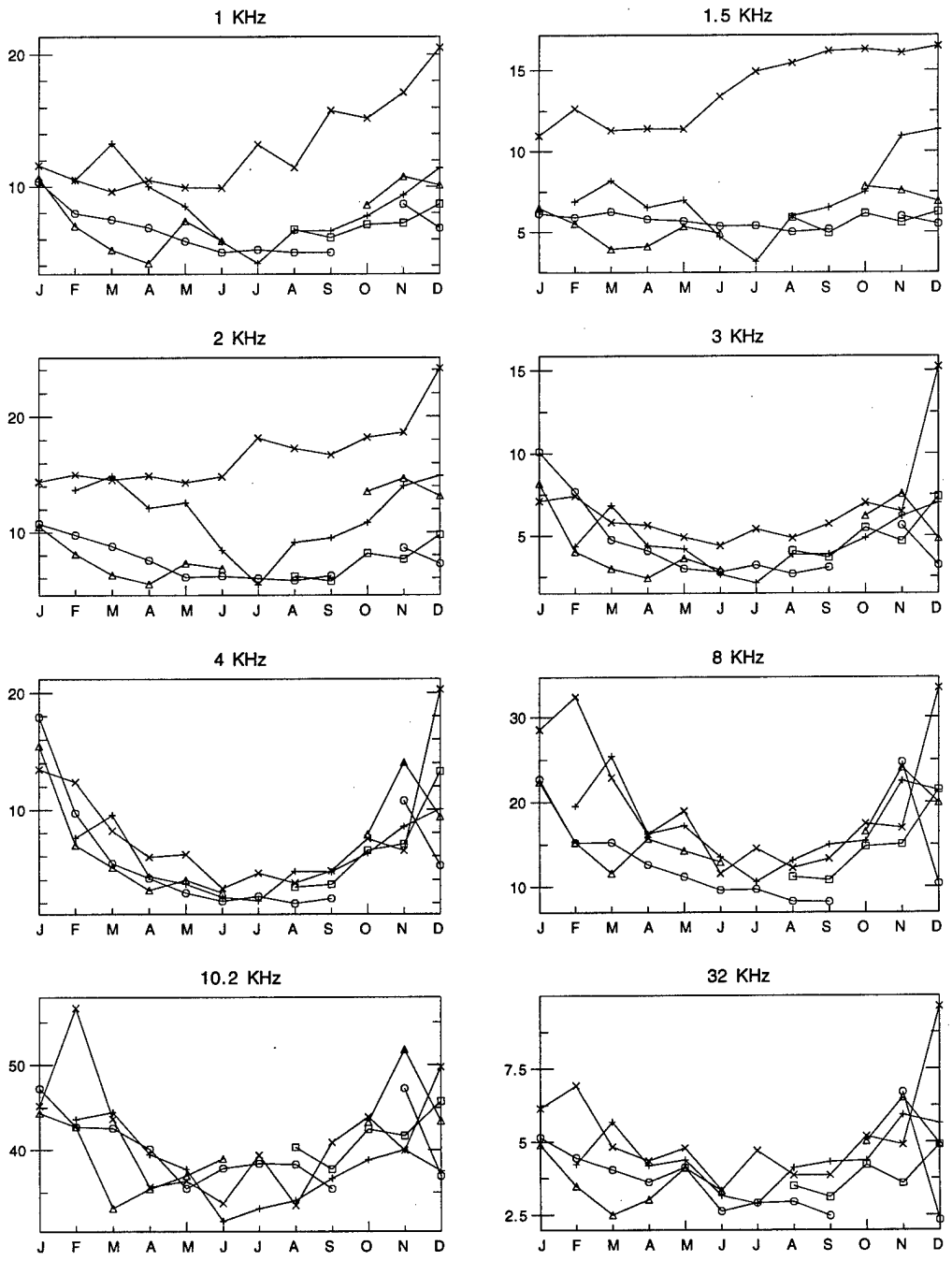

Figure 85: Monthly variation of ELF/VLF radio noise at Dunedin, New Zealand, for the eight highest-frequency channels and the 12-16 UT time block, each year shown individually. The years 1986 to 1990 are included.

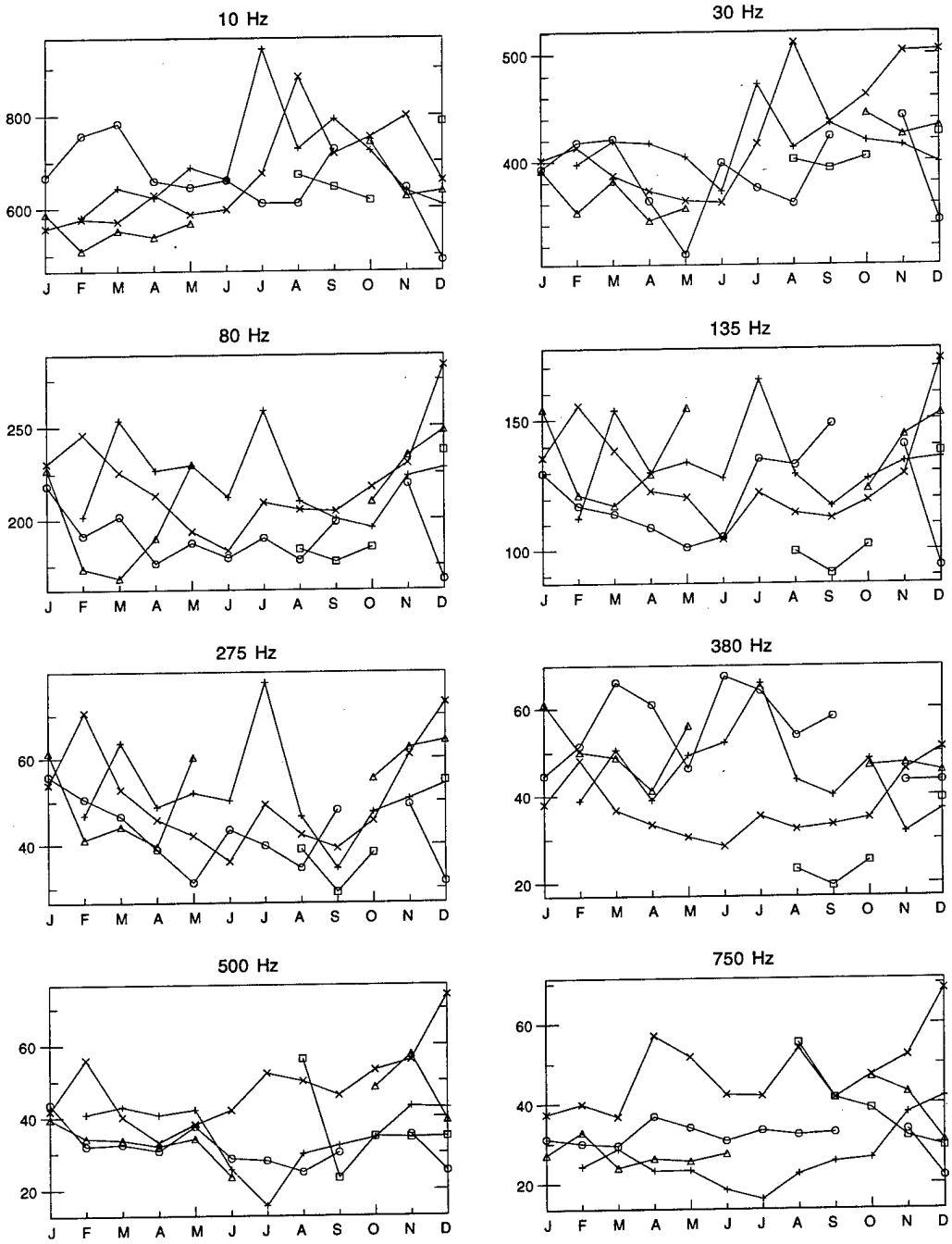

Figure 86: Monthly variation of ELF/VLF radio noise at Dunedin, New Zealand, for the eight lowest-frequency channels and the 16-20 UT time block, each year shown individually. The years 1986 to 1990 are included.

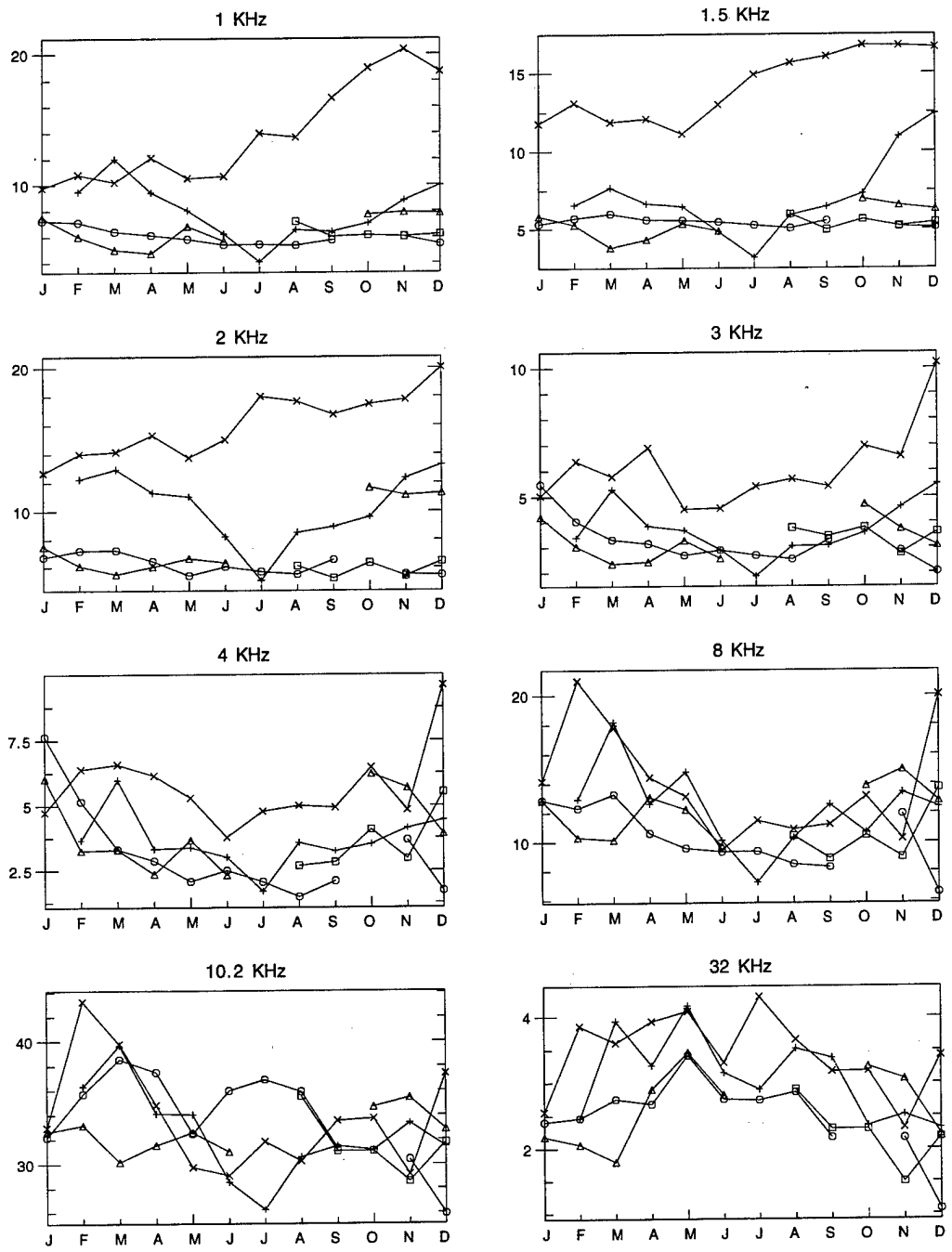

Figure 87: Monthly variation of ELF/VLF radio noise at Dunedin, New Zealand, for the eight highest-frequency channels and the 16-20 UT time block, each year shown individually. The years 1986 to 1990 are included.

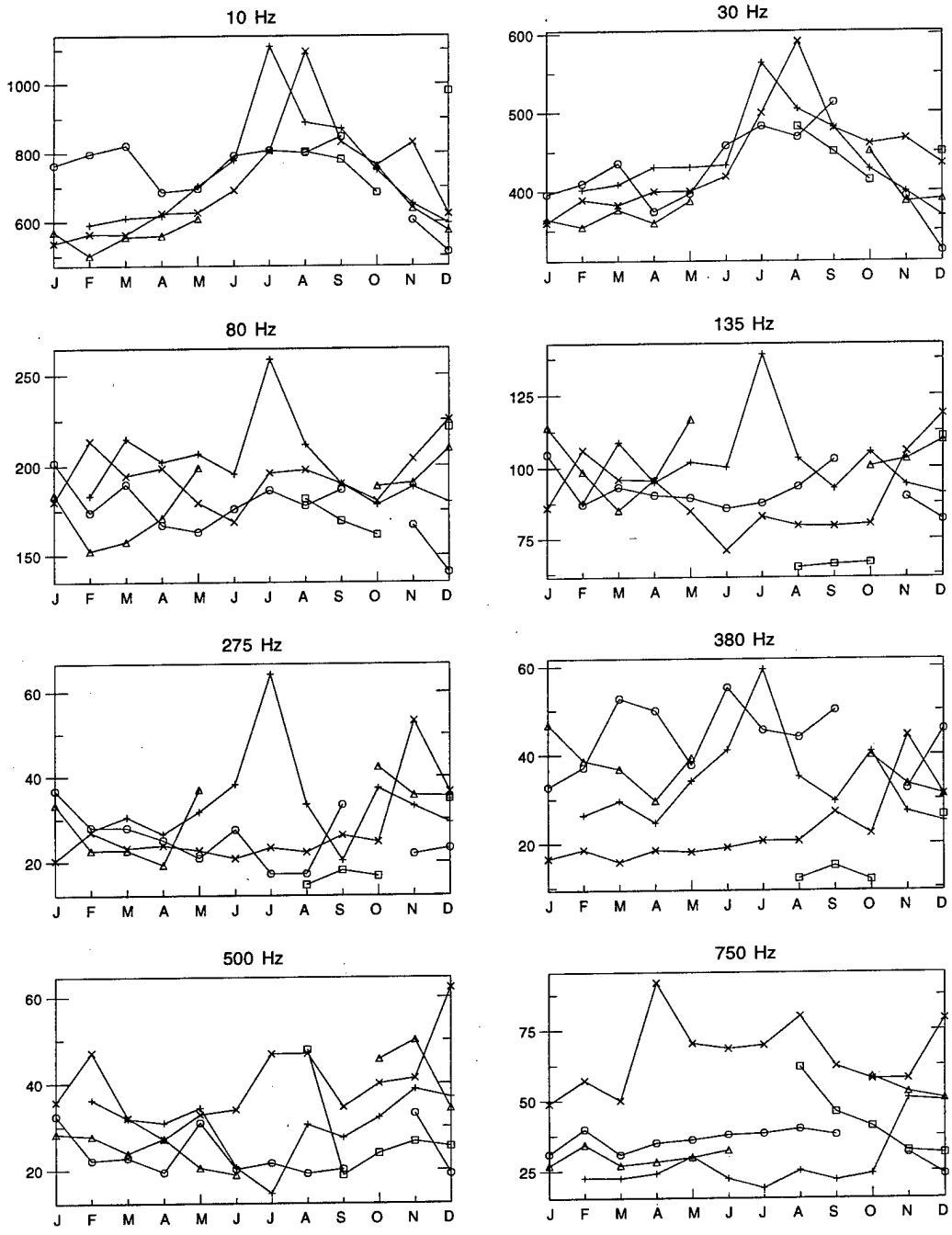

Figure 88: Monthly variation of ELF/VLF radio noise at Dunedin, New Zealand, for the eight lowest-frequency channels and the 20-24 UT time block, each year shown individually. The years 1986 to 1990 are included.

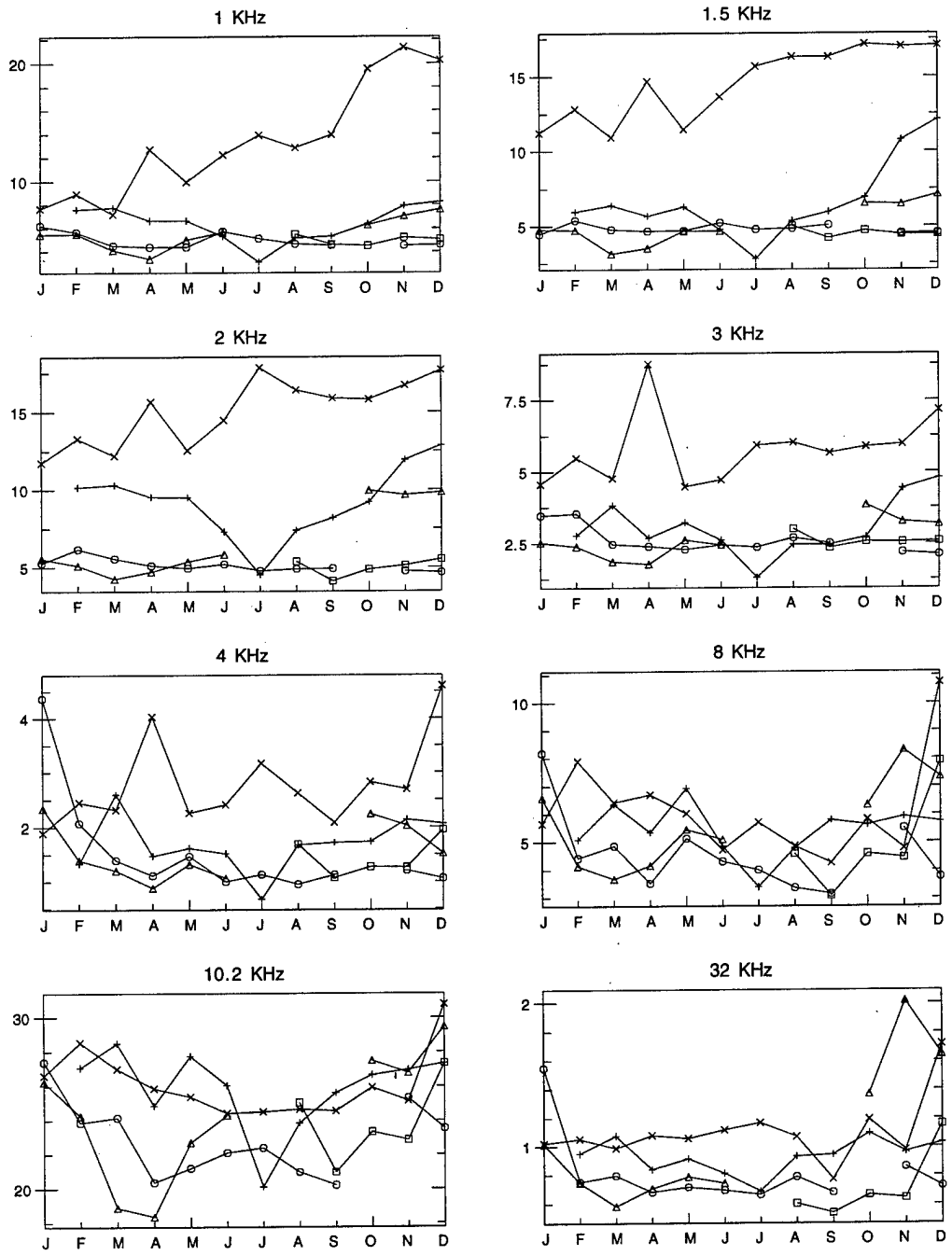

Figure 89: Monthly variation of ELF/VLF radio noise at Dunedin, New Zealand, for the eight highest-frequency channels and the 20-24 UT time block, each year shown individually. The years 1986 to 1990 are included.

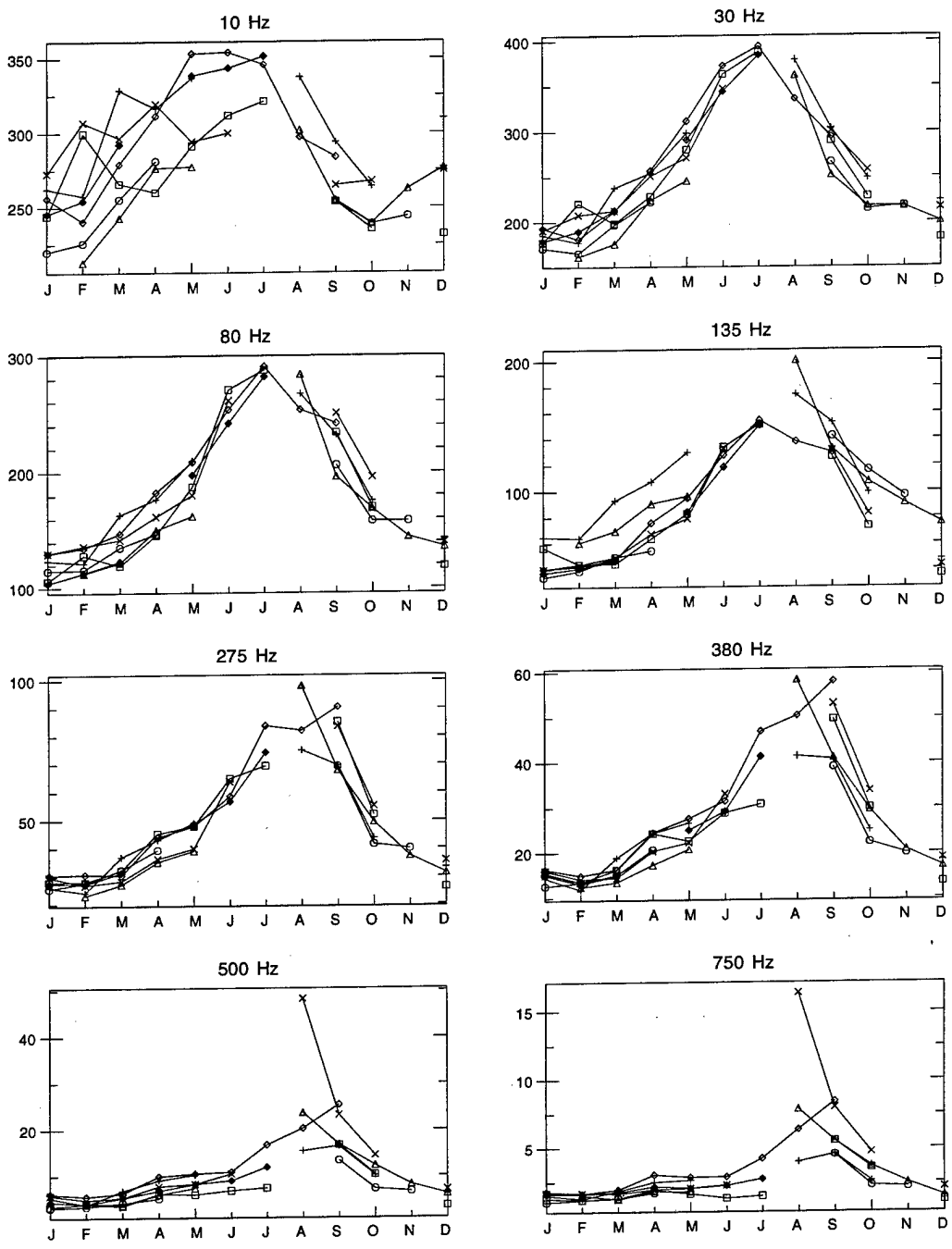

Figure 90: Monthly variation of ELF/VLF radio noise at Søndrestrøm, Greenland, for the eight lowest-frequency channels and the 00-04 UT time block, each year shown individually. The years 1986 to 1991 and the year 1993 are included.

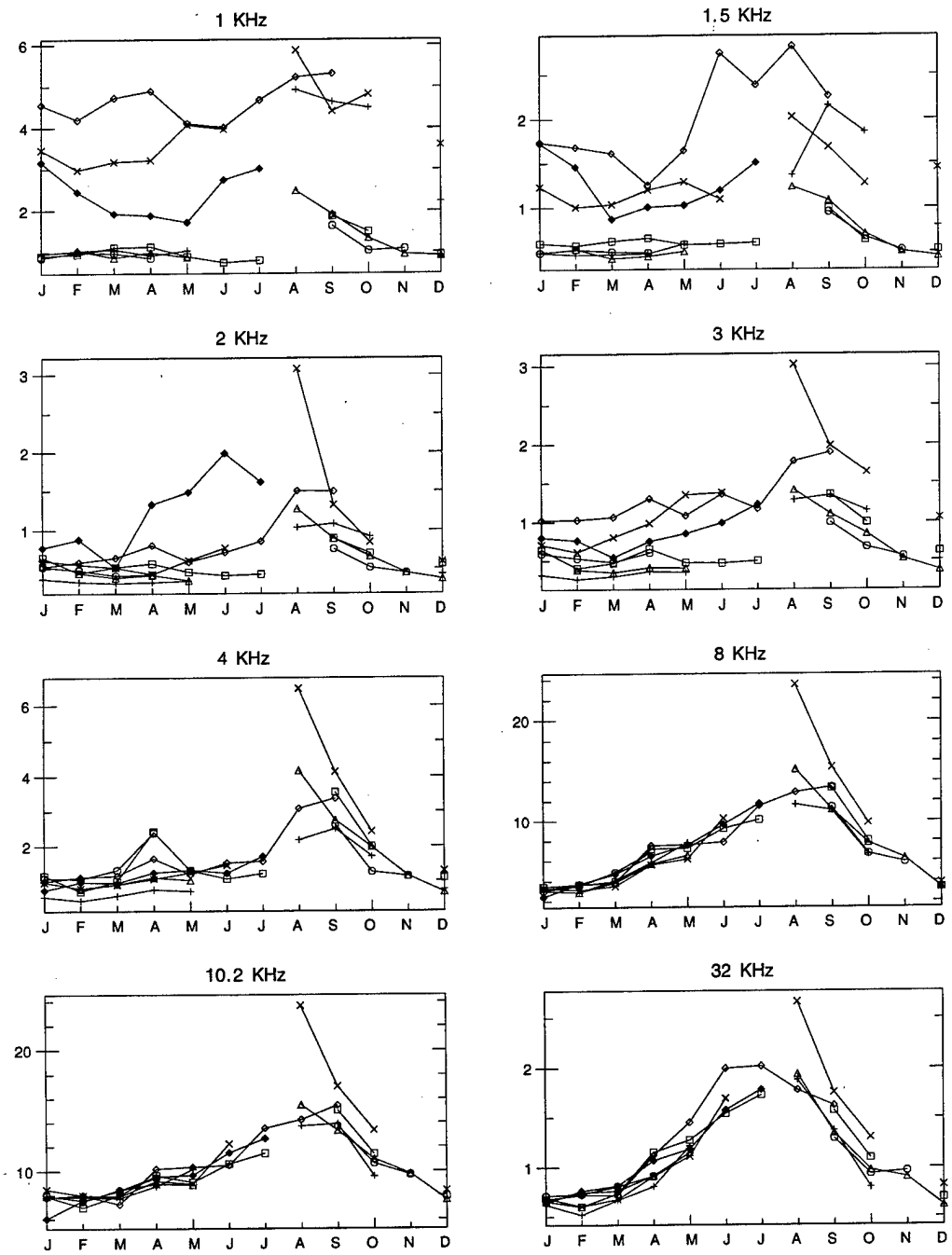

Figure 91: Monthly variation of ELF/VLF radio noise at Søndrestrøm, Greenland, for the eight highest-frequency channels and the 00-04 UT time block, each year shown individually. The years 1986 to 1991 and the year 1993 are included.

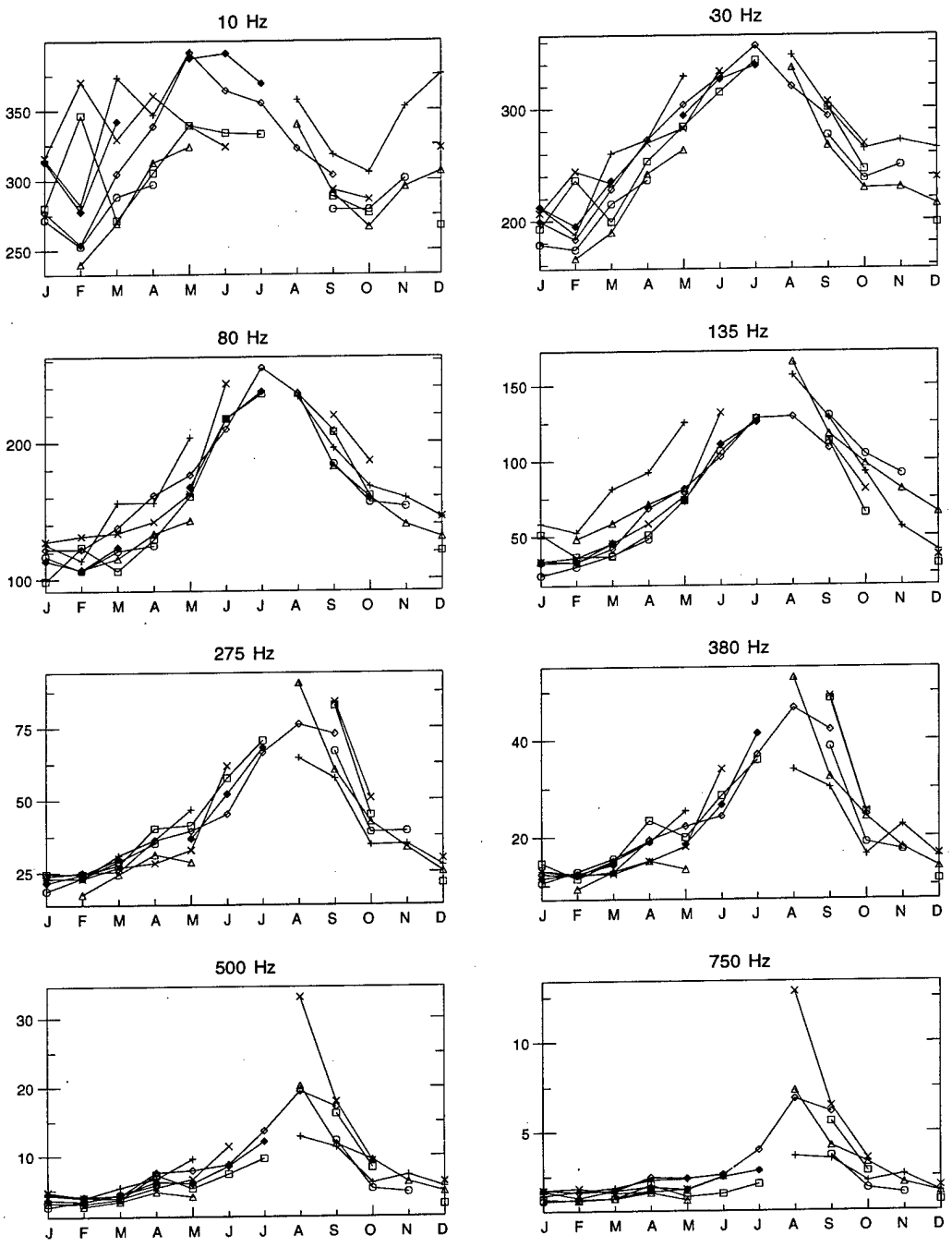

Figure 92: Monthly variation of ELF/VLF radio noise at Søndrestrøm, Greenland, for the eight lowest-frequency channels and the 04-08 UT time block, each year shown individually. The years 1986 to 1991 and the year 1993 are included.

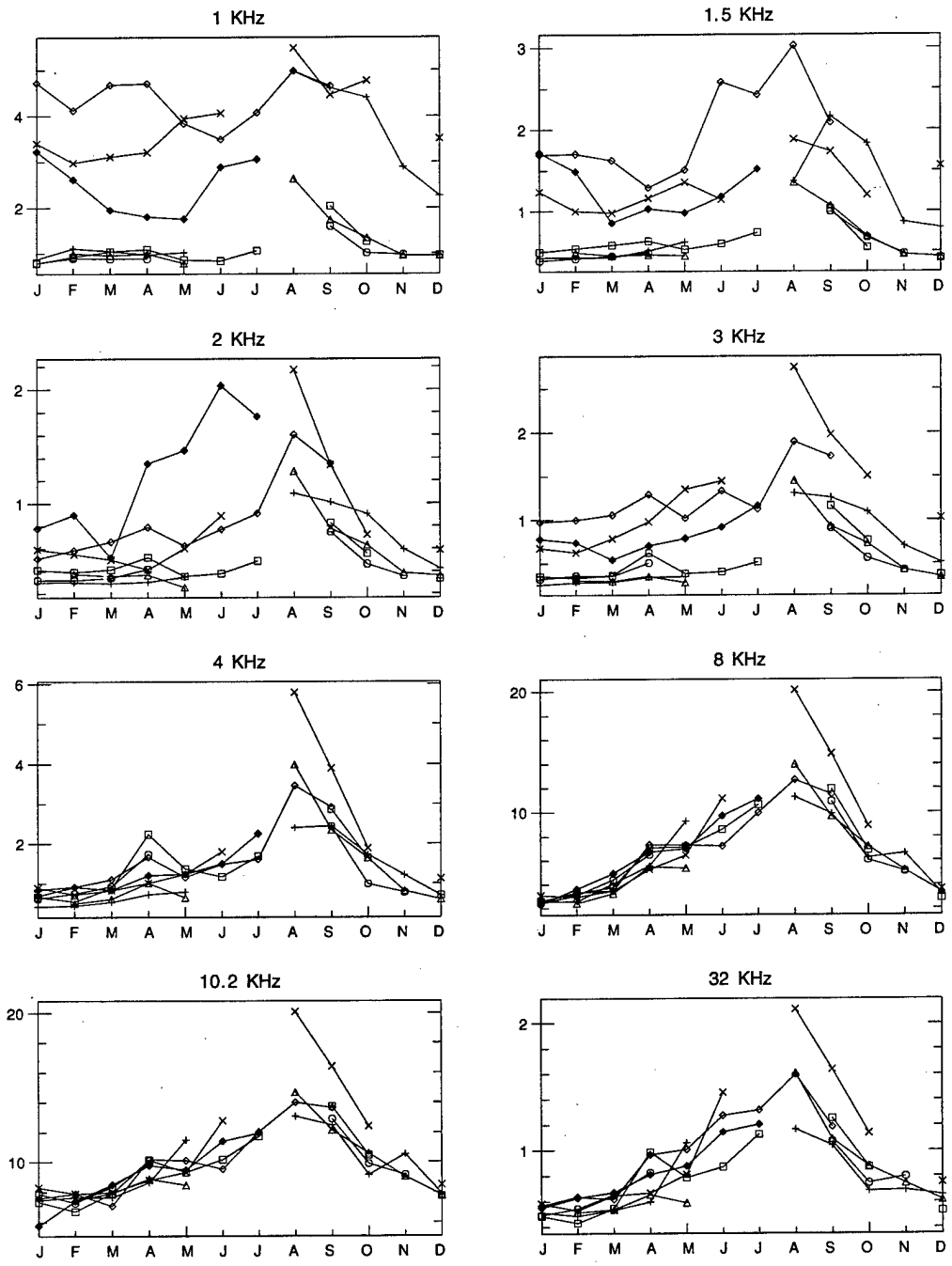

Figure 93: Monthly variation of ELF/VLF radio noise at Søndrestrøm, Greenland, for the eight highest-frequency channels and the 04-08 UT time block, each year shown individually. The years 1986 to 1991 and the year 1993 are included.

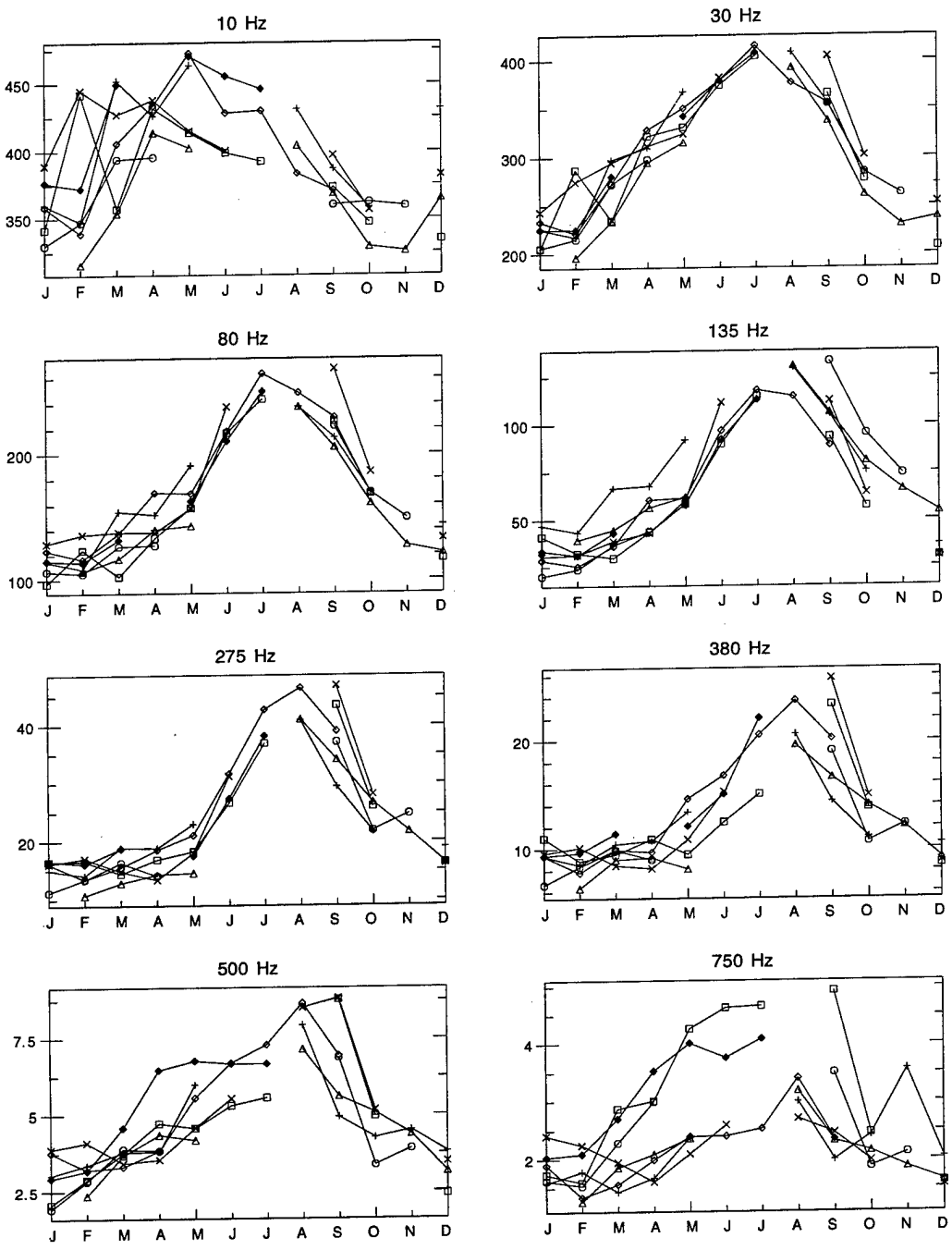

Figure 94: Monthly variation of ELF/VLF radio noise at Søndrestrøm, Greenland, for the eight lowest-frequency channels and the 08-12 UT time block, each year shown individually. The years 1986 to 1991 and the year 1993 are included.

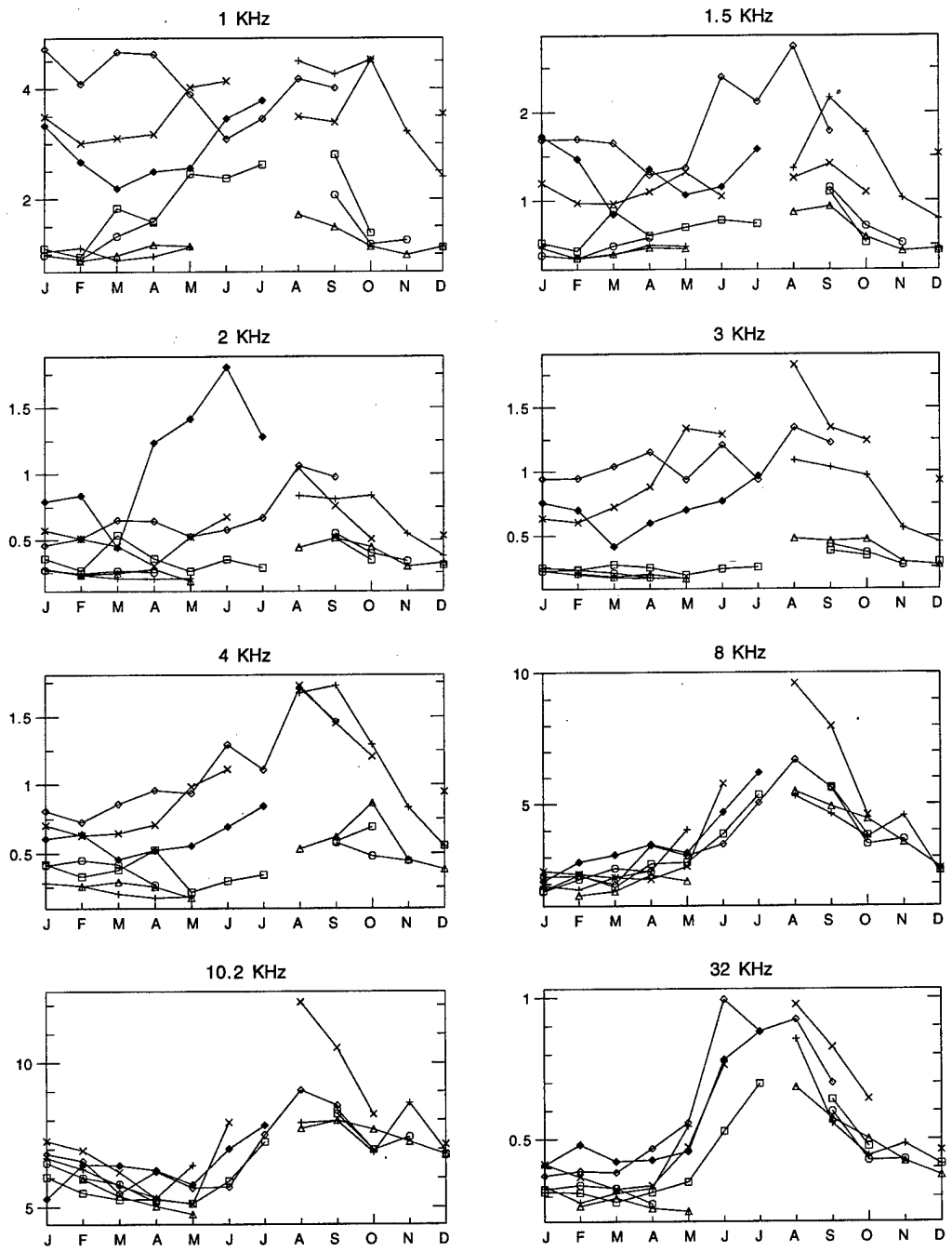

Figure 95: Monthly variation of ELF/VLF radio noise at Søndrestrøm, Greenland, for the eight highest-frequency channels and the 08-12 UT time block, each year shown individually. The years 1986 to 1991 and the year 1993 are included.

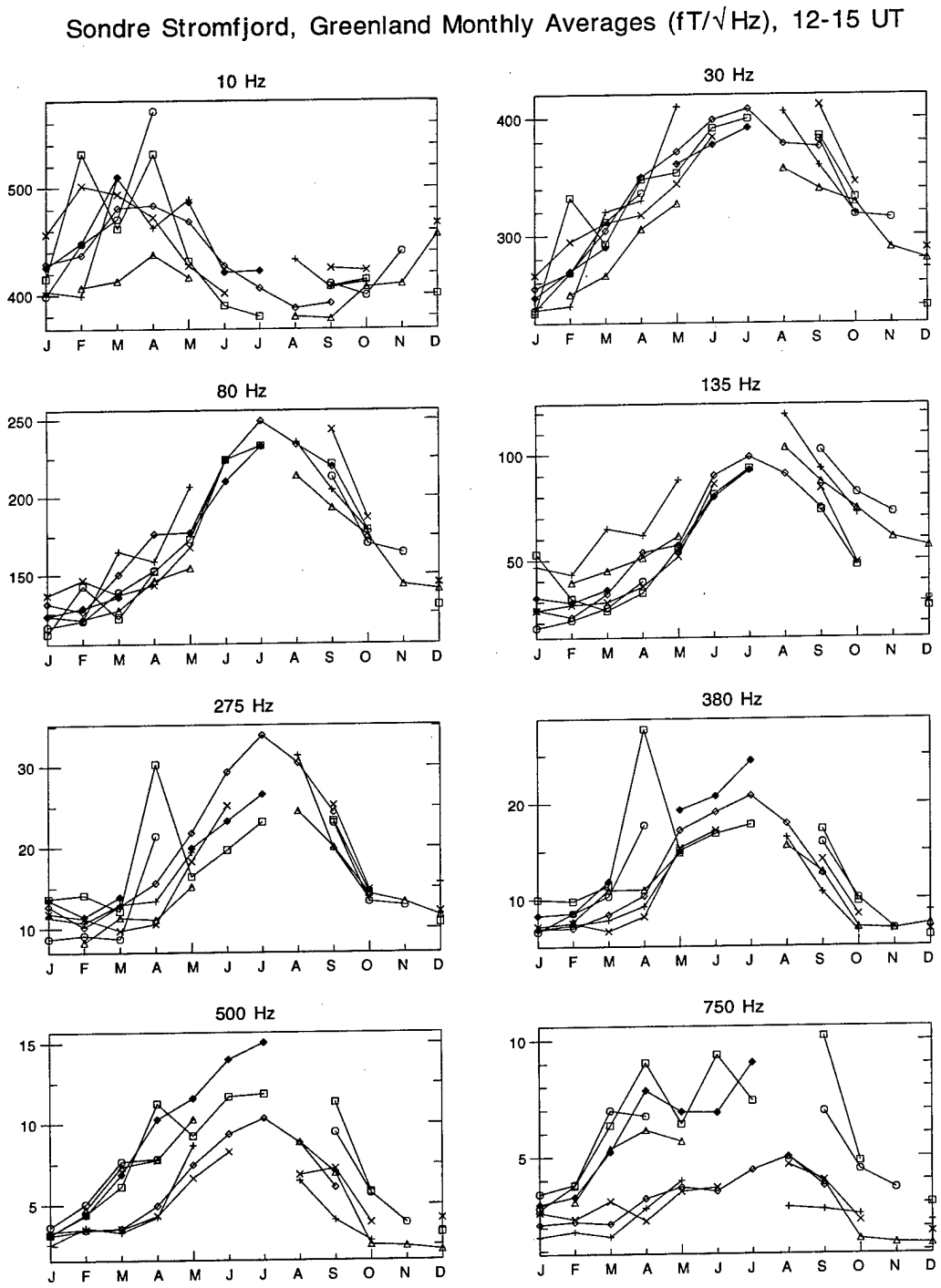

Figure 96: Monthly variation of ELF/VLF radio noise at Søndrestrøm, Greenland, for the eight lowest-frequency channels and the 12-16 UT time block, each year shown individually. The years 1986 to 1991 and the year 1993 are included.

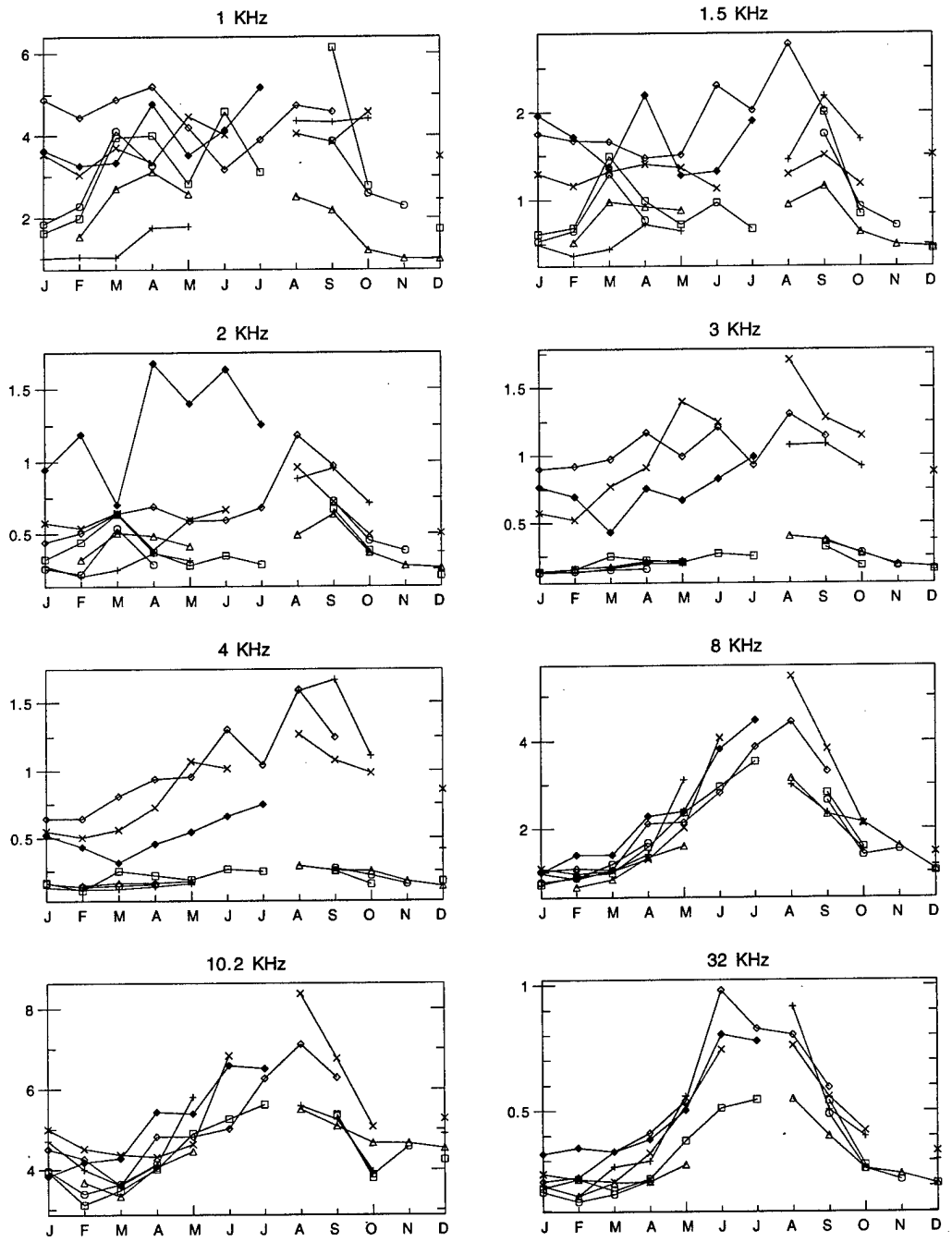

Figure 97: Monthly variation of ELF/VLF radio noise at Søndrestrøm, Greenland, for the eight highest-frequency channels and the 12-16 UT time block, each year shown individually. The years 1986 to 1991 and the year 1993 are included.

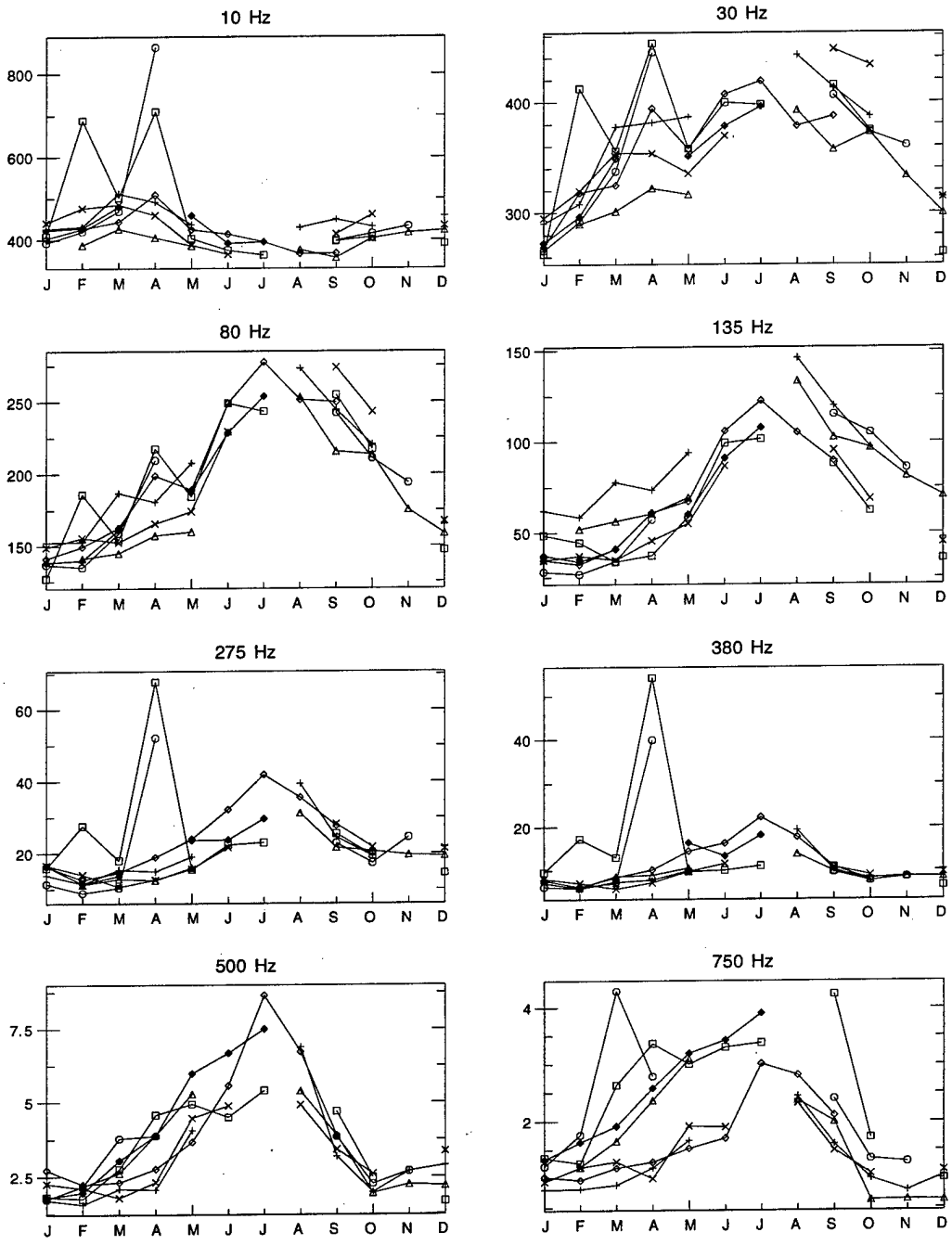

Figure 98: Monthly variation of ELF/VLF radio noise at Søndrestrøm, Greenland, for the eight lowest-frequency channels and the 16-20 UT time block, each year shown individually. The years 1986 to 1991 and the year 1993 are included.

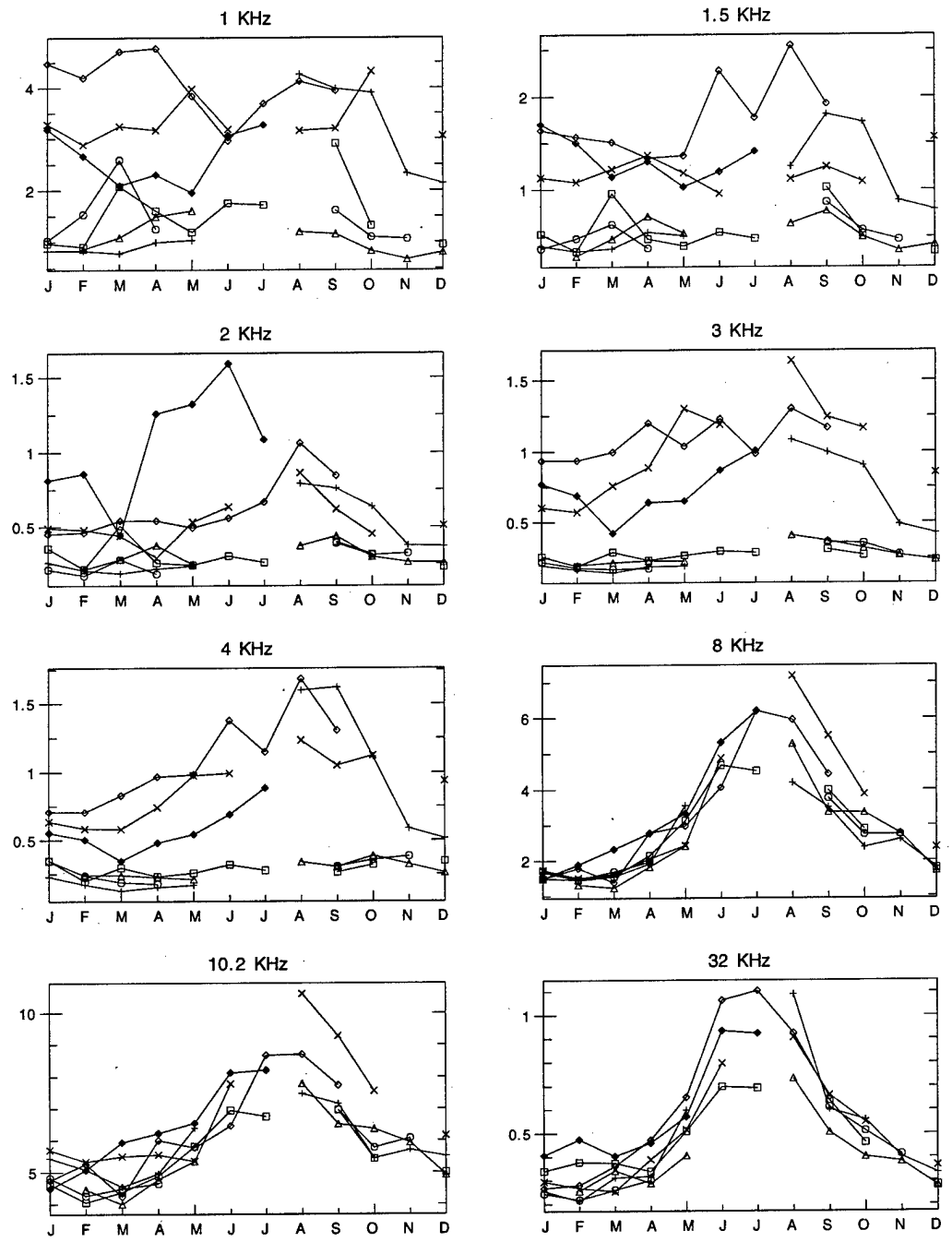

Figure 99: Monthly variation of ELF/VLF radio noise at Søndrestrøm, Greenland, for the eight highest-frequency channels and the 16-20 UT time block, each year shown individually. The years 1986 to 1991 and the year 1993 are included.

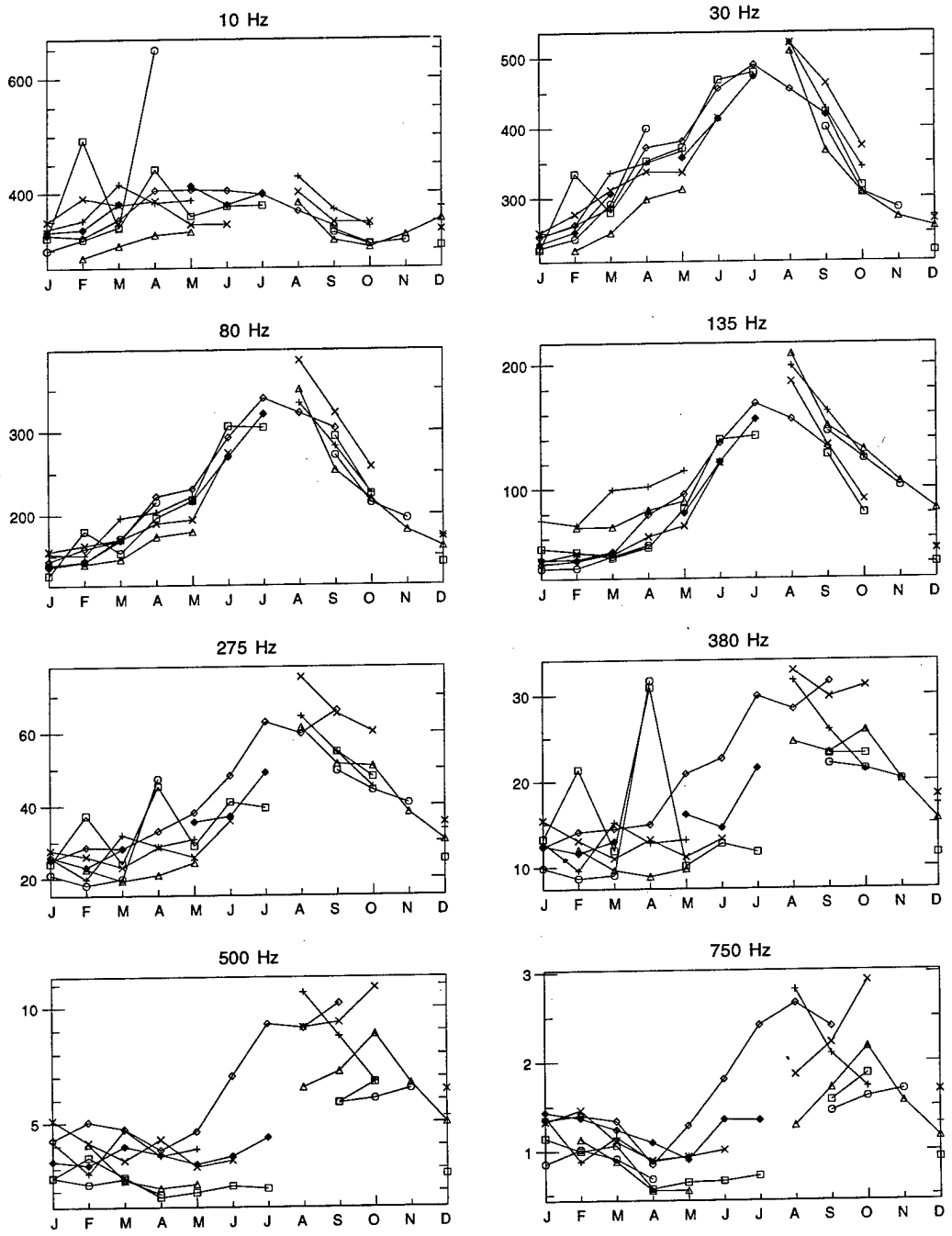

Figure 100: Monthly variation of ELF/VLF radio noise at Søndrestrøm, Greenland, for the eight lowest-frequency channels and the 20-24 UT time block, each year shown individually. The years 1986 to 1991 and the year 1993 are included.

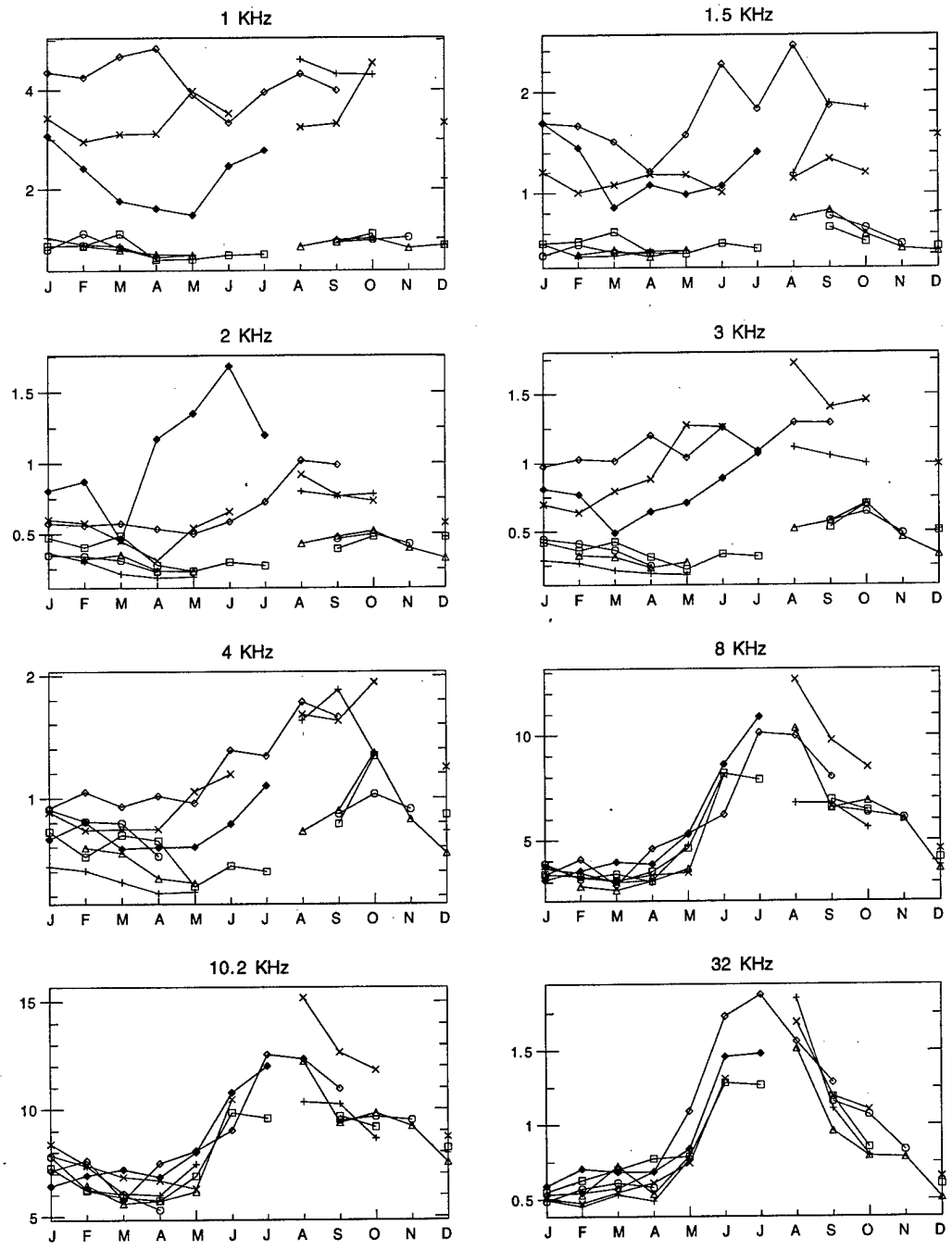

Figure 101: Monthly variation of ELF/VLF radio noise at Søndrestrøm, Greenland, for the eight highest-frequency channels and the 20-24 UT time block, each year shown individually. The years 1986 to 1991 and the year 1993 are included.

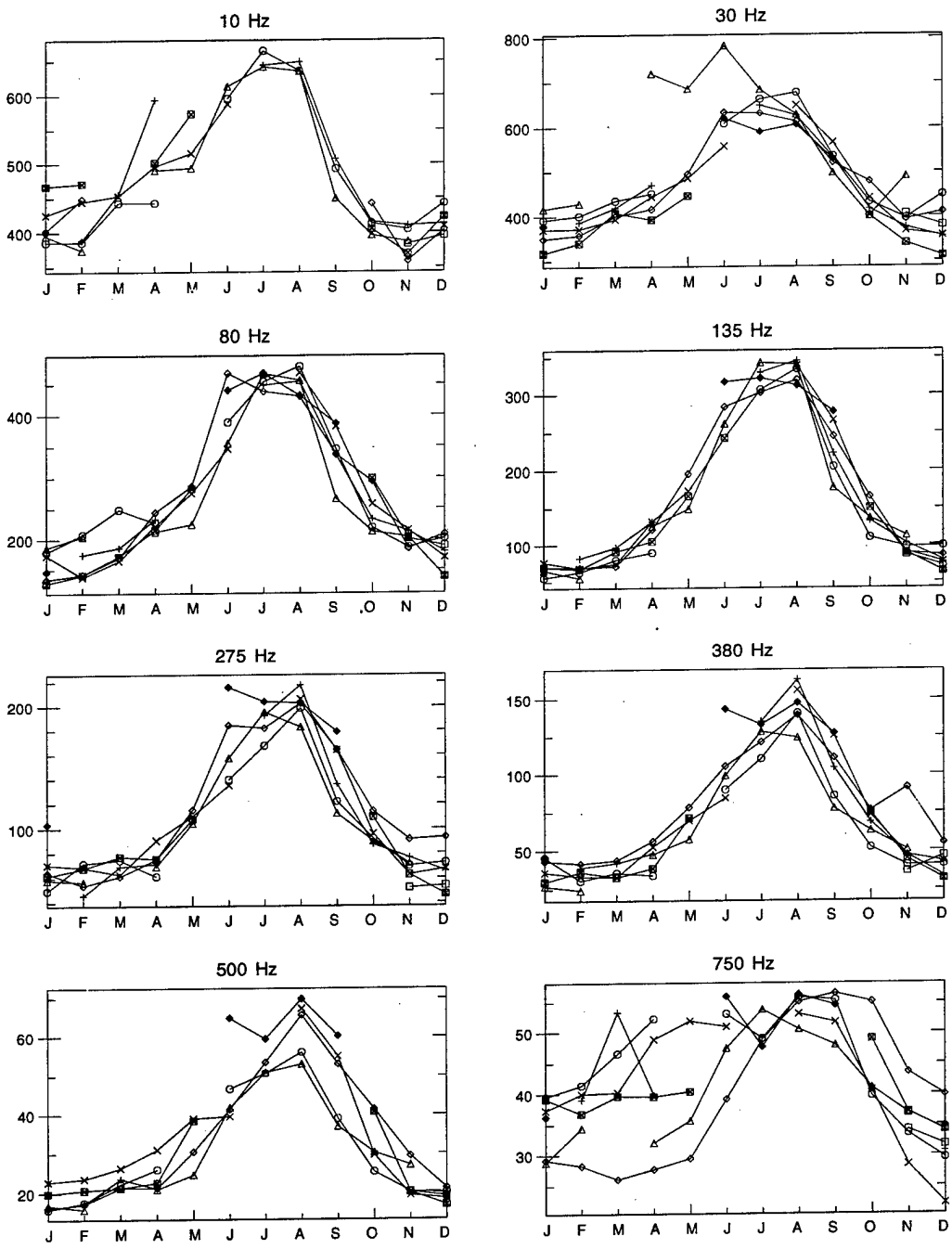

Figure 102: Monthly variation of ELF/VLF radio noise at Stanford, California, for the eight lowest-frequency channels and the 00-04 UT time block, each year shown individually. The years 1986 to 1993 are included.

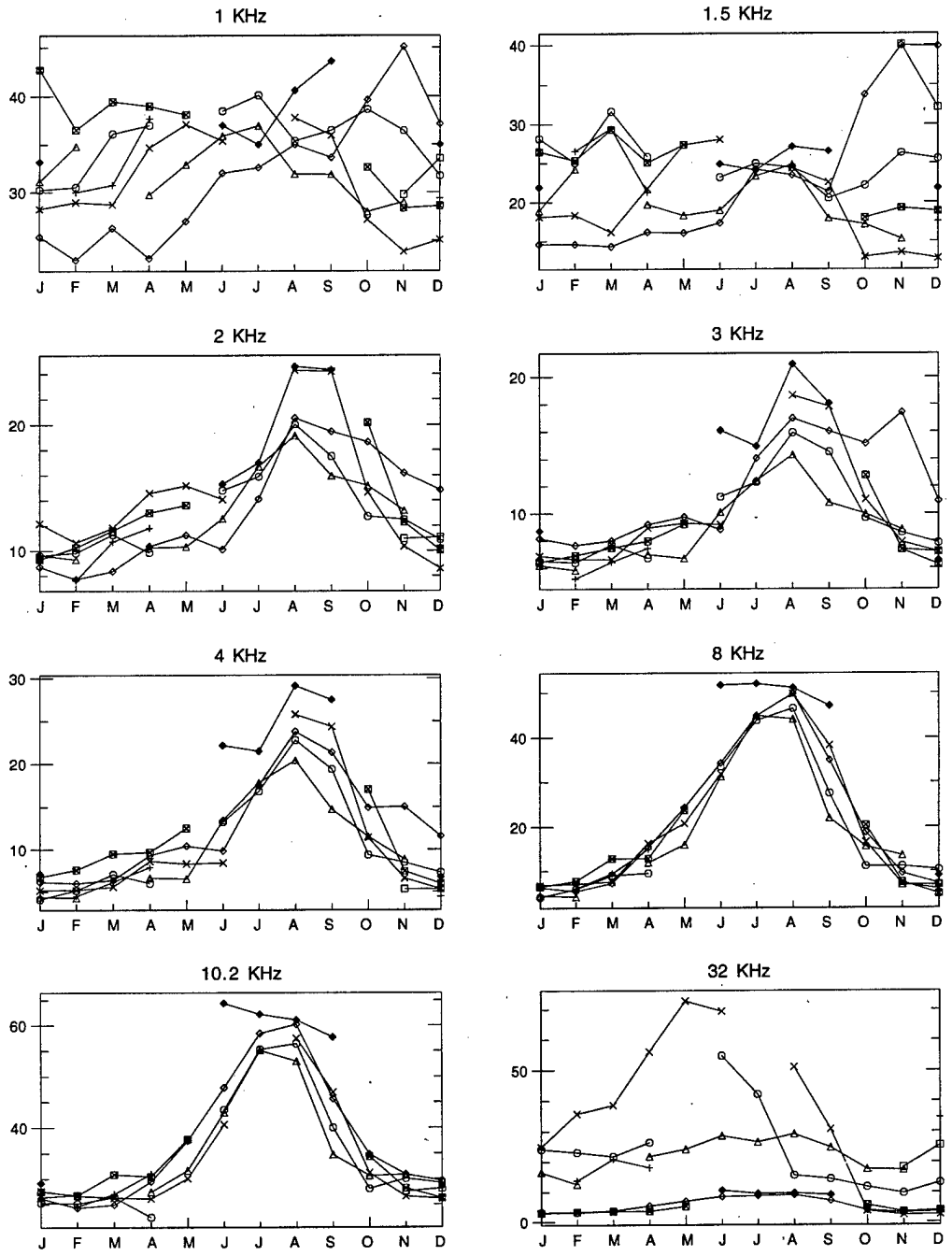

Figure 103: Monthly variation of ELF/VLF radio noise at Stanford, California, for the eight highest-frequency channels and the 00-04 UT time block, each year shown individually. The years 1986 to 1993 are included.

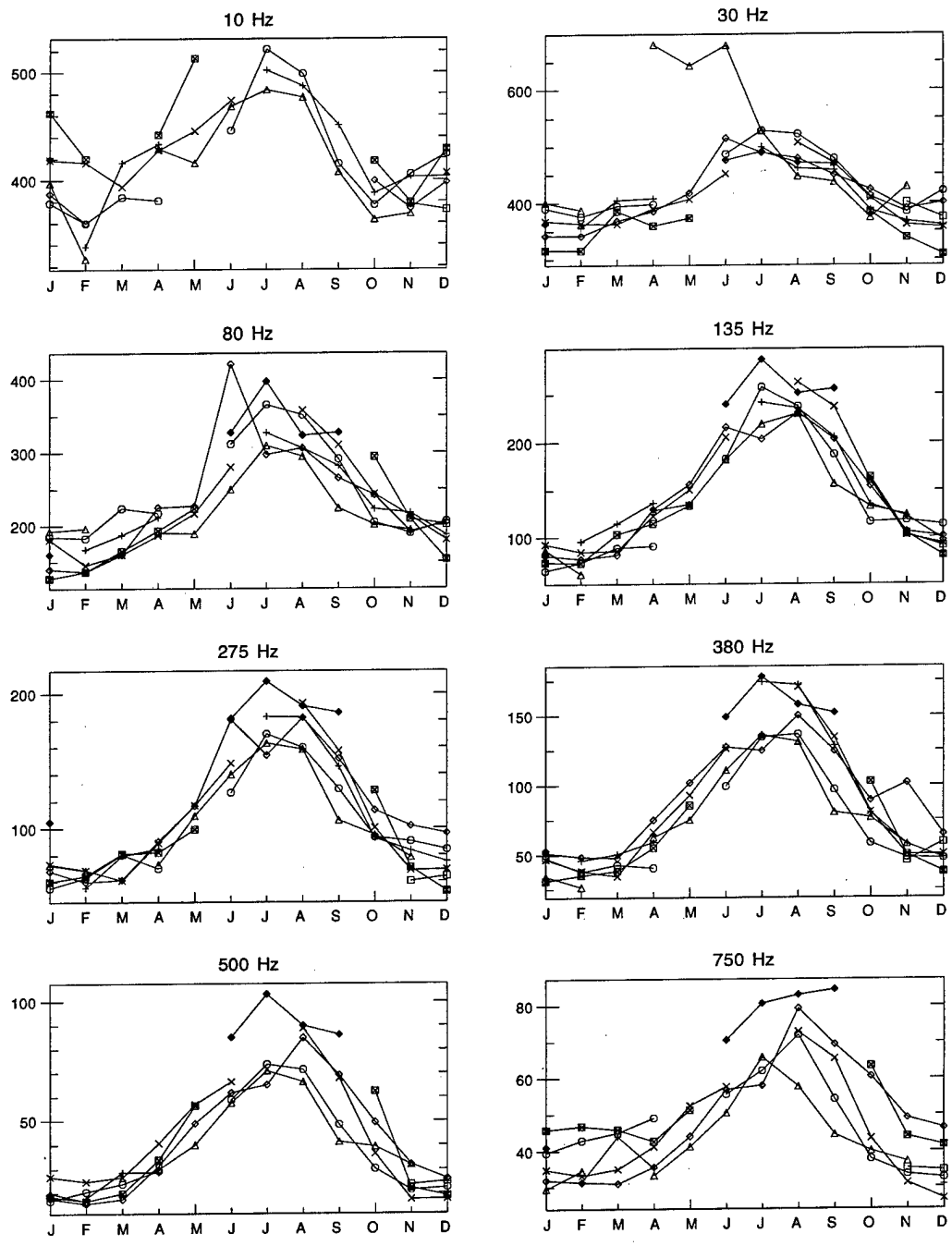

Figure 104: Monthly variation of ELF/VLF radio noise at Stanford, California, for the eight lowest-frequency channels and the 04-08 UT time block, each year shown individually. The years 1986 to 1993 are included.

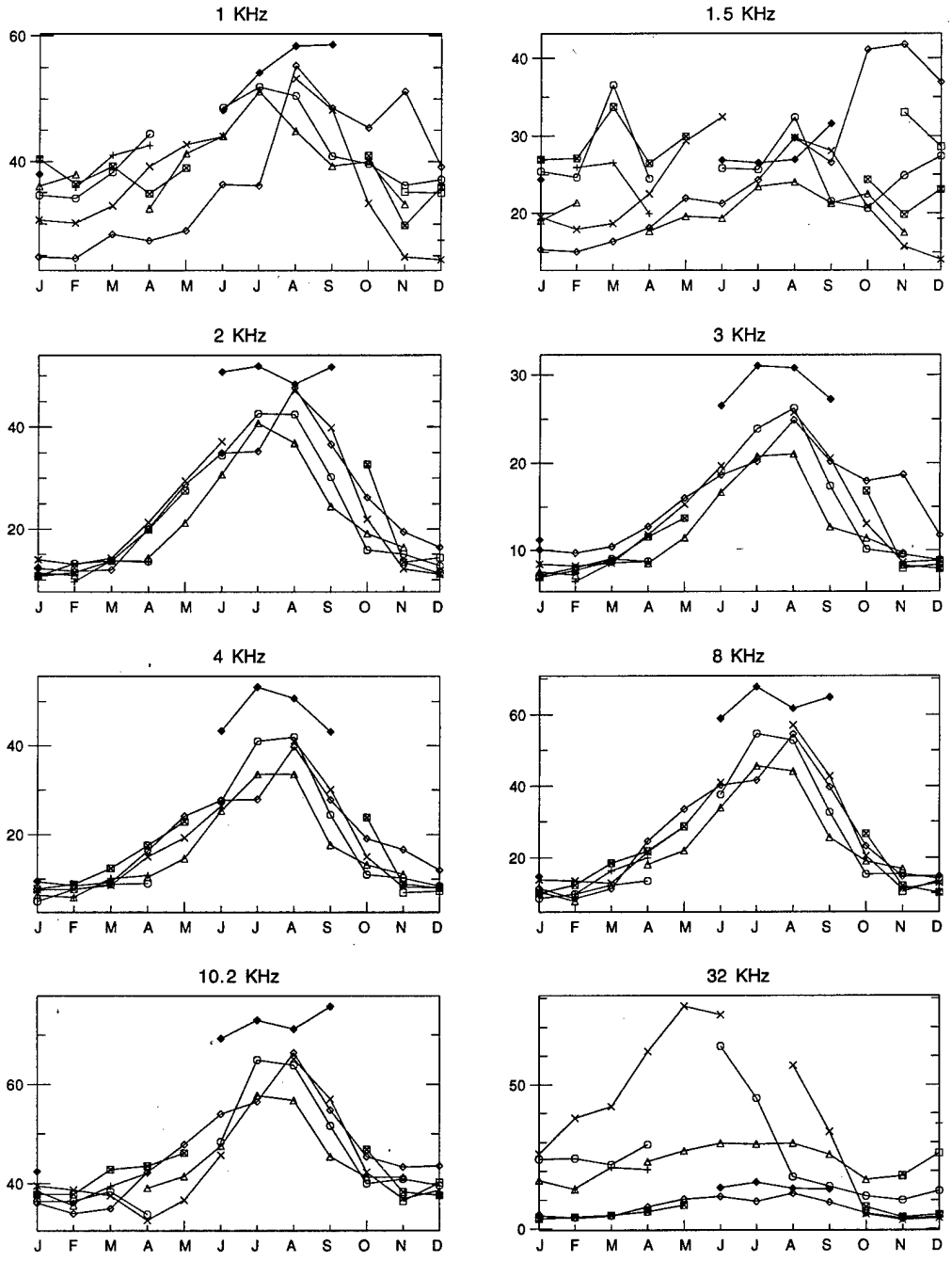

Figure 105: Monthly variation of ELF/VLF radio noise at Stanford, California, for the eight highest-frequency channels and the 04-08 UT time block, each year shown individually. The years 1986 to 1993 are included.

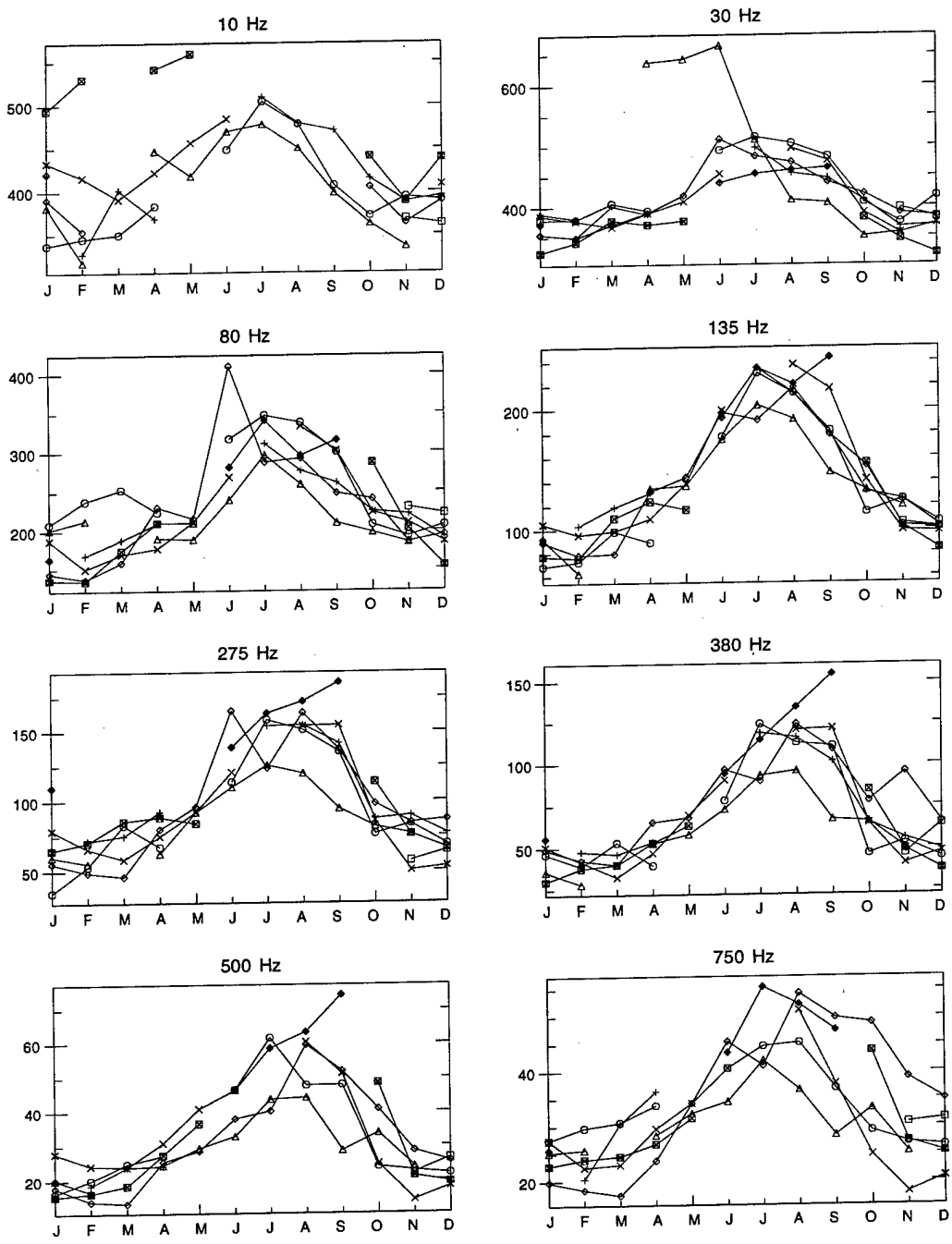

Figure 106: Monthly variation of ELF/VLF radio noise at Stanford, California, for the eight lowest-frequency channels and the 08-12 UT time block, each year shown individually. The years 1986 to 1993 are included.

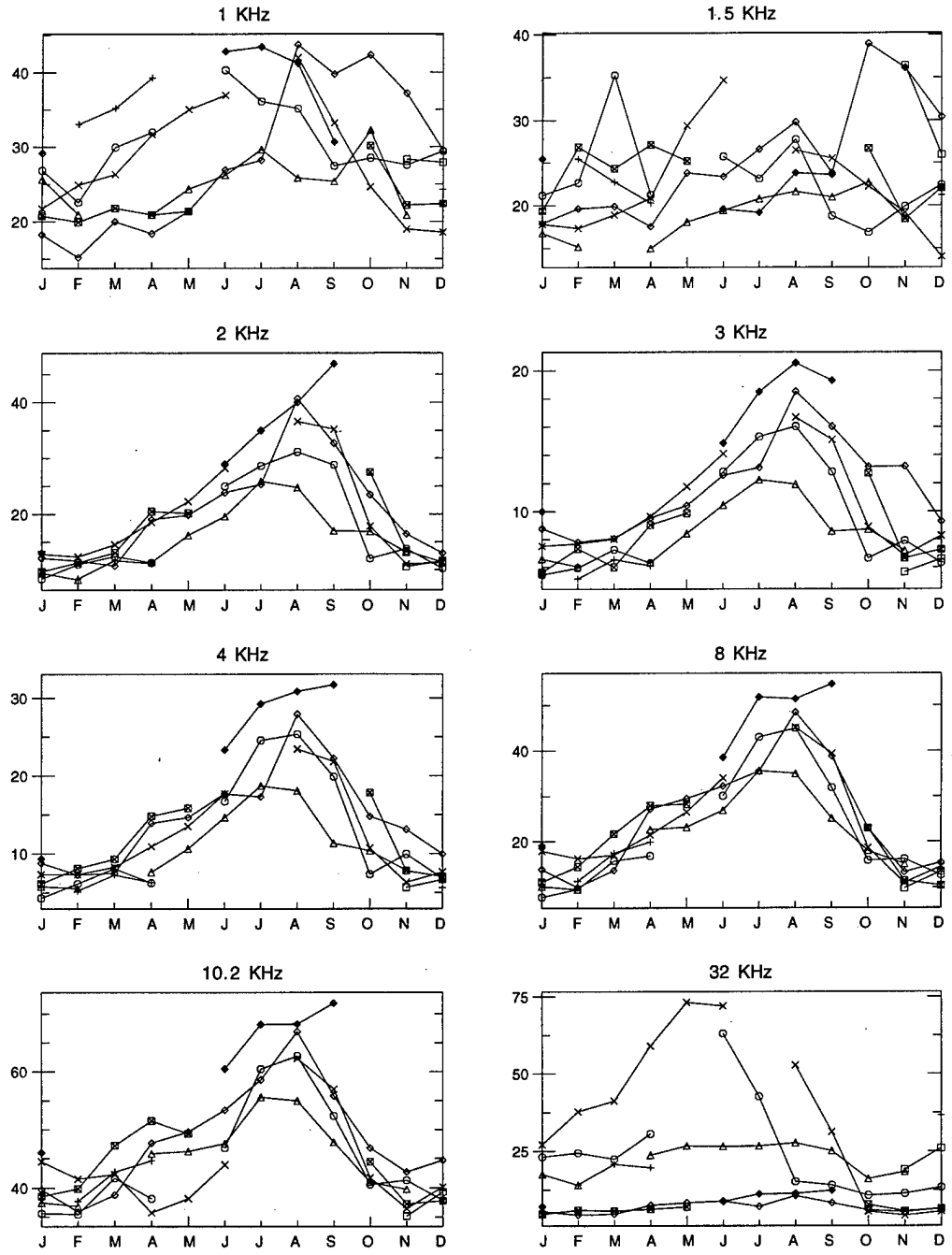

Figure 107: Monthly variation of ELF/VLF radio noise at Stanford, California, for the eight highest-frequency channels and the 08-12 UT time block, each year shown individually. The years 1986 to 1993 are included.

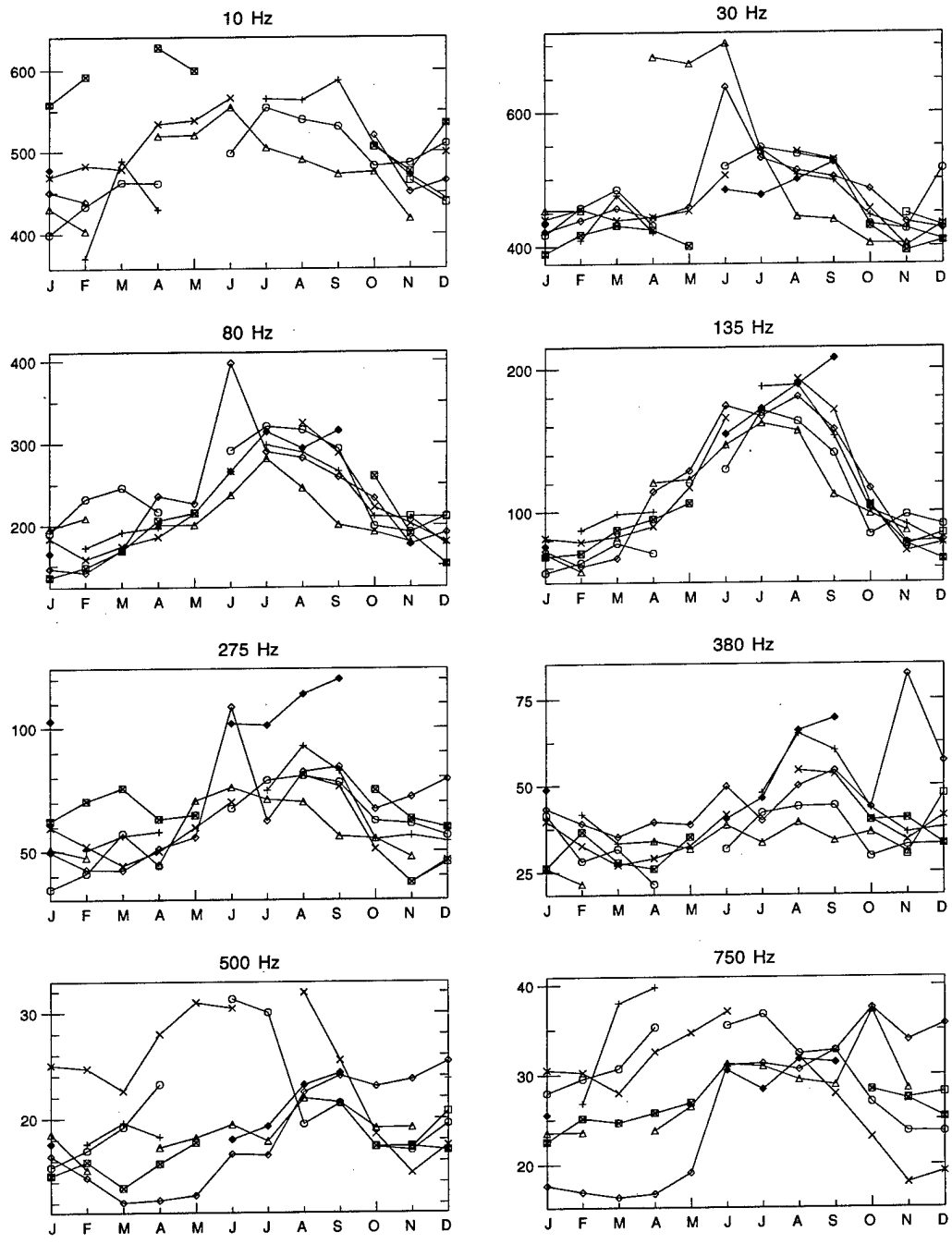

Figure 108: Monthly variation of ELF/VLF radio noise at Stanford, California, for the eight lowest-frequency channels and the 12-16 UT time block, each year shown individually. The years 1986 to 1993 are included.

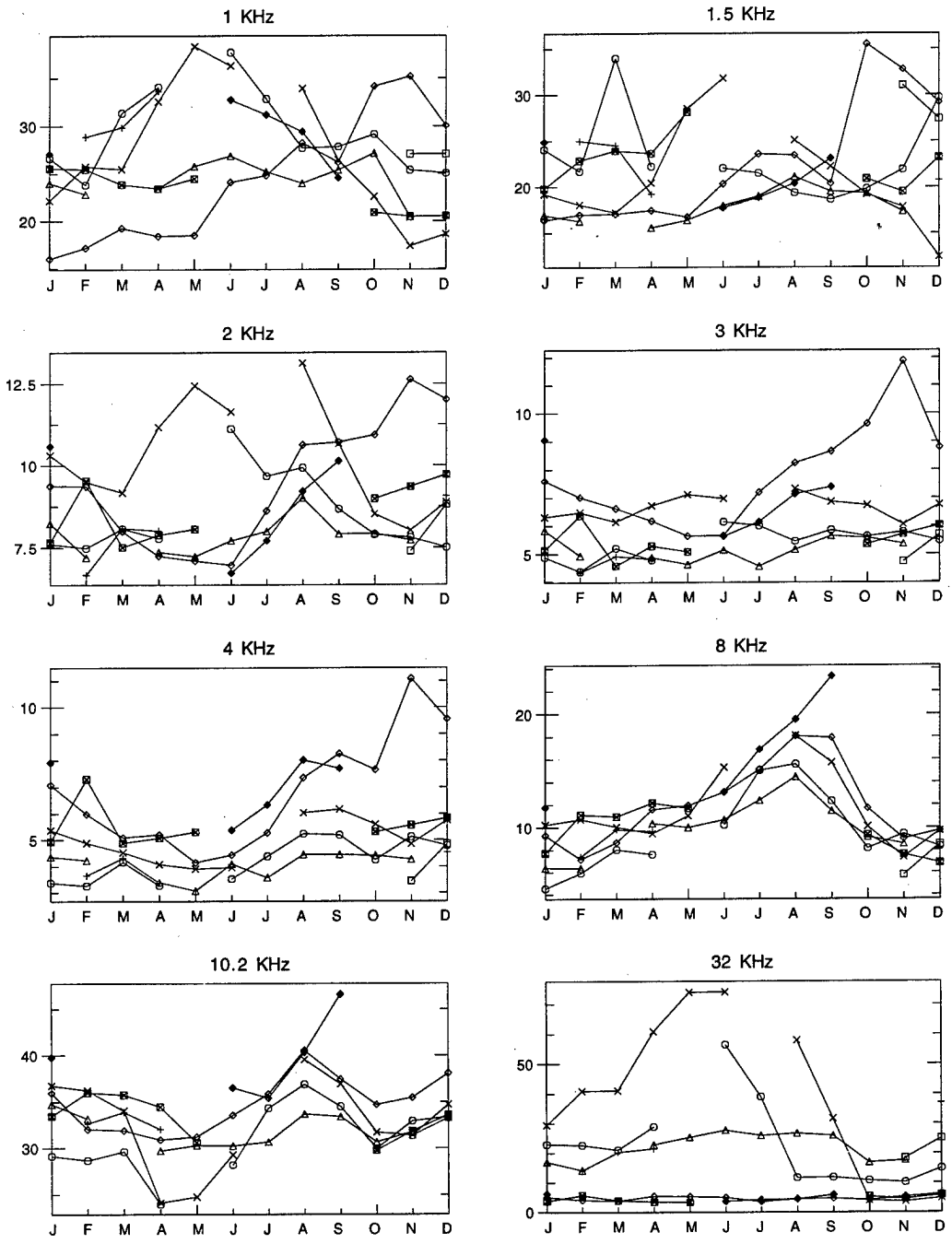

Figure 109: Monthly variation of ELF/VLF radio noise at Stanford, California, for the eight highest-frequency channels and the 12-16 UT time block, each year shown individually. The years 1986 to 1993 are included.

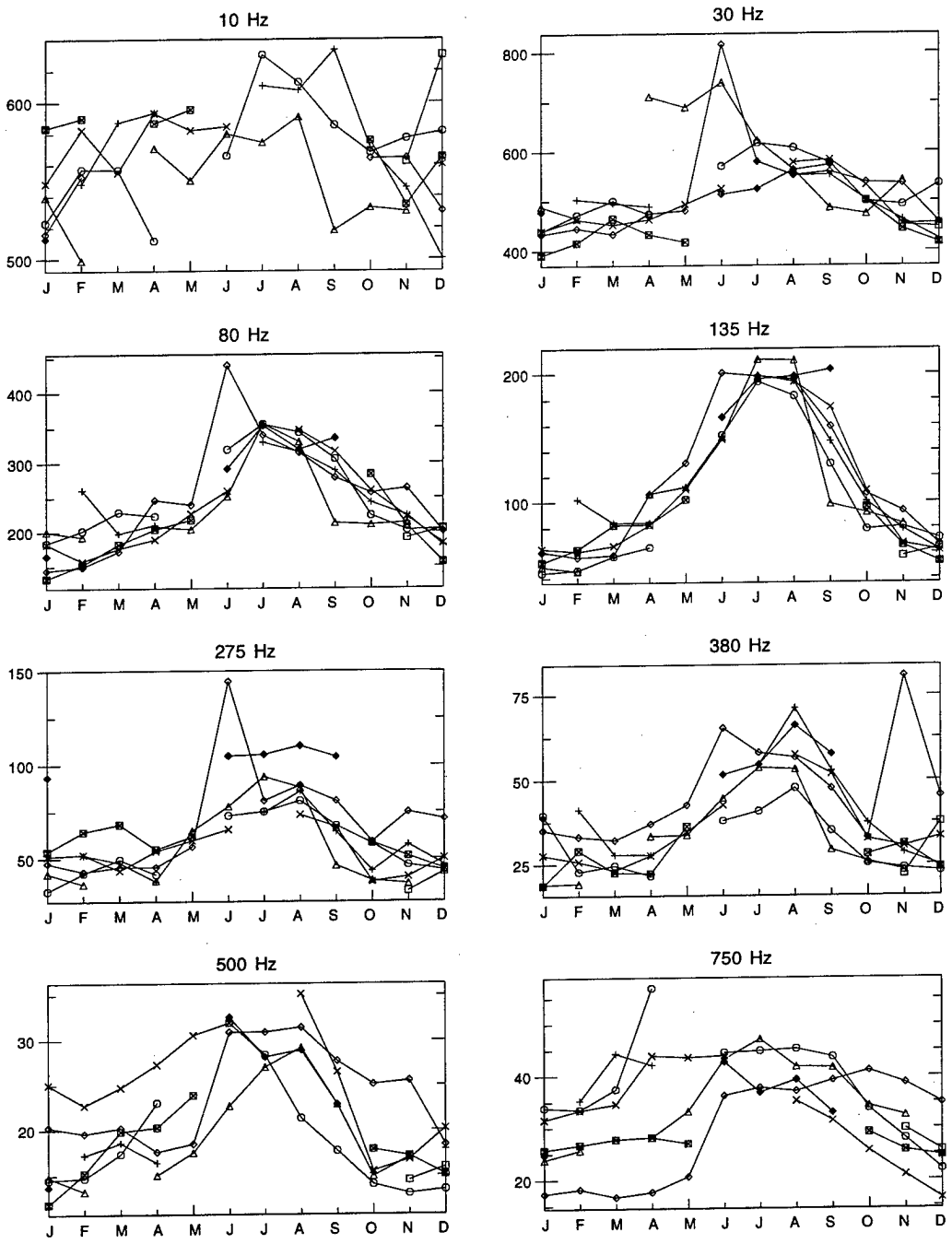

Figure 110: Monthly variation of ELF/VLF radio noise at Stanford, California, for the eight lowest-frequency channels and the 16-20 UT time block, each year shown individually. The years 1986 to 1993 are included.

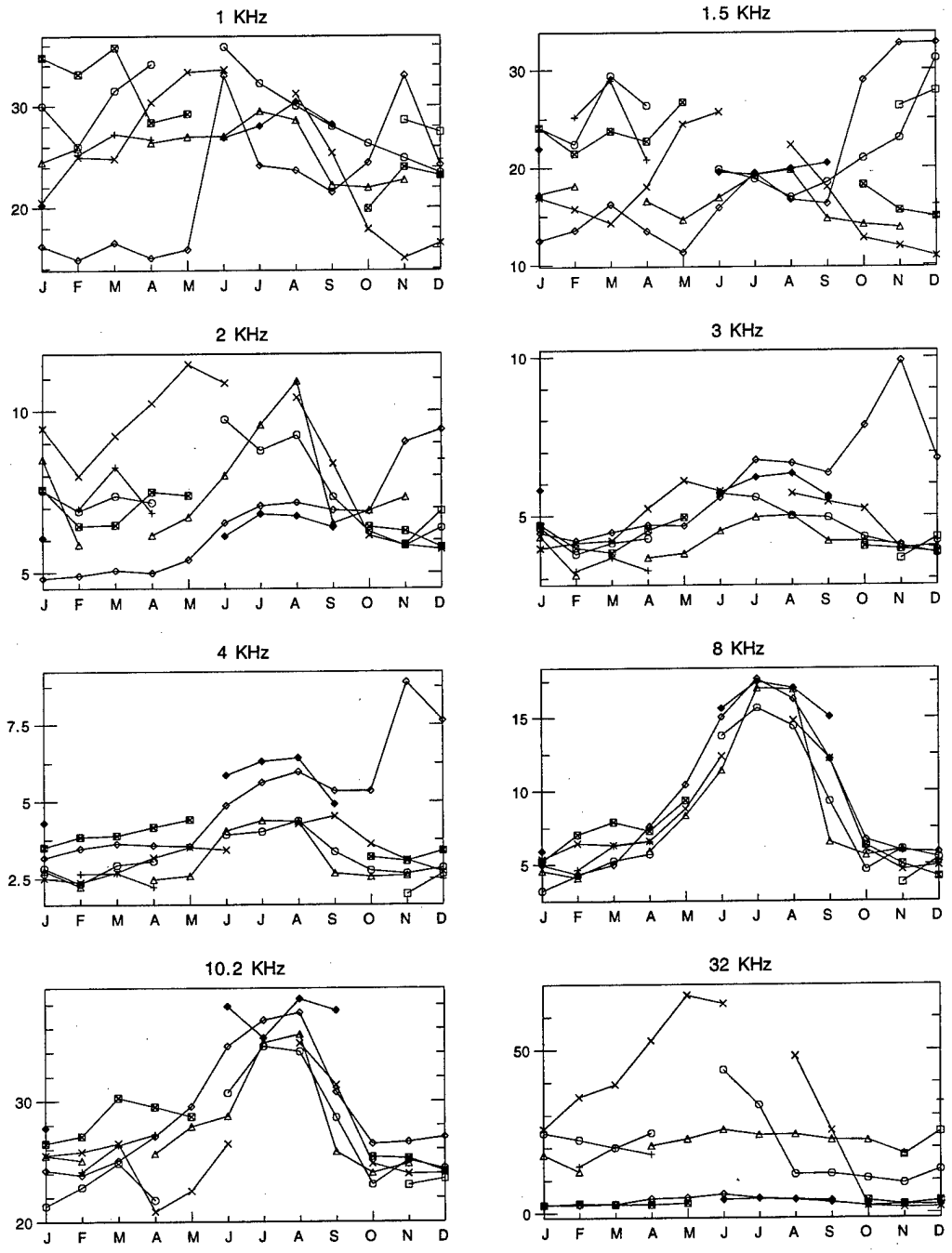

Figure 111: Monthly variation of ELF/VLF radio noise at Stanford, California, for the eight highest-frequency channels and the 16-20 UT time block, each year shown individually. The years 1986 to 1993 are included.

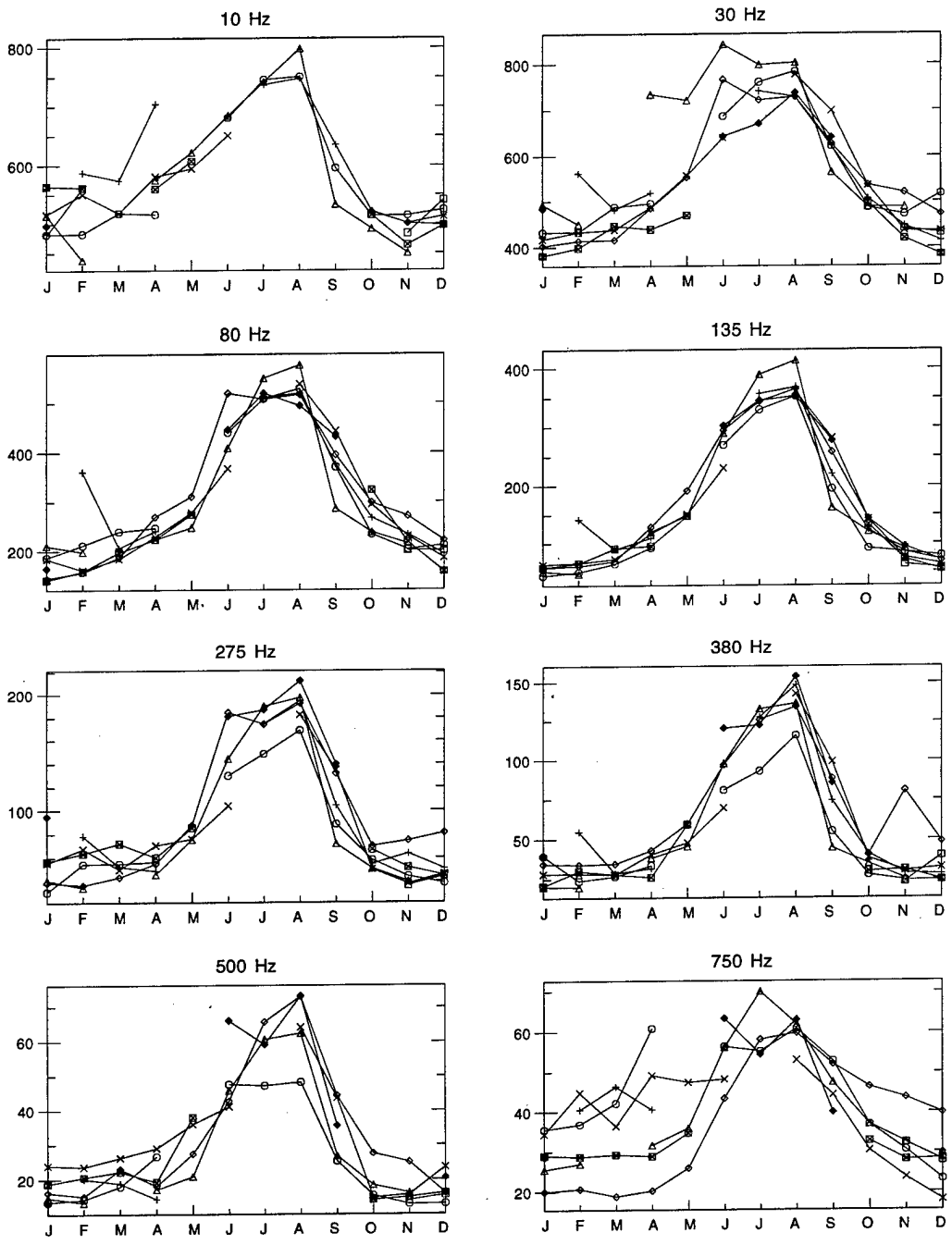

Figure 112: Monthly variation of ELF/VLF radio noise at Stanford, California, for the eight lowest-frequency channels and the 20-24 UT time block, each year shown individually. The years 1986 to 1993 are included.

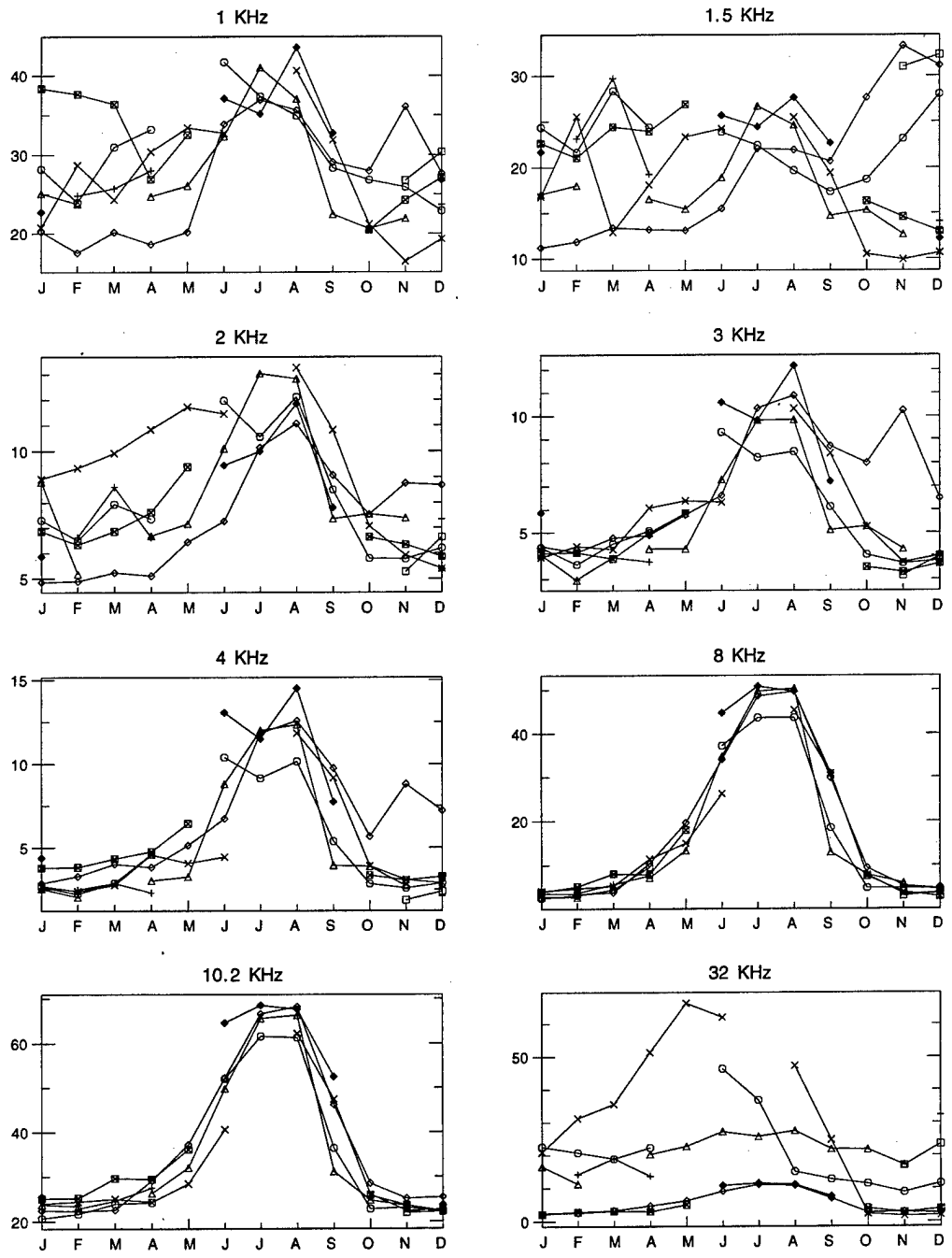

Figure 113: Monthly variation of ELF/VLF radio noise at Stanford, California, for the eight highest-frequency channels and the 20-24 UT time block, each year shown individually. The years 1986 to 1993 are included.